Seismic Performance Assessment of Buildings
Volume 1 – Methodology

Prepared by

APPLIED TECHNOLOGY COUNCIL
201 Redwood Shores Parkway, Suite 240
Redwood City, California 94065
www.ATCouncil.org

Prepared for

FEDERAL EMERGENCY MANAGEMENT AGENCY
Michael Mahoney, Project Officer
Robert D. Hanson, Technical Monitor
Washington, D.C.

ATC MANAGEMENT AND OVERSIGHT
Christopher Rojahn (Project Executive Director)
Jon A. Heintz (Project Manager)
Ayse Hortacsu

PROJECT MANAGEMENT COMMITTEE
Ronald O. Hamburger (Project Technical Director)
John Gillengerten
William T. Holmes **
Peter J. May
Jack P. Moehle
Maryann T. Phipps*

STEERING COMMITTEE
William T. Holmes (Chair)
Roger D. Borcherdt
Anne Bostrom
Bruce Burr
Kelly Cobeen
Anthony B. Court
Terry Dooley
Dan Gramer
Michael Griffin
R. Jay Love
David Mar
Steven McCabe
Brian J. Meacham
William J. Petak

* ATC Board Contact
** ex-officio

RISK MANAGEMENT PRODUCTS TEAM
John D. Hooper (Co-Team Leader)
Craig D. Comartin (Co-Team Leader)
Mary Comerio
Allin Cornell
Mahmoud Hachem
Gee Hecksher
Judith Mitrani-Reiser
Peter Morris
Farzad Naeim
Keith Porter
Hope Seligson

STRUCTURAL PERFORMANCE PRODUCTS TEAM
Andrew S. Whittaker (Team Leader)
Gregory Deierlein
John D. Hooper
Yin-Nan Huang
Laura Lowes
Nicolas Luco
Andrew T. Merovich

NONSTRUCTURAL PERFORMANCE PRODUCTS TEAM
Robert E. Bachman (Team Leader)
Philip J. Caldwell
Andre Filiatrault
Robert P. Kennedy
Helmut Krawinkler
Manos Maragakis
Gilberto Mosqueda
Eduardo Miranda
Keith Porter

FEMA

nehrp

RISK MANAGEMENT PRODUCTS CONSULTANTS
Travis Chrupalo
D. Jared DeBock
Armen Der Kiureghian
Scott Hagie
Curt Haselton
Russell Larsen
Juan Murcia-Delso
Scott Shell
P. Benson Shing
Farzin Zareian

STRUCTURAL PERFORMANCE PRODUCTS AND FRAGILITY DEVELOPMENT CONSULTANTS
Jack Baker
Dhiman Basu
Dan Dolan
Charles Ekiert
Andre Filiatrault
Aysegul Gogus
Kerem Gulec
Dawn Lehman
Jingjuan Li
Eric Lumpkin
Juan Murcia-Delso
Hussein Okail
Charles Roeder
P. Benson Shing
Christopher Smith
Victor Victorsson
John Wallace

NONSTRUCTURAL PERFORMANCE PRODUCTS AND FRAGILITY DEVELOPMENT CONSULTANTS
Richard Behr
Greg Hardy
Christopher Higgins
Gayle Johnson
Paul Kremer
Dave McCormick
Ali M. Memari
William O'Brien
John Osteraas
Elizabeth Pahl
John Stevenson
Xin Xu

FRAGILITY REVIEW PANEL
Bruce Ellingwood
Robert P. Kennedy
Stephen Mahin

VALIDATION/VERIFICATION TEAM
Charles Scawthorn (Chair)
Jack Baker
David Bonneville
Hope Seligson

SPECIAL REVIEWERS
Thalia Anagnos
Fouad M. Bendimerad

Notice

Cover photograph – Collapsed building viewed through the archway of an adjacent building, 1999 Chi-Chi, Taiwan earthquake (courtesy of Farzad Naeim, John A. Martin & Associates, Los Angeles, California).

Foreword

The Federal Emergency Management Agency (FEMA) is committed to reducing the ever-increasing cost that disasters inflict on our country. Preventing losses before they happen by building to withstand anticipated forces is one of the key components of mitigation, and is the only truly effective way of reducing the impact of disasters on our country. One of the most promising tools that can be used to reduce damage from an earthquake, or other similar disaster, is performance-based design.

Performance-Based Seismic Design (PBSD) is a concept that permits the design and construction of buildings with a realistic and reliable understanding of the risk of life, occupancy and economic loss that may occur as a result of future earthquakes. PBSD is based on an evaluation of a building's design to determine the probability of experiencing different types of losses, considering the range of potential earthquakes that may affect the structure. The desired performance level for a building, along with a specified level of seismic shaking, are defined at the initiation of the design process. Decision-makers then select one or more of these performance levels along with an input ground motion, scenario event, or earthquake hazard level for which this performance is to be achieved. The designer then conducts a performance assessment, which is intended to determine whether the various performance levels are met or exceeded at the selected hazard level. Following the PBSD process, the building design would then be adjusted until the performance assessments indicate a risk of loss that is deemed acceptable by the building owner or regulator.

Current building codes are prescriptive in nature and are intended principally to provide a life-safety level of protection when a design-level event, such as an earthquake, occurs. While codes are intended to produce buildings that meet a life-safety performance level for a specified level of ground shaking, they do not provide designers with a means to determine if other performance levels would be achieved. During a design level earthquake, a code-designed building could achieve the goal of preventing loss of life or life-threatening injury to building occupants, but could still sustain extensive structural and nonstructural damage and be out of service for an extended period of time. In a number of cases, the damage may be too costly to repair, leading to demolition. While some current design guidance, codes, and standards for existing buildings incorporate some performance-based design

concepts, these contain older criteria that do not address all of the necessary issues.

The PBSD process can be used by a building owner or design team to design new buildings, or the seismic upgrade of existing buildings, that are more loss-resistant than buildings designed using traditional prescriptive procedures. It can also be used to design buildings with a higher confidence of performing as intended after a design event. PBSD can also be used to improve the prescriptive provisions of current building codes so that more consistent and reliable performance can be attained.

The FEMA 349, *Action Plan for Performance Based Seismic Design*, was published by FEMA in April 2000. The FEMA-349 *Action Plan* extended over a period of ten years, and required an estimated $20 million to $27 million in funding (1998 dollars). At that time, FEMA was unable to fund such an undertaking, and the plan was not implemented. During that time, the three National Science Foundation-funded Earthquake Engineering Research Centers were all performing research related to performance-based seismic design. In particular, the Pacific Earthquake Engineering Research Center (PEER) had made significant progress in this area, and approached FEMA with an interest in assisting in such an effort.

In 2001, FEMA contracted with the Applied Technology Council (ATC) to initiate the Project Planning Phase of a multi-year effort to develop PBSD, following the general approach outlined in the FEMA 349 *Action Plan*. Under this contract, work included the development of a project management process and work plan; conduct of two workshops to receive outside input on project needs and goals; consensus on the definitions of performance to be used as the basis for performance based seismic design; development of a new Program Plan based on the FEMA 349 *Action Plan*; and initiation of the process for quantifying structural and nonstructural component performance. The Project Planning Phase was completed in 2006 with the publication of FEMA 445, *Next-Generation, Performance-Based Seismic Design Guidelines, Program Plan for New and Existing Buildings*.

In 2006, FEMA then contracted with ATC to initiate Phase 1 Development of a Seismic Performance Assessment Methodology. This work built upon work completed during the Project Planning Phase, as well as research performed by others, including the three Earthquake Engineering Research Centers and other universities, private industry, various construction materials trade associations, and individual product manufacturers and suppliers who have performed research to facilitate the use of their products and materials in a performance-based design environment. Phase 1

developmental work was completed in 2012 with the publication of FEMA P-58, *Seismic Performance Assessment of Buildings*, *Volume 1 – Methodology*, *Volume 2 – Implementation Guide*, and a series of supporting electronic materials and background technical information. For practical implementation of the methodology, work included the development of an electronic tool, referred to as the *Performance Assessment Calculation Tool*, or PACT, to help capture building inventory data, input a given earthquake shaking probability or intensity, apply specific fragilities and consequences to each building component, and present the results of a large number of runs, or realizations, in a logical format.

Unlike earlier versions of performance-based seismic design, FEMA P-58 methodology utilizes performance measures that can be understood by decision makers. Performance objectives relate to the amount of damage the building may experience and the consequences of this damage including: potential casualties; loss of use or occupancy; and repair and reconstruction costs. They can also be used to assess potential environmental impacts, including generation of waste, expenditure of energy, or creation of greenhouse gases.

The typical building design process is based on designers selecting, proportioning and detailing building components to satisfy prescriptive criteria contained within the building code. While most code criteria were developed with the intent of providing some level of seismic performance, the intended performance is often not obvious, and the design's actual ability to provide this performance is seldom evaluated. Using the FEMA P-58 methodology, owners, designers and other stakeholders will jointly identify the desired building performance characteristics at the beginning of a project. Then as design decisions are made, the effect of these decisions on a building's performance can be evaluated to assure that the final design will be capable of achieving the desired performance.

Although FEMA is supporting the development of PBSD, there will always be a need for the current prescriptive-based building codes, especially for the majority of buildings designed and constructed with marginal engineering involvement. PBSD will best be utilized for critical facilities or other structures where performance is an issue, for buildings where the cost of increased performance can be justified, or for buildings that will benefit from additional reliability associated with increased engineering design involvement.

As part of FEMA's ongoing commitment to PBSD, contracting has begun on the Phase 2 developmental effort, which will use the FEMA P-58 seismic

performance assessment methodology to develop performance-based seismic design guidelines and stakeholder guidelines. It is envisioned that this five-year effort will also include capturing any necessary improvements to the FEMA P-58 methodology and associated products as they are used in conducting the work.

FEMA wishes to express its sincere gratitude to all who were involved in this project and in the development of the FEMA P-58 methodology. The entire development team numbered more than 130 individuals, and it is not possible to acknowledge them all here. However, special thanks are extended to: Ronald Hamburger, Project Technical Director; Robert Bachman, Nonstructural Team Leader; John Hooper, Risk Management Team Leader; Andrew Whittaker, Structural Products Team Leader; William Holmes, Steering Committee Chair; and Jon Heinz, ATC Project Manager. The hard work and dedication of these individuals, and all who were involved in this project, have immeasurably helped our nation move towards making performance-based seismic design a reality, and towards reducing losses suffered by the citizens of our country in future earthquakes.

Federal Emergency Management Agency

Preface

In 2001, the Applied Technology Council (ATC) was awarded the first in a series of contracts with the Federal Emergency Management Agency (FEMA) to develop Next-Generation Performance-Based Seismic Design Guidelines for New and Existing Buildings. These projects would become known as the ATC-58/ATC-58-1 Projects. The principal product under this combined 10-year work effort was the development of a methodology for seismic performance assessment of individual buildings that properly accounts for uncertainty our ability to accurately predict response, and communicates performance in ways that better relate to the decision-making needs of stakeholders.

This report, *Seismic Performance Assessment of Buildings, Volume 1 – Methodology*, and its companion products, together describe the resulting methodology as well as the development of basic building information, response quantities, fragilities, and consequence data used as inputs to the methodology. The procedures are probabilistic, uncertainties are explicitly considered, and performance is expressed as the probable consequences, in terms of human losses (deaths and serious injuries), direct economic losses (building repair or replacement costs), and indirect losses (repair time and unsafe placarding) resulting from building damage due to earthquake shaking. The methodology is general enough to be applied to any building type, regardless of age, construction or occupancy; however, basic data on structural and nonstructural damageability and consequence are necessary for its implementation.

To allow for practical implementation of the methodology, work included the collection of fragility and consequence data for most common structural systems and building occupancies, and the development of an electronic *Performance Assessment Calculation Tool* (PACT) for performing the probabilistic computations and accumulation of losses.

This work is the result of more than 130 consultants involved in the development of the methodology and underlying procedures, collection of available fragility data, estimation of consequences, development of supporting electronic tools, implementation of quality assurance procedures, and beta testing efforts. ATC is particularly indebted to the leadership of Ron Hamburger, who served as Project Technical Director, John Hooper and Craig Comartin, who served as Risk Management Products Team Leaders,

Andrew Whittaker, who served as Structural Performance Products Team Leader, Bob Bachman, who served as Nonstructural Performance Products Team Leader, and the members of the Project Management Committee, including John Gillengerten, Bill Holmes, Peter May, Jack Moehle, and Maryann Phipps.

ATC would also like to thank the members of the Project Steering Committee, the Risk Management Products Team, the Structural Performance Products Team, the Nonstructural Performance Products Team, the Fragility Review Panel, the Validation/Verification Team, and the many consultants who assisted these teams. The names of individuals who served on these groups, along with their affiliations, are provided in the list of Project Participants at the end of this report.

ATC acknowledges the Pacific Earthquake Engineering Research Center (PEER), and its framework for performance-based earthquake engineering, as the technical basis underlying the methodology. In particular, the work of Tony Yang, Jack Moehle, Craig Comartin, and Armen Der Kiureghian, in developing and presenting the first practical application of the PEER framework, is recognized as the basis of how computations are performed and losses are accumulated in the methodology.

Special acknowledgment is extended to C. Allin Cornell and Helmut Krawinkler for their formative work in contributing to risk assessment and performance-based design methodologies, and to whom this work is dedicated.

ATC also gratefully acknowledges Michael Mahoney (FEMA Project Officer) and Robert Hanson (FEMA Technical Monitor) for their input and guidance in the conduct of this work, and Peter N. Mork, Bernadette Hadnagy, and Laura Samant for ATC report production services.

Jon A. Heintz
ATC Director of Projects

Christopher Rojahn
ATC Executive Director

Dedication

This report, *Seismic Performance Assessment of Buildings*, is dedicated to the memory of C. Allin Cornell and Helmut Krawinkler, longtime faculty colleagues at Stanford University.

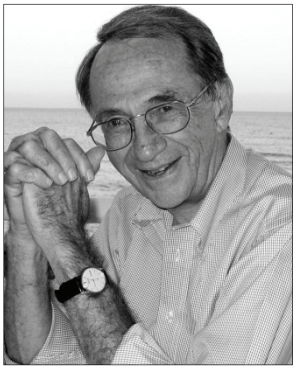

C. Allin Cornell

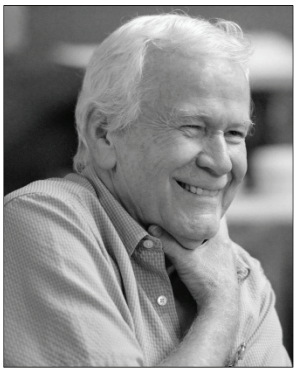

Helmut Krawinkler

Allin brought rigorous mathematical approaches for uncertainty assessment into structural engineering, seismology, and geophysics. His continuous major contributions to risk and reliability analysis over the years have formed the basis for modern seismic risk assessment methodologies. Helmut specialized in structural design and behavior with ground-breaking research on seismic design and nonlinear structural response. His work established principles underlying modern building code provisions and formed the basis of current performance-based design methodologies.

Following the 1994 Northridge earthquake, Allin and Helmut began a close collaboration on the FEMA-funded SAC Steel Project, developing seismic design criteria for steel moment frame construction. In this regard, they were a perfect complement to one another – a combination of rigorous probabilistic thinking with an understanding of nonlinear structural behavior and design. This close collaboration continued to grow in work with the Pacific Earthquake Engineering Research Center (PEER), ultimately leading to the formalization of the PEER framework for performance-based earthquake engineering, the theoretical basis on which this report is based.

In 2000, Allin and Helmut reflected on the ultimate goal of performance-based engineering, "*The final challenge is not in predicting performance or estimating losses; it is in contributing effectively to the reduction of losses and the improvement of safety. We must never forget this."* Allin and Helmut were true visionaries whose contributions to performance-based design and earthquake engineering are immeasurable. Their professional contributions won them both many accolades, including two of engineering's highest honors – election to the National Academy of Engineering and receipt of the George W. Housner Medal from the Earthquake Engineering Research Institute. Beyond their professional achievements, they were both delightful, fun-loving, and thoughtful individuals whose spirits live on through their pioneering ideas and the many lives they touched in positive ways.

Table of Contents

Foreword ..... **iii**

Preface ..... **vii**

Dedication ..... **ix**

List of Figures ..... **xvii**

List of Tables ..... **xxiii**

1. Introduction **1-1**
- 1.1 Background 1-1
- 1.2 The Need for Next-Generation Performance-Based Seismic Design Procedures 1-2
- 1.3 The Performance-Based Design Process 1-3
- 1.4 Scope 1-4
- 1.5 Basis 1-6
- 1.6 Limitations 1-7
- 1.7 Products 1-8
- 1.8 Organization and Content 1-10

2. Methodology Overview **2-1**
- 2.1 Performance Measures 2-1
- 2.2 Factors Affecting Performance 2-2
- 2.3 Uncertainty in Performance Assessment 2-3
- 2.4 Types of Performance Assessment 2-5
  - 2.4.1 Intensity-Based Assessments 2-5
  - 2.4.2 Scenario-Based Assessments 2-5
  - 2.4.3 Time-Based Assessments 2-5
- 2.5 The Methodology 2-6
  - 2.5.1 Assemble Building Performance Model 2-6
  - 2.5.2 Define Earthquake Hazards 2-7
  - 2.5.3 Analyze Building Response 2-8
  - 2.5.4 Develop Collapse Fragility 2-9
  - 2.5.5 Performance Calculations 2-9

3. Assemble Building Performance Model **3-1**
- 3.1 Introduction 3-1
- 3.2 Basic Building Data 3-2
- 3.3 Occupancy 3-3
- 3.4 Population Models 3-4
- 3.5 Fragility and Performance Groups 3-5
  - 3.5.1 Fragility Groups 3-6
  - 3.5.2 Performance Groups 3-9

3.5.3 Unit and Normative Quantities 3-11
3.6 Damage States 3-13
3.6.1 General 3-13
3.6.2 Damage Logic 3-14
3.6.3 Correlation 3-15
3.7 Demand Parameters 3-16
3.8 Component Fragility 3-17
3.8.1 Fragility Functions 3-17
3.8.2 Experimentally Derived Fragilities 3-19
3.8.3 Common Fragilities 3-20
3.8.4 Calculated Fragilities 3-22
3.9 Consequence Functions 3-29
3.9.1 Repair Costs 3-29
3.9.2 Repair Time 3-31
3.9.3 Unsafe Placards 3-33
3.9.4 Casualties 3-34
3.10 Fragility Specifications 3-35

4. Define Earthquake Hazards 4-1
4.1 Introduction 4-1
4.2 Building Location and Site Conditions 4-2
4.2.1 Seismic Environment and Hazard 4-2
4.2.2 Location 4-2
4.2.3 Local Soil Effects 4-2
4.3 Ground Motion Prediction Equations 4-3
4.4 Nonlinear Response-History Analysis 4-6
4.4.1 Introduction 4-6
4.4.2 Target Acceleration Response Spectra 4-7
4.4.3 Ground Motion Selection and Scaling 4-8
4.5 Simplified Analysis 4-11
4.5.1 Introduction 4-11
4.5.2 Intensity-Based Assessment 4-11
4.5.3 Scenario-Based Assessment 4-12
4.5.4 Time-Based Assessment 4-12

5. Analyze Building Response 5-1
5.1 Scope 5-1
5.2 Nonlinear Response-History Analysis 5-1
5.2.1 Introduction 5-1
5.2.2 Modeling 5-2
5.2.3 Number of Analyses 5-7
5.2.4 Floor Velocity 5-9
5.2.5 Quality Assurance 5-9
5.2.6 Uncertainty 5-10
5.3 Simplified Analysis 5-14
5.3.1 Introduction 5-14
5.3.2 Modeling 5-15
5.3.3 Analysis Procedure 5-16
5.4 Residual Drift 5-23

6. Develop Collapse Fragility 6-1
6.1 Introduction 6-1
6.2 Nonlinear Response-History Analysis 6-2

6.2.1 Introduction 6-2
6.2.2 Incremental Dynamic Analysis 6-2
6.2.3 Limited-Suite Nonlinear Analysis 6-3
6.2.4 Mathematical Models 6-4
6.3 Simplified Nonlinear Analysis 6-5
6.4 Judgment-Based Collapse Fragility 6-7
6.5 Collapse Modes 6-8

7. Calculate Performance 7-1
7.1 Introduction 7-1
7.2 Realization Initiation 7-2
7.3 Collapse Determination 7-3
7.3.1 Collapse Mode 7-4
7.3.2 Casualties 7-5
7.3.3 Repair Cost and Time 7-5
7.4 Simulation Demands 7-5
7.4.1 Simplified Analysis 7-5
7.4.2 Nonlinear Response History Analysis 7-6
7.5 Damage Calculation 7-7
7.5.1 Sequential Damage States 7-7
7.5.2 Simultaneous Damage States 7-8
7.5.3 Mutually Exclusive Damage States 7-9
7.6 Loss Calculation 7-9
7.7 Time-Based Assessments 7-11

8. Decision Making 8-1
8.1 Introduction 8-1
8.2 Code Equivalence 8-1
8.3 Scenario-Based Assessments 8-2
8.4 Time-Based Assessments 8-4
8.5 Probable Maximum Loss 8-7

Appendix A: Probability, Statistics, and Distributions A-1
A.1 Introduction A-1
A.2 Statistical Distributions A-1
A.2.1 Finite Populations and Discrete Outcomes A-1
A.2.2 Combined Probabilities A-2
A.2.3 Mass Distributions A-3
A.2.4 Continuous Distributions A-4
A.3 Common Forms of Distributions A-6
A.3.1 Normal Distributions A-6
A.3.2 Cumulative Probability Functions A-7
A.3.3 Lognormal Distributions A-8
A.4 Probabilities over Time A-11

Appendix B: Ground Shaking Hazards B-1
B.1 Scope B-1
B.2 Ground Motion Prediction Models B-1
B.3 Fault Rupture Directivity and Maximum Direction Shaking B-3
B.4 Probabilistic Seismic Hazard Assessment B-4
B.4.1 Introduction B-4

B.4.2 Probabilistic Seismic Hazard Assessment Calculations B-5
B.4.3 Inclusion of Rupture Directivity Effects B-12
B.4.4 Deaggregation of Seismic Hazard Curves and Epsilon B-13
B.4.5 Conditional Mean Spectrum and Spectral Shape B-15
B.5 Vertical Earthquake Shaking B-19
B.5.1 Introduction B-19
B.5.2 Procedure for Site Classes A, B and C B-19
B.5.3 Procedure for Site Classes D and E B-19
B.6 Soil-Foundation-Structure Interaction B-20
B.6.1 General B-20
B.6.2 Direct Soil-Foundation-Structure-Interaction Analysis B-20
B.6.3 Simplified Soil-Foundation-Structure-Interaction Analysis B-21
B.7 Alternate Procedure for Hazard Characterization for Scenario-Based Assessment Using Nonlinear Response-History Analysis B-25

Appendix C: Residual Drift C-1
C.1 Introduction C-1
C.2 Prediction of Residual Drift C-1
C.3 Model to Calculate Residual Drift C-5
C.4 Proposed Damage States for Residual Drift C-6

Appendix D: Component Fragility Specifications D-1
D.1 Provided Specifications D-1

Appendix E: Population Models E-1
E.1 Population Models E-1

Appendix F: Normative Quantities F-1
F.1 Normative Quantities F-1

Appendix G: Generation of Simulated Demands G-1
G.1 General G-1
G.2 Nonlinear Response-History Analysis G-1
G.2.1 Introduction G-1
G.2.2 Algorithm G-2
G.2.3 Sample Application of the Algorithm G-4
G.2.4 Matlab Code G-11
G.3 Simplified Analysis G-14

Appendix H: Fragility Development H-1
H.1 Introduction H-1
H.1.1 Purpose H-1
H.1.2 Fragility Function Definition H-1
H.1.3 Derivation Methods H-3
H.1.4 Documentation H-4
H.2 Fragility Parameter Derivation H-5
H.2.1 Actual Demand Data H-5
H.2.2 Bounding Demand Data H-6

H.2.3 Capable Demand Data H-9
H.2.4 Derivation H-11
H.2.5 Expert Opinion H-11
H.2.6 Updating H-12
H.3 Assessing Fragility Function Quality H-14
H.3.1 Competing Demand Parameters H-14
H.3.2 Dealing with Outliers using Pierce's Criterion H-14
H.3.3 Goodness of Fit Testing H-15
H.3.4 Fragility Functions that Cross H-17
H.3.5 Assigning a Single Quality Level to a Fragility Function H-17

Appendix I: Rugged Components I-1
I.1 Rugged Components I-1

Appendix J: Collapse Fragility Development Using Incremental Dynamic Analysis J-1
J.1 Introduction J-1
J.2 Basic Procedure J-1
J.3 Mathematical Models J-2
J.4 Ground Motion Selection and Scaling J-2
J.5 Collapse Fragility Development J-4

Appendix K: Sliding and Overturning K-1
K.1 Introduction K-1
K.2 Overturning K-1
K.3 Sliding K-4

Glossary L-1

Symbols M-1

References N-1

Project Participants O-1

List of Figures

Figure 1-1 Flow chart of the performance-based design process 1-3

Figure 2-1 Hypothetical building performance function 2-4

Figure 2-2 Flow chart of the performance assessment methodology 2-6

Figure 2-3 Loss calculation flow chart 2-10

Figure 2-4 Realization flow chart 2-10

Figure 2-5 Typical building repair fragility 2-12

Figure 2-6 Seismic hazard curve used in time-based assessments 2-13

Figure 2-7 Example time-based performance curve 2-14

Figure 3-1 Definition of floor number, story number, and story height 3-3

Figure 3-2 Plot of default variation in population (relative to expected peak population) by time of day for commercial office occupancies 3-5

Figure 3-3 Example performance groups for a three-story office building 3-10

Figure 3-4 Example family of fragility curves for special steel moment frames 3-18

Figure 3-5 Overturning of unanchored object. 3-27

Figure 3-6 Sample consequence function for cost of repair 3-31

Figure 3-7 Basic identifier information for a typical fragility specification 3-35

Figure 3-8 Fragility information for a typical fragility specification 3-36

Figure 3-9 Consequence information for a typical fragility specification 3-36

Figure 4-1 Illustration of the differences between three ground-motion prediction equations 4-5

Figure 4-2 Response spectra with different probabilities of exceedance derived from a single ground-motion prediction equation for an earthquake scenario 4-6

Figure 4-3 Example hazard curve showing selection, intensity intervals, midpoints and corresponding mean annual frequencies of exceedance 4-11

Figure 5-1 Generalized component force-deformation behaviors 5-3

Figure 5-2 Generalized force-deformation relationship of ASCE/SEI 41-06 5-3

Figure 5-3 Comparison of cyclic versus in-cycle degradation of component response 5-4

Figure 5-4 Definition of floor, story numbers and floor heights above grade 5-16

Figure 6-1 Sample Incremental Dynamic Analysis Results for a hypothetical building 6-3

Figure 6-2 Illustration of Collapse Fragility estimated using nonlinear analysis at several intensity levels 6-4

Figure 6-3 Global force-displacement relationship in SPO2IDA 6-6

Figure 6-4 Sample SPO2IDA results for the example of Figure 6-3 ... 6-7

Figure 7-1 Performance calculation flow chart 7-3

Figure 7-2 Representative collapse fragility for a hypothetical building structure 7-4

Figure 7-3 Illustration of assumed variability in demands associated with simplified analysis 7-6

Figure 7-4 Illustration of variability in demands associated with nonlinear response-history analysis 7-7

Figure 7-5 Illustration of determining sequential damage state for a performance group for a given realization 7-8

Figure 7-6 Sample repair cost loss curve 7-10

Figure 7-7 Sample repair cost deaggregation by performance group 7-11

Figure 7-8 Distribution of mean annual total repair cost 7-11

Figure 7-9 Seismic hazard curve and time-based loss calculations ... 7-12

Figure 7-10 Example cumulative probability loss distributions for a hypothetical building at four ground motion intensities .. 7-14

Figure 8-1 Hypothetical Peformance Function for building illustrating calculation of the mean value of a performance measure 8-3

Figure 8-2 Hypothetical annual performance function for building illustrating calculation of mean annual value of performance measure 8-4

Figure A-1 Probability mass function indicating the probability of the number of "heads-up" outcomes in four successive coin tosses A-4

Figure A-2 Probability density function of possible concrete cylinder strengths for a hypothetical mix design A-5

Figure A-3 Calculation of probability that a member of the population will have a value within a defined range A-5

Figure A-4 Probability density function plots of normal distributions with a mean value of 1.0 and coefficients of variation of 0.1, 0.25, and 0.5 ..... A-7

Figure A-5 Cumulative probability plots of normal distributions with a mean value of 1.0 and coefficients of variation of 0.1, 0.25, and 0.5 ..... A-8

Figure A-6 Probability density function plots of lognormal distributions with a median value of 1.0 and dispersions of 0.1, 0.25, and 0.5 ..... A-9

Figure A-7 Cumulative probability plots of lognormal distributions with a median value of 1.0 and dispersions of 0.1, 0.25, and 0.5 ..... A-9

Figure B-1 Site-to-source distance definitions B-3

Figure B-2 Fault rupture directivity parameters B-4

Figure B-3 Steps in probabilistic seismic hazard assessment B-5

Figure B-4 Source zone geometries B-6

Figure B-5 Variations in site-to-source distance for three source zone geometries B-7

Figure B-6 Conditional probability calculation B-9

Figure B-7 Seismic hazard curve for Berkeley, California B-11

Figure B-8 Sample de-aggregation of a hazard curve B-14

Figure B-9 Sample geometric-mean response spectra for negative-, zero- and positive-ε record sets with each record in the sets scaled to a) $S_a(0.8s) = 0.5\ g$ and b) $S_a(0.3s) = 0.5\ g$ B-15

Figure B-10 UHS for a 2% probability of exceedance in 50 years and original and scaled CMS for a rock site in San Francisco B-18

Figure B-11 Conditional Spectrum for Sa(1s) with 2% probability of exceedance in 50 years for a rock site in San Francisco B-18

Figure B-12 Analysis for soil foundation structure interaction B-21

Figure B-13 Reductions in spectral demand due to kinematic interaction..... B-24

Figure B-14 Calculation of spectral accelerations given a lognormal distribution B-26

Figure C-1 Idealized incremental dynamic analysis presenting transient and residual story drifts. C-2

Figure C-2 Idealized response characteristics for elastic-plastic (EP), general inelastic (GI) and self-centering (SC) systems C-3

Figure C-3 Idealized model to estimate residual drift from story drift. C-5

Figure E-1 Plot of default variation in population (relative to expected peak population) by time of day for: (a) Commercial office; and (b) Education – elementary school occupancies..... E-3

Figure E-2 Plot of default variation in population (relative to expected peak population) by time of day for: (a) Education – middle school; and (b) Education – high school occupancies..... E-3

Figure E-3 Plot of default variation in population (relative to expected peak population) by time of day for: (a) Healthcare; and (b) Hospitality occupancies E-4

Figure E-4 Plot of default variation in population (relative to expected peak population) by time of day for: (a) Multi-Unit Residential; and (b) Research occupancies E-4

Figure E-5 Plot of default variation in population (relative to expected peak population) by time of day for: (a) Retail; and (b) Warehouse occupancies..... E-5

Figure G-1 Generation of simulated vectors of correlated demand parameters. G-4

Figure G-2 Relationships between demand parameters G-5

Figure G-3 Joint probability density functions G-5

Figure H-1 Illustration of (a) fragility function, and (b) evaluating individual damage-state probabilities H-2

Figure H-2 Example form for soliciting expert opinion on component fragility H-13

List of Tables

Table 1-1 Structural Systems and Components for which Fragility and Consequence Data have been Provided 1-5

Table 1-2 Building Occupancies for which Nonstructural Component Data and Population Models have been Provided 1-5

Table 3-1 Recommended Default Peak Population Models..... 3-5

Table 3-2 Example Fragility Groups for 2-story Moment-resisting Steel Frame Office Structure 3-7

Table 3-3 Normative Quantities for Healthcare Occupancy 3-12

Table 3-4 Default Material Property Dispersions, β_M, for Structural Materials..... 3-24

Table 3-5 Default Values of Uncertainty, β_C, Associated with Construction Quality..... 3-24

Table 5-1 Default Descriptions and Values for β_c 5-12

Table 5-2 Default Descriptions and Values for β_q 5-13

Table 5-3 Default Dispersions Ground Motion Variability 5-14

Table 5-4 Correction Factors for Story Drift Ratio, Floor Velocity and Floor Acceleration for 2 to 9 Story Buildings..... 5-20

Table 5-5 Correction Factors for Story Drift Ratio, Floor Velocity and Floor Acceleration for 10 to 15 Story Buildings..... 5-20

Table 5-6 Default Dispersions for Record-to-Record Variability and Modeling Uncertainty 5-22

Table 6-1 Sample Probabilities that the Specified Portion of a Building Will be Involved in the Collapse..... 6-9

Table A-1 Values of the Gaussian Variate in Normal Distributions for Common Probabilities A-7

Table B-1 Ground Motion Prediction Models B-2

Table B-2 Values of η_i for Generating a Distribution of $S_{ai}(T)$ B-26

Table C-1 Damage States for Residual Story Drifts C-7

Table C-2 Sample Transient Story Drift, Δ / h, Associated with the Residual Story Drift Damage States of Table C-1 ..... C-8

Table D-1 List of Provided Fragility Specifications D-3

Table E-1 Default Variation in Population by Time of Day and Day of Week for Different Occupancies E-1

Table E-2 Default Variation in Population by Month, Relative to Expected Peak Population for Different Occupancies E-5

Table F-1 Normative Quantities for Commercial Office Occupancies F-2

Table F-2 Normative Quantities for Education (K-12) Occupancies F-4

Table F-3 Normative Quantities for Healthcare Occupancies F-6

Table F-4 Normative Quantities for Hospitality Occupancies F-8

Table F-5 Normative Quantities for Multi-Unit Residential Occupancies F-10

Table F-6 Normative Quantities for Research Occupancies F-12

Table F-7 Normative Quantities for Retail Occupancies F-14

Table F-8 Normative Quantities for Warehouse Occupancies F-16

Table G-1 Matrix of Analytically Determined Demand Parameters, *X* G-5

Table G-2 Natural Logarithm of Demand Parameters, $\mathbf{Y}$ G-6

Table G-3 Covariance Matrix of Demand Parameters Y, $\boldsymbol{\Sigma}_{\mathbf{YY}}$ G-6

Table G-4 Matrix $\mathbf{D}_{\mathbf{Y}}$ for the Sample Problem G-7

Table G-5 Matrix $\mathbf{L}_{\mathbf{Y}}$ for the Sample Problem G-7

Table G-6 Matrix of Simulated Demand Parameters (first 10 vectors of 10000) G-8

Table G-7 Ratio of Simulated to Original Logarithmic Means G-8

Table G-8 Ratio of Entries in Simulated and Original $\boldsymbol{\Sigma}_{\mathbf{YY}}$ Matrices G-8

Table G-9 Natural Logarithm of Demand Parameters, $\mathbf{Y}'$ G-9

Table G-10 Covariance Matrix of Demand Parameters $\mathbf{Y}'$, $\boldsymbol{\Sigma}_{\mathbf{Y'Y'}}$ G-9

Table G-11 Matrix $\mathbf{D}_{Y'}$ for the Sample Problem G-9

Table G-12 Matrix $\mathbf{D}_{pp}$ for the Sample Problem G-10

Table G-13 Matrix $\mathbf{L}_{Y'}$ for the Sample Problem G-10

Table G-14 Matrix $\mathbf{L}_{np}$ for the Sample Problem G-10

Table G-15 Matrix of Simulated Demand Parameters (first 10 vectors of 10000) G11

Table G-16 Ratio of Simulated to Original Logarithmic Means..... G-11

Table G-17 Ratio Of Entries in Simulated and Original $\mathbf{\Sigma}_{Y'Y'}$ Matrices G-11

Table H-1 Values of z H-10

Table H-2 Parameters for Applying Peirce's Criterion H-16

Table H-3 Critical Values for the Lilliefors Test H-17

Table H-4 Fragility Function Quality Level H-18

Table I-1 List of Rugged Components I-2

Chapter 1
Introduction

This report describes a general methodology and recommended procedures to assess the probable seismic performance of individual buildings based on their unique site, structural, nonstructural, and occupancy characteristics. Performance is measured in terms of the probability of incurring casualties, repair and replacement costs, repair time, and unsafe placarding. The methodology and procedures are applicable to new or existing buildings, and can be used to: (1) assess the probable performance of a building; (2) design new buildings to be capable of providing desired performance; or (3) design upgrades for existing buildings to improve their performance.

In this methodology, performance is measured in terms of the probability of incurring casualties, repair and replacement costs, repair time, and unsafe placarding.

Performance can be assessed for a particular earthquake scenario or intensity, or considering all earthquakes that could occur, and the likelihood of each, over a specified time period.

The general methodology and procedures can be applied to seismic performance assessments of any building type, regardless of age, construction or occupancy. However, implementation requires basic data on the vulnerability of structural and nonstructural components to damage (fragility), as well as estimates of potential casualties, repair costs, and repair times (consequences) associated with this damage.

1.1 Background

Performance-based seismic design is a formal process for design of new buildings, or seismic upgrade of existing buildings, with the specific intent that the buildings will be able to achieve specified performance objectives in future earthquakes. Performance objectives relate to expectations regarding the amount of damage a building may experience and the consequences of that damage.

The typical building design process is not performance-based. In the typical process, design professionals select, proportion, and detail building components to satisfy prescriptive criteria contained within the building code. Many of these criteria were developed with the intent to provide some level of seismic performance; however, the intended performance is often not obvious, and the actual ability of the resulting designs to provide the intended performance is seldom evaluated or understood.

Performance-based design in its current form originated in the 1990s. Present-generation performance-based design is based on the Federal Emergency Management Agency (FEMA) report, FEMA 273, *NEHRP*

Guidelines for the Seismic Rehabilitation of Buildings (FEMA, 1997), which addressed seismic strengthening of existing buildings, and outlined initial concepts of performance levels related to damageability and varying levels of seismic hazard. Its successor documents, FEMA 356, *Prestandard and Commentary for the Seismic Rehabilitation of Buildings* (FEMA, 2000), and the American Society of Civil Engineer (ASCE) Standard ASCE/SEI 41-06, *Seismic Rehabilitation of Existing Buildings* (ASCE, 2007) define current practice for performance-based seismic design in the United States.

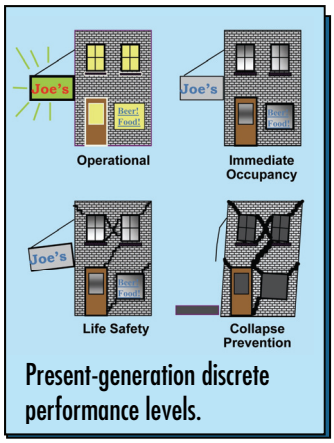

Present-generation discrete performance levels.

In present-generation procedures, performance is expressed in terms of a series of discrete performance levels identified as Operational, Immediate Occupancy, Life Safety, and Collapse Prevention. These performance levels are applied to both structural and nonstructural components, and are assessed at a specified seismic hazard level. Although they established a vocabulary and provided a means by which engineers could quantify and communicate seismic performance to clients and other stakeholders, implementation of present-generation procedures in practice uncovered certain limitations and identified enhancements that were needed.

1.2 The Need for Next-Generation Performance-Based Seismic Design Procedures

Limitations in present-generation procedures included: (1) questions regarding the accuracy and reliability of available analytical procedures in predicting actual building response; (2) questions regarding the level of conservatism present in acceptance criteria; (3) the inability to reliably and economically apply performance-based procedures to the design of new buildings; and (4) the need for alternative ways of communicating performance to stakeholders that is more meaningful and useful for decision-making purposes.

In order to fulfill the promise of performance-based engineering, FEMA began planning the development of next-generation procedures to address the above limitations. The FEMA 349 *Action Plan for Performance Based Seismic Design* was prepared by the Earthquake Engineering Research Institute (EERI) in 2000. Using this plan as a basis, FEMA initiated the first of a series of projects with the Applied Technology Council in 2001, which would become known as the ATC-58/ATC-58-1 Projects.

The first step in this work was to update the FEMA 349 *Action Plan*, which resulted in the publication of FEMA 445, *Next-Generation, Performance-Based Seismic Design Guidelines, Program Plan for New and Existing Buildings* (FEMA, 2006). As outlined in FEMA 445, the objectives of the ATC-58/ATC-58-1 Projects were to:

- Develop a framework for performance assessment that properly accounts for, and adequately communicates to stakeholders, limitations in our ability to accurately predict response, and uncertainty in the level of earthquake hazard;
- Revise the discrete performance levels defined in present-generation procedures to create new performance measures that better relate to the decision-making needs of stakeholders;
- Create procedures for estimating these new performance measures for both new and existing buildings;
- Expand current nonstructural procedures to explicitly assess the damageability and post-earthquake condition of nonstructural components and systems; and
- Modify current structural procedures to assess performance based on global response parameters, so that the response of individual components does not unnecessarily control the prediction of overall structural performance.

1.3 The Performance-Based Design Process

In the performance-based design process, design professionals, owners, and other stakeholders jointly identify the desired building performance characteristics at the outset of the project. As design decisions are made, the effects of these decisions are evaluated to verify that the final building design is capable of achieving the desired performance. Figure 1-1 presents a flow chart for the performance-based design process.

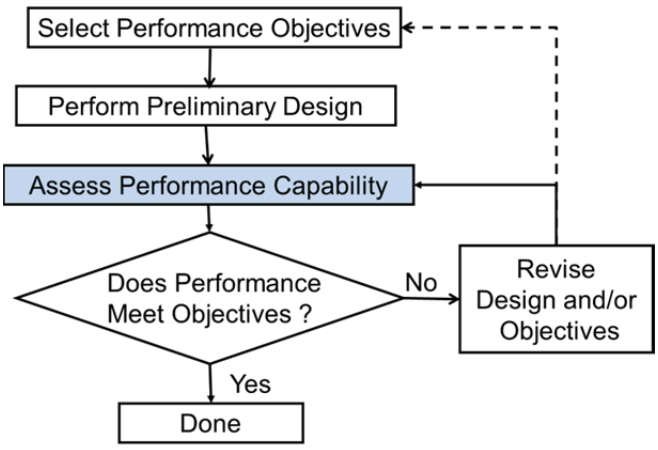

Figure 1-1 Flow chart of the performance-based design process

The process initiates with selection of one or more performance objectives. Each performance objective is a statement of the acceptable risk of incurring

damage or loss for identified earthquake hazards. Decision-makers including owners, developers, design professionals, and building officials will typically participate in the selection of performance objectives. This process may consider the needs and desires of a wider group of stakeholders, including prospective tenants, lenders, insurers, and the general public. The needs and opinions of others can have an indirect impact on the design of a building, but these groups generally do not have an opportunity to directly participate in the design process.

Once performance objectives are selected, designs must be developed and the performance capability determined. As a minimum, basic building design information includes: (1) the location and characteristics of the site; (2) building size, configuration, and occupancy; (3) structural system type, configuration, strength, and stiffness; and (4) type, location, and character of finishes and nonstructural systems. For new buildings, preliminary design information must be developed to a sufficient level of detail to allow determination of performance capability. In the case of existing buildings, basic building design information is already defined, but preliminary retrofit measures must be developed (if necessary).

Performance assessment is the process used to determine the performance capability of a given building design. In performance assessment, engineers conduct structural analyses to predict building response to earthquake hazards, assess the likely amount of damage, and determine the probable consequences of that damage.

Following performance assessment, engineers compare the predicted performance capability with the desired performance objectives. If the assessed performance is equal to or better than the stated performance objectives, the design is adequate. If the assessed performance does not meet the performance objectives, the design must be revised or the performance objectives altered, in an iterative process, until the assessed performance and the objectives match.

1.4 Scope

Performance assessment is the primary focus of the general methodology and recommended procedures contained herein.

Seismic performance assessment (shaded box in Figure 1-1), is the portion of the performance-based design process that is the primary focus of the methodology and recommended procedures contained herein. Seismic performance is expressed in terms of potential casualties, repair and replacement costs, repair time, and unsafe placarding resulting from earthquake damage. The methodology can be expanded to consider additional consequences such as environmental impacts, and could be

adapted to assess performance for other hazards and extreme loading conditions, but such enhancements have not been included in the current version of the methodology.

Table 1-1 lists the structural systems for which fragility and consequence data have been provided. Table 1-2 lists the building occupancies for which information on common nonstructural components, contents, normative quantities, and population models have been provided.

Performance assessment for other structural systems and occupancies is possible. Data necessary for such assessments can be developed using procedures included as part of the methodology.

Table 1-1 Structural Systems and Components for which Fragility and Consequence Data have been Provided

Material	System	Comments
Concrete	Beam-column frames	Conventionally reinforced, with or without modern seismic-resistant detailing
	Shear walls	Shear or flexurally controlled, with or without seismic-resistant detailing
	Slab-column systems	Post-tensioned or conventionally reinforced, with or without slab shear reinforcement
Masonry	Walls	Special or ordinary reinforced masonry walls, controlled by shear or flexure
Steel	Moment frames	Fully restrained, pre- or post-Northridge, Special, Intermediate, and Ordinary detailing
	Concentrically braced frames	"X"-braced, chevron-braced, single diagonals, special, ordinary, or nonconforming detailing
	Eccentrically braced frames	Flexure or shear links at mid-span of link beam
	Light-framed walls	Structural panel sheathing, steel panel sheathing or diagonal strap bracing
	Conventional floor framing	Concrete-filled metal deck, untopped steel deck, or wood sheathing
Timber	Light-framed walls	Structural panel sheathing, gypsum board sheathing, cement plaster sheathing, let-in bracing, and with or without hold downs

Table 1-2 Building Occupancies for which Nonstructural Component Data and Population Models have been Provided

Occupancy	Comment
Commercial Office	None
Education (K-12)	Typical elementary, middle school, high school classrooms
Healthcare	General in-patient hospitals, medical equipment excluded
Hospitality	Hotels and motels
Multi-Unit Residential	Also applicable to single-family detached housing
Research	Special purpose laboratory equipment excluded
Retail	Shopping malls and department stores
Warehouse	Inventory excluded

Performance assessment for other structural systems and occupancies is possible. Data necessary for such assessments can be developed using procedures included as part of the methodology. These procedures involve the use of laboratory testing of individual components and assemblies, analytical evaluation, statistical information on the actual performance in past earthquakes, or expert judgment. It is envisioned that future research and product development activities will include the development of additional fragility and consequence data for systems and components not provided herein.

1.5 Basis

Performance measures serving as the basis for the assessment process were developed with input from an expanded group of stakeholders including commercial real estate investors, insurers, lenders, attorneys, and architects. This group was assembled at an invitational workshop held in Chicago, Illinois (ATC, 2002), and the collective opinions of this group were used to select the concepts of casualties, direct and indirect economic losses, and downtime, which have been used to express and measure consequences in the methodology.

The technical basis of the methodology is the framework for performance-based earthquake engineering developed by researchers at the Pacific Earthquake Engineering Research Center (PEER) during the period 1997–2010.

The technical basis of the methodology is the framework for performance-based earthquake engineering developed by researchers at the Pacific Earthquake Engineering Research Center (PEER) during the period 1997–2010. The PEER framework (Moehle and Deierlein, 2004) applies the total probability theorem to predict earthquake consequences in terms of the probability of incurring particular values of performance measures or outcomes including casualties, repair costs, and downtime. Under the PEER framework, earthquake performance is computed as a multi-level integral of the probability of incurring earthquake effects of differing intensity, over all intensities; the probability of experiencing building response (drifts, accelerations, component demands) of different levels, given an intensity of shaking; the probability of incurring damage of different types, given building response; and the probability of incurring specific consequences given that the damage occurs.

Closed form solution of the integral is difficult, even for simple structural systems, and is problematic for systems as complex as real buildings. In 2004, an application of this framework was developed utilizing a modified Monte Carlo approach to implement the integration using inferred statistical distributions of building response obtained from limited suites of analyses. This application, described in Yang et al. (2009), is the basis of the

performance assessment calculations and accumulation of consequences as implemented in the methodology.

1.6 Limitations

This report and its companion products provide a general methodology and recommended procedures to assess the probable performance of individual buildings subjected to future earthquakes. Specifically, the methodology assesses the likelihood that building structural and nonstructural components and systems will be damaged by earthquake shaking, and estimates the potential casualties, repair and replacement costs, repair time, and unsafe placarding that could occur as a result of such damage.

Performance assessment in this methodology is limited to consideration of consequences that occur within the occupied building envelope. However, earthquake shaking can also result in loss of power, water, and sewage due to damage at offsite utilities, and earthquake casualties can occur outside the building envelope when damage generates debris that falls onto surrounding property. Earthquake shaking can also cause other significant building impacts, both inside and outside the building envelope, including initiation of fires and release of hazardous materials. Construction of models to assess these additional impacts are possible, but beyond the scope of this effort.

Performance assessment in this methodology is limited to consideration of consequences that occur within the occupied building envelope.

Earthquake effects also include ground fault rupture, landslide, liquefaction, lateral spreading, seiches, and tsunamis. Although the general methodology could be used to assess impacts from these effects, such assessment is beyond the scope of the current methodology and its companion products. Engineers conducting seismic performance assessments should, as a minimum, qualitatively evaluate these other effects, and, if judged significant, report appropriate limitations to decision-makers.

Assessment of building performance in future earthquakes inherently entails significant uncertainty. The methodology and procedures presented herein use state-of-the-art techniques to express the effect of these uncertainties on probable building performance. Extensive quality assurance measures were undertaken to validate the basic methodology and products as part of the developmental process. These included:

Assessment of building performance in future earthquakes inherently entails significant uncertainty.

- Widespread presentation of the basic methodology and procedures at project workshops, technical conferences and symposia, and publication of interim products in refereed journals.
- Independent review of the underlying theory and methods by a validation and verification team consisting of expert researchers and practitioners with specialized knowledge in seismic performance and probabilistic

theory, and implementation of a series of quality control recommendations to incrementally validate the procedures during development.

- Independent review of the component fragility development process by teams of engineers and researchers familiar with structural and nonstructural seismic performance, as well as detailed review of the quality of data and consistent application of procedures by a panel of independent experts knowledgeable in structural reliability theory and seismic performance.
- Independent review of the consequence development process, and detailed review of the quality of the resulting cost and repair data, by a knowledgeable construction cost estimator.
- Independent review of the calculation algorithms embedded in supporting electronic materials by designated members of the project development team.
- A series of benchmark performance evaluations conducted on representative building types ranging from low-rise masonry, to mid-rise concrete and steel, to high-rise structures, by teams of researchers and graduate students that implemented the methodology under a variety of assumptions to explore the rationality of results.

Regardless of quality assurance measures undertaken, it is possible that the performance of individual buildings in actual earthquakes may be better or worse than indicated by assessments conducted in accordance with this methodology. Further, the accuracy of any performance assessment will depend on data and calculations generated by individual users. No warranty is expressed or implied regarding the accuracy, completeness, or usefulness of performance assessments made using any information, product, or procedure comprising the methodology, and users of this methodology assume all liability arising from such use.

1.7 Products

Products include this volume, an implementation guide, supporting electronic materials, and background technical information.

The resulting products have been organized into a series of volumes consisting of a description of the basic methodology, guidance on implementation, supporting electronic materials, and background technical information. These include:

Seismic Performance Assessment of Buildings, Volume 1 – Methodology. Volume 1 is the fundamental product of this work. It presents the general methodology for conducting seismic performance assessments, and describes

the necessary information and recommended procedures for developing basic building information, response quantities, fragilities, and consequence data used as inputs to the methodology.

Seismic Performance Assessment of Buildings, Volume 2 – Implementation Guide. Volume 2 provides guidance on implementing a seismic performance assessment using the methodology, and includes specific instructions on how to assemble and prepare the input data necessary for the *Performance Assessment Calculation Tool* (PACT). It contains a user's manual and examples illustrating the performance assessment process, including selected calculation and data generation procedures.

Seismic Performance Assessment of Buildings, Volume 3 – Supporting Electronic Materials. Volume 3 consists of a series of electronic products assembled to assist engineers in conducting seismic performance assessments. The following tools and supporting data are included:

- *Performance Assessment Calculation Tool* (PACT) – PACT is an electronic calculation tool, and repository of fragility and consequence data, that performs the probabilistic calculations and accumulation of losses described in the methodology. It includes a series of utilities used to specify building properties and update or modify fragility and consequence information in the referenced databases.
- Fragility Database – The Fragility Database is an Excel workbook that is used to manage and maintain all provided fragility and consequence data outside of PACT, and update database information within PACT.
- Fragility Specification – The Fragility Specification is a PDF file displaying the contents of the fragility database. Each fragility specification contains fragility and consequence data for the component of interest, in a one-page format. Damage states are illustrated with photos of representative damage, when available.
- Normative Quantity Estimation Tool – The Normative Quantity Estimation Tool is an Excel workbook designed to assist in estimating the type and quantity of nonstructural components typically present in buildings of a given occupancy and size.
- Consequence Estimation Tools – The Structural and Nonstructural Consequence Estimation Tools are Excel workbooks that provide the basis for provided consequence data, and can be used to assist in estimating consequences for custom fragility specifications.
- *Static Pushover to Incremental Dynamic Analysis* (SPO2IDA) – SPO2IDA is an Excel workbook application that was originally

developed by Vamvatsikos and Cornell (2006). This tool uses empirical relationships from a large database of incremental dynamic analysis results to convert static pushover curves into probability distributions for building collapse as function of ground motion intensity.

- Collapse Fragility Tool – The Collapse Fragility Tool is an Excel workbook application that fits a lognormal distribution to collapse statistics obtained from a series of nonlinear dynamic analysis at different ground motion intensity levels.

Seismic Performance Assessment of Buildings, Volume 4 – Technical Background Documents. Volume 4 contains a series of reports documenting the technical background and source information for key aspects of the methodology, including simplified analysis procedures, fragility development procedures, estimation of peak floor velocity, scaling of ground motion records, residual drift computations, downtime modeling, building population modeling, validation and verification studies, and results from beta testing efforts.

Seismic Performance Assessment of Buildings, Volume 5 – Structural Fragility Background Documents. Volume 5 contains a series of reports documenting the technical background and source data for structural fragilities provided with the methodology.

Seismic Performance Assessment of Buildings, Volume 6 – Nonstructural Fragility Background Documents. Volume 6 contains a series of reports documenting the technical background and source data for nonstructural fragilities provided with the methodology.

1.8 Organization and Content

This volume presents the overall seismic performance assessment methodology and describes the recommended procedures for developing information used as inputs to the methodology. Readers are cautioned to become thoroughly acquainted with the information contained in this volume before attempting to conduct building performance assessments using PACT.

Chapter 2 presents an overview of the methodology including discussion of the specific performance measures used and the types of assessments that can be conducted.

Chapter 3 describes the development of building-specific performance models by assembling all the data necessary to assess building performance.

Chapter 4 describes methods to characterize seismic hazards for use in the methodology.

Chapter 5 provides guidelines for two alternative methods of structural analysis used to predict building response.

Chapter 6 presents alternative procedures for characterizing susceptibility to collapse as a function of ground shaking intensity.

Chapter 7 describes the calculation procedures used to determine the probable damage that a building will sustain and the consequences of damage in terms of casualties, repair costs, repair time, unsafe placarding, and other potential impacts.

Chapter 8 illustrates some methods for using data obtained from performance assessment in the project planning and design process.

Appendix A provides a basic tutorial on probability and statistics and the types of probability distributions used to represent uncertainty in the methodology.

Appendix B provides detailed information on seismic hazard evaluation and ground motion prediction models.

Appendix C presents information on residual drift estimation and discusses limitations on the ability of structural analysis to reliably predict residual drift.

Appendix D lists the types of structural and nonstructural components and contents for which fragility and consequence data are provided in the accompanying databases.

Appendix E presents recommended building population models for common building occupancies.

Appendix F provides a tabulation of the typical quantities of nonstructural components and contents found in buildings of differing occupancy or use.

Appendix G describes the algorithm used to generate multiple vectors of simulated demands as part of the performance assessment process.

Appendix H provides guidelines for development of fragility functions for individual building components for use in performance assessment.

Appendix I tabulates a list of building components that are generally considered rugged and therefore, insignificant to the performance assessment process.

Appendix J describes the incremental dynamic analysis procedure to determine a building's susceptibility to collapse.

Appendix K describes the basis used to determine vulnerability of unanchored components to sliding or overturning.

Chapter 2
Methodology Overview

2.1 Performance Measures

This methodology expresses performance in terms that are meaningful to decision-makers.

A performance measure is a means of quantifying the consequences of a building's earthquake response in terms that are meaningful to decision-makers. Historically, decision-makers have used a number of different performance measures.

Since the publication of ASCE/SEI 31-03, *Seismic Evaluation of Existing Buildings* (ASCE, 2003), and ASCE/SEI 41-06, *Seismic Rehabilitation of Existing Buildings* (ASCE, 2007), building officials and engineers have commonly used a series of standard discrete performance levels, termed *Operational*, *Immediate Occupancy*, *Life Safety* and *Collapse Prevention*, to characterize expected building performance. These performance levels are defined by acceptable ranges of strength and deformation demand on structural and nonstructural components, with implicit qualitative relationships to probable levels of damage, casualties, post-earthquake occupancy and repair consequences.

Many financial institutions including lenders, investment funds, and insurers use Probable Maximum Loss (PML), Scenario Expected Loss (SEL), and Scenario Upper Bound loss (SUL) as preferred performance measures. These performance measures are quantitative statements of probable building repair cost, typically expressed as a percentage of building replacement value. Some building owners, developers, and tenants have also relied on these performance measures to quantify seismic performance.

This seismic performance assessment methodology expresses performance as the probable damage and resulting consequences of a building's response to earthquake shaking. The consequences, or impacts, resulting from earthquake damage considered in this methodology are:

- **Casualties.** Loss of life, or serious injury requiring hospitalization, occurring within the building envelope.
- **Repair cost.** the cost, in present dollars, necessary to restore a building to its pre-earthquake condition, or in the case of total loss, to replace the building with a new structure of similar construction;

- **Repair time.** The time, in weeks, necessary to repair a damaged building to its pre-earthquake condition; and
- **Unsafe placarding.** A post-earthquake inspection rating that deems a building, or portion of a building, damaged to the point that entry, use, or occupancy poses immediate risk to safety.

For a number of reasons, it is impossible to predict any of these impacts precisely. Therefore, the methodology expresses performance in the form of probable impacts, considering inherent uncertainties. This approach for measuring performance has several advantages. These performance measures (casualties, repair costs, repair time, and unsafe placarding) are more meaningful to decision-makers and more directly useful in the decision-making process than the standard discrete performance levels that have traditionally been used. Also, PML, SEL and SUL measures of performance can be directly and objectively derived using a probabilistic approach. Finally, uncertainty in performance assessment is explicitly acknowledged, and if properly used, can assist design professionals in avoiding liability associated with the possible perception of warranties associated with performance assessments and performance-based designs.

2.2 Factors Affecting Performance

The amount of earthquake damage that a building experiences, and the consequences of that damage in terms of casualties, repair costs, repair time, and unsafe placarding, depends on a number of factors. These include:

- the intensity of ground shaking and other earthquake effects experienced by the building;
- the building's response to ground shaking and other earthquake effects, and the resulting force, deformation, acceleration, and velocity demands experienced by the structural and nonstructural components, contents, and occupants;
- the vulnerability of the building components, systems, and contents to damage;
- the number of people, and the type, location, and amount of contents present within the building envelope when the earthquake occurs;
- the interpretation of visible evidence of damage by inspectors performing post-earthquake safety investigations;
- the specific details and methods of construction used in performing repairs; and

- the availability of labor and materials, the efficiency of individual contractors, and their desire for profit in the post-disaster construction environment.

This methodology explicitly evaluates each of these factors in the development of building performance functions. However, there are other important factors associated with the actions people take in response to a future earthquake that the methodology does not consider because they are inherently unpredictable. Factors that are not considered, but can affect the magnitude of earthquake impacts, include:

- the speed and quality of care given to injured individuals;
- the speed with which building owners engage design professionals, obtain necessary approvals, and engage contractors to implement repair actions; and
- a decision to conduct repairs while a building remains occupied, or to vacate a building and allow full access to construction crews.

2.3 Uncertainty in Performance Assessment

Each factor affecting seismic performance has significant uncertainty in our ability to know or predict specific values. The fault that will produce the next earthquake, where along the fault the rupture will initiate, or the magnitude of shaking that will occur are not known with any certainty. Nor is there a complete understanding of the subsurface conditions that seismic waves must pass through between the fault rupture and the building site. As a result, the intensity, spectral shape, or wave form of future earthquake shaking cannot be precisely predicted.

Each factor affecting seismic performance has significant uncertainty in our ability to know or predict specific values.

The cumulative result of these and other uncertainties is that it is not possible to precisely assess the seismic performance of a building.

While the ability to develop analytical models of structures is constantly improving, models are still imprecise. Typical structural models are based on assumptions of material strength, cross-section geometry, and details of construction. Damping is estimated using rules of thumb. The effects of soil-structure interaction, elements designed to resist only gravity loads, and nonstructural components are commonly neglected. Therefore, response predictions are inherently uncertain, and it is not known whether structural analyses are under-predicting or over-predicting the actual response of a building.

Using response quantities from structural analyses, and the observed behavior of similar elements tested in the laboratory or in past earthquakes, it is possible to predict the levels of damage that structural and nonstructural components might sustain. However, components tested in a laboratory may

not be identical to components in an actual building, and the forces and deformations imposed in the laboratory may not be identical to those predicted in the structural analysis or experienced in an actual earthquake. Therefore, predictions of the type and amount of damage are likely to be somewhat inaccurate.

Similarly, it is not possible to predict the exact time of day, or day of the week, when an earthquake will occur, the number of people that will be within the building at that time, and the type or amount of contents and furnishings that are present. Once damage is predicted, it is difficult to know the exact repair techniques that will be specified to repair damaged components, or how efficiently the repairs will be constructed.

The cumulative result of these and other uncertainties is that it is not possible to precisely assess the seismic performance of a building, whether that performance is measured by casualties, repair costs, repair time, or other impacts. It is, however, possible to express performance measures in the form of performance functions. Performance functions are statistical distributions that indicate the probability that losses of a specified or smaller magnitude will be incurred as a result of future earthquakes. Appendix A provides a brief introduction to such distributions.

Performance functions express the probability of incurring earthquake impacts. This methodology provides a means of determining performance functions.

Figure 2-1 presents a performance function for a hypothetical building and given intensity of shaking. In the figure, the horizontal axis represents the size of the impact (e.g., number of casualties, repair cost, or weeks of construction time) while the vertical axis indicates the probability that the actual impact will be equal to or less than this value.

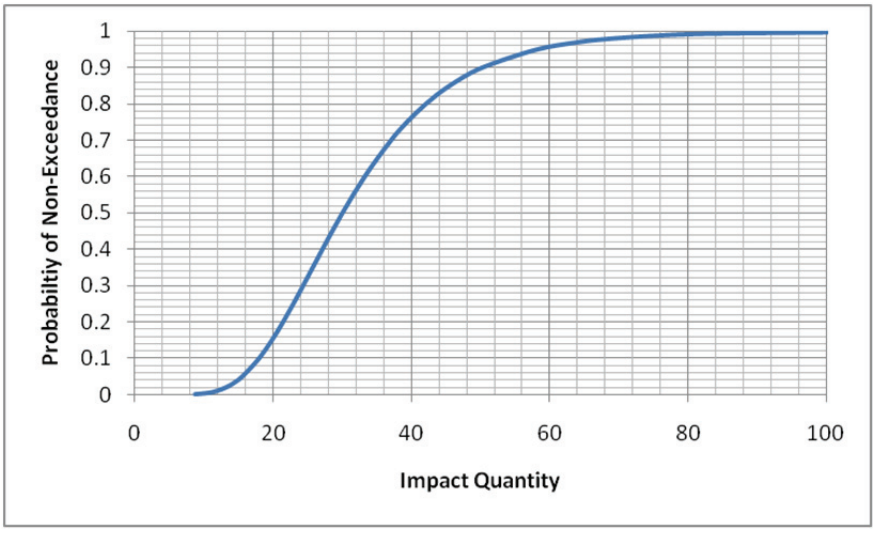

Figure 2-1 Hypothetical building performance function.

The methodology and procedures presented in this report describe a means to determine these performance functions.

2.4 Types of Performance Assessment

This methodology can be used to develop three different types of performance assessment: intensity-based, scenario-based, and time-based assessments.

2.4.1 Intensity-Based Assessments

Intensity-based assessments evaluate a building's probable performance assuming that it is subjected to a specified earthquake shaking intensity. Shaking intensity is defined by 5% damped, elastic acceleration response spectra. This type of assessment can be used to assess a building's performance in the event of design earthquake shaking consistent with a building code response spectrum, or to assess performance for shaking intensity represented by any other response spectrum**.**

Intensity-based assessments evaluate performance for a user-selected acceleration response spectrum.

2.4.2 Scenario-Based Assessments

Scenario-based assessments evaluate a building's probable performance assuming that it is subjected to a specified earthquake scenario consisting of a specific magnitude earthquake occurring at a specific location relative to the building site. Scenario assessments may be useful for buildings located close to one or more known active faults. This type of assessment can be used to assess a building's performance in the event of a historic earthquake on these faults is repeated, or a future projected earthquake occurs.

Scenario-based assessments evaluate performance for a user-defined earthquake magnitude and site distance.

Scenario-based assessments are very similar to intensity-based assessments except that they consider uncertainty in the intensity of earthquake shaking, given that the scenario occurs. Results of scenario-based assessments are performance functions similar to Figure 2-1, except that the probable performance is conditioned on the occurrence of the scenario earthquake rather than a specific shaking intensity.

2.4.3 Time-Based Assessments

Time-based assessments evaluate a building's probable performance over a specified period of time (e.g., 1-year, 30-years, or 50-years) considering all the earthquakes that could occur in that time period, and the probability of occurrence associated with each earthquake. Time-based assessments consider uncertainty in the magnitude and location of future earthquakes as well as the intensity of motion resulting from these earthquakes.

Time-based assessments evaluate performance over time, considering all possible earthquakes and their probability of occurrence.

The time period for time-based assessment depends on the interests and needs of the decision-maker. Assessments based on a single year are useful for cost-benefit evaluations used to decide between alternative performance criteria. Assessments over longer periods of time are useful for other decision-making purposes. Chapter 8 provides additional information on decision-making uses for performance assessment results.

Time-based assessments provide performance functions that are similar to Figure 2-1, except that the vertical axis of the function expresses the frequency that an impact magnitude (e.g., number of casualties, repair costs, or weeks of construction time) will be exceeded in a period of time, typically one year. Once the performance function for a one-year time period has been developed, it can easily be converted to other time periods (see Appendix A).

2.5 The Methodology

This Section provides a brief introduction to the steps that comprise the performance assessment methodology. Figure 2-2 is a flow chart that illustrates the relationship between these steps and identifies the chapters providing more detailed discussion of each step.

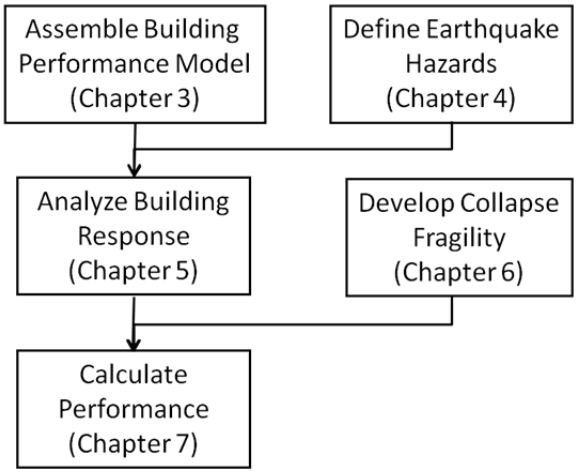

Figure 2-2 Flow chart of the performance assessment methodology.

2.5.1 Assemble Building Performance Model

The building performance model defines the building assets at risk and their exposure to seismic hazards.

The building performance model is an organized collection of data used to define the building assets at risk and their exposure to seismic hazards. This data includes definition of:

- Structural components and assemblies that can be damaged by the building's response to earthquake shaking. Data must include information on the types of damage these components can sustain, the structural demands that cause this damage, and the consequences of this

damage in terms of risk to human life, repair methods, repairs costs, repair time, and post-earthquake building occupancy due to unsafe placarding.

- Nonstructural systems, components, and contents that do not provide significant resistance to gravity or earthquake loading but can be damaged by the building's response to earthquake shaking. Data must include the location of these components in the building, their vulnerability to damage of different types, and the consequences of this damage, in terms of generation of life-threatening debris, repair methods, repairs costs, repair time, and influence on post-earthquake building occupancy.
- Occupancy, including the distribution of people within the building envelope and the variability of this distribution over time of day and day of the year.

Vulnerable building components are categorized into fragility groups and performance groups. Fragility groups are sets of similar components that have the same potential damage characteristics in terms of vulnerability and consequences. Performance groups are subsets of a fragility group that will experience the same earthquake demands in response to earthquake shaking. Chapter 3 introduces the fragility specification used to define damage and consequence data, and describes the categorization of components into fragility groups and performance groups.

2.5.2 Define Earthquake Hazards

This methodology addresses earthquake performance associated with ground shaking.

Earthquake effects include ground shaking, ground fault rupture, liquefaction, lateral spreading, land sliding, and tsunami inundation. Each of these effects can occur with different levels of severity, or intensity, ranging from imperceptible to highly damaging. Earthquake hazard is a quantification of the intensity of these effects and the site-specific probability that effects of a given intensity will be experienced. Presently, this methodology addresses consequences associated with building damage due to earthquake ground shaking. It can, however, be extended to include consideration of other earthquake effects.

Ground shaking hazards are specified in different ways, depending on the type of assessment and the type of structural analysis used to quantify earthquake response. These are described below and in more detail in Chapter 4.

Intensity-based assessments consider building response to a single acceleration response spectrum. Depending on the type of structural analysis

used, ground shaking intensity is characterized in the form of discrete spectral response accelerations extracted from a reference spectrum, or suites of ground motion records that have been selected and scaled for consistency with this spectrum.

Scenario-based assessments consider building response to an earthquake scenario at a defined magnitude and distance from the site. Shaking hazards are represented by a median acceleration response spectrum and period-dependent dispersions obtained from the ground motion prediction model or attenuation relationship used to derive the spectrum. Analyses are conducted using discrete spectral response accelerations derived from the median spectrum, or ground motion records that are scaled to be consistent with the distribution of possible spectra.

For time-based assessments, ground shaking hazards are characterized by a series of mean seismic hazard curves at different structural periods. Each hazard curve is a plot of the mean annual frequency of exceedance of spectral response acceleration of different amplitudes at a particular structural period. These hazard curves are used to derive a series of acceleration response spectra to represent a range of ground shaking intensities across a meaningful range of exceedance probabilities and structural response. Analyses are conducted using discrete spectral response accelerations derived from spectra at each intensity, or ground motion records that are scaled to be consistent with these spectra.

2.5.3 Analyze Building Response

Structural analysis is used to predict a building's response to earthquake shaking in the form response quantities, or demands, that can be associated with structural and nonstructural damage. Demands typically include peak values of story drift ratio in each of two orthogonal directions, floor velocity, floor acceleration, and residual drift ratio. It is possible to use other demand parameters, such as individual component strength or deformation demands, if a building includes components for which damage is better correlated with such parameters.

Building response can be simulated using nonlinear response-history analysis or a simplified procedure based on equivalent lateral forces.

Chapter 5 describes the use of two analysis procedures for response prediction: (1) nonlinear response-history analysis; and (2) simplified analysis based on equivalent lateral force methods. Nonlinear response-history analysis can be used for any structure, and can provide values for any demand parameter that is simulated in the model. Simplified analysis is valid for regular, low-rise, and mid-rise structures, with limited nonlinear response, and will provide values for peak transient floor acceleration, floor velocity

and story drift ratio only. Also included in Chapter 5 is an approximate procedure to estimate residual drift ratio from peak story drift ratio and yield story drift ratio.

2.5.4 Develop Collapse Fragility

Most casualties occur as a result of partial or total building collapse. To assess potential casualties, it is necessary to define the probability of incurring structural collapse as a function of ground motion intensity and the modes of structural collapse that are possible (e.g., single-story, multi-story, full-floor, or partial floor). These are represented in the form of collapse fragility functions. Chapter 6 describes means of establishing collapse fragilities using a combination of structural analysis and judgment.

Most casualties occur as a result of building collapse.

2.5.5 Performance Calculations

To account for the many uncertainties inherent in factors affecting seismic performance, the methodology uses a Monte Carlo procedure to perform loss calculations. This is a highly repetitive process in which building performance is calculated for each of a large number (hundreds to thousands) of realizations. Each realization represents one possible performance outcome for the building, considering a single combination of possible values of each uncertain factor.

Each realization represents one possible performance outcome. The methodology uses Monte Carlo analysis to explore uncertainty in the possible range of outcomes.

Chapter 7 describes the calculation procedures used to assess probable performance with explicit consideration of uncertainty. As a matter of practicality, these calculations are best performed using a computer, and a companion *Performance Assessment Calculation Tool* (PACT) is provided along with the methodology.

Intensity-based and Scenario-based Assessments

For intensity and scenario-based assessments, the performance calculations are nearly identical. Figure 2-3 and Figure 2-4 provide flow charts illustrating the performance calculation process for intensity- and scenario-based assessments. For each type of assessment, the possible consequences of building performance (casualties, repair costs, repair time, unsafe placarding) are calculated many times to explore the effect of uncertainty on the predicted outcome. Each repetition is termed a realization, and represents one possible performance outcome for the particular earthquake intensity or scenario being analyzed. The calculation is repeated for R realizations, where R might be on the order of 1000 or more. These outcomes are ordered from smallest to largest and a performance curve (similar to Figure 2-1) is constructed as a plot of the percentage of realizations with outcomes that exceed each value. Key steps in the process are described below.

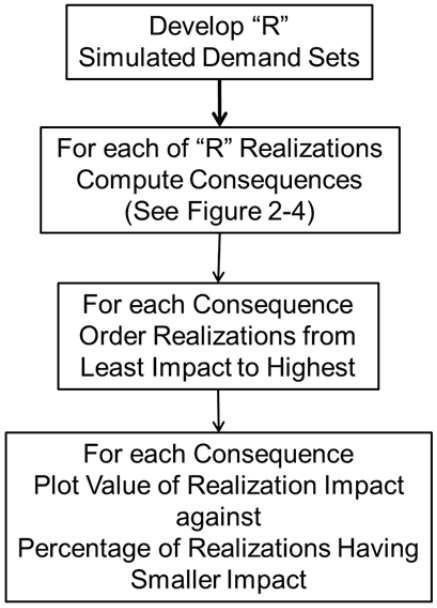

Figure 2-3 Loss calculation flow chart.

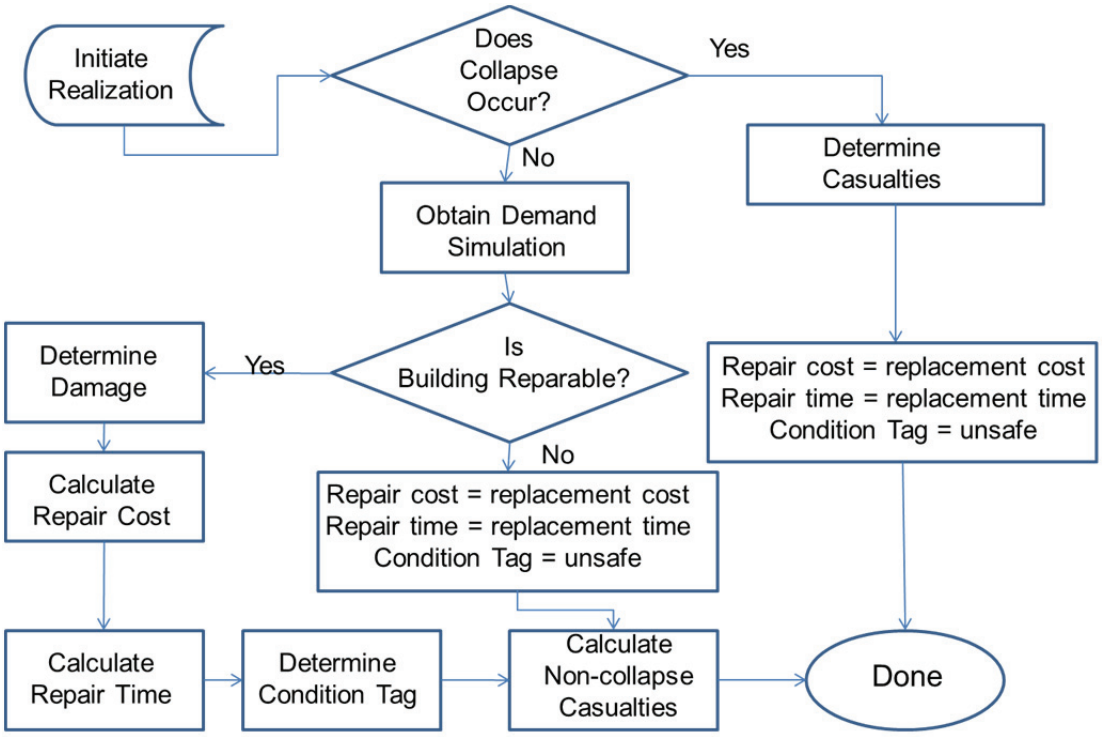

Figure 2-4 Realization flow chart.

Simulate vectors of structural response. The process initiates with determining how many realizations, *R*, will be evaluated. Results from the structural analysis are used to generate a series of *R* simulated demand sets. The simulated demand sets reflect the correlation between the various demand parameters predicted in the analyses, as well as uncertainties

inherent in demand predictions, and in the case of scenario-based assessment, uncertainties associated with the spectral content of the ground motion. Appendix G describes the mathematical procedure for deriving the set of simulated demands in the form of a matrix [m x R], where each column in the matrix is one simulated set of demands. For each of the R realizations, a unique set of possible earthquake performance outcomes is determined using the steps in Figure 2-4.

Determine if collapse occurs. The first step in each realization is to determine if the building has collapsed using a collapse fragility function. By entering the collapse fragility function with the intensity of ground motion for the realization, the probability of collapse is determined. A random number generator is used to select an integer between 1 and 100. If the selected number is less than or equal to the probability of collapse indicated by the collapse fragility, then the building is deemed to have collapsed. When collapse occurs, the building is assumed to be a total loss and the repair cost and repair time are taken as the building replacement values, including consideration of demolition and removal of debris from the site.

Calculate building collapse casualties. To calculate casualties, it is necessary to determine a time of day and day of the week at which the realization occurs, again using a random number generator. Using a time-dependent population model appropriate for the building occupancy, along with the randomly generated day and time, the number of people present in the area of collapse is determined. Using casualty functions appropriate to the type of construction, percentages of the population at risk in the collapsed area will be classified as serious injuries or fatalities.

The methodology does not predict casualties that could occur outside the building envelope resulting from debris falling on adjacent properties. To predict such casualties it would be necessary to have a population model for the area immediately surrounding the building. For tall buildings, exterior population models would need to extend to a considerable distance from the building, and would potentially include many other buildings. Although the logic could be extended to include such modeling, implementation is beyond the scope of the current methodology.

Obtain Simulated Demands. If the random number generation and collapse fragility suggest the building does not collapse in a given realization, it is necessary to associate one of the previously generated sets of simulated demand vectors with the realization. Each simulated demand set in the

[*m* x *R*] matrix of simulated demands is associated with one realization in which collapse does not occur.

Determine Damage. If the building has not collapsed in a given realization, the set of simulated demands is used to determine a damage state for each vulnerable component in the building. Damage states are assigned on a performance group basis. Each performance group has an associated series of damage states and fragility functions that describe the probability that components within the group will be damaged to a given level. Random number generation is used to determine which damage state, if any, is experienced by each component in the realization.

Calculate Consequences. Using damage states and associated consequence functions, the magnitude of consequences associated with the damage in each component is determined. In calculating consequences, consideration is given to the volume of repairs that must be made, as well as uncertainties associated with repair technique, contractor efficiency, and pricing.

Determine if building is reparable. The simulated set of demands for each realization includes an estimate of the residual drift ratio at each level of the building. Following computation of damage and consequences in each performance group, the maximum residual drift ratio is used, together with a building repair fragility, to determine if repair is practicable. A typical building repair fragility is a lognormal distribution with a median value of 1% residual drift ratio, and a dispersion of 0.3, as shown in Figure 2-5.

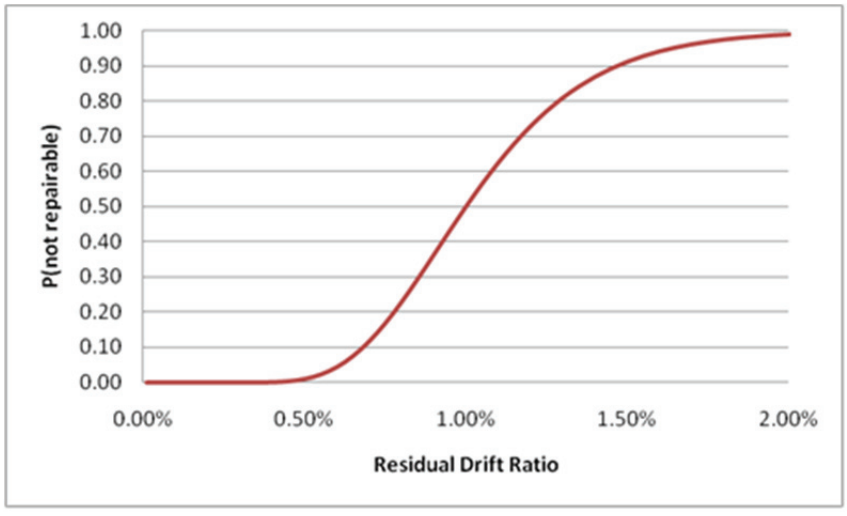

Figure 2-5 Typical building repair fragility.

At a residual drift ratio of 0.5%, this fragility indicates that building repair is a virtual certainty. At a residual drift ratio of 2.0%, however, it is a virtual certainty that the building will not be repaired. As with collapse

determination, a random number generator is used to select an integer between 1 and 100. If this number is equal to or less than the probability of irreparability, as determined by the building repair fragility at the residual drift ratio for the realization, then the building is deemed irreparable for that realization. If irreparable, repair cost and repair time are taken as the building replacement values, including consideration of demolition and removal of debris from the site. The building is also assumed to be assigned an unsafe placard.

Time-based Assessments

In time-based assessments, a more complex process is used. Time-based assessments compute the probable building performance outcomes considering all possible intensities of shaking that might be experienced by the building within the specified time period, and weights the outcome from each intensity by the probability that such shaking will occur.

To perform this calculation, it is necessary to obtain a hazard curve for the site that provides the annual frequency of exceedance of ground motions with different intensities. Figure 2-6 is one such curve for a hypothetical site, showing the annual frequency of exceedance of a ground motion intensity parameter, e. Chapter 4 and Appendix B provide detailed information on how to develop hazard curves.

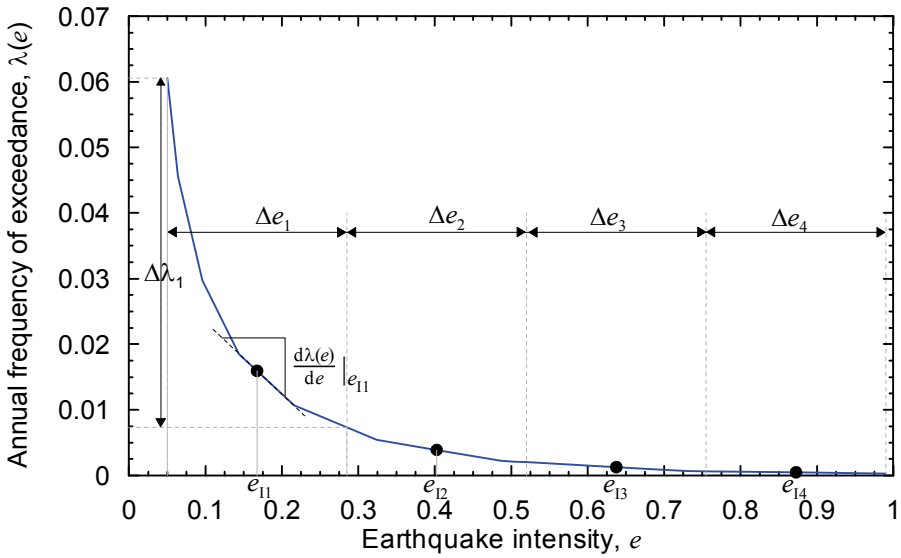

Figure 2-6 Seismic hazard curve used in time-based assessments.

The hazard curve is divided into a series of intervals, illustrated as the intervals Δe_i in the figure. The annual frequency of occurrence of ground motion having an intensity that falls within each interval is equal to the difference between the annual frequencies of exceedance of the ground

shaking intensities at each end of the interval. For each intensity interval on the hazard curve, an intensity-based assessment is performed for the intensity at the mid-point of the interval. The resulting performance outcomes are then weighted by the annual frequency of occurrence of intensities within that interval. The results of these assessments are summed over all of the intervals to form a time-based performance curve, as shown in Figure 2-7.

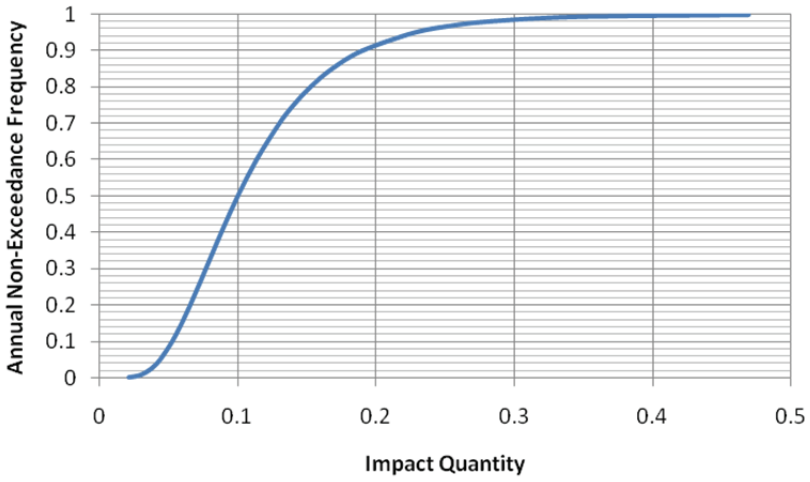

Figure 2-7 Example time-based performance curve.

Chapter 3

Assemble Building Performance Model

3.1 Introduction

This chapter describes the process for assembling the building performance model. The building performance model is an organized collection of data necessary to define building assets that are vulnerable to the effects of earthquake shaking. This includes definition of:

The building performance model is an organized collection of all data necessary to define the building assets at risk.

- Basic building data including building size, replacement cost, and replacement time.
- Occupancy, including the distribution of people within the building envelope and the variability of this distribution over time, and the type and quantity of nonstructural components and contents present in the building.
- Vulnerable structural elements and assemblies in sufficient detail to quantify their location within the building and the demands they will experience during response to earthquake shaking; their vulnerability to damage caused by earthquake-induced deformations and forces; and the consequences of this damage, in terms of collapse potential and generation of life-threatening debris, necessary repair actions, and influence on post-earthquake building occupancy due to unsafe placarding.
- Vulnerable nonstructural systems, components and contents in sufficient detail to quantify their location within the building and the demands they will experience during response to earthquake shaking; their method of installation as it effects their vulnerability to damage; and the consequences of this damage, in terms of generation of falling hazards and life-threatening debris, necessary repair actions, and influence on post-earthquake building occupancy.

The building performance model includes population models, fragility groups, and performance groups. Components and assemblies that provide measurable resistance to deformation are classified as structural whether or not they are intended to be part of the gravity or seismic-force-resisting systems. Elements and components that are vulnerable to damage are

assigned a fragility within the building performance model. Elements and components that are not vulnerable to damage are not included in the performance model, although the costs associated with these elements must be considered in the total building replacement cost. Appendix I provides a list of component types that, in most cases, can be considered rugged (i.e., not vulnerable to damage related to earthquake shaking).

3.2 Basic Building Data

Basic building data includes:

- the number of stories, story height, floor area at each level; and
- the total replacement cost, core and shell replacement cost, replacement time, and total loss threshold.

Total replacement cost is used to compute the cost associated with damage that renders the building irreparable. This can occur when the total cost of repairing all of the damaged components and systems exceeds a threshold value, discussed below; when residual story drift ratio exceeds a level that permits practical repair; or when collapse occurs. In order to replace a damaged building it is necessary to demolish the damaged structure and remove it from the site. Therefore, the replacement cost not only includes the cost to replace the building "in-kind" but also the cost to demolish the damage building and clear the site of debris. Demolition and site clearance can increase the building-only replacement cost up to 20% to 30%.

Total loss threshold allows use of a pre-set repair cost at which owners are likely to elect to replace the building. Past studies suggest a value of 40% of replacement cost as a reasonable threshold for many buildings.

The total loss threshold is used to set a pre-determined cap on the level of repair effort, at which a building is likely to be replaced rather than repaired. Past studies suggest that many owners elect to replace buildings rather than repair them, when the projected repair cost exceeds about 40% of replacement cost. Of course many factors, including the building's age, its occupancy, status as a historic landmark, the economic health of its surrounding neighborhood and individual profitability affect these decisions. The Federal Emergency Management Agency uses a threshold value of 50% when contemplating whether a damaged structure should be replaced or repaired.

Figure 3-1 defines the system used to number floors and stories. A floor level and the story immediately above it are always assigned the same number. Building roofs are designated Floor N+1, where N is the total number of stories. In the figure, Floor 1 is assigned to the ground floor, assuming that basement construction and contents are rugged. If significant damage and loss can occur in basement levels, floor numbering initiates at the lowest vulnerable level.

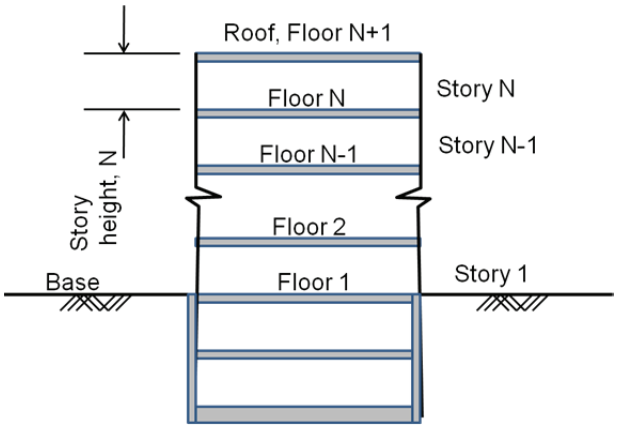

Figure 3-1 Definition of floor number, story number, and story height.

3.3 Occupancy

Occupancy categorizes the primary use of a building or portion of a building

As used in this methodology, occupancy categorizes a building's primary use or uses. The primary functions for occupancy are to:

- establish a population model (i.e., the number of people present at different times of the day and different days of the year for use in assessing potential casualties); and
- define, on an approximate basis without the need for performing a building-specific inventory, the type and quantities of nonstructural building components and contents.

Population and inventory model information is provided for eight occupancies. Users can modify this information or develop their own models.

Population models and inventories are provided for the following occupancies:

- Commercial office
- Education (K-12) – typical elementary, middle school, and high school classrooms
- Healthcare – general in-patient hospitals; medical equipment excluded
- Hospitality – hotels and motels
- Multi-Unit Residential – also applicable to single-family detached housing
- Research – special purpose laboratory equipment excluded
- Retail – shopping malls and department stores
- Warehouse – inventory excluded

It is possible to create building-specific inventories of nonstructural components for occupancies not covered by this list. Adaptive use of the

provided occupancies, however, greatly facilitates building performance modeling.

3.4 Population Models

Population models define the number of people present in the building by occupancy, time of day, day of the week and month of the year

Building population models define the number of people present per 1,000 square feet of building floor space. Population models include definition of the peak population, that is, the number of people likely to be present at times of peak occupancy, and the fraction of this peak population likely to be present at other times, characterized by:

- time of day;
- day of the week (weekday or weekend); and
- month of the year.

Variation by month is used to characterize the effect of holidays. Rather than designating specific days as holidays, the methodology pro-rates weekday populations by the number of holidays per month divided by the total number of weekdays, on average, for that month.

Population models also include an Equivalent Continuous Occupancy. This is a time-weighted average population. It represents the number of persons present, on average, throughout the year, considering all times of day and days of the week. Using the peak population, it is possible to generate a "worst-case" estimate of casualties, assuming that earthquakes occur during times of peak occupancy. This may be useful for evaluating casualties in buildings that have large assemblies when occupied, but which are occupied only occasionally such as large auditoriums, sports venues and similar buildings. Using the equivalent continuous occupancy population enables rapid estimate of mean casualties, considering that earthquake occurrence is random in time. However, using equivalent continuous occupancy does reduce the apparent dispersion in casualty estimates. Using the point-in-time model of population, it is possible to develop a better understanding of the uncertainty in casualties associated with time of earthquake occurrence. However, it is necessary to perform a large number of realizations, on the order of several thousand, to do this in a meaningful way and this can consume significant processing time.

Population patterns vary with time of day (e.g., hours of operations, lunch time fluctuations), and day of week (weekdays vs. weekends). Table 3-1 presents peak populations for each of the provided occupancies. Table 3-1 also indicates the time of day during which these peak populations are expected to occur. Figure 3-2 shows an example of the time-dependent

variation of population, as a percentage of peak population, for commercial office occupancies. Appendix E contains similar data for the other provided occupancies.

Table 3-1 Recommended Default Peak Population Models

Occupancy Description	Peak Population Model (Occupants per 1000 sq. ft.)	Peak Population Model - Time of Day
Commercial office	4.0	Daytime (3 pm)
Education (K-12): Elementary Schools	14.0	Daytime
Education (K-12): Middle Schools	14.0	Daytime
Education (K-12): High Schools	12.0	Daytime
Healthcare	5.0	Daytime (3 pm)
Hospitality	2.5	Nighttime (3 am)
Multi-unit residential	3.1	Nighttime (3 am)
Research Laboratories	3.0	Daytime (3 pm)
Retail	6.0	Daytime (5 pm)
Warehouse	1.0	Daytime (3 pm)

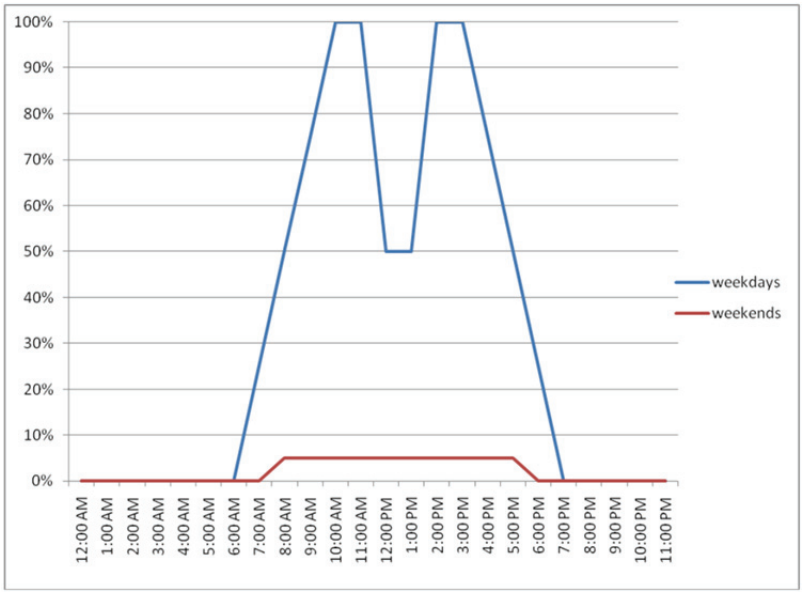

Figure 3-2 Plot of default variation in population (relative to expected peak population) by time of day for commercial office occupancies.

3.5 Fragility and Performance Groups

All vulnerable structural components, nonstructural components, and contents are categorized by fragility groups and performance groups. The

quantity of nonstructural components and contents in a building and within each performance group can be determined by conducting a building-specific inventory. Alternatively quantities can be assigned based on typical quantities found in buildings of similar occupancy and size.

3.5.1 Fragility Groups

A fragility group is a collection of similar component or systems, each of which has the same damageability and consequences of damage. A performance group is that subset of a fragility group subject to the same demands.

A fragility group is a collection of components, or assemblies, all of which have similar:

- construction characteristics, including details of construction, details of manufacture and installation techniques;
- potential modes of damage;
- probability of incurring these damage modes, when subjected to earthquake demands
- potential consequences resulting from the damage, assuming that the components are installed in the same locations.

A fragility group can comprise individual components (e.g., pendant light fixtures), or assemblies of components (e.g., interior fixed partitions including the metal studs, gypsum board sheathing and wall coverings).

Components and assemblies that are of similar, but not identical construction may have to be assigned to different fragility groups, in order to correctly characterize their susceptibility to damage and the consequences of such damage. For example, fixed interior partitions throughout a building could all be assigned to the same fragility group, if they are all of the same height, all installed in the same manner and all have the same wall coverings. However, if some of the interior partitions are installed with slip tracks at their top to permit the walls to move independently of the structure under seismic shaking and some are provided with fixed top connections, each type would have to be assigned to a different fragility group, as each would have different susceptibility to damage under the same earthquake shaking. Similarly, partitions with ceramic tile finish would cost more to repair than walls that are simply painted and should be assigned to different fragility groups than walls without such finish.

Fragility groups are identified using a classification system based on the Uniformat II system described in NISTIR 6389.

Each fragility group is identified by a unique classification number based on recommendations contained in NISTIR 6389, *UNIFORMAT II Elemental Classification for Building Specifications, Cost Estimating and Cost Analysis* (NIST, 1999). Fragility classification numbers take the form: A1234.567. The first letter in the classification system indicates the overall component category and is one of the following:

- A–Substructure
- B–Shell
- C –Interiors
- D–Services
- E – Equipment and furnishings
- F – Special construction and demolition

The first two numbers provides the next categorization. For instance, B10 represents superstructure components while B20 represents exterior enclosures. The next two numbers identify a unique component. For example, the classification for reinforced concrete shear walls is B1044. The identifiers after the decimal provide variations of the basic component and are used to identify different configurations, conditions of installation, material quantities, demand levels, and other attributes.

Table 3-2 lists a sample set of fragility groups that could be used in the performance model for a 2-story, steel frame office building. The table includes a NISTIR fragility classification number, a description of the covered component, and the predictive demand parameter used to assess damage.

Table 3-2 Example Fragility Groups for 2-story Moment-resisting Steel Frame Office Structure

Fragility Classification Number	Description	Demand Parameter
B1035.011	Structural Steel Special Moment Frame	Story drift ratio parallel to frame
B2020.001	Glazing	Story drift ratio parallel to wall
D3031.000	Mechanical Equipment	Floor acceleration
D1014.010	Hydraulic Elevators	Peak ground acceleration
C1011.001	Interior Partitions	Story drift ratio parallel to wall
C3032.001	Suspended Ceiling	Floor acceleration
E2022.010	Bookcases & File Cabinets	Floor acceleration
E2022.020	Desktop Equipment	Floor acceleration

The fragility groups listed in Table 3-2 are at an elementary level. Each of these fragility groups will typically include a number of sub-groups assigned as necessary to identify slight differences in the damageability or consequences for the components. For example, the fragility group D3031.000 “Mechanical Equipment” could have a number of sub-groups, including D3031.011 “Chillers installed with seismic anchorage” and D3031.012 “Chillers installed without seismic anchorage”.

Appendix D contains a summary of provided fragility groups, categorized by general system type and NISTIR fragility classification number. Complete fragility information including potential damage states, the relationship between demand and damage, and the consequences of damage are contained in an electronic database referenced by the companion *Performance Assessment Calculation Tool* (PACT).

User-defined fragility groups can be developed to suit the needs of a specific building. When a new fragility group is created, or an existing fragility group is modified, a new NISTIR fragility classification number must be assigned to the new group. The following logic is recommended for establishing fragility groups, when the provided fragility groups are not adequate to define the assets at risk in a particular building:

1. **Identify the components that are likely to suffer damage and contribute to potential losses.** These are components that both can be damaged and will have significant impact on building performance if they are damaged. Components that are inherently rugged and not subject to significant damage for credible levels of demand need not be considered. For example, in a steel frame building, floor beams that are not part of the building's seismic force resisting system will not typically be damaged by earthquake shaking and generally need not be considered. Also, some nonstructural components (e.g., toilet fixtures) can often be neglected as they are inherently rugged and generally not damaged by earthquake shaking. Appendix I provides a listing of components typically considered rugged.

   Some components may not be damaged by earthquake shaking, but can be affected by damage or required repairs for other components. For example, a conduit embedded in an interior partition, by itself is inherently rugged. However, if the partition is sufficiently damaged to require complete replacement, it will be necessary to replace the conduit, even though the conduit was not damaged. In this case, the wall, and not the conduit, would be assigned to the fragility group. The fact that the wall contains the conduit, however, is acknowledged in determining the consequences of wall damage. Similarly, if a fire sprinkler line breaks, the resulting water spray would damage carpets and furnishing below it that are otherwise rugged. As with the conduit embedded in the wall, it is not be necessary to define fragility groups for the carpet and other rugged items, but rather, to account for their potential damage as part of the consequences of sprinkler system failure.

2. **Group components into logical sets considering normal design and construction process and specification sections**. Interior partitions is a fragility group common to many buildings. Partitions are constructed out of a series of individual components including cold-formed steel framing, gypsum wallboard, fasteners, drywall tape, plaster, and paint. Since these items have both a design and construction relationship and tend to be damaged as an assembly, they should be included as a common assembly in a single fragility group. Despite the fact that these subcomponents are grouped together as an assembly, it is important to recognize that if the design or construction of one is changed, for example, the manner in which the studs attach to the floors above and below, this change will likely affect the damageability of the entire assembly. Similarly, repair of damage for one component is likely to involve others in the group.

3. **Group components into fragility groups such that all components in the group are damaged by a single demand parameter.** The probability that any building component (or collection) of components will be damaged must be tied to a single demand parameter such as story drift ratio, floor acceleration, floor velocity, or plastic rotation. Damage to all fragility group components is assumed to be dependent on the same type of demand, for example floor acceleration, for all possible damage states. However, not all fragility group components need actually experience the same value of demand. For example, the partitions at a building's third story can be assigned to the same fragility group as those on the second story even though the demands (story drift ratio) will likely be different in the two stories.

4. Group components into fragility groups such that fragilities, damage states and consequence functions are logical for monitoring and repair. All components placed in a single fragility group should have similar damage states and similar consequences of damage. Interior partitions and exterior cladding should be placed in different fragility groups because the damage states for each will likely be different—they will be damaged at different levels of drift—and the consequences of the damage to interior partitions are different than the consequences of damage to exterior cladding. These damage characteristics are categorized in the form of fragility functions, as discussed in Section 3.8.

3.5.2 Performance Groups

Performance groups are a further sub-categorization of fragility groups. A performance group is that set of fragility group members that are subject to

the same earthquake demands (e.g., story drift, floor acceleration or velocity in a particular direction at a particular floor level).

Performance groups are a sub-categorization of fragility groups; all members of a performance group are subject to the same earthquake demands

Figure 3-3 illustrates the concept of performance groups for a three-story reinforced concrete office structure. As depicted in the figure, most performance groups are organized by story (1st through 3rd) and direction (N-S and E-W) since their predictive demand parameter is story drift parallel ratio to their orientation. For instance, the 1st story N-S shear walls comprise one performance group, while the 2nd story N-S shear walls comprise a different performance group even though they are from the same fragility group: concrete shear walls (B1044.011). Similar performance groups are used for curtain walls and glazing.

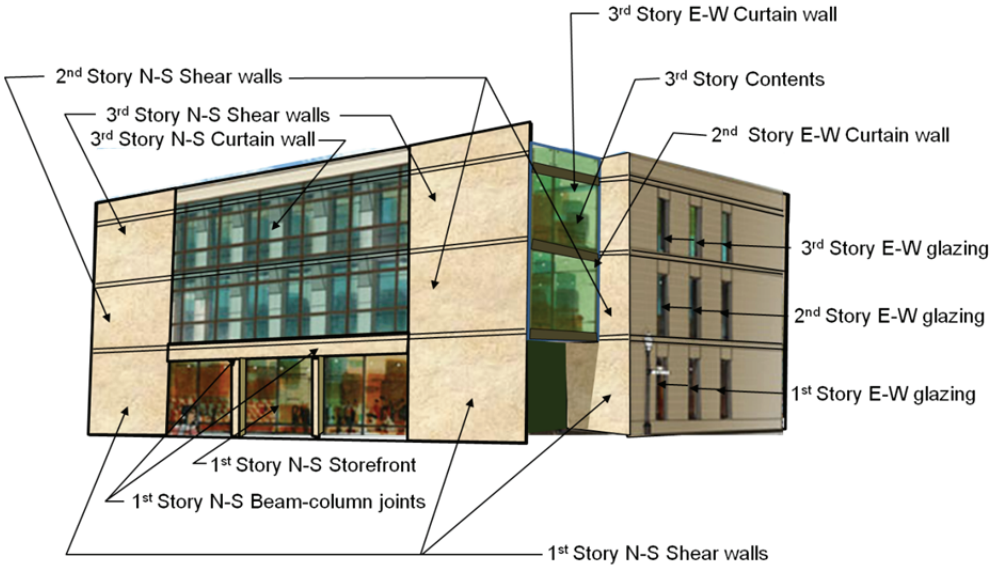

Figure 3-3 Example performance groups for a three-story office building.

Contents, however, are assigned to performance groups independent of direction since the predictive demand parameter for fragility groups associated with contents is floor acceleration. Contents at each of the 1st, 2nd and 3rd stories would each be assigned to their own unique performance groups since the floor accelerations vary by level. Other performance groups whose damage is associated with floor acceleration include ceiling systems, sprinklers and mechanical equipment.

For acceleration-sensitive components, it is important to differentiate between the level at which demands are imparted to the component, and the level at which impacts will occur if the component experiences damage. Suspended components, such as ceilings, fire suppression sprinklers, and pendant light fixtures, experience acceleration demands from the level they are suspended from, but if they fail, will cause consequences in the level

below. In this methodology, such suspended system components are assigned to the floor that is impacted by their failure. Special flags are used to identify that such components are associated with demands obtained for the floor or roof level at the top of the story.

3.5.3 Unit and Normative Quantities

Standard units of measure and normative quantities are associated with typical fragility groups on an occupancy basis, to assist in the development of the building inventory

It is necessary to identify the quantity of components in each performance group in meaningful units of measure. This methodology uses units of measure that are amenable to computation of damage in a logical manner that relates to damageability and the consequences of this damage. For example, large distinct components like elevators, air handlers, and beam-column moment connections are measured in individual units (or "each"). However, many other components have other units. For example, low aspect ratio shear walls (aspect ratios less than 1-to-1) are measured in units of H x H panels because damage in these walls often can be segregated into panels of this size. Sprinkler piping is measured in units of thousands of linear feet because historically, when leaks have occurred in these systems, a leak rate of 1 per 1,000 feet is common. The units of measure for particular fragility groups are defined in the fragility specification form, described in Section 3.10. A complete listing of the units of measure for common fragility groups is contained in the companion electronic data base product.

The quantity of components present within a performance group is described by the number of units of measure present. Thus, for an office building, the 4^{th} floor, east-west interior partitions performance group might have 20 – 100-ft-long units, indicating the presence of a total of 2,000 linear feet of partition wall. Quantities of components in a particular building can be obtained either by performing building-specific inventories, using drawings or on-site surveys, or by using typical (normative quantities) for given occupancies, factored by building size measures.

While the quantity of nonstructural components can be established from a building's design drawings (architectural, mechanical, electrical and plumbing), this level of detail is not typically known until late in the design process and also is subject to change over the years.

Databases of normative quantities are available that define the quantity of nonstructural components and contents in buildings of typical occupancies. Normative quantities provide a reasonable estimate of the quantity of components and contents likely to be present on a 1,000 square foot basis and simplify the process of performance model assembly.

Appendix F provides a tabulation of normative quantities for the occupancies provided with the methodology. Normative quantities are based on a detailed analysis of approximately 3,000 buildings across typical occupancies. This broad range of input permits normative quantity estimates at the 10th, 50th, and 90th percentile levels. These percentile levels are provided to enable consideration of the differences found in individual buildings. Table 3-3 shows an example of the normative quantity information provided for healthcare occupancies, including 10th, 50th, and 90th percentile quantities.

Table 3-3 Normative Quantities for Healthcare Occupancies

Normative Quantity Type	Unit of Measurement	10-Percentile Quantity	50-Percentile Quantity	90-Percentile Quantity
Cladding				
Windows or Glazing Area	100 SF per 1 gsf	4.0E-04	1.4E-03	3.1E-03
Interior Partition Length	100 LF per 1 gsf	7.5E-04	1.1E-03	1.4E-03
Ceilings				
Ceiling - Lay in tile percentage	%	N/A	80%	N/A
Ceiling - Gypsum board percentage	%	N/A	8%	N/A
Ceiling - Exposed percentage	%	N/A	8%	N/A
Ceiling - Other (high end) percentage	%	N/A	4%	N/A
Elevators	EA per 1 gsf	1.2E-05	2.8E-05	9.8E-05
Plumbing				
Cold Domestic Water Piping - 2 ½ inch diameter or smaller	1,000 LF per 1 gsf	8.0E-05	1.1E-04	1.3E-04
Gas supply piping	1,000 LF per 1 gsf	5.0E-06	1.0E-05	1.5E-05
HVAC				
Chiller capacity	TN per 1 gsf	2.9E-03	3.3E-03	3.7E-03
Boiler capacity	BTU per 1 gsf	40.000	50.000	65.000
Air Handling Units	CFM per 1 gsf	0.800	1.000	1.250
HVAC Ducts – less than 6 sq. feet	1,000 LF per 1 gsf	5.0E-05	7.5E-05	9.0E-05
HVAC in-line Drops & Diffusers	EA per 1 gsf	1.6E-02	2.0E-02	2.2E-02
Piping				
Steam & Chilled Water Piping - 2 ½ inch diameter or smaller	1,000 LF per 1 gsf	0.0E+00	2.0E-05	1.5E-05
Electrical				
Standby generators	KVA per 1 gsf	3.5E-03	5.0E-03	1.5E-02
Fire Protection				
Sprinkler Piping	20 LF per 1 gsf	1.0E-02	1.1E-02	1.3E-02
Sprinkler Drops	EA per 1 gsf	1.0E-02	1.2E-02	1.4E-02

Typically, the 50th percentile values are appropriate for estimating nonstructural component quantities. Where more information is known about the building occupancy, values between the 10th percentile and 90th percentile can be selected and is the primary purpose for their listing.

Occupancy-specific quantities associated with typical tenant-furnished equipment and contents are not included. For instance, normative quantity information for hospital equipment including imaging equipment, surgical devices, specialty lighting are not provided. This information, along with the related fragilities, must be supplied on a building-specific basis.

In addition to the listing in Appendix F, a nonstructural component calculation spreadsheet tool is provided as a companion product to this report. The implementation guide describes the use of this tool.

3.6 Damage States

3.6.1 General

Damage is characterized as a series of discrete damage states representing the different levels of possible damage

Although building and component damage generally occurs as a continuum with the scope and extent of damage increasing as demand increases; rather than using a continuous range of possible damage states, each fragility group is assigned a series of discreet damage states to characterize the different levels of damage that can occur. Each damage state is associated with a unique set of consequences consisting of:

- a unique probable repair action, with associated repair consequences;
- a unique potential for "unsafe" placard assignment;
- a unique potential impact on casualties;

or a combination of these.

Not all damage states will have significant consequences of all of these types. Damage states meaningful for one performance measure (e.g., repair action) may not be significant for another performance measure (e.g. casualties). Each damage state represents a unique set of consequences considering these performance measures. For example, for a hypothetical exterior cladding component, meaningful damage states could include:

- Cracking of sealant joints, permitting moisture and/or air intrusion. Such damage will have no consequences with regard to casualties, safety placard placement or long-lead times. However, over the long term, the damage will present building maintenance issues, and therefore will require repair consisting of sealant joint replacement. This will result in limited repair costs with an associated short repair time.

- Damage consisting of visible cracking of the panels. To repair this unsightly damage, the cladding must be removed from the building and replaced. This damage will likely have more severe cost consequences and will result in a longer repair time. Casualties, safety placards and or long-lead times are not impacted in this damage state.
- Damage consisting of panel connection failure, and pieces of the cladding falling off the building. This damage will likely have similar repair consequences as that described previously (replacement of the panels) but will also have potential casualty impacts (when the cladding falls from the building, although this methodology only tracks casualties within the building envelope) and may have severe occupancy impacts as the building might be deemed unsafe for occupancy and placarded as such, until the cladding is repaired.

When a fragility group has more than one damage state, damage states can be sequential, mutually exclusive or simultaneous

3.6.2 Damage Logic

For a particular component type, damage states must have a logical inter-relationship. The several possible logical relationships include:

- *Sequential* relationship. Sequential damage states must occur in sequential order, with one state occurring before another is possible. Sequential damage states represent a progression of damage from none to higher and higher levels as demand increases. Generally, as damage moves from one state to the next, more serious consequences accrue. For example, for a concrete component whose behavior is controlled by flexure, the damage states may include: 1) hairline cracking repaired with simple patching and painting; 2) large open cracks requiring injection with epoxy and 3) spalling with buckling of reinforcing steel, requiring replacement of bent or fractured reinforcing bars and crushed concrete.
- *Mutually exclusive* relationship. Mutually exclusive damage states exist when the occurrence of one damage state precludes the occurrence of other damages states. Each mutually exclusive damage state must have a conditional probability of occurrence, given that the component is damaged. For example, the previously discussed concrete component might reach a level of demand at which, either (a) the flexural cracks lengthen and widen (80% chance) or (b) the behavior mode transitions to shear with the formation of a more serious crack pattern (20% chance). The probabilities for all mutually exclusive damage states must sum to 100 percent.

- *Simultaneous* relationship. Simultaneous damage states can, but need not, coexist with one another, if the component is damaged. Each simultaneous damage state is assigned a conditional probability of occurrence given that the component is damaged. The sum of the conditional probabilities for all simultaneous damage states will generally exceed 100% as some states will occur at the same time. Elevators are an example of components with simultaneous damage states. Damage can consist of one or more conditions each with its own independent probability of occurring, given that the elevator has become damaged (e.g. damaged controls (30%), damaged vane and hoistway switches (20%), damaged entrance and car door (30%), oil leak in hydraulic line (10%). Other states are also possible, but not covered here for brevity.

3.6.3 Correlation

Individual performance groups can be designated as having either correlated or uncorrelated damage. If a performance group is designated as correlated this means that all components within the group will always be in the same damage state. If a performance group is designated as uncorrelated, then each performance group component can have different damage.

Performance groups can be identified as having correlated or uncorrelated damage. Specifying correlation significantly reduces computational effort and time but understates the potential dispersion in performance

Damage state correlation can be used to indicate the existence of a condition where failure of one element will necessarily require simultaneous failure of all elements within the performance group. An example of this condition would be a series of identical braced frames, all within a single line of resistance in a story. If lateral deformation of the brace line is sufficient to induce buckling in one of the braces in this frame, it is likely that all of the braces will buckle, as forces will redistribute from the buckled brace to adjacent braces triggering their buckling. Similarly, identical braces on separate lines of resistance will likely exhibit uncorrelated behavior as the building deformation along different framing lines will likely be different, resulting in different probabilities of damage on each line. One way to model this condition would be to assign a separate performance group to each line of bracing, and then designate that components within each performance group are correlated.

From a practical perspective, designation of performance group components as correlated results in reduced computational effort in the performance calculation process as for each realization, it is only necessary to identify a single damage state for each performance group. For uncorrelated components, it is necessary to determine a unique damage state for each component in the group, greatly increasing computation effort. In reality, most building components will not have perfectly correlated damage states.

Designation of performance groups as correlated, when they are not, should have small effect on the mean performance outcomes, but can significantly affect computed dispersion.

If the probability of incurring unsafe post-earthquake placarding is an important consequence, correlation should not be used unless there is reason to believe that damage occurrence for a particular performance group actually is correlated. This is because the probability of incurring an unsafe placard is determined by comparing the percentage of components damaged to certain states against trigger percentage quantities. If an assumption of correlation is used then the number of realizations that reach the trigger percentage will be overstated resulting in an unrealistically high calculated probability for unsafe placards.

3.7 Demand Parameters

Story drift, floor acceleration and floor velocity are the most typical demand parameters; however, other demand parameters can be defined

Although actual damage can occur as a result of complex relationships between damageability and component demands of various types, in this methodology, the occurrence of all damage states within a fragility group is predicted by a single demand parameter. The selected demand parameter is the one that best predicts the occurrence of the several damage states with the least amount of uncertainty. For most structural systems (e.g., shear walls, steel braces, steel and concrete moment frames) along with many nonstructural components, story drift ratio is that demand parameter. Floor acceleration and floor velocity are also commonly used. When appropriate, it is possible to define other demand parameters, such as plastic rotations demands, axial forces and other demands on individual beams, columns, braces, etc.

Since most buildings include drift-sensitive components that generally align with each of the building's principal orthogonal axes, e.g. exterior walls, drifts in both directions are required to calculate performance. Failure modes related to acceleration or velocity such as those associated with failure of base anchorage of mechanical equipment and sliding of unanchored or unbraced components are insensitive to the direction of application of the demand. Others, such as tall book cases, may be sensitive to demand directionality; however, it may be very difficult to determine the actual orientation of such objects with respect to the building's primary axes. Therefore, for behavior modes that are velocity or acceleration dependent, damage states are determined based on an estimate of the maximum peak value independent of direction. This methodology estimates maximum peak floor acceleration and velocity by multiplying the maximum value obtained from analysis in either of the two directions by a factor of 1.2. The 1.2 factor

is an approximation that accounts for vector summation effects for the velocity or acceleration, while acknowledging that the peak value of these quantities is unlikely to occur simultaneously along the two axes. It is possible to change this factor. Also, if an acceleration- or velocity-sensitive component's behavior is direction-sensitive and its orientation is known, its fragility can be designated as sensitive to demand in a particular direction.

Other demand parameters can be developed as appropriate for the damage states being defined. For instance, plastic hinge rotation for beams and columns in moment frames could be used. For some nonstructural components, peak floor velocity may be a better indicator of damage than peak floor acceleration. Any single demand parameter can be selected; the one selected should best predict the onset of damage with the least amount of uncertainty. Each fragility group can use only one demand parameter for all damage states.

3.8 Component Fragility

3.8.1 Fragility Functions

The type and extent of damage a component will incur, given that it experiences a particular demand, is uncertain. Component fragility functions are statistical distributions that indicate the conditional probability of incurring damage given a value of demand. Fragility functions are assumed to be lognormal distributions. A unique fragility function is required for each sequential damage state, and for each group of mutually exclusive or simultaneous damage states.

Component fragility functions are distributions that indicate the conditional probability of incurring a damage state given a value of demand. This methodology assumes lognormal distributions.

Figure 3-4 presents a representative family of sequential fragility curves for a reduced beam section (RBS) special steel moment frame beam-column connection. For this fragility group, three damage states: DS_1, DS_2, and DS_3, are defined:

- DS_1: Beam flange and web local buckling requiring heat straightening of the buckled region.
- DS_2: Lateral-torsional distortion of the beam in the hinge region requiring partial replacement of the beam flange and web, and corresponding construction work to other structural and nonstructural components.
- DS_3: Low-cycle fatigue fracture of the beam flanges in the hinge region requiring replacement of a large length of beam in the distorted/fractured region, and corresponding construction work to other structural and nonstructural components.

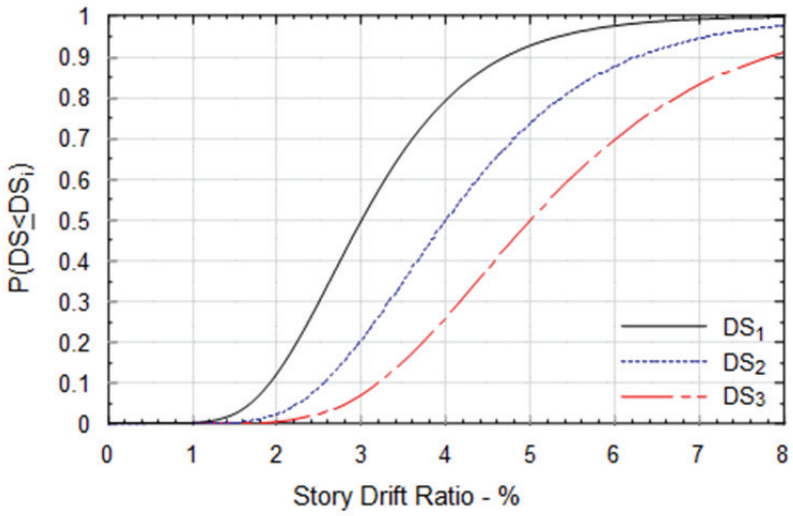

Figure 3-4 Example family of fragility curves for special steel moment frames.

Each damage state fragility function is defined by a median demand value, θ_{DS}, at which there is a 50% chance that the damage state will initiate, and a dispersion β_{DS} that indicates the uncertainty that damage will initiate at this particular value of demand. If a large number of components are subjected to demand, θ_{DS}, and the performance of these components is uncorrelated, half of the components will have entered the damage state and half will not.

The dispersion is associated solely with uncertainty in the onset of damage as a function of demand and is independent of uncertainty associated with the intensity of shaking or the prediction of demand. As the value of β_{DS} increases the shape of the curve becomes flatter, indicating a wider range of demand values over which there is significant probability for the damage state to initiate. The dispersion reflects variability in construction and material quality, the extent that the occurrence of damage is totally dependent on a single demand parameter, and the relative amount of knowledge or data on the components likely behavior.

For the damage states represented in Figure 3-4, median and dispersion values are: *DS1* - θ = 3% story drift ratio; β = 0.35; *DS2* - θ = 4% story drift ratio, β = 0.35 and for *DS3* θ = 5% story drift ratio, β = 0.35. Therefore at a story drift ratio of 4%:

- the probability of having some damage is the probability that DS_1 will have occurred, or 80%, since these damage states are sequential, and DS_1 must occur before any of the other states can.

- the probability of no damage (neither Damage State DS_1, DS_2, nor DS_3have occurred) is 20% (=1.00-0.80),
- the probability of damage in state DS_1 (assumed to be representative of damage between curves DS_1 and DS_2) is 30% (=0.80-0.50), the probability of damage in state DS_2 is 24% (=0.50-0.26) and the probability of damage in state DS_3 is 26% (=0.26-0).

For each realization in which building collapse is not predicted, the demands are used together with the component fragility functions for all performance groups in the building to determine the damage state for each component. Taken together, the damage states for all of the components that comprise the building define a building damage state.

3.8.2 Experimentally Derived Fragilities

Component fragilities may be developed by laboratory testing, from earthquake experience data, by analysis, by judgment or by a combination of these.

Component fragility functions can be developed by laboratory testing, collecting data on the behavior of similar components in real earthquakes, analysis, judgment, or a combination of these methods. Appendix H presents quantitative procedures for developing fragility functions. FEMA 461, *Interim Testing Protocols for Determining the Seismic Performance Characteristics of Structural and Nonstructural Components* (FEMA, 2007), presents recommended procedures for performance of laboratory tests intended to develop fragility functions.

Appendix H provides detailed procedures for developing the median (θ) and dispersion (β) values for a fragility function for the following five conditions of data:

- *Actual Demand Data*: When test data is available from a sufficient number of specimens and each tested component actually experienced the damage state of interest at a known value of demand.
- *Bounding Demand Data*: When test data or earthquake experience data are available from a sufficient number of specimens, but the damage state of interest only occurred in some specimens. For the other specimens, testing was terminated before the damage state occurred or the earthquake did not damage the specimens. The value of the maximum demand to which each specimen was subjected is known for each specimen. This maximum demand need not necessarily be the demand at which the damage state initiated.
- *Capable Demand Data*: When test data or earthquake experience data are available from a sufficient number of specimens, but the damage state of interest did not occur in any of the specimens. The maximum value of demand that each specimen was subjected to is known.

- *Derivation*: When no test data are available, but it is possible to model the behavior and analytically estimate the level of demand at which the damage state of interest will occur.
- *Expert Opinion*: When no data are available and analysis of the behavior is not feasible, but one or more knowledgeable individuals can offer an opinion as to the level of demand at which damage is likely to occur, based either on experience or judgment.

All five of these approaches were used in the development of fragility functions provided in a companion database.

3.8.3 Common Fragilities

Over 700 standard fragilities have been developed as part of this methodology and are included in an electronic data base as a companion to this Volume.

Using the procedures of Section 3.8.2 and available test data, numerous fragility functions for common structural and nonstructural components have been developed. Appendix D presents a complete listing of these fragilities. An electronic data base that is a companion to this Volume presents the actual fragility functions. Summaries of the data used to determine these fragility functions can be found in *Background Reports* published as another companion product to this Volume.

The provided fragilities cover many common structural systems including:

- Moment-resisting steel frames;
- Moment-resisting concrete frames;
- Steel braced frames;
- Steel eccentrically-braced frames;
- Concrete shear walls (low- and high-aspect ratio walls);
- Masonry shear walls;
- Light-framed wood walls;
- Concrete slab-column frames; and
- Ordinary steel beam-column framing.

For many of these systems, provided fragilities capture the range of performance capability from high ductility to ordinary ductility. For example, the overall steel braced frame category includes fragilities for those that:

- conform to AISC 341 requirements for special concentrically braced frames (high ductility)

- conform only to the requirements of AISC 360 (ordinary ductility)
- consist of different structural member sections, including HSS, WF, (high ductility to ordinary ductility)
- consist of gusset plate designs using varying limit state assumptions (high ductility to ordinary ductility)

In addition, variations based on configuration have also been developed. For example, concentrically-braced steel frame systems include the following configurations:

- X-bracing;
- Single diagonal; and
- Chevron.

Similar variations are provided for the other structural system fragility groups. Differences in consequence functions, especially those related to repair costs, further expands the list of fragilities. While the damage states and associated repair measures for a specific fragility group may be identical, the difference in the quantity of material damaged required the development of additional fragility groups to reflect the difference in repair costs. For instance, fragility groups for low-aspect ratio concrete shear walls include variations for the following wall thicknesses:

- less than 8 inches
- 8-to-16 inches
- 16-to-24 inches

For each of these wall thicknesses, the fragility list is further expanded to include the following variation in heights:

- Less than 15 feet
- 16-to-24 feet
- 25-to-40 feet

Similar variations based on configuration and material quantity are provided for the other structural system fragility groups as well. Appendix D presents a complete listing of all available fragility groups and a companion electronic database provides complete details of the specific contents of each provided fragility group.

Fragility groups have also been developed for many nonstructural components. As with the structural components, variations have been developed to account for configurations and situations that are likely to be encountered in buildings.

Appendix D and the Implementation Guide provide additional detail regarding the provided fragility groups and selecting the appropriate ones for use in building performance modeling.

3.8.4 Calculated Fragilities

Some component types and damage modes require building-specific calculation of fragility. This methodology includes four separate procedures to calculate fragility parameters.

Some component types and damage modes, for example, anchorage failure of mechanical equipment, require building-specific calculation of the fragility parameters. The procedures below provide estimated fragility parameters for components with failure modes, the onset of which can be predicted using design formulations contained within industry standard design specifications, such as ACI 318-11, *Building Code Requirements for Structural Concrete and Commentary* (ACI, 2011), and ANSI/AISC 360-10, *Specification for Structural Steel Buildings* (AISC, 2010). These procedures can also be used to estimate fragility parameters for components and failure modes for which industry design standards do not provide a capacity, but which nonetheless, can be predicted using a rational calculation procedure based on considerations of engineering mechanics. Separate procedures are presented, based on the type of limit state associated with the damage. These include procedures for:

- Strength-limited damage states;
- Ductility-limited damage states;
- Displacement-limited damage states;
- Code-based limit states;
- Overturning limit states; and,
- Sliding limit states

These procedures should be used only when the common fragilities of Section 3.8.3 are not applicable and suitable test data for use with the procedures of Section 3.8.2 is unavailable.

Strength-limited Damage States

This procedure is applicable to the calculation of fragility parameters for damages states that occur as a limit to essentially elastic behavior. The procedure initiates by determining the component design strength ϕR_n in

accordance with an appropriate industry standard. For ductile behavioral modes, such as flexure, determine the median strength as:

$$\theta_{ductile} = C_q e^{(2.054\beta)} \phi R_n \quad (3\text{-}1)$$

For brittle failure modes determine the median strength as:

$$\theta_{brittle} = C_q e^{(2.81\beta)} \phi R_n \quad (3\text{-}2)$$

where, the dispersion β and coefficient C_q are determined as described below.

Determine the total dispersion, β, as a function of the uncertainty in material strength (β_M), inherent variability in the design equation's ability to predict actual failure demand (β_D), and the uncertainties associated with construction quality (β_C).

Design equations for brittle failure modes have higher inherent uncertainty than do those for ductile failure modes. Material strength variability (β_M) is a function of the material itself. Wood tends to have higher variability than does concrete due to the uncertainty associated with grading procedures and the non-uniformity of individual pieces of wood. Some grades of steel, such as ASTM A992 have relatively low material strength variability, while others, such as A36, may have variability comparable to that of concrete.

The combined uncertainty β is computed from the equation:

$$\beta = \sqrt{\beta_D^2 + \beta_M^2 + \beta_C^2} \quad (3\text{-}3)$$

For ductile failure modes that are well predicted by classical methods of engineering mechanics, such as the yield strength of a prismatic member loaded in flexure, a value of the design uncertainty, β_D, equal to 0.05 is recommended. For ductile failure modes with more complex behavioral characteristics, such as elastic buckling of a bar, a larger value of the design uncertainty, on the order of 0.1, is recommended.

For brittle failure modes, such as tensile failure of a wood post, shear failure of lightly reinforced concrete, and crushing failure of masonry or concrete, a higher design uncertainty value is recommended. This can be attained either by reference to commentary underlying the design standard, or by reference to the fundamental research upon which the design standard is based. Alternatively, a default value for the design uncertainty, β_D, for brittle failure modes may be taken as 0.25.

Recommended values for the material strength uncertainty, β_M, may be obtained from industry data, or lacking this, the values shown in Table 3-4 may be used.

Table 3-4 Default Material Property Dispersions, β_M, for Structural Materials

Material	Condition	Dispersion, β_M
Steel	All grades except A36	0.10
	A36	0.15
Concrete	Ready-mix conforming to ASTM C-94	0.12
	Other – based on cylinder test results	a
Wood	Machine-stress graded	0.12
	Visually graded	0.20
	Ungraded	0.30
Masonry	Engineered concrete or brick masonry conforming to ACI 530.1	0.15
	Other masonry	0.25

a For concrete with unknown construction control, compute β as the coefficient of variation obtained from tests on cores removed from the structure. If the coefficient of variation exceeds 0.15, not less than 6 tests should be performed to determine the coefficient of variation

Table 3-5 provides recommended values for the uncertainty associated with construction quality, β_C, based on consideration of the sensitivity of a particular behavioral mode to construction quality and the level of quality control that is provided in construction. For example, the yield strength of a steel bar will be essentially insensitive to the effects of construction quality, other than through the potential variability in cross section dimensions, regardless of the extent of quality control provided. However, the strength of a post-installed expansion anchor is very sensitive to the quality of installation as reflected by hole size and tightening condition.

Table 3-5 Default Values of Uncertainty, β_C, Associated with Construction Quality

Sensitivity to Construction Quality	Degree of Construction Quality Control		
	Very Good	Average	Low
Low	0	0	0
Moderate	0	.1	.15
High	0	.15	.25

The coefficient, C_q, in equations 3-1 and 3-2 adjusts the value of the median based on the sensitivity of the behavioral mode to construction quality; the extent to which this is included in the resistance factors used to ascertain

design strength; and the severity of the potential effects of poor construction quality. The C_q coefficient should be established based on judgment and an understanding of the probable value of the capacity, given poor quality control. The value of C_q will normally be taken as unity. However, in some conditions a lesser value is warranted. For example, a post-installed tension anchor, where it is uncertain whether the anchor has been properly set, a judgmental value taken as the average of that for a proper installation and that of an improper installation can be used.

Ductility-limited Damage States

Some damage states in ductile elements will initiate when inelastic deformation of the element reaches a particular ductility. Without appropriate test data to characterize the ductility at which some damage states occur, estimates of this ductility are, at best, highly uncertain. When appropriate test data are not available, the following procedure can be used to characterize ductility-limited damage states:

1. Calculate the median value and dispersion for the onset of yield of the element, per the procedures for strength-limited damage states described above.

2. Calculate the median deformation of the element, δ_y, at the onset of yield, using elastic deformation analysis under the applied median yield load.

3. Judgmentally classify the behavioral mode as one of "limited ductility" associated with a μ of 2, "moderate ductility" associated with a μ of 4, or high ductility associated with a μ of 6, where μ is the ratio of deformation at onset of a damage state to deformation at yield.

4. Calculate the median displacement demand for the onset of the damage states as $\theta = \mu\delta_y$.

5. Calculate the dispersion β for the damage state as:

$$\beta = \sqrt{\beta_1^2 + 0.16} \leq 0.6 \qquad (3\text{-}4)$$

where β_1 is the dispersion associated with the onset of yield, calculated per the procedures for strength-based damage states described above.

Displacement-limited Damage States

Some damage states are best characterized based on an imposed displacement. An example of this would be an expansion joint at which

beams rest upon a bearing seat of limited length, or an attachment for a precast cladding panel, that relies on a slotted connection to accommodate movement. In such situations, the median displacement demand at initiation of failure should be taken as the calculated available length of travel based on the specified travel allowance dimension (for example, slotted hole length, length of bearing seat). The dispersion should be set based on an evaluation of the likelihood that the initial position of the structure is out of tolerance. The normal construction tolerance can be considered to represent one standard deviation on the displacement dimension. The dispersion can be taken as equal to the coefficient of variation calculated approximately as the standard deviation value divided by the median.

Code-based Limit States

In some cases, there may not be sufficient information available to calculate the capacity of a component, for example the anchorage of an equipment item, either because the anchorage itself has not yet been designed, or for an existing installation, the details of the anchorage are not known. In such cases, if the code-based design capacity that the installation should comply with is known, the following procedure can be used:

1. Compute the assumed design strength (or displacement capacity) of the installation in terms of a convenient demand parameter, such as spectral acceleration, force, or story drift ratio. This presumed code-based capacity is taken as the value of ϕR_n.

2. Decide whether the damage state is a ductile or brittle mode. If it is unknown which of the two is likely, a separate calculation can be performed for each assumption, and the average results used. Regardless, use a value of the coefficient C_q of 0.5.

3. Assign a default dispersion, β, to the behavior, of 0.5.

4. If the mode is considered to be ductile, use equation 3-1 to determine the median value of the demand parameter, θ. If the mode is considered to be nonductile, use equation 3-2 to determine the median value.

Unanchored Component Overturning

This procedure has been adapted from Section 7.1,A.2 and Appendix B of ASCE/SEI 43-05, *Seismic Design Criteria for Structures, Systems, and Components in Nuclear Facilities* (ASCE, 2005). The procedure uses peak total floor velocity V_{PT} as the demand parameter. V_{PT} is defined as the peak value of the sum of the ground velocity and the relative velocity between the

ground and the floor. It can also be visualized as the peak velocity, during earthquake response, of the floor relative to a fixed point in space.

Fragility parameters include the median peak total floor velocity, $\hat{V}_{PT}$, at which overturning initiates and a dispersion to reflect the uncertainty. The method assumes that unanchored objects exhibit an oscillatory rocking behavior until a critical displacement is reached at which the object becomes unstable and topples. This displacement produces a tipping angle that exceeds the object's critical balance point. The spectral characteristics of the ground motion and the object's rocking frequencies and damping are used to derive $\hat{V}_{PT}$. Appendix K presents the assumptions, derivation and basis for the procedure.

Primary assumptions include: the component has rectangular shape, height 2*h*, width 2*b*, uniform weight distribution and is assumed to overturn about a single weak axis with the smallest base dimension 2*b*. Figure 3-5 defines these primary parameters.

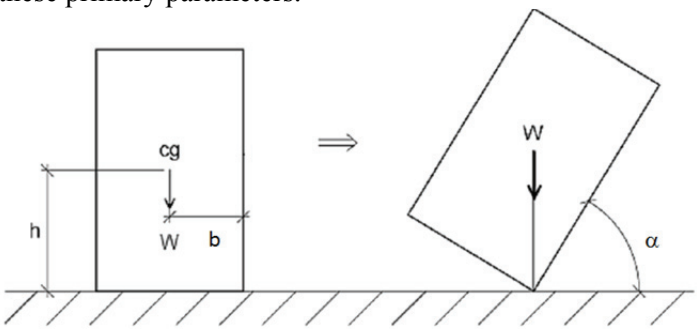

Figure 3-5 Overturning of unanchored object.

The procedure initiates with determination of the critical tipping angle, α, at which the component will become statically unstable, given by the equation:

$$\alpha = \arctan\left(\frac{b}{h}\right) \tag{3-5}$$

A spectral acceleration capacity of the object, S_{aO} is determined from the critical tip angle α and the component's dimensions as:

$$S_{aO} = \frac{2B}{\alpha} \tag{3-6}$$

where *B* is given by the equation:

$$B = \cos(\alpha) + \frac{b}{h}\sin(\alpha) - 1 \tag{3-7}$$

To determine whether sliding or overturning is likely to occur, the value of S_{aO} is compared with the static coefficient of friction μ_S. A value of S_{aO} that is greater than μ_S indicates the object will likely slide rather than overturn, while a value less than μ_S indicates the object will overturn.

The component's effective rocking frequency f_r and damping ratio, β_r are determined from the equations:.

$$f_r = \frac{1}{2\pi}\sqrt{\frac{2gB}{C_3\alpha^2 h}} \tag{3-8}$$

$$\beta_r = \frac{\gamma}{\sqrt{4\pi^2 + \gamma^2}} \tag{3-9}$$

where:

$$C_3 = \frac{4}{3}\left(1 + \left(\frac{b}{h}\right)^2\right) \tag{3-10}$$

$$C_R = 1 - \frac{2\left(\frac{b}{h}\right)^2}{C_3} \tag{3-11}$$

$$\gamma = -2ln\left(C_R\right) \tag{3-12}$$

Finally, the estimated median peak total floor velocity $\hat{V}_{PT}$ is obtained from the equation:

$$V_{PT} = \frac{S_{ao}g}{2\pi f_r D_{amp}} \tag{3-13}$$

Where D_{amp} is give by the equation:

$$D_{amp} = 2.31 - 0.41\ln\left(100\beta_r\right) \tag{3-14}$$

A dispersion of 0.5 is recommended for this fragility.

Unanchored Component Sliding

The procedure for determining fragility parameters for sliding of unanchored components is similar to that for component overturning described above, and is also based on procedures contained in *ASCE 43-05*. Like the procedures for overturning, the basis of the procedures for sliding are presented in Appendix K.

The procedure for sliding relies on definition of a critical sliding displacement, δ, at which the component will either slide off of a mounting surface or slide into some other object, resulting in damage. As is the case for overturning, the fragility function is defined by a median value of the peak floor velocity $\hat{V}_{PT}$ and dispersion β.

Before determining sliding fragility parameters for a component, it is necessary to determine whether the object is likely to overturn or slide. The previous section provides information on how to make this determination. Assuming that a determination is made that sliding is more likely to occur than overturning, the median value of peak floor velocity at which the component will slide a distance δ is determined from the equation:

$$\hat{V}_{PT} = \frac{\sqrt{2\mu_D g\delta}}{1.37} \qquad 3\text{-}15)$$

Where μ_D is the dynamic coefficient of friction between the component and its supporting surface, g, is the acceleration due to gravity and δ is the available sliding displacement. As with overturning, a dispersion of 0.5 is recommended.

3.9 Consequence Functions

Consequence functions are distributions of the likely consequences of a component damage state translated into repair costs, repair time, potential for unsafe placards, casualties and other impacts. For each damage state, fragility definitions include repair descriptions that provide the necessary information to develop the associated repair costs and times. To facilitate casualty estimation, each damage state description also includes a discussion as to whether life safety hazards are associated with the damage, and if they are, the affected area in which life safety hazards will likely occur. Damage state descriptions also include text describing the extent to which the occurrence of the damage is likely to result in posting of an unsafe placard being.

Consequence functions are distributions of the likely consequences of component damaged translated into repair costs, repair time and other impacts.

Consequence functions for each of these impacts are developed based on these descriptions, using the procedures described below.

3.9.1 Repair Costs

Repair costs include consideration of all necessary construction activities to return the damaged components to their pre-earthquake condition. Repair costs do not include work associated with bringing a non-conforming installation or structure into compliance with newer criteria. They assume

Repair costs include the cost of all construction activities necessary to return the damaged component to their pre-earthquake condition.

repair or replacement "in-kind". The repair costs are based on the repair measures outlined for the specific damage state and include all the steps a contractor would implement to conduct the repair including:

- Shore the surrounding structure (if necessary);
- Remove or protect contents adjacent to the damaged area;
- Protect the surrounding area from dust, noise, etc. with a temporary enclosure;
- Remove architectural and MEP systems, as necessary, to obtain access to the repair;
- Procure new materials and transport them to the site;
- Perform the repair;
- Replace architectural and MEP systems, as necessary; and
- Replace contents.

The methodology accounts for efficiencies of scale, occupancy-specific conditions that affect repair effort, height within the building, and the difficulty associated with working at upper floors; and the effect of hazardous materials, such as lead-based paint and asbestos in determining repair cost and repair time

For many repairs, the cost to protect the surrounding area is greater than the cost of the repair itself. The cost of accessing the damaged area to conduct repairs will also affect repair costs. It is more difficult, and, hence, more costly, to repair damage on the 10th floor of a building than on the 1st floor. Likewise, the type of occupancy within the damaged area can affect repair costs. Occupancies such as healthcare and research laboratories will likely have access restrictions and will require enhanced protection measures. Finally, hazardous materials located within the damage area will affect the repair approach. All three of these will result in an increase in repair costs. This methodology includes "macro-factors", provided on a story-by-story basis, to take such effects into account. The Implementation Guide provides additional detail regarding use of these factors.

Calculation of repair costs also includes consideration of efficiencies of scale in construction operations. When a large quantity of the same type of construction work is necessary, contractor mobilization, demobilization and overhead costs can be spread over a larger volume of work, resulting in reduced unit rates. For each damage state, repair costs are described with the following parameters illustrated in Figure 3-6:

- *Lower quantity:* the quantity of repair actions of a give type, below which there is no cost discount to reflect efficiency in construction operations
- *Maximum cost:* This is the cost to perform a unit damage state repair, without any efficiency of scale being obtained.

- *Upper quantity:* the quantity of repair work, above which no further efficiencies of scale are attainable
- *Minimum cost:* the minimum cost that can be attained for a unit repair operation, considering all possible efficiencies of scale
- *Dispersion:* the uncertainty associated with the unit cost.

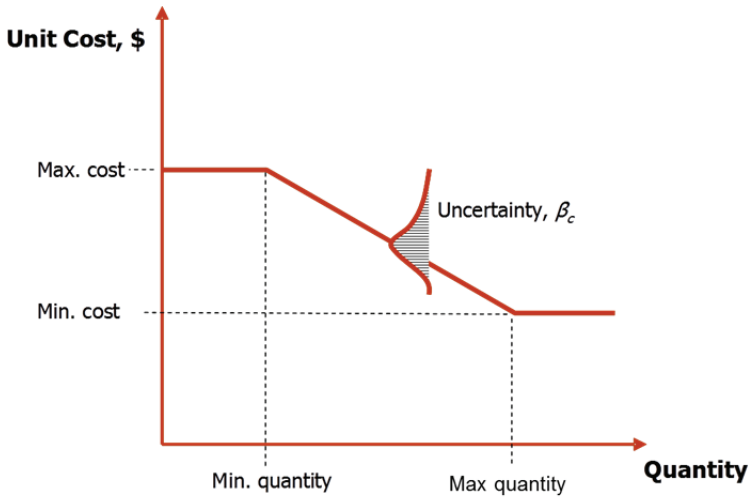

Figure 3-6 Sample consequence function for cost of repair.

The distribution of the repair costs is derived from costs that represent the 10th, 50th , and 90th percentile estimates. Both lognormal and normal distributions are developed from the repair cost data and the curve with the best fit is used.

Repair cost is computed for a reference standard location in the United States at a reference period of time (2011), neglecting uncertainty in contractor pricing strategies or construction cost escalation. Construction cost indices are used to adjust these standard costs for the building-specific location and to adjust for inflation. Any convenient construction cost index can be used if normalized to the standard location and time.

3.9.2 Repair Time

The actual time that a building will be unusable for beneficial occupancy is very difficult to determine. Factors that can affect this include:

Repair time is limited to the number of labor hours associated with the required repair.

- The party responsible for performing repairs – i.e., the owner or tenants;
- Whether the party responsible for performing repairs has the necessary financial resources to pay for the needed repairs;

- The availability of design professionals to design repair operations and the availability of contractors to perform these operations;
- Whether or not the contractor has free access to the building to conduct the repairs or if the building remains in service and the contractor must limit their activity at any time to small portions of the building; and
- Whether the building has been placarded as "unsafe", and the length of time necessary to convince the building official that it is safe to conduct repair operations within the building.

These uncertainties make estimation of overall occupancy interruption time an intractable problem. Therefore, these procedures provide the following measures of occupancy interruption:

1. The length of time necessary to conduct repairs,
2. The need to procure items with long lead-times, and
3. The probability that the building will be placarded as unsafe for occupancy.

In order to estimate repair time, each damage state includes a time-related consequence function that indicates the number of labor hours associated with the required repair. An important parameter in developing repair time estimates is the number of workers that can occupy the building at the same time. The methodology includes a "maximum worker per square foot" parameter that accounts for this. This number can depend on whether the building is occupied during construction as well as the available labor in the region.

Repair time, like repair cost, can benefit from efficiency of scale when a large quantity of a specific repair action must be undertaken. These effects are described in the fragility specification through the following parameters:

- *Lower quantity:* the minimum quantity of a given repair action, below which there is no time efficiency.
- *Maximum time:* the maximum number of labor hours necessary to implement a repair action without efficiency of scale.
- *Upper quantity:* maximum quantity of a repair action above which there is no further efficiency.
- *Minimum time:* the minimum number of labor hours per unit repair action, considering possible economies of scale.
- *Dispersion:* the uncertainty associated with the labor effort associated with a given repair action.

Similar to repair costs, the distribution for repair time is derived from time allocations that represent the 10^{th}-, 50^{th}- and 90^{th}-percentile estimates. Both lognormal and normal distributions are developed from the repair time data and the curve with the best fit is used in the methodology

Both serial and parallel repair strategies are estimated as part of the methodology. The serial repair strategy assumes that repairs are performed on one floor at a time while parallel assumes that repairs can be done on all floors at the same time. Neither repair time estimate will likely represent the actual schedule used for a particular building; however, the two repair time estimates should bound the probable time required.

Finally, repair time can be greatly affected by long-lead times for procurement of critical equipment and components (e.g., HVAC equipment and elevators). If a damage state requires replacement of a component that is associated with a long-lead time, this is indicated in the fragility specification and is flagged as part of the methodology.

Downtime estimates associated with unsafe placards is not considered; rather the likelihood of such placards for each performance group and the building as a whole is established.

3.9.3 Unsafe Placards

Unsafe placards can be a primary source for damage-related downtime and could have an effect on the actual repair time given the presumed dangerous state of the building. An estimate of the downtime associated with such placards is not included as part of the methodology. However, the likelihood of receiving an unsafe placard as a result of damage to a performance group is established. The actual time associated with this can be estimated on a case-by-case basis and added to the repair time estimate.

Each damage state associated with a fragility group is identified as having a potential to result in an unsafe placard or not. The majority of nonstructural fragility groups will not result in an unsafe placard. Although nonstructural damage could be an indicator of potential structural damage, it usually does not, by itself, pose a life safety risk. However, the most severe damage states in nearly all of the structural fragility groups will trigger a potential for an unsafe placard since the structure's stability has been compromised sufficient to result in a life safety risk.

For those damage states that are determined to have potential to produce unsafe placards, the median quantity of damage that would trigger such a placard is provided. For example, for ACI-compliant special moment-resisting frames (B1041.001), it is estimated that if 20% of the beam-column joints reach damage state 3 for a performance group, an unsafe placard is likely.

The probability that the building will receive an unsafe placard is determined by considering the probability of obtaining such a placard based on damage sustained by components in each of the performance groups. It is assumed that the potential for receiving an unsafe placard based on the damage sustained by components in one performance group is not correlated with that for other performance groups. This allows determination of the total probability of receiving an unsafe placard using the formula:

$$P(U_T) = \begin{Bmatrix} 1-\left[1-P\left(U_1\right)\right]*\left[1-P\left(U_2\right)\right]*\cdots*\left[1-P\left(U_i\right)\right]* \\ \cdots*\left[1-P\left(U_n\right)\right]*\left[1-P\left(C\right)\right] \end{Bmatrix} \quad (3\text{-}15)$$

where, $P(U_T)$ is the total probability of receiving an unsafe placard; $P(U_i)$ is the probability of receiving an unsafe placard because of damage to performance group "i"; $P(C)$ is the probability of building collapse and "n" is the total number of performance groups. In the above, $P(U_i)$ is given by:

$$P\left(U_i\right) = \frac{k}{N} \quad (3\text{-}16)$$

where, k is the number of realizations in which performance group "i" resulted in an unsafe placard and N is the total number of realizations evaluated.

3.9.4 Casualties

Building collapse is the principle cause of earthquake casualties; this methodology does, however, estimate casualties associated with falling debris and other component damage.

Although building collapse is the principle cause of earthquake casualties (defined as death and serious injuries), some damage states associated with individual components or assemblies can have potential casualty consequences. These are generally associated with falling debris, for example glazing falling out of its frame and injuring nearby occupants, but can also be associated with the release of hot water, steam or toxic materials.

Casualties caused by building collapse are determined based on the building's collapse modes (See Section 6.5) and the number of estimated occupants (See Section 7.3). For individual components, the each damage state description includes a "flag" indicating whether a life-safety hazard exists for the damage state. If the answer is "yes", then a casualty-affected planar area is estimated along with the probability that individuals within that affected area are likely to incur serious injury or death.

As the name implies, the casualty-affected planar area represents the planar area proximate to a component, where the component's damage could result in casualties. The affected area is typically larger than that occupied by the

component to account for the uncertainty in the area where debris, spray or other release may occur.

Not all of the occupants within the planar area will become casualties, resulting in the need to identify the percentage of individuals within the area that are likely to be injured. For example, for electronic equipment on wall mount brackets (E2022.021), the casualty-affected area is 16 SF, while the unit itself may only be 5-10 SF, and the percentage for serious injury and death is 10% and 5%, respectively. These statistics are judgmentally determined.

3.10 Fragility Specifications

All of the damage, fragility, and consequence data associated with a fragility group are recorded on a standard fragility specification form. Over 700 fragility specifications have been developed as part of the methodology and are available in an electronic database.

The basic identifier, fragility, and consequence information for a typical fragility specification is illustrated in Figure 3-7, Figure 3-8, and Figure 3-9, respectively.

NISTIR Classification	B1049.002a		
Name	Reinforced concrete flat slabs- columns without shear reinforcing .2<Vg/Vo<.4, no continuity reinf		
Description	Costing is on a per joint basis		
Construction Quality: [1]	ACI 318-56, ACI 318-63, ACI 318-89, ACI 318-95, ACI 318-99, ACI 318-05		
Seismic Installation Conditions:	Not applicable		
Normative Quantity (unit):	Each	Each	
Demand Parameter (unit):	Story Drift	Unit less	
Number of Damage States:	2		
Damage State:	DS1	DS2	
Type of Damage State:	Sequential	Sequential	
DS Hierarchy	Seq{DS1,DS2}		
Descriptions	Yield strain of the slab flexural reinforcement has been exceeded, spalling of concrete may/may not occur, slab exhibits large enough crack widths to allow epoxy injection	Punching occurs, causing significant spalling of concrete. Epoxy injection is no longer expected to be sufficient to restore the required strength and stiffness to the slab and the slab-column connection.	

Figure 3-7 Basic identifier information for a typical fragility specification.

Illustrations	B1049.001a-DS1-1.JPG	B1049.001a-DS2-1.JPG
Damage State Probability:	1.00	1.00
Fragility Parameters		
Median Demand, θ:	0.02	0.035
Data dispersion, β_d:	0.4	0.4
Uncertainty, β_u:	0.1	0.1
Total Dispersion, β:	0.4	0.4
Correlation (Yes / No)	NO	
Directionality (Yes / No)	NO	
Quality Ratings		
Data Quality	Average	
Data Relevance	Average	
Documentation Quality	Average	
Rationality	Superior	
Consequence Functions		
Repair Description	Prepare work area for epoxy injection, inject epoxy into 40 feet of crack (30 feet top, 10 feet bottom of slab) per 100 square feet of floor panel, replace and repair finishes; replace furnishings, ceilings, mechanical, electrical and plumbing systems.	Shore damaged area in the two stories below. Remove 100 square feet of concrete slab per column, preserving the slab reinforcement; lap splice 30 new 10 foot long rebar with existing rebar; place formwork; recast concrete slab; remove forms, replace and repair finishes; replace furnishings, ceilings, mechanical, electrical, and plumbing systems Cracks wide enough to be grouted are included in the portion of slab to be demolished and recast.

Figure 3-8 Fragility information for a typical fragility specification.

Long Lead Time (Yes / No)	NO			NO		
Repair Costs:	P_{10}	P_{50}	P_{90}	P_{10}	P_{50}	P_{90}
Repair Cost by Damage State:	1.93E+04	3.62E+04	5.09E+04	3.43E+04	4.95E+04	7.67E+04
Best fit mean:		3.55E+04			5.06E+04	
Best Fit Distribution:		Normal			LogNormal	
Quantity Plateau (Min Qty, Max Qty)	3.00		10.00	3.00		10.00
Average Repair Cost (Min Qty, Max Qty)	3.99E+04		3.26E+04	5.45E+04		4.46E+04
CV or beta (Min Qty, Max Qty)	0.35		0.35	0.32		0.32
Quantity Unit:		EA			EA	
Repair Time:	P_{10}	P_{50}	P_{90}	P_{10}	P_{50}	P_{90}
Repair Time by Damage State:	4.77E+01	8.95E+01	1.26E+02	8.47E+01	1.22E+02	1.89E+02
Best fit mean:		8.76E+01			1.25E+02	
Best Fit Distribution:		Normal			LogNormal	
Quantity Plateau (Min Qty, Max Qty)	3.00		10.00	3.00		10.00
Average Repair Time (Min Qty, Max Qty)	9.85E+01		8.06E+01	1.35E+02		1.10E+02
CV or beta (Min Qty, Max Qty)	0.35		0.35	0.32		0.32
Quantity Unit:		EA			EA	
LifeSafety Hazard:						
Potential non-collapse casualties? (Yes / No)	NO			NO		
Casualty-affected Planar Area (sf) per Normative Unit:	Not Applicable			Not Applicable		
Serious Injury (Median, Dispersion)	0%	0.00		0%	0.00	
Death (Median, Dispersion)	0%	0.00		0%	0.00	
Post-event Tagging Flag:		NO			YES	
Red Tag Trigger (Median, Dispersion)	Not Applicable	Not Applicable		10%	0.50	

Figure 3-9 Consequence information for a typical fragility specification.

Chapter 4
Define Earthquake Hazards

4.1 Introduction

Earthquake ground shaking is characterized by target acceleration response spectra. For the Simplified Analysis method, spectral response acceleration parameters are derived from these spectra. For nonlinear response history analysis, earthquake acceleration time series (ground motions) are selected and scaled to be representative of the target spectra.

This methodology addresses ground shaking. Engineers should perform qualitative assessment of other hazards that could cause damage including ground fault rupture, landslide, liquefaction, lateral spreading and tsunamis.

Seismic hazards other than ground shaking can cause damage and significantly impact performance. These hazards can include ground fault rupture, liquefaction, lateral spreading, landslides, and inundation from offsite effects such as dam failure or tsunami. This methodology does not presently address these other hazards. As a minimum, engineers should conduct a qualitative assessment of the potential impact of these other hazards and, if this impact is potentially significant acknowledge that performance predicted using this methodology does not include these effects.

Earthquake shaking occurs in three dimensions, and can be completely defined by two orthogonal horizontal components and one vertical component. However, vertical shaking is not a key contributor to damage in most buildings and has little effect on performance. Therefore, for most buildings, only horizontal earthquake shaking must be addressed. Appendix B presents procedures that can be used to characterize vertical shaking, when deemed significant. Appendix B also presents background information on ground shaking characterization that may be useful for some readers.

For intensity-based assessments, ground shaking intensity can be represented by any user-defined acceleration response spectrum. For scenario-based assessments, ground shaking intensity is represented by acceleration response spectra derived for specific magnitude-distance pairs using ground motion prediction equations, also called attenuation relationships. For time-based assessments, ground-shaking intensity is represented by a series of seismic hazard curves and acceleration response spectra derived from these curves associated at selected annual exceedance frequencies.

For nonlinear response-history analysis, shaking effects are assessed by simultaneously evaluating response to orthogonal pairs of horizontal ground

motion components. The ground motion pairs are scaled for consistency with the target response spectrum for the desired ground shaking intensity level. For simplified analysis, shaking is characterized by spectral response accelerations at the first mode period along each axis.

4.2 Building Location and Site Conditions

4.2.1 Seismic Environment and Hazard

Earthquake hazard is defined by the earthquake sources, the propagation of seismic waves to the building location and modifications applicable to the local site conditions.

Earthquake shaking hazards are dependent on site location with respect to causative faults and sources and, regional and site-specific geologic characteristics. Local topographic conditions (e.g., hills, valleys, canyons) can also modify the character of shaking however, this is not a significant factor for most sites and is neglected here.

4.2.2 Location

Time-based assessments require seismic hazard curves that predict the annual frequency of exceedance of key spectral response parameters. To develop hazard curves, the site's exact location (longitude and latitude) must be identified. Latitude and longitude should be defined to a minimum of three decimal places.

For scenario-based assessments, the distance from the building site to the causative fault must be known. For intensity-based assessments, the site location need not be defined.

4.2.3 Local Soil Effects

The properties of site soils must be defined to enable:

- selection of appropriately shaped spectra for intensity-based assessments
- selection of appropriate ground motion prediction equations for scenario-based assessments, and/or
- development of seismic hazard curves and response spectra for time-based assessments

In the Western United States it is generally sufficient to define the soil conditions to a depth of 30 m (100 ft.) from the ground surface. As a minimum, it will be necessary to have sufficient data to characterize the Site Class in accordance with the ASCE 7-10 Standard (ASCE, 2010) so that site coefficients can be assigned. For sites categorized as Site Class E or F, additional information will be necessary to permit the necessary site response analysis. This information will generally include the depth, classification and shear wave velocity of materials in the soil column above bedrock.

4.3 Ground Motion Prediction Equations

Ground motion prediction equations are used to derive acceleration response spectra for use in scenario-based assessments, and also form the basis for probabilistic seismic hazard analyses used to develop the hazard curves needed for time-based assessments. Ground motion prediction equations provide estimated values of ground shaking intensity parameters, such as peak ground acceleration, peak ground velocity and spectral response acceleration at particular structural periods, for user-specified combinations of earthquake magnitude and site-to-source distance (e.g., $M_W 7$ from a source 12 km from the building site) and other parameters.

Ground motion prediction equations provide estimates of spectral response accelerations for specified earthquake magnitude and site to source distance based on statistical analysis of past strong ground motion recordings.

Earthquake researchers derive ground motion prediction equations by performing regression analyses on the values of intensity parameters obtained from strong motion recordings of past earthquakes against distance, magnitude and other parameters. Horizontal ground shaking is a vector quantity that varies in orientation and amplitude throughout an earthquake's duration. Strong motion recordings used to develop ground motion prediction equations are typically obtained from pairs of instruments arranged to capture orthogonal components of motion. At any instant of time, each component of recorded motion will have different amplitude and neither may be the maximum component that occurred at the given point of time. Most ground motion prediction equations now provide geometric mean (geomean) spectral response accelerations that represent the quantity:

$$S_{gm}(T) = \sqrt{S_x(T) \times S_y(T)} \qquad (4\text{-}1)$$

where $S_x(T)$ and $S_y(T)$ are orthogonal components of spectral response acceleration at period T. The X and Y directions may represent the actual recorded orientations, or may represent a rotated axis orientation. Some equations rotate the motion to capture fault-normal and fault-parallel orientations, while others use an arbitrary rotation intended to capture a maximum orientation. The geomean approximately represents a statistical mean response, with actual shaking response in any direction as likely to be higher as it is lower than the geomean. Maximum response acceleration can be as much as 130% of the geomean or more, while the minimum response acceleration can be less than 80% of the geomean or less. Except within a few kilometers of the zone of fault rupture, the orientation of maximum spectral response with respect to the strike of the fault is random and varies with period.

Scenario assessments can be used to assess the effects of a repeat of a historic earthquake or to explore the effects of a maximum-magnitude event

on a nearby fault. The US Geological Survey posts information on best-estimate maximum magnitudes for active faults in the Western United States and the Inner Mountain seismic region at http://earthquake.usgs.gov/hazards/qfaults/.

Fault directivity effects can have substantial effect on the amplitude, duration and period content of shaking and should be considered for scenario-based assessments if the building site is located within 20 to 30 km of the presumed fault rupture zone and the selected earthquake magnitude is M_w 6 or greater. Directivity should be specified as: forward directivity (rupture progresses towards the site); reverse directivity (rupture progresses away from the site); null directivity; or unspecified directivity (random direction of rupture progression). Appendix B and NIST GCR 11-917-15, *Selecting and Scaling Earthquake Ground Motions for Performing Response-History Analyses* (NIST, 2011), provide guidance on fault-rupture directivity and its inclusion in hazard calculations.

At sites located within the forward directivity region, and within 20 km of the rupture zone of large magnitude (M_w 6.0 or greater) strike-slip faulting, ground shaking often exhibits directionality with shaking in the fault normal direction exhibiting significant velocity pulses as well as significantly larger amplitude than does shaking in the fault parallel direction. Hazard assessments on sites within this distance should account for these effects.

Some ground motion prediction equations are quite complex and require spreadsheet or other electronic computation tools for proper implementation. The simpler models, often called attenuation relationships can take the basic form:

$$\ln Y = c_1 + c_2 M - c_3 \ln R - c_4 R + \gamma \qquad (4\text{-}2)$$

where Y is the median value of the strong-motion parameter of interest (e.g., geometric mean spectral acceleration at a particular period), M is the earthquake magnitude, R is the source-to-site distance, and γ is a standard error term. Additional terms can be used to account for other effects including near-source directivity faulting mechanism (strike slip, reverse and normal), and site conditions.

Although many ground motion prediction equations have been developed, most apply to a specific geographic region, based on the data set of ground motion records used to develop the relationships. It is important to ensure that the selected equation is appropriate to the particular building site and earthquake source.

Appendix B lists selected North American ground motion prediction equations. The Open Seismic Hazard Analysis website, http://www.opensha.org/, provides a ground motion prediction equation plotter (under the dialog box Applications) that can be downloaded from the website and used to generate median spectra and dispersions for the listed relationships including three Next Generation Attenuation relationships (Boore and Atkinson, B_A; Campbell and Bozorgnia, C_B; Chiou and Youngs, C_Y) used by the USGS to produce the national seismic hazard maps referenced by ASCE 7-10.

For a particular earthquake scenario and site, different attenuation relationships can provide significantly different estimates of the probable values of spectral response acceleration. These differences result from differences in the data set of records used to develop each relationship and differences in the functional form of the relationships. Figure 4-1 illustrates these differences by presenting the value of 0.2-second spectral response acceleration derived using three different relationships for an M_w 7.25 event and an M_w 5.0 event for site-to-source distances ranging from 1 km to 100 km. The differences between ground motion prediction equations are sources of uncertainty associated with determining ground motion intensity for a scenario.

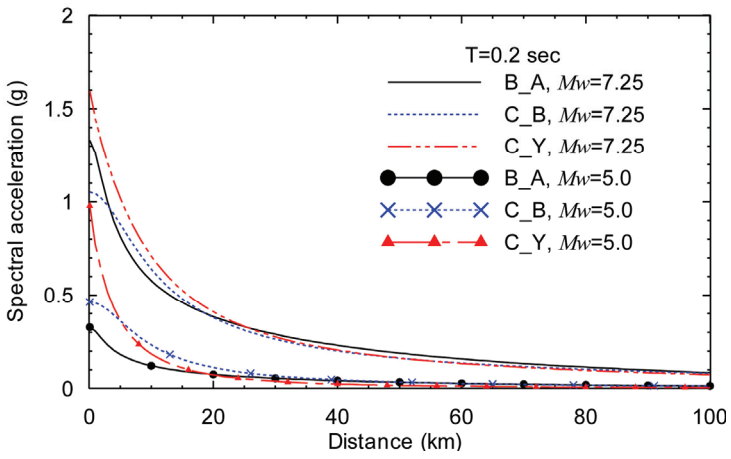

Figure 4-1 Illustration of the differences between three ground-motion prediction equations.

Some prediction equations use shear-wave velocity in the upper 30 *m* of soil as an input variable while others are applicable only for a particular soil type. If the selected equation has an input variable for shear wave velocity in the upper 30 *m*, the site-specific value should be used for seismic hazard calculations.

If the selected equation uses a generic description of the reference soil type (e.g., soft rock) and reports the reference shear wave velocity, spectra so calculated should be adjusted for the site-specific shear wave velocity in the upper 30 *m* of the soil column using either site-response analysis or site class factors such as those used in ASCE-7 and other references.

Ground motion prediction equations can be used to develop acceleration response spectra by repeatedly applying the equation to a range of periods.

In addition to uncertainties associated with the differences in response accelerations derived from different attenuation relationships, each equation includes a measure of uncertainty associated with the lack of perfect match between the values predicted by the model and the measured values of acceleration upon which they were based. Some models permit calculation of a distribution of response acceleration values. Figure 4-2 illustrates this with plots of response spectra for different probabilities of exceedance, all derived from a single ground motion prediction equation for an M_w 7.25 earthquake.

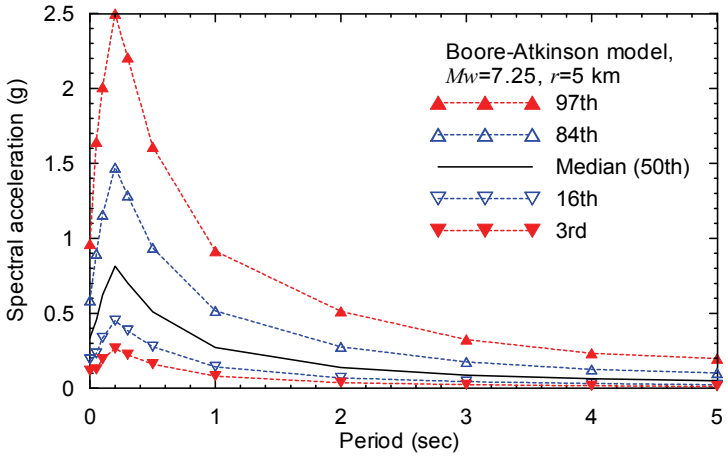

Figure 4-2 Response spectra with different probabilities of exceedance derived from a single ground-motion prediction equation for an earthquake scenario.

4.4 Nonlinear Response-History Analysis

4.4.1 Introduction

This section describes recommended procedures for selecting and scaling acceleration histories for use with nonlinear response-history analysis. The basic procedure consists of:

1. Developing an appropriate target acceleration response spectrum;

2. Selecting an appropriate suite of earthquake ground motions; and
3. Scaling the motions for consistency with the target spectrum.

The procedures presented in this Section are applicable to intensity-based, scenario-based and time-based assessments. Appendix B, Section B.7 provides an alternate procedure for use with scenario-based assessments that explicitly considers uncertainty in ground motion.

4.4.2 Target Acceleration Response Spectra

For intensity-based assessments any spectrum of the user's choice can be used. The spectral shape should be consistent with the site's geologic characteristics. For scenario-based assessments, the target spectrum should be derived directly from an appropriate ground motion prediction equation. For time-based assessments, one spectrum is required for each of the several seismic hazard intervals used for analysis. These seismic hazard intervals are selected from the site seismic hazard curve. Either: Uniform Hazard Spectra, Conditional Mean Spectra or Conditional Spectra can be used (Appendix B describes all three types). For intensities having high annual exceedance frequency, the Uniform Hazard and Conditional Mean spectra should have similar shape. For intensities having low annual exceedance frequency, the amplitude of a Conditional Mean Spectra will be smaller at some periods than the Uniform Hazard Spectrum as the Conditional Mean Spectrum quantifies a less conservative and more realistic "scenario spectrum" for the particular intensity. The Conditional Spectrum differs from the Conditional Mean Spectrum only in that it considers uncertainty in spectral values. The use of either Conditional Mean Spectra or Conditional Spectra will provide more accurate estimates of median story drift and acceleration response for a given intensity of earthquake shaking than Uniform Hazard Spectra but additional effort is required to generate these spectra.

If Conditional Mean Spectra are used, it is necessary to select an appropriate period, upon which to condition the spectra. If a building has identifiable modes associated primarily with translational response aligned approximately with two orthogonal axes, *X* and *Y*, the corresponding fundamental translational periods associated with each axis are respectively denoted T_1^X and T_1^Y. Conditional Mean Spectra should be developed, as described further in Appendix B, based on the hazard at period $\overline{T}$, the average of periods T_1^X and T_1^Y. For buildings without identifiable response modes in each of the *X* and *Y* axes, $\overline{T}$ should be taken as the period of the fundamental mode T_1.

4.4.3 Ground Motion Selection and Scaling

Basic procedures for ground motion selection and scaling include:
1) develop an appropriate target response spectra;
2) select a suite of ground motions; and
3) scale that suite for consistency with the spectrum.

The intent of ground motion selection and scaling is to obtain a set of motions that will produce unbiased estimates of median structural response when used with nonlinear response-history analysis. Limited study suggests that when the spectral shape of the selected motions matches the target spectrum well, relatively few records can provide a reasonable prediction of median response along the building height. When there is significant scatter in spectral shape of the selected records or a poor fit to the target spectrum, eleven or more pairs of motions may be needed to produce reasonable estimates of median response. Regardless fewer than 7 motion pairs should not be used.

After defining the target spectrum, ground motions are selected and scaled such that in average, they reasonably match the target spectrum over the period range T_{min} to T_{max}. For buildings with identifiable translational response modes in each of the X and Y axes, T_{max} is taken as twice the larger value of T_1^X or T_1^Y. For buildings without identifiable response modes in each of the X and Y axes, T_{max} is taken as twice the period of the fundamental period T_1. Period T_{min} is taken as the smaller of $0.2T_1^X$ or $0.2T_1^Y$. If substantial response and damage can occur due to response in modes having periods smaller than T_{min} (e.g., in high-rise buildings where multiple higher modes may contribute significantly to the acceleration and drift response) T_{min} should be selected sufficiently small to capture these important behaviors.

Select records with spectral shape similar to that of the target spectrum. Where good fit is obtained, 7 pairs of motions may be adequate. When poorer fit is obtained, at least 11 pairs are recommended.

To the extent possible, selected pairs of earthquake ground motions should have spectral shape similar to that of the target spectrum over the range of periods $T_{min} \le T \le T_{max}$. Additional factors to consider include selecting records having faulting mechanism, earthquake magnitude, site-to-source distance and local geology that are similar to those that dominate the seismic hazard at the particular intensity level, although these are not as significant as the overall spectral shape. Ground motions are available from a number of sources, including www.peer.berkeley.edu and www.cosmos-eq.org.

The subsections below present procedures to scale acceleration time series for each assessment type. For near-fault sites in the forward directivity region and/or for buildings equipped with velocity-sensitive nonstructural components and systems, ground motion selection and scaling should also consider the amplitude and shape of the scaled velocity time series.

4.4.3.1 Intensity-Based Assessment

Intensity-based assessments require a user-selected target acceleration response spectrum and suites of *n* ground motions scaled for compatibility with this spectrum. The following procedure should be used to scale the suite of records to the target spectrum:

1. Select the target response spectrum.
2. Select a candidate suite of ground motion pairs from available data sets of recorded motions.
3. Using equation 4-1, construct the geomean spectrum for each ground motion pair over the period range: $T_{min} \le T \le T_{max}$. Compare the geomean shape with that of the target. Select ground motion pairs with geomean spectra that are similar in shape to the target response spectrum within the period range $T_{min} \le T \le T_{max}$. Discard motion pairs that do not fit the shape of the target spectrum adequately.
4. Amplitude-scale both components of each ground motion pair by the ratio of $S_a(\bar{T})$ obtained from the target spectrum to the geometric mean $S_a(\bar{T})$ of the recorded components, where $\bar{T}$ is the average of periods T_1^X or T_1^Y.

4.4.3.2 Scenario-Based Assessments

Scenario-based assessments require a median response spectrum for the scenario derived from a ground motion prediction model; a measure of the dispersion associated with this spectrum; and, suites of *n* ground motion pairs scaled for compatibility with the target spectrum. Ground motion intensity is assumed to be lognormally distributed with median value θ and dispersion β. In this procedure, dispersion is indirectly considered in the procedures for response calculation (Chapter 5). Appendix B, Section B.7 presents an alternate procedure for ground motion selection that explicitly considers ground motion dispersion. If this alternative procedure is used, modeling uncertainty, discussed in Chapter 5, must be adjusted to avoid double counting.

Ground motions should be selected and scaled using the following procedure:

1. Select the scenario magnitude and site-to-source distance.
2. Select an appropriate ground motion prediction model for the region, site soil type and source characteristics.
3. Establish the period range ($T_{\max}$, $T_{\min}$).

4. Construct a median spectrum in the period range ($T_{\max}$, $T_{\min}$) using the selected ground motion prediction models.
5. Select and scale suites of *n* ground motion pairs per Steps 2 through 4 of Section 4.4.4.1 Intensity-based Assessment, above.

4.4.3.3 Time-Based Assessments

Time-based performance assessments require seismic hazard curves for spectral acceleration $S_a(\overline{T})$ and suites of ground motion pairs selected and scaled to match spectra derived from the seismic hazard curves in the period range $T_{min} \le T \le T_{max}$ over a range of exceedance probabilities. The hazard curve includes explicit consideration of ground motion uncertainty. The following two-step procedure should be used to determine analysis intensities for time-based assessments:

Step 1 – Select Intensity Range

Select a range of ground motion exceedance probabilities and corresponding spectral response accelerations, $S_a(\overline{T})$ appropriate to the structure. Select exceedance probabilities ranging from those associated with intensities that cause negligible damage to complete loss. For new buildings designed to conform to a recent edition of ASCE 7 an acceptable range is:

- Minimum exceedance frequency such that $S_a(\overline{T}) = S_a^{\min} = 0.05\ g$ for $\overline{T} \le 1$ second and $0.05 / \overline{T}\ \ g$ otherwise
- Maximum exceedance frequency of 0.0002. Take $S_a^{\max}$ as $S_a(\overline{T})$ at this exceedance frequency.

Older, non-ductile buildings are more likely to experience damage at low levels of shaking and to collapse at moderate levels of shaking than modern code-compliant buildings. For such buildings, the range of spectral accelerations suggested above should be modified. Specifically the upper limit should be adjusted so that no more than 2 of the intensities of shaking described below trigger collapse. The lower bound limit on spectral acceleration should be selected such that it does not result in damage to either structural or nonstructural components.

Step 2 – Select Analysis Intensities

Structural analysis will be performed at a series of intensities spanning the range of intensities selected in Step 1. The following procedure should be used to identify the analysis intensities:

1. Develop a seismic hazard curve for $S_a(\overline{T})$.

2. Compute the spectral accelerations $S_a^{\min}$ and $S_a^{\max}$ per Step 1 above.
3. Split the range of spectral acceleration, $S_a^{\min}$ to $S_a^{\max}$ into *m* (suggested *m* = 8) intervals; identify the midpoint spectral acceleration in each interval and the corresponding mean annual frequency of exceedance (See Figure 4-3).
4. Calculate the mean annual frequency of spectral demand within each interval $\Delta\lambda_i$ from the hazard curve and record these frequencies
5. Develop a target spectrum for the mean annual frequency of exceedance of each midpoint spectral acceleration.
6. For *each* target spectrum, select and scale suites of *n* ground motion pairs per Steps 2 through 4 of Section 4.4.4.1 (intensity-based assessment).

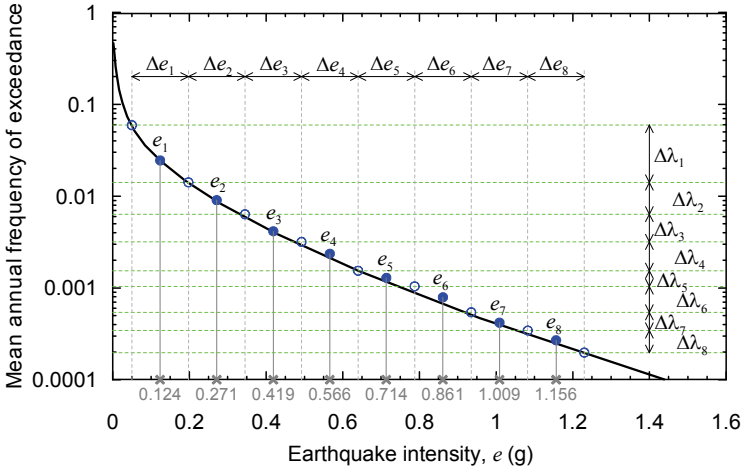

Figure 4-3 Example hazard curve showing selection, intensity intervals, midpoints and corresponding mean annual frequencies of exceedance.

4.5 Simplified Analysis

4.5.1 Introduction

This section presents procedures to characterize earthquake hazard for use with simplified analysis.

4.5.2 Intensity-Based Assessment

Earthquake intensity is defined by any user-defined 5%-damped, elastic horizontal acceleration response spectrum. Simplified analysis uses the spectral response accelerations at the fundamental period of translational response in each of two orthogonal directions, T_1^X and T_1^Y, derived from that spectrum.

4.5.3 Scenario-Based Assessment

The following procedure should be used to characterize earthquake hazard for scenario-based assessment using simplified analysis:

1. Select the magnitude and site to source distance for the scenario event.
2. Select an appropriate ground motion prediction equation for the region, site and source characteristics.
3. Determine the median values of the spectral response acceleration at the periods of the first translational mode along each axis of the building, T_1^X and T_1^Y.

4.5.4 Time-Based Assessment

Time-based assessment makes use of site-specific seismic hazard curves. See Section 4.4.3.3 for additional explanation, and guidance on selection of an acceptable range of intensities. Divide the hazard curve into *m* intervals (8 is recommended – See Section 4.4.4.3) of spectral acceleration, $S_a(\overline{T})$, where $\overline{T}$ is the average of the periods of fundamental translation response in each of the building's two orthogonal response directions. The *m* intervals of spectral acceleration should span the range of interest from shaking that causes no damage to complete loss. The following procedure should be used to characterize earthquake hazard for time-based assessment using simplified analysis:

1. Develop a seismic hazard curve for $S_a(\overline{T})$.
2. Compute the spectral accelerations $S_a^{\min}$ and $S_a^{\max}$.
3. Split the range of spectral acceleration, $S_a^{\min}$ to $S_a^{\max}$ *g*, into *m* intervals; identify the midpoint spectral acceleration in each interval and the corresponding mean annual frequency of exceedance, λ, at each end.
4. Calculate the mean annual frequency of spectral demand in each interval $\Delta\lambda_i$ (see Figure 4-3) from the hazard curve and record these frequencies
5. Develop a uniform hazard spectrum for each mean annual frequency of exceedance of Step 3.
6. For *each* of the *m* uniform hazard spectra, determine the values of the spectral response acceleration at the periods of the first translational mode along each axis of the building, T_1^X and T_1^Y.

Chapter 5
Analyze Building Response

5.1 Scope

Structural analysis provides estimates of median values of key structural response parameters that are predictive of damage including peak floor acceleration and velocity, peak transient and residual story drift.

Structural analysis is used to evaluate building response to earthquake shaking and produce estimated median values of key structural response parameters that are predictive of structural and nonstructural damage including peak floor accelerations and velocities, story drift ratios and residual drift ratios. This chapter presents two alternative structural analysis procedures that can be used for this purpose and to estimate dispersion in structural response. These procedures are not suitable for evaluation of building collapse. Use the procedures of Chapter 6 for that purpose.

Section 5.2 presents guidelines for using nonlinear response-history analysis to predict median response and dispersion. Section 5.3 describes a simplified procedure to predict median response and dispersion using elastic static analysis and knowledge of the structure's yield strength. Section 5.4 presents equations for calculating residual drift ratio, based on the results of either nonlinear response-history analysis or simplified analysis.

5.2 Nonlinear Response-History Analysis

5.2.1 Introduction

Nonlinear response history analysis can be used for performance assessment for any structure and for any ground shaking intensity. The analysis produces statistics for demands that are predictive of performance including story drift ratios, floor accelerations and velocities. These statistics are used to estimate median values and dispersions of each demand of interest, and to derive correlations between these different demand parameters.

Buildings should be modeled, analyzed and assessed as three-dimensional assemblies of components, including foundation and soil-structure interaction effects as appropriate. All structural framing and nonstructural components that contribute significant stiffness and/or strength should be explicitly included in the analytical model. Although a complete treatment of the subject is beyond the scope of this report, Subsection 5.2.2 provides limited guidance on mathematical modeling of structural and nonstructural components. Further guidance on nonlinear modeling considerations can be

found in *NEHRP Seismic Design Technical Brief No. 4, Nonlinear Structural Analysis for Seismic Design: A Guide for Practicing Engineers* (NIST, 2010), and PEER/ATC-72-1, *Modeling and Acceptance Criteria for Seismic Design and Analysis of Tall Buildings* (ATC, 2010). Subsection 5.2.3 discusses the number of ground motions pairs needed for analysis. Subsection 5.2.4. discusses recommended measures to assure the mathematical model is appropriate and analysis results are meaningful, while subsection 5.2.5 presents recommendations to characterize demand parameter uncertainties.

5.2.2 Modeling

General

Models should include all elements that provide measurable resistance to lateral displacement. Models should use nonlinear representation of components, unless it can be demonstrated they will remain elastic.

All modeled components should typically include nonlinear representation of force-deformation behavior. Elastic component representations should be substituted for nonlinear component models only if elastic response of the element is confirmed for the shaking intensities analyzed. Components can be modeled using a variety of techniques, ranging from frame elements with concentrated springs or hinges to detailed finite element and fiber type models. Whatever type model is used, it should be verified against test data and/or appropriate idealized backbone response curves, such as those in ASCE/SEI 41-06, *Seismic Rehabilitation of Existing Buildings* (ASCE, 2007) and PEER/ATC-72-1. Strength and stiffness degradation in all components and elements should be considered to the extent they are expected to significantly influence structural response for the ground motion intensities considered.

The goal of analysis is to provide an estimate of the building's response and that of its components to earthquake shaking. Median values of model parameters (e.g., initial stiffness, Q_y, or Δ_p in the force-deformation relationship of Figure 5-1) should be used if known. However, mean (expected) values are more commonly available than median values and can be used where insufficient information is available to accurately characterize the distribution and the median value.

Component force--deformation relationships

Hysteretic models should be benchmarked against cyclic laboratory test data or be referenced to standard industry approaches

Element and component models will often be enveloped by force-displacement relationships like those shown in Figure 5-1, with a single force parameter (axial lozc, shear or moment), Q, compared to a characteristic displacement (or rotation) parameter, Δ. For convenience, the curves shown in the figure are idealized as piecewise linear plots, but actual behavior is typically curvilinear. Regardless, the discrete characteristic strength and

deformation quantities shown in the figure are useful indices to either calibrate or validate component models.

Component backbone relationships can generally be characterized as being envelopes of either monotonic or cyclic loading response. Cyclic envelopes are not unique and depend on the cyclic loading protocol used in component testing. Force-deformation behavior is typically characterized by an initial stiffness, yield strength, peak strength, plastic deformations to the peak and ultimate points, and a residual strength. As shown, the deformation capacities, peak and residual strengths typically degrade with repeated cyclic loading.

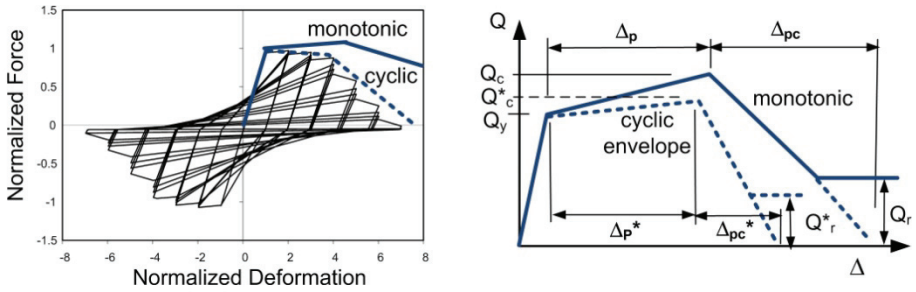

Figure 5-1 Generalized component force-deformation behaviors.

Many force-deformation relationships used for seismic assessments, such as those presented in ASCE/SEI 41-06, and reproduced in Figure 5-2, are defined based on a cyclic envelope curve so as to approximately capture cyclic effects that are not modeled directly in the analysis. Ideally, the cyclic envelope should be based on tests conducted using a standard loading protocol, such as given by ATC-24, *Guidelines for Cyclic Seismic Testing of Components of Steel Structures* (ATC, 1992), which represents the loading demands of a characteristic earthquake. Referring to Figure 5-2, the "a", "b" and "c" parameters of the ASCE/SEI 41-06 nonlinear force-deformation relationships are comparable to the Δ_p*, Δ_{pc}* and Q_r* parameters of Figure 5-1.

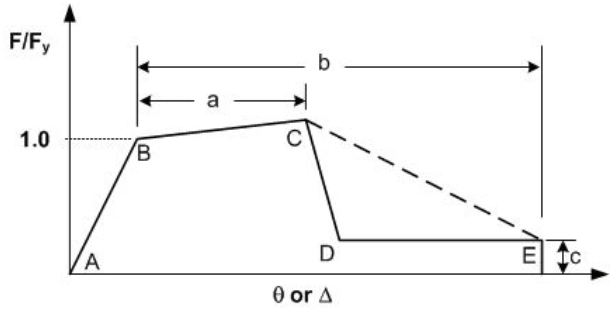

Figure 5-2 Generalized force-deformation relationship of ASCE/SEI 41-06.

The choice of backbone curve (monotonic or cyclic) will depend on whether the analysis model is capable of directly simulating the degradation of the backbone curve. Direct modeling of cyclic degradation begins with a monotonic backbone curve and degrades this relationship as the analysis proceeds, in accordance with the load path that is imposed on the component. Indirect modeling of cyclic degradation does not adjust the component backbone curve based on the specific load path, but instead, uses the cyclic envelope to define the component backbone in analysis. While it is desirable to employ direct modeling, relatively few commercial analysis software codes employ elements capable of this and indirect modeling must often be used.

Component models should account for cyclic and in-cycle strength degradation, either explicitly or implicitly

In general, the envelope of component response described by the backbone curve has a more significant effect on response than the characteristics of the cyclic loading (such as pinching behavior) between the peak excursions. As shown in Figure 5-3, cyclic degradation is often differentiated between "cyclic" and "in-cycle" degradation. Cyclic degradation is associated with the decrease in stiffness and yield strength that occurs between subsequent cycles, whereas "in-cycle" degradation occurs during a loading excursion within a cycle. Studies have shown that in-cycle degradation has a more significant effect on response, especially at large deformations beyond the peak strength (ATC, 1996; FEMA, 2005) than does "cyclic" degradation. The differences between the two are less significant for ductile components where the imposed deformations do not exceed the peak strength (less than Δ_p or Δ_p* in Figure 5-1). Further details on modeling degradation and its effects on behavior are provided in PEER/ATC-72-1, *NEHRP Seismic Design Technical Brief No. 4*, FEMA P-440A (FEMA, 2009c), and Ibarra et al. (2005).

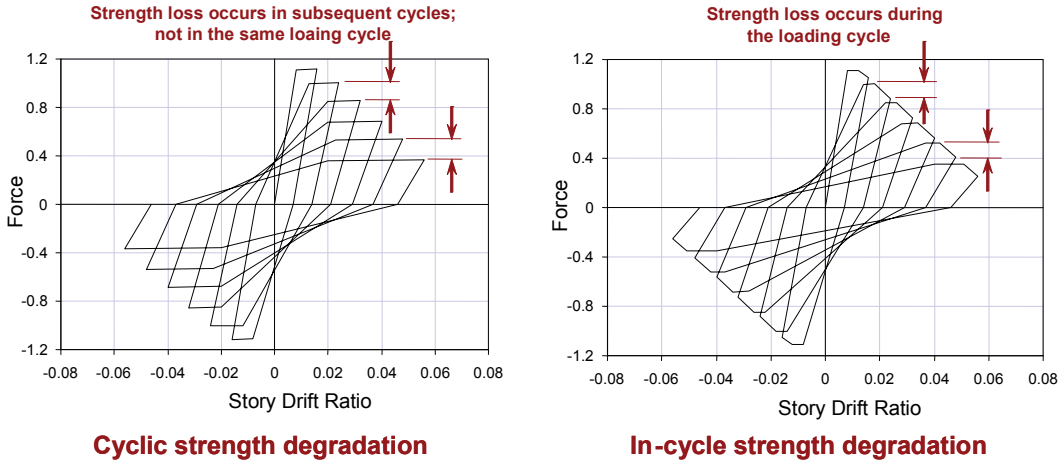

Figure 5-3 Comparison of cyclic versus in-cycle degradation of component response (FEMA, 2009c).

Geometric Nonlinear Effects

P-Δ effects can significantly increase displacements and internal member forces in the post-yield region of response. Therefore, P-Δ effects, should be accounted for in nonlinear analysis, even where elastic design provisions would otherwise allow them to be neglected.

Gravity Loads

Gravity loads incorporated in the analysis should be based on the expected dead and live loads and should including the structure's entire seismic mass. Gravity loads should typically include about 25% of the unreduced design live load.

Damping

In nonlinear dynamic analyses, most energy dissipation is modeled directly through hysteretic response of the structural components. Therefore, equivalent viscous damping assigned to the dynamic analysis model should be limited to that energy dissipation that is not otherwise captured by element hysteresis. Generally, this includes energy dissipation associated with components that are modeled as elastic but where limited cracking or yielding occurs; architectural cladding, partitions and finishes, that are not modeled; and foundations and the soil (if soil-structure interaction effects are not modeled). Equivalent viscous damping should typically be assigned in the range of 1% to 5% of critical damping in the building's predominant vibration modes. Values of 3% or less should be used for tall buildings and other structures where the damping effect of foundations and nonstructural cladding is small relative to the structural characteristics. PEER/ATC-72-1 provides further guidance on modeling of damping.

Most energy dissipation should be explicitly modeled. Equivalent viscous damping to account for components that are not modeled should typically be limited to 5% or less. In tall buildings, equivalent viscous damping should be limited to 3% or less.

Where energy dissipation components (dampers) are installed in a structural system, these components should be modeled explicitly using appropriate component models, including velocity terms to capture viscous effects and/or nonlinear springs to capture hysteretic effects.

Floor diaphragms

Floor diaphragms should be modeled using appropriate stiffness assumptions. A diaphragm can be classified as rigid if the maximum in-plane lateral deformation of the diaphragm is less than one half of the average drift in the stories above and below the subject diaphragm for the same intensity of shaking. Diaphragms that do not meet this criterion and diaphragms where significant shear transfer between vertical lines of resistance will occur, such as at out-of-plane offset discontinuities, should not be considered rigid and should be modeled explicitly using finite elements. Mass should be

distributed across the footprint of diaphragms to capture torsional and in-plane response. If diaphragms are incapable of remaining elastic at the response levels investigated, a nonlinear representation should be used.

Soil-foundation-structure interaction

Foundation rocking and sliding should be modeled, where this will occur. Soil-foundation-structure interaction should be modeled for structures on soft sites, that are deeply embedded, have large footprints and short fundamental periods.

Foundations likely to uplift or slide at the ground shaking intensities of interest should be modeled to capture these effects. Where foundation compliance will either significantly alter the structure's dynamic properties or change the structure's deformation pattern, this should also be modeled. This effect will generally be greatest for stiff buildings (small fundamental period) founded on soft soils. NIST GCR 12-917-21, *Soil-Structure Interaction for Building Structures* (NIST 2012), notes that this effect is likely to be significant for buildings with a computed fixed-base first mode period of $10V_s/h$ where V_s is the soil shear wave velocity in the upper 30 meters and h is 2/3 of the building height. The NIST report further notes that significant reductions in short period spectral demands are also likely for foundations that are deeply embedded (e.g. buildings with basements) or have large footprint. Nonlinear models of soil in the immediate building vicinity should be included in structures having these conditions. Alternatively, approximate methods of soil foundation structure interaction, such as those in FEMA 440, *Improvement of Nonlinear Static Seismic Analysis Procedures* (FEMA, 2005), can also be used.

Appendix B presents limited guidance on modeling soil-foundation-structure systems together with a discussion of the likely impact of soil-foundation-structure interaction as a function of building and foundation type and geometry, soil type and depth to bedrock, and related issues. NIST GCR 12-917-21 provides more guidance on detailed procedures that can be used, together with example applications of these procedures.

Foundation embedment

Seismic hazard assessments commonly assume that structures are located in the free field, that is, the sites are far-removed from buildings or other structures. Depending on the site and the building's dynamic characteristics, free-field motions may differ substantially from those actually experienced by a building's embedded foundation, with the greatest differences occurring for buildings with deeply embedded foundations and/or soft soil sites. For structures with basements exceeding one story in depth, consideration should be given to developing estimates of ground motion at the structure's base, rather than in the free-field. Site response analysis can be used for this purpose. Appendix B provides additional discussion on this topic.

Non-simulated deterioration and failure modes

Ideally, all significant modes of component deterioration and failure should be incorporated directly into the nonlinear analysis model. In new buildings that employ ductile detailing and capacity design concepts, the analysis can usually simulate the complete response, since inelastic deformations are concentrated in ductile elements and force demands in non-ductile (strength-controlled) elements are shielded by the yielding elements. However, in many existing buildings and new buildings that do not have well-defined yield zones protected by ductile detailing, there may be non-ductile rapid strength and stiffness degradation that is not captured in the nonlinear analysis. For example, sudden degradation in response may occur through premature shear failures in concrete columns or walls, torsional-flexural buckling of laterally un-braced steel members, or connection and splice failures. In such cases, care should be taken to assure that modeling does not over-estimate available structural resistance. Particular attention should be given to failure modes that may trigger building collapse.

Foundations are rarely included in building models but can be damaged by earthquake shaking. Damage to vulnerable foundation components can be treated as non-simulated failure modes but the appropriate fragility and consequence functions will need to be assigned to the foundations to include them in the loss calculations. For buildings with vulnerable foundations, analysis runs that produce failure-level demands on foundations should not be considered valid for purposes of obtaining response statistics.

5.2.3 Number of Analyses

The number of analyses required for each scenario or intensity level depends on the extent that spectra for the ground motions match the target spectrum.

The number of ground motion pairs necessary to obtain valid estimates of median response depends on how well the geomean spectral shape of the scaled motions matches that of the target spectrum in the period range T_{min} to T_{max} as further discussed in Chapter 4. Limited study suggests that when good match between the spectral shape of the selected motions and the target spectrum is obtained, use of relatively few records can provide a reasonable prediction of median response. When ground motions are selected without consideration of spectral shape, analyses using eleven pairs of properly scaled motions can provide a reasonable estimate (+/-20%) of median response with 75% confidence (Huang et al., 2008B). Use of fewer than 7 motion pairs is not recommended regardless of the goodness of fit of the spectra for the scaled motions to that of the target because of the extremely poor predictions of record to record variability obtained from such small suites of ground motions.

For time-based assessments, nonlinear analyses are conducted at *m* different intensity levels representing intervals along the site seismic hazard curve (see Section 4.4.4.3). A value of $m = 8$ is recommended although it may be possible to use fewer intervals for some structures and seismic hazard environments. At each intensity level, at least 7 motion pairs should be used, as described above, and if selected motions do not have appropriate spectral shape to match the target spectrum for the intensity, as many as 11 or more motions may be appropriate.

When performing nonlinear response history analysis at values of ground shaking intensity $S_a(\bar{T})$ that approach the structure's median collapse capacity, it is likely that one or more of the *n* sets of ground motion pairs will result in prediction of structural collapse, evidenced by solution instability, predicted story drift ratio that exceeds the structural model's range of analytical validity, or predicted demands that suggest the onset of one or more non-simulated collapse modes, such as shear failure of a flat slab – column joint.

While it is possible to obtain additional ground motions pairs and perform additional analyses to replace the motions that produce collapse, this is not always necessary, and for shaking intensities where the collapse probability is high, impractical and unnecessary. The following procedures are recommended when analytically predicted collapse is encountered in *q* or more sets of the *n* ground motion pairs selected for a ground motion intensity:

- In this methodology, the simulated demands used for loss calculation are conditioned on the structure not having collapsed. If an analysis predicts collapse, its results should not be included in the demand set for that ground motion intensity. Therefore the analysis results from any ground motion pair that results in prediction of collapse, either simulated or non-simulated should not be included in the suites of analyses used to predict loss. However, these analyses can be used to develop the structure's collapse fragility as further described in Chapter 6.
- If the remaining number of ground motion pairs for which collapse did not occur (n-q) is greater than or equal to 7, it is acceptable to use the remaining (n-q) analyses to obtain estimates of demand for this ground motion intensity. No further analyses are required at this ground motion intensity level.
- If the remaining number of ground motion pairs for which collapse did not occur is less than 7 and the fraction of the total analyses for this ground motion intensity q/n for which collapse is predicted is 0.3 or

less, it is likely that the remaining $(n - q)$ sets of analysis results at this ground motion intensity will not provide a valid estimate of the demands, given that collapse does not occur. Therefore, additional ground motion pairs should be selected and scaled for this shaking intensity and additional analyses performed until either 7 valid sets of analysis results are obtained or the fraction $\acute{q}/\acute{n}$ exceeds 0.3 where: $\acute{n}$ is the total number of ground motion pairs analyzed including the additional ground motion pairs, those that predicted collapse and those that did not, and $\acute{q}$ is the total number of ground motion pairs that predict collapse, including any additionally selected ground motion pairs that predict collapse.

- If the fraction of ground motion pairs that predict collapse, q/n, or $\acute{q}/\acute{n}$ exceeds 0.3, then the losses at this intensity level are likely to be dominated by collapse and the accuracy of the demand estimates obtained from the remaining sets of analyses is less critical. Therefore, in this case, it is not necessary to obtain additional ground motion pairs, or to perform additional analyses.

5.2.4 Floor Velocity

Typical outputs from nonlinear response-history analysis include peak values of story drifts and element strength demands and nonlinear deformations in individual components. Although some component fragility functions use component strength or deformation demand as the predictive parameter for damage, more generally, component fragility functions predict damage based on story drift ratio, floor acceleration or floor velocity. Most structural analysis software does not directly provide results in the form of floor accelerations or velocities and some post-processing may be needed to obtain these quantities. Floor velocity can be calculated floor by floor by numerical differentiation, the simplest form of which consists of dividing the difference in floor displacements at adjacent time steps by the time step size. If the analysis software does not directly calculate floor acceleration this can be obtained by taking a second numerical differential by dividing the difference in computed floor velocities at adjacent time steps by the time step size.

5.2.5 Quality Assurance

Nonlinear analysis is a complex process. To assure meaningful results, models should be carefully checked to establish their reliability.

Nonlinear analysis, models should be carefully checked to establish their reliability. The following are suggested steps:

- Results of linear dynamic analyses (response spectrum) should be compared to results of the nonlinear response history analyses to assess the degree of nonlinearity in the structure under various ground motion

intensities and to confirm that under low intensity motion, the nonlinear model is behaving in a manner consistent with the linear model.

- Nonlinear static lateral and gravity load analyses should be used to interrogate inelastic mechanisms, plastic deformations, and inelastic force redistributions and to confirm these with expected behavior.
- Nonlinear analyses should be run with and without P-Δ effects to establish the sensitivity of the results to gravity loads and large deformations.
- Hysteretic response plots of selected components (from nonlinear response history analysis) should be reviewed for conformance with the modeled response.

5.2.6 Uncertainty

It is usually impractical to perform sufficient numbers of analyses on sufficient numbers of structural models to obtain reliable reliable estimates of demand uncertainty from analysis.

Nonlinear response-history analysis is used to provide estimated *median* values of demand parameters (component deformations and forces, story drift ratio, floor acceleration, and floor velocity). If a sufficient number of nonlinear analyses are performed on a number of mathematical models with varied modeling assumptions, it is possible to explicitly calculate demand uncertainties associated with modeling assumptions (around the estimated median values) and the relationships or correlations between these demand parameters. However, it is usually not practical to perform sufficient numbers of analyses to obtain valid information on either response dispersion or demand parameter correlation. In this methodology, demand parameters dispersions are estimated based on judgments about the uncertainty inherent in response calculation. Despite the probable inaccuracies in demand parameter correlation indicated by small suites of analyses, this correlation information is used, due to lack of better available information.

Three sources of demand parameter uncertainty are considered: modeling uncertainty; analysis or record-to-record variability; and ground motion variability; as discussed below. Chapter 7 and Appendix G describe how the computed variability in record-to-record response is augmented to account for modeling uncertainty and, for scenario-based assessments, ground motion variability.

Modeling Uncertainty

The demand (floor accelerations and velocities, story drift ratios and residual drift ratios) distributions for selected ground motion intensities are characterized by median values and dispersions. Median values and dispersions can be obtained through development and *probabilistic analysis*

of a large family of building models whose component mechanical properties are random variables with user-specified distributions. However, the computational effort required to do this is very large. Therefore, best-estimate analysis models are used for analysis and calculated dispersions are augmented by judgmentally determined values to account for modeling uncertainty. .

Modeling uncertainty, β_m, results from inaccuracies in component modeling, damping and mass assumptions. For convenience these uncertainties are associated with building definition and quality assurance, β_c , and the quality and completeness of the nonlinear analysis model, β_q . The first of these, β_c , accounts for the possibility that the actual properties of structural elements, e.g. material strength, section dimensions, and rebar locations, may be different than those believed to exist. The latter, β_q, recognizes that our hysteretic models may not accurately capture the behavior of these elements, even if their construction is precisely known. The total modeling dispersion can be estimated using equation (5-1) and the information presented in the tables below.

Modeling uncertainty, β_m, accounts for our imprecise knowledge of a building's actual construction and also in accuracies in our ability to precisely model their inelastic behavior.

$$\beta_m = \sqrt{\beta_c^2 + \beta_q^2} \qquad (5\text{-}1)$$

Building definition and construction quality assurance. The value of the building definition dispersion, β_c , is assigned based on the quality and confidence associated with building definition. For an existing building, this will depend on the quality of the available drawings documenting the building's construction, and the level of field investigation performed to verify the documentation is accurate. For a new building this is determined based on assumptions as to how well the actual construction will match the design. Table 5-1 provides recommended values for β_c under representative conditions. Analysts should use individual judgment when selecting the values indicated in the table.

Model quality and completeness: The value of the dispersion, β_q, should be assigned on the basis of the completeness of the mathematical model and how well the structural component deterioration and failure mechanisms are understood and implemented. The dispersion should be selected on the basis of an understanding of how sensitive response predictions are to key structural parameters (e.g., strength/stiffness, deformation capacity, in-cycle and between cycle degradation of structural components) and the likely degree of inelastic response and deterioration. Table 5-2 provides guidance on the selection of β_q values.

Selection of β_q values should be guided by the expected degree of inelastic response and likelihood of component failure and building collapse. For example, component models in a building that is shaken in the elastic range only (i.e., no structural damage) need not address component deterioration and failure modes need not be simulated; a value of β_q=*0.1* is likely appropriate. Conversely, if collapse simulations are being performed, robust numerical models are required for all components expected to suffer significant damage. If such models have not been validated by large-scale testing, the model confidence should not be high, and a value of β_q in the range of 0.3 to 0.5 is likely appropriate.

Table 5-1 Default Descriptions and Values for β_c

Definition and Construction Quality Assurance	β_c
Superior Definition New Buildings - The building is completely designed and will be constructed with rigorous construction quality assurance, including special inspection, materials testing and structural observation. Existing Buildings - Drawings and specifications are available and field investigation confirms they are representative of the actual construction, or if not, that the actual construction is understood. Extensive material testing confirms the strength of materials.	.10
Average Definition New Buildings - The building is defined to the level typical in design development, or construction quality assurance and inspection are anticipated to be of limited quality. Existing Buildings. Documents defining the building's design are available and are confirmed by visual observation. Limited material testing generally confirms material properties.	0.25
Limited Definition New Buildings. Design is completed to a schematic or similar level of detail. Existing Buildings. Construction documents are not available and knowledge of the structural system is based on limited field investigation. Material properties are based on typical values for buildings of the type, location and construction age.	0.40

Regardless of the relative values of β_c and β_q, derived using *Tables 5-1 and 5-2*, the total uncertainty computed using equation 5-1 should never be taken greater than 0.5.

Table 5-2 Default Descriptions and Values for β_q

Model Quality and Completeness	β_q
Model quality: The numerical model is robust over the anticipated range of response. Strength and stiffness deterioration and all likely failure modes are modeled explicitly. Model accuracy is established with data from large-scale component tests through failure. *Completeness*: The mathematical model includes all structural components and nonstructural components in the building that contribute strength and/or stiffness.	.10
Model quality: The numerical model for each component is robust over the anticipated range of displacement or deformation response. Strength and stiffness deterioration is fairly well represented, though some failure modes are simulated indirectly. Accuracy is established through a combination of judgment and large-scale component tests. *Completeness*: The mathematical model includes most structural components and nonstructural components in the building that contribute significant strength and/or stiffness.	0.25
Model quality: The numerical model for each component is based on cyclic envelope curve models of ASCE/SEI 41-06 or comparable guidelines, where strength and stiffness deterioration and failure modes are incorporated indirectly. *Completeness*: The mathematical model includes all structural components in the lateral-force-resisting system.	0.40

Record-to-Record Variability

For structures having nonlinear response or response in multiple modes, each record will produce somewhat different predictions of peak response quantities (or demands), resulting in record to record variability. Unless a very large number of ground motion pairs, on the order of 30 or more, are used, dispersion values obtained from the analyses will generally not be accurate. Large suites of records are needed to capture this effect properly.

Use of a smaller number of ground motions, will either underestimate or overestimate true record-to-record variability in each demand parameter and also the correlation between demand parameters. This methodology assumes that computed record-to-record response variability and demand correlation coefficients computed using small numbers of ground motions are sufficiently accurate.

Ground Motion Variability

For scenario-based assessment, it is necessary to account for uncertainty in the shape and amplitude of the target spectrum. Table 5-3 lists suggested values for ground motion spectral demand dispersion, β_{gm}, based on widely accepted ground motion prediction equations for Western North America (WNA); the Central and Eastern United States (CEUS); and the Pacific North West (PNW). The values of β_{gm} appropriate to the specific ground motion

prediction equations used to derive the target spectrum should be substituted for these.

Table 5-3 Default Dispersions Ground Motion Variability

$\bar{T}, T_1$ (sec)	β_{gm} [1]		
	WNA	CEUS	PNW
<0.20	0.60	0.53	0.80
0.35	0.60	0.55	0.80
0.5	0.61	0.55	0.80
0.75	0.64	0.58	0.80
1.0	0.65	0.60	0.80
1.50	0.67	0.60	0.85
2.0+	0.70	0.60	0.90

Residual Drift

Residual drift ratios for each analysis should be determined using the procedures of Section 5.4

5.3 Simplified Analysis

5.3.1 Introduction

Simplified procedures use linear structural models and estimate of the structure's lateral yield strength to estimate median values of response parameters.

The simplified procedure uses linear mathematical structural models and an estimate of the structure's lateral yield strength to estimate median values of response parameters. Structures are assumed to have independent translational response in each of two horizontal axes (denoted *X* and *Y*). Separate analysis is performed along each axis. The affects of vertical earthquake shaking, torsion and soil-foundation-structure interaction are neglected.

Assumptions that underlie the simplified procedure include:

(a) building framing is independent along each horizontal axis, permitting the framing systems along each axis to be uncoupled and torsional response ignored;

(b) the building is regular in plan and elevation (i.e., there are no substantial discontinuities in lateral strength and stiffness);

(c) story drift ratios do not exceed 4 times the corresponding yield drift ratio, so that the assumptions of elastic-plastic (bilinear) response at the component level is not compromised by excessive degradation in strength and stiffness;

(d) *P*-Δ effects are not included, therefore, story drifts ratios are limited to 4%, beyond which may *P*-Δ effects may become important; and

(e) building height is less than 15 stories.

To the extent that buildings do not conform to these assumptions, the results of simplified analysis may not be reliable. Even for buildings that do conform to the above assumptions, the simplified procedures entail much greater uncertainty as to the true value of the medians and also the dispersion associated with the demands. Therefore, this procedure will result in projections of performance that are somewhat different from and entail greater uncertainty than when the nonlinear methods are used.

5.3.2 Modeling

Mathematical models should appropriately represent the building's distribution of mass and stiffness. All elements that contribute significantly to the building's lateral strength or stiffness should be included in the model, whether or not these elements are considered to be structural or nonstructural, or part of the seismic force-resisting system. ASCE/SEI 41-06 provides guidance for modeling the strength and stiffness of typical building elements.

The mathematical model should appropriately represent the building's distribution of stiffness and mass and should include all elements that significantly contribute to the building's lateral strength or stiffness, whether or not they are considered structural or part of the lateral force resisting system.

The mathematical model is used to establish the building's first mode period and shape in each of two orthogonal axes. These periods and mode shapes are used to compute pseudo lateral forces which are statically applied to the model to determine story drift ratios. This information, together with estimates of the peak ground acceleration, peak ground velocity and the structure's yield strength, is used to compute median estimates of peak story drift ratio, peak floor acceleration and peak floor velocity in each building direction.

The structure's lateral yield strength can be estimated by either nonlinear static analysis, per ASCE/SEI 41-06, plastic analysis or, for building's designed in accordance with ASCE/SEI 7-10, *Minimum Design Loads for Buildings and Other Structures* (ASCE, 2010), using the response modification factor, R, and the overstrength factor, Ω_0. This latter approach is appropriate only when minimal information is available as to the structure's actual design, as may occur during schematic or preliminary design phases. In these phases, the structure's yield strength can be taken in the range given by formula 5-2 below. Individual judgment as to the structure's actual strength must be applied in evaluating equation (5-2).

$$\frac{1.5S_a(T)W}{R/I} \le V_y \le \frac{\Omega_o S_a(T)W}{R/I} \qquad (5\text{-}2)$$

In the above formula, $S_a(T)$ is the structure's design spectral response acceleration, as defined in ASCE/SEI 7-10, evaluated at its fundamental

period in the direction under consideration, and R, Ω_o and I are the elastic design coefficients appropriate to the structural system and occupancy.

5.3.3 Analysis Procedure

Figure 5-4 presents the definitions of floor and story numbers and story height adopted for use with the Simplified procedures. An independent analysis for each of two principal orthogonal building axes is required.

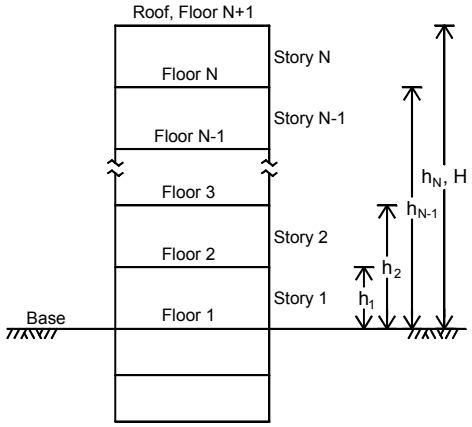

Figure 5-4 Definition of floor, story numbers and floor heights above grade.

Pseudo Lateral Force

In each direction, a pseudo lateral load, V, is used to compute story drift ratios, velocities and accelerations. The load V in each direction is computed using equation (5-3):

$$V = C_1 C_2 S_a\left(T_1\right) W_1 \tag{5-3}$$

where C_1 is an adjustment factor for inelastic displacements; C_2 is an adjustment factor for cyclic degradation; $S_a(T_1)$ is the 5% damped spectral acceleration at the fundamental period of the building in the direction under consideration, for the selected level of ground shaking; and W_1 is the building's first modal weight in the direction under consideration, but cannot be taken as less than 80% of the total weight, W. If building response is elastic, coefficients C_1 and C_2 are set equal to 1.0.

The first modal weight, W_1, can be calculated as

$$W_1 = \frac{\left(\sum_{j=2}^{N+1} w_j \phi_{j1}\right)^2}{\sum_{j=2}^{N+1} w_j \phi_{j1}^2} \tag{5-4}$$

where w_j is the lumped weight at floor level j (see Figure 5-4), ϕ_{j1} is the jth floor ordinate of the first mode deflected shape and N is the number of floors in the building *above* the base. In the absence of calculation per equation 5-4, W_1 can be set equal to $C_{sm}W$, where C_{sm} is defined in ASCE/SEI 41-06.

The adjustment factor, C_1, is computed as:

$$\begin{aligned} C_1 &= 1 + \frac{S-1}{0.04a} && \text{for } T_1 \le 0.2\,\text{sec} \\ &= 1 + \frac{S-1}{aT_1^2} && \text{for } 0.2 < T_1 \le 1.0\,\text{sec} \\ &= 1 && \text{for } T_1 > 1.0\,\text{sec} \end{aligned} \tag{5-5}$$

where T_1 is the fundamental period of the building in the direction under consideration, a is a function of the soil site class (= 130, 130, 90, 60 and 60 for ASCE/SEI 7-10 site classes A, B, C, D and E, respectively) and S is a strength ratio given by equation (5-6):

$$S = \frac{S_a(T_1)W}{V_{y1}} \tag{5-6}$$

where V_{y1} is the (estimated) yield strength of the building in first mode response, and W is the total weight. V_{yt} should be determined by a suitable nonlinear static analysis procedure, such as that contained in ASCE/SEI 41-06. If S has a value less than or equal to 1.0 then C_1 is taken as having a value of 1.0.

When the value of S is less than or equal to 1.0, C_2 is also taken as unity. When S has a value greater than 1.0, the adjustment factor C_2 is computed as:

$$\begin{aligned} C_2 &= 1 + \frac{(S-1)^2}{32} && \text{for } T_1 \le 0.2\,\text{sec} \\ &= 1 + \frac{1}{800}\frac{(S-1)^2}{T_1^2} && \text{for } 0.2 < T_1 \le 0.7\,\text{sec} \\ &= 1 && \text{for } T_1 > 0.7\,\text{sec} \end{aligned} \tag{5-7}$$

If the building incorporates viscous or viscoelastic damping devices, the 5% damped spectral acceleration ordinate should be replaced by the value that corresponds to the first mode damping in the building. The procedures of ASCE/SEI 41-06 can be used to estimate the damping in a building equipped with viscous or viscoelastic energy dissipation devices and to adjust the response spectrum for the effects of damping other than 5%.

Median Estimates of Demand

Estimates of median story drift ratio, Δ_i^*, floor acceleration, a_i^*, and floor velocity V_i^* are computed in the following steps:

1. Determine the distribution of the pseudo lateral force *V* obtained from equation 5-3, over the building height.
2. Apply the lateral forces to the elastic model and the floor displacements and uncorrected story drifts are determined. Story drifts are divided by story heights to obtain story drift ratios.
3. The story drift ratios are corrected to account for inelastic action and/or higher mode effects.
4. Peak ground acceleration is used to estimate peak floor acceleration at each floor.
5. Peak ground velocity is used to estimate peak floor velocity at each floor.

These steps are described in greater detail below.

Step 1 – Determine vertical distribution of force.

The pseudo lateral force, F_x, at floor level *x*, is given by:

$$F_x = C_{vx} V \tag{5-8}$$

where, C_{vx} is a vertical distribution factor given by:

$$C_{vx} = \frac{w_x h_{x-1}^k}{\sum_{j=2}^{N+1} w_j h_{j-1}^k} \tag{5-9}$$

w_j is the lumped weight at floor level *j*; h_{j-1} (h_{x-1}) is the height above the effective base of the building to floor level *j*; and *k* is equal to 2.0 for a first mode period greater than 2.5 seconds and equal to 1.0 for a first mode period less than or equal to 0.5 second (linear interpolation can be used for intermediate periods).

Step 2 – Compute floor displacements and story drift ratios

The lateral forces, F_x, at each level are simultaneously applied to the analytical model. The displacement of each floor relative to the base under these applied forces is computed. The uncorrected story drift ratio at each level, Δ_i, is determined as the difference between the lateral displacements of the floors immediately above and below the story, divided by the story height.

Step 3 – Correct story drift ratios for inelastic behavior and higher modes

Estimates of median story drift ratio, Δ_i^*, at each level "*i*" are computed from the formula:

$$\Delta_i^* = H_{\Delta i}\left(S, T_1, h_i, H\right)\Delta_i \qquad (5\text{-}10)$$

where $H_{\Delta i}\left(S, T_1, h_i, H\right)$ is the drift correction factor for story *i* computed using equation (5-11):

$$\ln\left(H_{\Delta i}\right) = a_0 + a_1 T_1 + a_2 S + a_3 \frac{h_i}{H} + a_4 \left(\frac{h_i}{H}\right)^2 + a_5 \left(\frac{h_i}{H}\right)^3, \; S \geq 1, \; i = 1 \text{ to } N \qquad (5\text{-}11)$$

and the values of the coefficients a_0 through a_5 are obtained from Table 5-4 for structures less than 9 stories in height and Table 5-5 for structure 10-15 stories in height, respectively. In this formula, *S* is the strength ratio previously defined; T_1 is the first mode period; and *H* is the total building height above the base.

Step 4 – Convert peak ground acceleration to peak floor acceleration

At the building base, take peak floor acceleration as equal to the peak ground acceleration. At other floor levels, *i*, the estimated median peak floor acceleration, a_i^*, is derived from the peak ground acceleration using the formula:

$$a_i^* \quad H_{ai} \; S, T, h_i, H \quad pga_i \quad i = 2 \text{ to } N+1 \qquad (5\text{-}12)$$

where *pga* is the peak ground acceleration and $H_{ai}(S, T_1, h_i, H)$ is the acceleration correction factor for floor *i* calculated using equation 5-13:

$$\ln\left(H_{ai}\right) = a_0 + a_1 T_1 + a_2 S + a_3 \frac{h_i}{H} + a_4 \left(\frac{h_i}{H}\right)^2 + a_5 \left(\frac{h_i}{H}\right)^3, \; S \geq 1, \; i = 2 \text{ to } N+1 \qquad (5\text{-}13)$$

Obtain the values of coefficients a_0 through a_5 from Table 5-4 for structure 9 stories or less in height and Table 5-5 for structures 10 to15 stories in height. If the building response is elastic, set *S* equal to 1 in equation (5-13).

Step 5 – Convert peak ground velocity to peak floor velocity accounting for inelastic action and higher mode effects

At the building base the peak floor velocity is taken as the peak ground velocity (*PGV*). The peak ground velocity can be calculated by seismic hazard analysis for intensity- or time-based assessments or using a ground motion prediction equation for a scenario-based assessment. If this information is unavailable, the peak ground velocity along each building axis

can be estimated by dividing the spectral velocity at a period of one second by 1.65 (Newmark and Hall 1982, Huang et al. 2012).

Table 5-4 Correction Factors for Story Drift Ratio, Floor Velocity and Floor Acceleration for 2 to 9 Story Buildings

	Frame type	a_0	a_1	a_2	a_3	a_4	a_5
Story drift ratio	Braced	0.90	-0.12	0.012	-2.65	2.09	0
	Moment	0.75	-0.044	-0.010	-2.58	2.30	0
	Wall	0.92	-0.036	-0.058	-2.56	1.39	0
Floor velocity	Braced	0.15	-0.10	0	-0.408	0.47	0
	Moment	0.025	-0.068	0.032	-0.53	0.54	0
	Wall	-0.033	-0.085	0.055	-0.52	0.47	0
Floor acceleration	Braced	0.66	-0.27	-0.089	0.075	0	0
	Moment	0.66	-0.25	-0.080	-0.039	0	0
	Wall	0.66	-0.15	-0.084	-0.26	0.57	0

Table 5-5 Correction Factors for Story Drift Ratio, Floor Velocity and Floor Acceleration for 10 to 15 Story Buildings

	Frame type	a_0	a_1	a_2	a_3	a_4	a_5
Story drift ratio	Braced	1.91	-0.12	-0.077	-3.78	6.43	-3.42
	Moment	0.67	-0.044	-0.098	-1.37	1.71	-0.57
	Wall	0.86	-0.036	-0.076	-4.58	6.88	-3.24
Floor velocity	Braced	0.086	-0.10	0.041	0.45	-2.89	2.57
	Moment	-0.020	-0.068	0.034	0.32	-1.75	1.53
	Wall	-0.11	-0.085	0.11	0.87	-4.07	3.27
Floor acceleration	Braced	0.44	-0.27	-0.052	3.24	-9.71	6.83
	Moment	0.34	-0.25	-0.062	2.86	-7.43	5.10
	Wall	-0.13	-0.15	-0.10	7.79	-17.52	11.04

Spectral velocity at a period of 1 second can be derived from spectral acceleration a t a period of one second using the formula:

$$S_v(1) = \frac{S_a(1)}{2\pi} g \tag{5-14}$$

where $S_a(1)$ is the spectral acceleration at 1 second period. Peak ground velocity can then be approximated as:

$$PGV = \frac{S_v(1)}{1.65} \tag{5-15}$$

At other floor levels, *i*, the estimated median peak floor velocity v_i^* relative to a fixed point in space is computed from the peak ground velocity using the formula:

$$v_i^* \quad H_{vi} \; S,T,h_i,H \quad v_{si} \quad i \quad 2 \text{ to } N \quad 1 \tag{5-16}$$

where H_{vi} is computed from the equation:

$$\ln\left(H_{vi}\right) = a_0 + a_1 T_1 + a_2 S + a_3 \frac{h_i}{H} + a_4 \left(\frac{h_i}{H}\right)^2 + a_5 \left(\frac{h_i}{h}\right)^3 \;,\; S \geq 1,\; i = 2 \text{ to } N+1 \tag{5-17}$$

where the coefficients a_0 through a_5 are given in Table 5-4 for structures 9 or fewer stories tall and Table 5-5 for structures 10 to 15 stories tall. The reference floor velocity v_{si} is determined from equation 5-18:

$$v_{si} = PGV + 0.3 \frac{T_1}{2\pi} \left(\frac{V_{y1}}{W_1 / g} \Gamma_1\right) \left(\frac{\delta_i}{\delta_r}\right) \tag{5-18}$$

where T_1 is the structure's first mode period, V_{y1} is the structure's effective yield strength in first mode response, W_1 is the first modal building weight taken not less than 80% of the total weight, Γ_1 is the first mode participation factor, δ_i is the uncorrected displacement of floor i estimated using the linear procedure, δ_r is the uncorrected roof displacement with respect to the building base estimated by the linear procedure before any correction, and all other terms have been previously defined.

Median Residual Drift Ratio

Residual drift ratios should be calculated using the story drift ratios computed above and the procedures of Section 5.4. Note that the simplified elastic procedure should not be used for computing story drift ratios in excess of four times the yield story drift ratio. The yield story drift ratio should be computed as discussed previously.

Dispersions in Response Calculations

To conduct performance assessments, it is necessary to develop distributions of story drift, floor acceleration and floor velocity, where the distributions capture the uncertainty in ground motion, β_{gm}, analysis, $\beta_{a\Delta}$, β_{aa}, and, β_{av}, and modeling, β_m. Table 5-6 lists default values of the dispersion to be used with the simplified analysis procedure. Linear interpolation can be used to estimate values of the β coefficients for intermediate values of T_1 and *S*.

Table 5-6 Default Dispersions for Record-to-Record Variability and Modeling Uncertainty

T_1 (sec)	$S = \frac{S_a(T_1)W}{V_{y1}}$	$\beta_{a\Delta}$	β_{aa}	β_{av}	β_m
0.20	≤ 1.00	0.05	0.10	0.50	0.25
	2	0.35	0.10	0.51	0.25
	4	0.40	0.10	0.40	0.35
	6	0.45	0.10	0.37	0.50
	≥ 8	0.45	0.05	0.24	0.50
0.35	≤ 1.00	0.10	0.15	0.32	0.25
	2	0.35	0.15	0.38	0.25
	4	0.40	0.15	0.43	0.35
	6	0.45	0.15	0.38	0.50
	≥ 8	0.45	0.15	0.34	0.50
0.5	≤ 1.00	0.10	0.20	0.31	0.25
	2	0.35	0.20	0.35	0.25
	4	0.40	0.20	0.41	0.35
	6	0.45	0.20	0.36	0.50
	≥ 8	0.45	0.20	0.32	0.50
0.75	≤ 1.00	0.10	0.25	0.30	0.25
	2	0.35	0.25	0.33	0.25
	4	0.40	0.25	0.39	0.35
	6	0.45	0.25	0.35	0.50
	≥ 8	0.45	0.25	0.30	0.50
1.0	≤ 1.00	0.15	0.30	0.27	0.25
	2	0.35	0.30	0.29	0.25
	4	0.40	0.30	0.37	0.35
	6	0.45	0.30	0.36	0.50
	≥ 8	0.45	0.25	0.34	0.50
1.50	≤ 1.00	0.15	0.35	0.25	0.25
	2	0.35	0.35	0.26	0.25
	4	0.40	0.30	0.33	0.35
	6	0.45	0.30	0.34	0.50
	≥ 8	0.45	0.25	0.33	0.50
2.0+	≤ 1.00	0.25	0.50	0.28	0.25
	2	0.35	0.45	0.21	0.25
	4	0.40	0.45	0.25	0.35
	6	0.45	0.40	0.26	0.50
	≥ 8	0.45	0.35	0.26	0.50

For intensity-based assessments and time-based assessments, separate values of dispersion for acceleration, velocity and drift demands are required. Story drift dispersion is given by:

$$\beta_{SD} = \sqrt{\beta_{a\Delta}{}^2 + \beta_m{}^2} \tag{5-19}$$

Dispersion in acceleration demand is given by:

$$\beta_{FA} = \sqrt{\beta_{aa}{}^2 + \beta_m{}^2} \tag{5-20}$$

Dispersion in velocity demand is given by:

$$\beta_{FV} = \sqrt{\beta_{av}^2 + \beta_m^2} \tag{5-21}$$

For scenario-based assessments, the values of story drift dispersion and floor acceleration dispersion must also include uncertainty in attenuation, β_{gm}, obtained from Table 5-3, and is respectively given by:

$$\beta_{SD} = \sqrt{\beta_{a\Delta}{}^2 + \beta_m{}^2 + \beta_{gm}{}^2} \tag{5-22}$$

$$\beta_{FA} = \sqrt{\beta_{aa}{}^2 + \beta_m{}^2 + \beta_{gm}{}^2} \tag{5-23}$$

$$\beta_{FV} = \sqrt{\beta_{av}^2 + \beta_m^2 + \beta_{gm}^2} \tag{5-24}$$

5.4 Residual Drift

Residual drifts predicted by nonlinear analysis are highly sensitive to the assumed component models including the post-yield hardening/softening slope and unloading response. Accurate statistical simulation of residual drifts requires the use of advanced component models with careful attention paid to cyclic hysteretic response and a large number of ground motion pairs.

Nonlinear analysis using hysteretic element properties available in nonlinear analysis software commonly used in design offices does not provide accurate assessments of residual drift.

Since such analysis is not presently practical for wide scale implementation, median residual drift ratio, denoted Δ_r, can be estimated as:

$$\begin{aligned} \Delta_r &= 0 && \Delta \le \Delta_y \\ \Delta_r &= 0.3\left(\Delta - \Delta_y\right) && \Delta_y < \Delta < 4\Delta_y \\ \Delta_r &= \left(\Delta - 3\Delta_y\right) && \Delta \ge 4\Delta_y \end{aligned} \tag{5-25}$$

where Δ is the median story drift ratio calculated by analysis and Δ_y is the median story drift ratio at yield calculated by analysis. Appendix C provides background information on the basis for these relationships.

The yield drift ratio, Δ_y, is the story drift ratio at which significant yielding in the structure occurs. For concentrically steel braced frame systems (or for squat wall systems), the yield drift ratio can be calculated as the story drift ratio associated with imposed story shear forces equal to the expected yield strength of the braces (or the expected shear strength of the walls). For moment frame systems, the yield drift ratio can be calculated as the story drift associated with story shear forces that cause (a) the beams and/or columns to reach their expected plastic moment capacity, taking into account the effect of axial forces in the members, or (b) the beam-column joint panel to reach its expected yield strength. The distribution of forces in the story under consideration can be calculated either based on the forces induced

using equivalent lateral forces, or alternatively, by applying a shear force at the floor above the story being evaluated with a lateral support imposed at the floor below the story being evaluated. In shear wall systems whose behavior is dominated by flexural yielding, the yield drift ratio is equal to the story drift ratio associated with the wall reaching its expected flexural strength under a lateral load distribution that reflects the dynamic response of the building.

When nonlinear response history analysis is used, calculate the residual drift ratio, Δ_i, using equation 5-18 and the story drift ratios calculated from the suite of analyses at each level. When simplified analysis is used, calculate the residual drift, Δ_r, at each level using value of median transient drift, Δ_i^*, calculated using the procedures of Section 5.3.

The dispersion in the residual drift is generally larger than that of the story drift. When Simplified Analysis is used, the total dispersion in the residual drift due to both record-to-record variability, β_a, and modeling, β_m, should be set equal to 0.8 (Ruiz-Garcia and Miranda, 2005). When response history analysis is used, the dispersion in residual drift, β_{RD}, can be taken from the equation:

$$\beta_{RD} = \sqrt{\beta_a^2 + \beta_{ARD}^2} \tag{5-26}$$

where β_a is the dispersion in residual drift obtained from the suite of analyses and β_{ARD} is set equal to 0.2.

Chapter 6
Develop Collapse Fragility

6.1 Introduction

This chapter presents several alternative procedures to establish building-specific collapse fragility functions that are necessary to perform meaningful assessments of potential casualties. The probability of building collapse is expressed as a function of spectral acceleration at the building's effective first mode period and is assumed to follow a lognormal distribution, defined by a median value, $\hat{S}_a(T)$, and dispersion, β.

The present state of art for collapse fragility function development is through use of Incremental Dynamic Analysis, a computationally intensive procedure described in FEMA P-695, *Quantification of Building Seismic Performance Factors* (FEMA, 2009n) and also in Appendix J of this report. This technique is rarely practical in non-research applications. A more practical alternative is to perform a limited suite of nonlinear response-history analyses at several intensity levels that produce some collapse predictions and to develop the collapse fragility function from the resulting collapse statistics. Collapse fragility functions for low-rise buildings can be approximated using a simplified procedure based on nonlinear static (pushover) analysis. Collapse fragilities for buildings conforming to the requirements of recent building codes can be inferred based on the target collapse resistance inherent in the building code.

Building collapse is generally associated with failure of the gravity-load framing system, either locally or globally. There are few examples of buildings overturning, aside from those that experienced soil or foundation (pile) failures. Excessive story displacements, which can lead to a near-complete loss of lateral stiffness, can trigger a failure of both vertical and horizontal components. In this methodology, collapse is defined as either:

Collapse is considered to occur if excessive sidesway leads to P-Δ instability or portions of the gravity load carrying system lose ability to continue to support gravity loads.

- sidesway failure, characterized by loss of lateral stiffness and development of P-Δ instability, or
- loss of vertical load carrying capacity of gravity framing members due to earthquake-induced building drifts.

Although analytical software such as LS-DYNA and ABAQUS that employ explicit solution techniques can directly simulate collapse, typical analytical

software used in engineering offices employ implicit solution techniques that are unable to do so. Instead, vertical collapse is assumed when numerical instability occurs in dynamic structural analysis or predicted lateral displacements exceed the modeling validity range, for example, when computed deformation demands on elements are larger than the range for which the hysteretic model is appropriate. Loss of vertical capacity in gravity framing components, typically predicted by excessive strength or deformation demands is included in the collapse assessment and development of collapse fragility functions.

6.2 Nonlinear Response-History Analysis

6.2.1 Introduction

Nonlinear response-history analysis is the most reliable method of establishing collapse fragility functions. The basic process entails performing large suites of nonlinear response-history analyses at multiple intensity levels ranging from intensities that produce near linear response to intensities that cause collapse, as evidenced by numerical instability, very large drift response, or demands exceeding the failure capacity of gravity-load bearing elements, for a large fractile of the analyses at the intensity level. A smooth lognormal distribution is fit to the fraction of ground motions at each intensity level that produced collapse predictions.

6.2.2 Incremental Dynamic Analysis

Incremental Dynamic Analysis, described in detail in *FEMA P-695*, though numerically intensive, can be used to derive collapse fragility functions.

Incremental Dynamic Analysis is an application used by researchers to determine collapse fragility functions for structures of different types. In this method, a large suite of suitable ground motion pairs, on the order of 20 or more, is selected. Each ground motion pair is scaled to an initial intensity level, characterized by a common value of the geomean spectral response acceleration at the structure's effective first mode period, $S_a\left(\overline{T}\right)$. The structure is subjected to nonlinear dynamic analysis, using each of these ground motion pairs, and the number of analyses that produce predictions of collapse is determined. Then, the ground motion amplitudes are incremented, and the process repeated until 50% or more of the analyses at the intensity level result in predicted collapse. The intensity $S_a\left(\hat{T}\right)_{50}$ at which 50% of the analyses predict collapse is taken as the median collapse intensity. A dispersion is fit to the collapse data and modified to account for other uncertainties. Figure 6-1 illustrates the data obtained from the Incremental Dynamic Analysis technique and the probabilistic distribution of collapse (collapse fragility function) inferred from the analysis for a

hypothetical structure. Appendix J provides more detailed guidance on this technique.

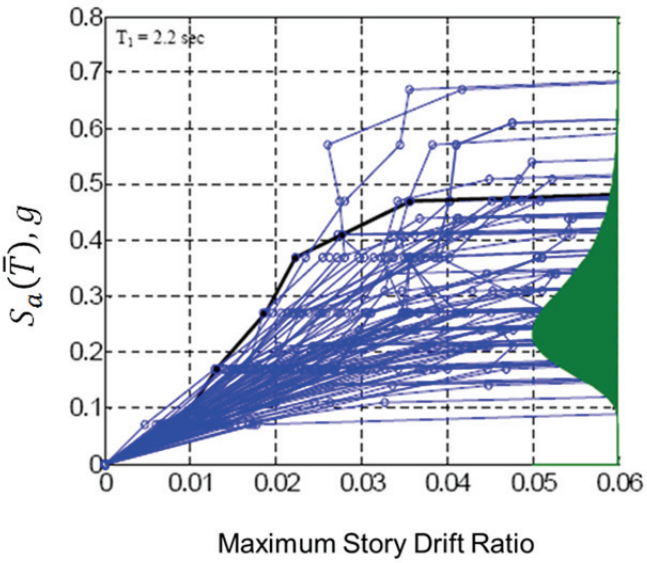

Figure 6-1 Sample Incremental Dynamic Analysis results for a hypothetical building.

6.2.3 Limited-Suite Nonlinear Analysis

In this approach, nonlinear response-history analyses are performed at a number of intensity levels, some of which produce predictions of collapse, where collapse is defined by one of the following:

- Numerical instability
- Simulated collapse
- Non-simulated collapse, consisting of predicted demands on one or more gravity load bearing elements that exceed the level at which they can continue to reliably support gravity load

Such analyses will be an inherent part of time-base assessment when nonlinear response-history analysis is used. At each intensity level, I, an estimated conditional probability of collapse, $P(C|I)$ is obtained from the equation:

$$P(C|I) = \frac{n}{N} \tag{6-1}$$

where, n is the number of analyses at intensity I for which collapse is predicted and N is the total number of analyses performed at intensity I. A plot of the estimated conditional probability of collapse can be developed as

a function of intensity and a lognormal distribution fitted to the data using an appropriate estimate of the dispersion, such as shown in Figure 6-2 below. A spreadsheet tool that automates the calculation for curve fitting is included in Volume 3. A dispersion of not less than 0.6 is recommended when this procedure is used.

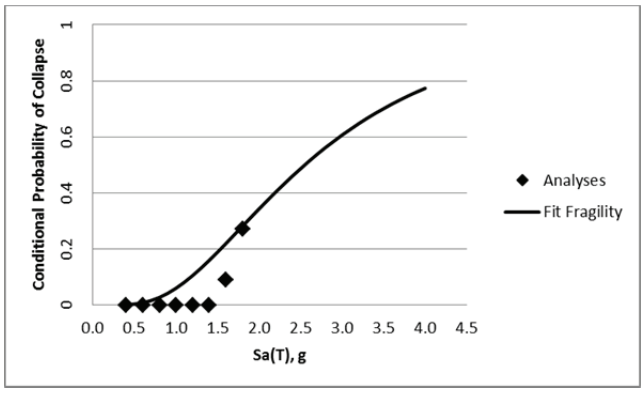

Figure 6-2 Illustration of collapse fragility estimated using nonlinear analysis at several intensity levels.

To obtain reliable estimates of collapse fragility, a large number of ground motions, on the order of 20, should be used. However, estimates obtained with as few as 7 analyses per intensity level are likely of comparable quality to those obtained using the simplified method described in Section 6.3, and of much better quality than obtained by the judgmental method described in Section 6.4. When fitting a lognormal distribution to the data obtained from such analyses, it is best to link the fitted curve to the data at a point near the median as small suites of analyses will produce very unreliable data when only a small fraction of the analyses predict collapse.

Figure 6-2 above illustrates this approach for a hypothetical structure for which time-based analysis is performed using suites of 10 nonlinear response history analyses each at values of $S_a\left(\overline{T}\right)$ of 0.4g, 0.6g, 0.8g, 1.0g, 1.2g, 1.4g, 1.6g, and 1.8g. In this example, the analyses predict three collapses at an intensity $S_a\left(\overline{T}\right)=1.8g$, one at 1.6g, and none at lower intensities. The lognormal distribution is fit to these data with a judgmentally selected median of 2.6g and a dispersion of 0.6. As noted above, the smoothed distribution has been fit to the upper data point, which is near the median.

6.2.4 Mathematical Models

Three-dimensional mathematical models should generally be used for collapse assessment. Two-dimensional (planar) models may be acceptable for buildings with regular geometries where the response in each orthogonal direction is independent and torsional response is not significant. When two-

dimensional models are used, the median collapse capacity, $\hat{S}_a(T)$, should be taken as the smaller of the value obtained for either direction.

Best-estimate properties should be used for each component in the mathematical model. Best-estimate models use median, or if median values are unavailable, mean properties of all force-deformation parameters, such as yield strength, yield deformation, post-yield stiffness, maximum strength, and deformation corresponding to maximum strength. Chapter 5 presents additional guidance for modeling structural components across the entire range of response, from elastic behavior through complete loss of resistance.

Ideally, nonlinear models should simulate all, or nearly all, possible modes of component deterioration and failure (e.g., axial, flexure, flexure-axial interaction, shear, and flexure-shear interaction). If a mode of deterioration or failure is not included in the model, its effect on collapse must be accounted for indirectly as a nonsimulated mode (see Section 6.2.4). Some building components, such as gravity-load resisting columns, may not be included in the building model but must be checked to either ensure they do not fail at story drifts smaller than those predicted by analysis at incipient building collapse, or the results of the analysis must be adjusted to account for the non-simulated failures. Non-simulated deterioration in components included in the mathematical model and components not included in the mathematical model should be assessed using appropriate collapse (loss of load-carrying capacity) limit state checks against demand parameters.

Ideally, models should simulate all possible modes of deterioration or failure. Nonsimulated modes, which are not included in the model must be indirectly evaluated for potential initiation at response levels below those at incipient simulated collapse.

For typical buildings, damping under earthquake motions is generally assumed to range between 2% and 5% of critical, depending on the building height, construction materials, and nonstructural components, with smaller values expected for high-rise, steel-framed buildings and larger values for low-rise, concrete-framed buildings. Since hysteretic damping is explicitly included in nonlinear analysis, common assumptions of 5% equivalent viscous damping are often inappropriate when analyzing response in the nonlinear range.

6.3 Simplified Nonlinear Analysis

Vamvatsikos and Cornell (2006) developed an analysis tool, known as SPO2IDA, to facilitate the development of approximate incremental dynamic analysis curves based on the results of nonlinear static analysis. This tool, which is provided in Volume 3 as an Excel workbook application, uses a user-defined global force-displacement relationship and a database of results from analyses of nonlinear single-degree-of-freedom models of varying profiles to generate surrogate incremental dynamic analysis curves, which

Nonlinear static analysis can be used with the SPO2IDA tool to provide representative collapse fragilities for regularly configured structures with uncoupled fundamental modes in each direction of response and limited higher mode behavior.

include some record-to-record variability. Use of this tool should be limited to low-rise structures that are regular in both plan and elevation, and whose seismic response is dominated by independent first translational modes along each principal axis.

To use the SPO2IDA tool, a pushover analysis, similar to the nonlinear static procedure described in ASCE/SEI 41-06*, Seismic Rehabilitation of Existing Buildings* (ASCE, 2007), is performed and the normalized force-displacement relationship such as that illustrated in Figure 6-3 is generated. The global base-shear, V , versus roof displacement, Δ , relationship is transformed to a relationship between a normalized spectral acceleration and global displacement ductility. The spectral acceleration, , is computed as $S_a = V / \left(C_m W / g \right)$. All terms have been defined in Chapter 5. The spectral acceleration is normalized by a variable, , which is equal in value to at the first control point as seen in the figure. The global displacement ductility, μ , is the ratio of the roof displacement, Δ , to the roof yield displacement. The coordinate of the yield point (first control point) in the SPO2IDA space is $(\mu, S_a / S_y = 1,1)$.

Figure 6-3 Global force-displacement relationship in SPO2IDA.

Figure 6-4 presents sample output from the SPO2IDA tool, which includes the results of the nonlinear static analysis illustrated in Figure 6-3 and the collapse fractile estimates, including the 16th, 50th (median) and 84th percentile predictions. The median collapse capacity, $\hat{S}_a$, for this example is approximately . Since a best estimate model is used to derive the nonlinear static analysis and also the collapse probability fractiles, dispersions due to record-to-record variability and modeling should be computed and used to derive the collapse fragility curve. A default dispersion of 0.6 is recommended for use with the SPO2IDA tool.

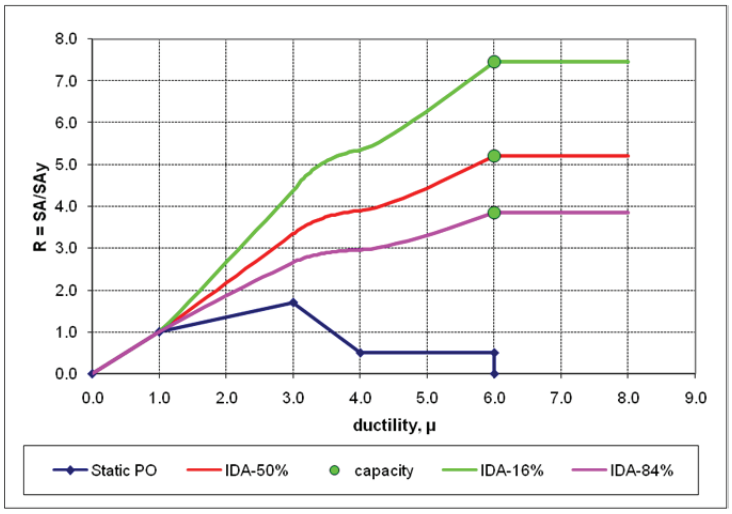

Figure 6-4 Sample SPO2IDA results for the example of Figure 6-3.

6.4 Judgment-Based Collapse Fragility

Judgment can be used to form approximations of collapse fragility but should not be regarded as reliable measures of a structure's collapse resistance

Collapse fragility curves can also be developed based on engineering judgment. As with any exercise of engineering judgment, the resulting assessments of performance will be only as good as the judgment used to develop the fragility.

The seismic design procedures contained in ASCE/SEI 7-10, *Minimum Design Loads for Buildings and Other Structures* (ASCE, 2010), are intended to provide less than a 10% chance that structures conforming to the requirements for Occupancy or Risk Category II will collapse if they experience Maximum Considered Earthquake shaking as defined in that standard. Recent studies funded under the National Earthquake Hazards Reduction program have used the methodology set forth in FEMA P-695 to confirm that some structural systems for which ASCE/SEI 7-10 specifies seismic design criteria are capable, on average, of meeting this criterion. These studies have generally used well-configured, regular structures. Further, some typical structures used in these studies have easily met this collapse resistance goal, while others have not. It can be expected that irregular structures with unfavorable configuration will not provide the same collapse probability as that intended by ASCE/SEI 7-10.

Regardless, the assumed collapse resistance can be used to generate approximate collapse fragilities for structures that generally conform to ASCE/SEI 7-10. This approach entails significantly greater uncertainty than the other two methods described above. The following procedure should be used for each of the building's primary directions and the lowest value of

median collapse capacity $\hat{S}_a\left(\overline{T}\right)$ so determined should be used:

Step 1. Determine the highest value of the spectral acceleration, $S_a(T)$, at the first mode period, that when used in the base shear equations of ASCE-7 results in a design that just satisfies the requirements of that standard and its referenced standards, assuming an occupancy importance factor of 1.0 and a redundancy coefficient of 1.0. This is the equivalent design spectral acceleration for the structure, S_{De}. If the equivalent lateral force procedure is used to make this determination, S_{De} should be taken as the highest value of the coefficient C_s defined in ASCE-7 at which the structure satisfies all applicable requirements.

Step 2. Compute the inferred median collapse capacity, $\hat{S}_a\left(T\right)$ at the building's fundamental period, T, from the formula:

$$\hat{S}_a\left(T\right) = 4.0 S_{De} \tag{6-2}$$

Step 3. Convert the computed median collapse capacity at the building's fundamental period to that at $\overline{T}$. For structures with :

$$\hat{S}_a\left(\overline{T}\right) = \frac{T}{\overline{T}} S_a\left(T\right) \tag{6-3}$$

For structures with :

$$\hat{S}_a\left(\overline{T}\right) = S_a\left(T\right) \tag{6-4}$$

Step 4. Take the dispersion as having a value of 0.7 for regular, well-configured structures, and 0.8 or higher for irregular structures or structures having configurations that otherwise are unfavorable to good seismic performance.

For archaic construction, the median value can be estimated on the basis of past experience; a dispersion of no less than 0.6 should be assumed.

If this method is used for a structure for which nonlinear response history analysis has been performed and the number of collapses predicted by the nonlinear analysis at different ground shaking intensities is not in relatively good agreement with that suggested by the derived collapse fragility, re-examination of either the analyses or the derived fragility is recommended.

6.5 Collapse Modes

In addition to determining the distribution of collapse probability, it is also necessary it is necessary to describe the likely collapse mode(s), the probability of occurrence of each, given that collapse occurs, the extent of

collapse in each mode at each story in the form of collapse area ratios, and the respective probabilities that people in areas of collapse will either become fatalities or serious injuries. Collapse area ratios indicate the percent of floor area at each level that is subject to collapse for each mode. Note that in some cases, collapse of one story, on top of another, can cause collapse in the lower story. This should be considered when generating collapse modes.

Collapse area ratios indicate the percent of floor area at each level that is subject to collapse for each mode.

Table 6-1 indicates representative collapse mode data for a hypothetical 4-story building with five separate modes of possible collapse. These include: mode 1 – total collapse of all stories; mode 2 –collapse in the first story only; mode 3 – collapse in the second story; mode 4 –collapse in the 3rd story and mode 5 –collapse in the 4th story. For each mode, the table shows the conditional probability of occurrence that the mode will occur; given that collapse occurs; and the collapse floor area ratio at each level. In addition to these data, it is necessary to designate the likelihood that persons in the collapse will either be injured or killed.

Table 6-1 Sample Probabilities that the Specified Portion of a Building will be Involved in the Collapse

ç	Mode 1	Mode 2	Mode 3	Mode 4	Mode 5
Collapse Mode Probabiltiy	0.2	0.2	0.2	0.2	0.2
Fatality Probability	1	0.9	0.9	0.9	0.9
Injury Probability	0	0.1	0.1	0.1	0.1
	Collapse Floor Area Ratios				
Roof	1	0	0	0	0
Floor 4	1	0	0	0	1
Floor 3	1	0	0	1	0
Floor 2	1	0	1	0	0
Floor 1	1	1	0	0	0

The collapsed floor area ratio identifies the total floor area at each level that will become the repository for debris from floors above. For this hypothetical example, it has been assumed that if a story collapses, the entire story is involved, as indicated by a collapse area ratio of 1.0 in the collapsed floors. It is possible to indicate only partial collapse within a story by using a fractional number less than 1 as the collapse area ratio.

The sum of the probabilities that collapse will occur in each mode must sum to a value of 1.0 when all modes are considered. It is typically not possible

to determine the various collapse modes that may occur in a building solely on the basis of analysis. Analysts will therefore have to use judgment to supplement the information obtained from the analyses in order to estimate which modes are viable for a particular structure, the appropriate floor area collapse ratio at each floor level for each mode, and the probability of occurrence of each mode, given that any collapse occurs.

It is also necessary to indicate the probabilities that each person in an impacted area will either become a fatality or incur serious injury. This is dependent on the type of construction involved. Analysts must rely on engineering judgment and data from past earthquakes to determine these probabilities. Past U.S. earthquake data suggest that most persons within unreinforced masonry bearing wall buildings with wood floors and roofs survive building collapse, as much of the heavy debris from the walls fall away from the building, rather than into it. In this form of construction, casualties are most common when people run out of these buildings during the earthquake and are struck by falling debris outside the building. Appropriate casualty probabilities for this type of construction may be on the order of 10% for fatalities and 30% for serious injuries. Conversely, collapse of reinforced concrete structures has typically resulted in many fatalities among people within the areas of floors impacted by falling debris. Fatality and injury probabilities for this type construction on the order of 0.9 and 0.1, respectfully, may be appropriate.

Chapter 7
Calculate Performance

7.1 Introduction

This chapter outlines the specific processes used to generated simulated demands, determine whether collapse occurs, determine damage, and compute casualties, repair costs and repair time. The procedures presented are those used for intensity-based assessment. Scenario-based assessments are performed in a similar manner. Time-based assessments, presented in the final section are performed as a series of occurrence frequency-weighted, intensity-based assessments.

A Monte Carlo process is used to explore variability in building performance outcomes for a particular ground motion intensity (or scenario). Ideally, this process would include performing structural analyses using a large suite of input ground motions, each representing the particular motion intensity of interest, with the properties of the analytical model randomly varied to account for modeling uncertainty. The analytical model would include structural and nonstructural systems and would be able to predict damage to each component, structural or nonstructural, as it occurs. The results of each single analysis would represent one possible building damage state, and the results of the large suite of analyses (thousands) would produce a smoothed distribution of possible building damage states that could be used to evaluate repair costs, casualties, and other earthquake consequences. At present, however, such an approach is impractical because the necessary modeling capability does not exist; the number of ground motions available for use in the analyses is insufficient and the solution time would be excessive.

Instead, analysis is used to predict demands that are indicative of damage. These demands are used together with the fragility and consequence functions described in Chapter 3 to predict earthquake damage and consequences over a distribution of possible earthquake response states. In this process, a small number of structural analyses are performed to estimate the median value of key building response parameters such as story drift ratios, floor accelerations, and floor velocities. These median estimates are converted into demand distributions based on assessment of variability of each of the random parameters, such as damping, element yield strength, and the likely effect of this variability on structural response. This approach,

albeit indirect and lacking the precision of large suites of analyses using appropriate distributions of strength and hysteretic properties, is computationally efficient and better suited to the analysis tools available at this time.

Realizations are used to determine the statistical distribution of performance outcomes. Each realization is one possible outcome.

In the Monte Carlo process used to assess performance, each possible earthquake outcome, including a set of demands (floor accelerations and velocities, and story drift ratios), damage, and performance consequences, is termed a realization. As part of the process of constructing realizations, the statistical distribution of demands derived from the structural analysis is used to construct a series of possible response states for the particular intensity of motion, termed simulations. The simulated demand set of maximum responses (simulation) used for a realization represents one possible set of peak response quantities that is statistically consistent with response calculated for the particular intensity of motion. Section 7.4 and Appendix G describe the process used to generate the hundreds to thousands of simulations (one simulation or demand set per realization) required to predict the distribution of building damage states for a particular motion intensity.

Subsequent sections describe the method of determining building damage states from sets of simulated demands. These procedures are repeated many times to determine the distribution of building damage and consequences over many realizations. Figure 7-1 shows the performance calculation process used to assess damage, followed by consequences in each realization, as described in the following sections. Not shown in the flow chart, and preceding the "Initiate Realization" step is the generation of all simulated demand sets, which for mathematical convenience is conducted ahead of the actual realizations.

7.2 Realization Initiation

Each realization initiates with determination of the time of day, and day of the year at which the earthquake has occurred. This information is used, together with the building's population model, to determine the number of people present. If desired, rather than allowing the building population to vary with time, the number of people present can be assumed to be either the peak population, or alternatively, the mean population. Chapter 3 provides additional information on population models.

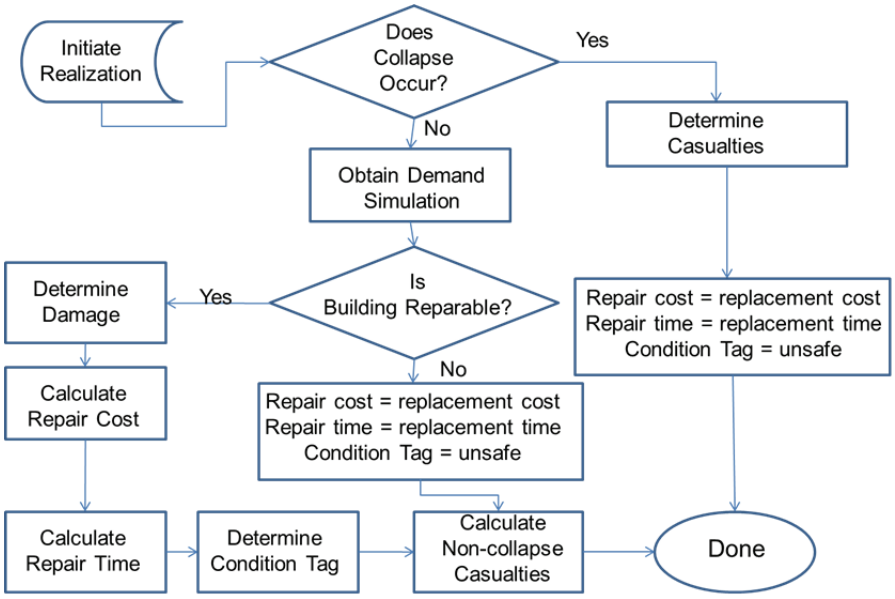

Figure 7-1 Performance calculation flow chart.

7.3 Collapse Determination

For each realization, a determination is made as to whether the building has collapsed, using the collapse fragility function described in Chapter 6. Figure 7-2 presents a collapse fragility function for a hypothetical building.

For each realization, a determination is made as to whether collapse has occurred.

As an example, at a ground motion intensity having a spectral acceleration at the building's fundamental period of 0.5g, Figure 7-2 indicates a 15% probability of building collapse. To determine if collapse has occurred, an integer in the range of 1 to 100 is randomly generated. For the example case of 0.5g ground shaking, if the random number is less than or equal to the conditional probability of collapse, factored by 100 (15 in this case), collapse is deemed to occur in this realization. If the number is greater than 15, collapse is deemed to not occur, and the performance calculation moves to the next step in the process, obtaining a simulated set of demands (see Section 7.4), as depicted in Figure 7-1.

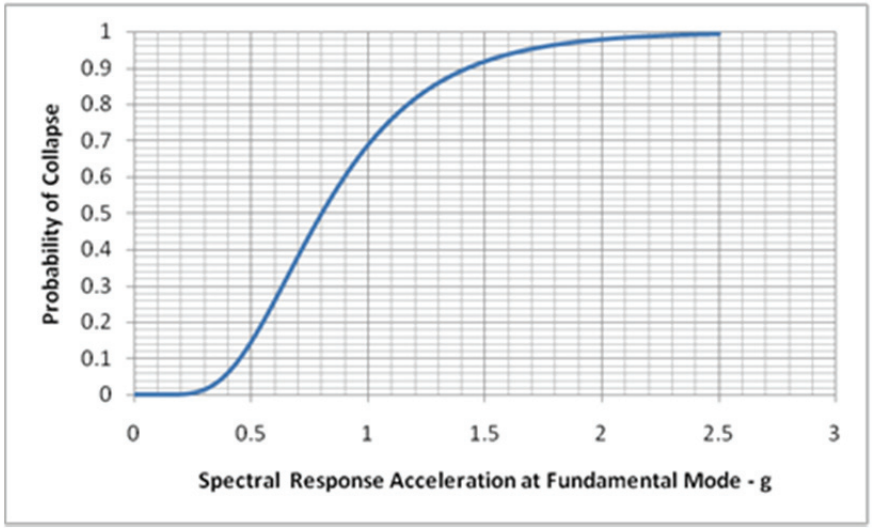

Figure 7-2 Representative collapse fragility for a hypothetical building structure.

7.3.1 Collapse Mode

The methodology allows for assessment of multiple collapse modes.

A structure may collapse in one of several modes, including collapse involving part of a single story or stories; an entire story or stories; or the entire building. Given that collapse is predicted, the mode must be determined to estimate casualties. As described in Chapter 6, the collapse fragility function includes identification of the possible collapse modes and the conditional probability of occurrence of each mode, given that collapse occurs, as well as the fraction of each floor subject to collapse debris. For complete collapse, the mode would identify that 100% of the floor area on each level is subject to collapse debris. For a single story collapse, with minor collapse on other floors, the mode would identify 100% for the floor area on the level associated with story collapse and lesser collapse debris percentages on other levels.

To determine which collapse mode has occurred in a realization, the collapse mode probabilities are assembled into an array ranging from 1 to 100, with n_i sequential numbers assigned to each mode, where n_i is the conditional probability of occurrence for mode "*i,*" factored by 100. Then, a number between 1 and 100 is randomly generated and the range in the array in which this number falls indicates the collapse mode that has occurred. For example, if a two story building has three potential collapse modes, consisting of first story collapse (50% probability), second story collapse (25% probability) and complete collapse (25%) these probabilities would be used to construct an array with numbers 1 through 50 assigned to collapse mode 1; numbers 51 to 75 to collapse mode 2 and 76 to 100 assigned to

collapse mode 3. A random number selection of 64 would indicate collapse mode 2 had occurred for this realization.

7.3.2 Casualties

Given determination that a collapse mode has occurred, the number of casualties is estimated based on the building population assumed present at the time of the realization, the associated fraction of floor area at each level subject to collapse, and additional casualty-specific information. For each collapse mode there are user-assigned mean fatality and injury rate ratios. These ratios describe, based on limited data from past earthquakes, the percent of occupants present in a collapsed floor area that will suffer fatality or injury. These probabilities are factored by the ratio of floor area subject to debris and the population present in the building to predicted deaths and injuries for the realization.

7.3.3 Repair Cost and Time

Given that the realization predicts collapse, repair cost and repair time are set equal to the building replacement values.

7.4 Simulation Demands

If collapse has not occurred, it is necessary to obtain a vector of simulated demands to predict the damage sustained by individual structural and nonstructural components and systems. Two different approaches are used for this purpose, depending on whether simplified analysis or nonlinear response-history analysis has been performed. Regardless of which analysis type is used, the generation of simulated demands occurs before the first realization is developed.

The demands used in the performance calculation are based on the analysis procedure used.

7.4.1 Simplified Analysis

The simplified analysis procedure of Chapter 5 results in a single vector of estimated median values of demand including peak floor acceleration and velocity, and story drift ratio at each level and also maximum residual drift ratio. It also results in an estimate of the associated dispersions.

For simplified analysis, a single set of peak demands are required.

For each realization, a number between 1 and 100 is randomly generated. This random number represents the percentile, within the lognormal distribution for determination of demands for this realization, respectively, using the dispersions for floor acceleration, floor velocity and story drift ratio and residual story drift ratio, as appropriate. In essence, this approach assumes that the building maintains the same response profile at a given intensity of ground motion, but with different amplitude. In other words, for

simplified analysis, it is assumed that there is perfect correlation between the various demands. If for a simulation, one demand is higher than the median by a particular measure, all are equally higher. Figure 7-3 illustrates this process by showing assumed deformed shapes for a hypothetical structure at different percentiles for four simulations. As described in Section 7.1, hundreds, and perhaps thousands, of simulations are needed to predict the distribution of building damage for a particular intensity of motion.

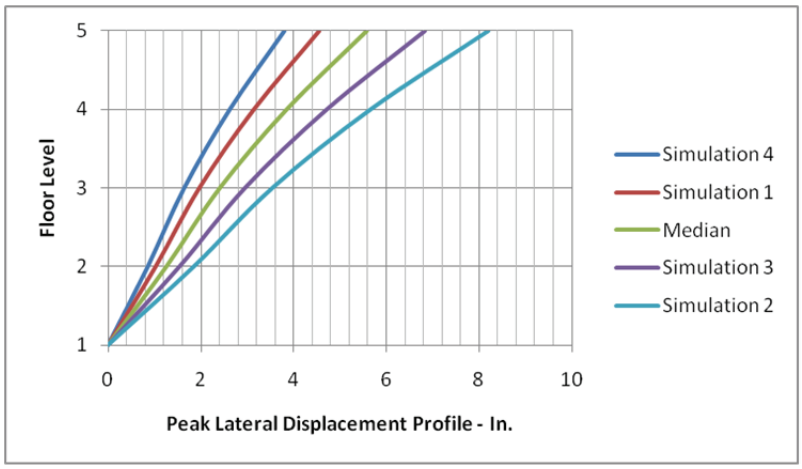

Figure 7-3 Illustration of assumed variability in demands associated with simplified analysis.

7.4.2 Nonlinear Response-History Analysis

Nonlinear response-history analysis produces a suite of demand vectors, assembled into a matrix.

The demands from each analysis are assembled into a vector containing the value of each of the demands (e.g., peak floor acceleration and velocity, peak and residual story drift ratio at each level in each direction) for that analysis. These vectors are assembled into a matrix, each column of the matrix presenting the results of one analysis and each row one demand parameter. The entries in the matrix are assumed to be a jointly lognormal distribution. The matrix can be manipulated (see Appendix G) to compute a vector of median demands (assumed to be the median vector derived from the suite of analyses), variances or dispersion, and a correlation matrix that indicates how each demand parameter varies with respect to all other demand parameters, such as drift ratio in the third story and acceleration on the fifth floor. Once this manipulation has occurred, the terms of the diagonal dispersion matrix are augmented using a root sum of squares approach to account for additional modeling uncertainty and ground motion uncertainty for scenario-based assessments.

The resulting simulated demand sets will have less uniformity than those obtained using the simplified procedure, and will more closely represent the possible demand sets the building could experience in a particular intensity

of shaking. Figure 7-4 illustrates this behavior for the same hypothetical structure of Figure 7-3. The structure's response profile varies in amplitude and shape from simulation to simulation. This is a more realistic treatment of potential variability than is possible using the simplified approach.

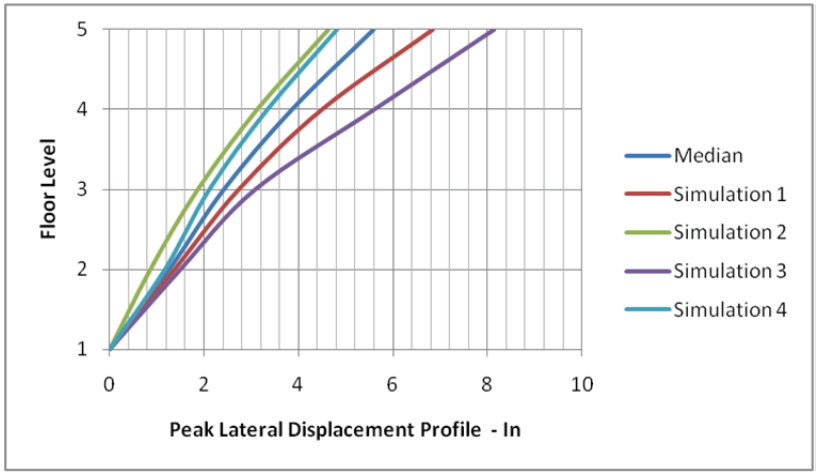

Figure 7-4 Illustration of variability in demands associated with nonlinear response-history analysis.

7.5 Damage Calculation

For each realization in which collapse is not predicted, a damage state is determined for each component utilizing the simulated set of demand vectors and the performance group fragility functions. The overall building damage state is the aggregate of the damage from all of the performance groups.

The process of determining the damage state for a performance group varies by damage state type and whether the damage is correlated or uncorrelated.

The damage state determination process for a performance group depends on the damage state type (sequential, simultaneous or mutually exclusive) and whether the damage is correlated or uncorrelated. Regardless, random number generation is used to determine the damage state for each component from its fragility function. For correlated damage states, every element of the performance group is assumed to have the same damage and the damage determination process is performed only one time for the performance group. For uncorrelated damage, each element of the performance group can have different damage and the damage determination process must be applied *n* times, where *n* is the number of elements in the performance group.

7.5.1 Sequential Damage States

Sequential damage states are states of increasing damage, with the logical relationship that one damage state cannot occur unless the prior, less severe damage state has also occurred. Each sequential damage state is assigned a range of numbers; damage state 1 ranging from (P_1 x 100) to (P_2 x 100), damage state 2 ranging from (P_2 x 100+1) to (P_3 x 100), and so on, where P_i

is the inverse probability of incurring damage state "*i*" at the demand level for the realization, as indicated by the performance group fragility. A random number below (P_1 x 100) indicates that no damage has occurred; a random number between (P_i x 100) and (P_{i+1} x 100) indicates damage state P_i has occurred. Figure 7-5 illustrates this process for a representative component. The figure shows the hypothetical fragility functions for three damage states and a hypothetical realization demand of 0.25g.

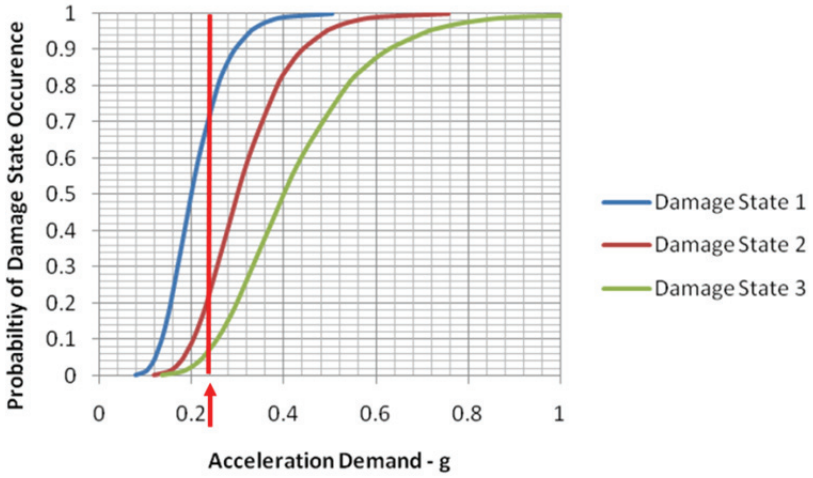

Figure 7-5 Illustration of determining sequential damage state for a performance group for a given realization.

For this hypothetical case, the probability of not incurring damage state 1 or higher is $P_1 = 1 - 0.75 = 0.25$; the probability of not incurring damage state 2 or higher is $1 - P_2 = 1 - 0.23 = 0.77$; and the inverse probability of not incurring damage state 3 is $P_3 = 1 - 0.06 = 0.94$. Therefore, the range of numbers assigned to no damage is from 1 to 25; the range to damage state 1 is from 26 to 77; for damage state 2 from 78 to 94; and for damage state 3 from 95 to 100. A random number of 97 for a realization falls within the highest range and would indicate that damage state 3 had occurred.

The fragility curves of Figure 7-5 do not overlap. In some instances, when two or more damage states have different dispersions, the curves may overlap, especially at the tails. For example, if the curve for DS2 crossed the curve for DS1 (because of a larger dispersion for DS2) at a probability of 0.1 (acceleration of 0.13g), for levels of acceleration less than that at the intersection point (0.13g) the probability of DS1 is set equal to 0, while the probability for DS2 is obtained directly from the curve for DS2.

7.5.2 Simultaneous Damage States

For simultaneous damage states, a first random number is selected to determine whether damage has occurred or not. If the random number is less

than the probability of incurring damage, than damage of some type has occurred. This could include any of the possible damage states as unique damage, or in any combination with the other possible damage states.

Each simultaneous damage state has an associated conditional probability of occurrence, given that the component is damaged. A random number is selected for each possible damage state and compared against the probability of the damage state's occurrence, to determine if the particular damage state has occurred in this realization. Unless one of the possible damage states always occurs (conditional probability of occurrence of 1.0), there will be some possibility, usually small, that the random number selection scheme will identify that none of the damage states have occurred. Since a determination has already been made that some damage state has occurred, when all of the random number evaluations for the damage states indicate the occurrence of no damage, the process is repeated, until at least one damage state occurs for the realization.

7.5.3 Mutually Exclusive Damage States

For mutually exclusive damage states, each damage state has a conditional probability of occurrence, given that damage occurs, and the sum of the conditional probabilities of occurrence must add up to 100%. The mutually exclusive damage states, DS_1, DS_2, and so on, are each assigned an array of numbers with the array for damage state 1 ranging from 1 to (P(DS_1) x 100), that for array 2 ranging from (P(DS_1) x 100+1) to (P(DS_1) +P(DS_2)) x 100, and so on. A random number is then generated between 1 and 100, and whichever range it falls within is the type of damage that occurs for the particular realization.

As an example, consider a hypothetical component that has three mutually exclusive damage states, DS_1, DS_2 and DS_3, with respective conditional probabilities of occurrence of 20%, 30% and 50%. The range of numbers assigned to damage state 1 is 1 to 20; for damage state 2 from 21 to 50; for damage state 3 from 51 to 100. A random number of 42 for a realization would indicate that damage state 2 has occurred.

7.6 Loss Calculation

Given that collapse does not occur, the losses are computed for each realization using the damage states for each component, calculated as described in the previous section. As described in Section 3.9, consequence functions for each damage state specify the likely consequences in terms of repair cost, repair time, and casualties and are used to calculate the associated losses for the given realization.

Each realization enables the development of a performance group damage state and the calculation of a single value of the loss. This loss value includes the efficiency of scale for the performance group as described in Section 3.9 and also takes into account the uncertainty in the calculation by taking into account the dispersion, β_c. Since the overall building loss is computed as the aggregate of the losses from all of the individual performance groups, global efficiencies of scale are not taken into account.

As described in Section 2.5, following computation of the damage states and consequences for all performance groups, the maximum residual drift ratio is evaluated to determine if it is sufficient to render the building impractical to repair. If the building is deemed irreparable, then the computed repair cost and time for the realization are discarded and the total replacement cost and times are used for the realization, instead.

The loss distributions are developed by repeating realization-specific damage and loss calculations many times.

The loss distribution is developed by repeating the realization-specific damage and loss calculation many times and sorting the losses in ascending or descending order to enable the calculation of the probability that the total loss will be less than a specific value for the given intensity of shaking. For example, if loss calculations are performed for 1,000 realizations, and the realizations are assembled in ascending order, the repair cost with a 90% chance of exceedance will be the repair cost calculated for the realization with the 100th largest cost, as 90% of the realizations will have a higher computed cost.

Figure 7-6 shows sample results of a scenario- or intensity-based cumulative loss distribution function for repair costs. In the figure, each point represents the repair cost determined for a single realization. The smooth curve is a lognormal distribution that has been fit to this data.

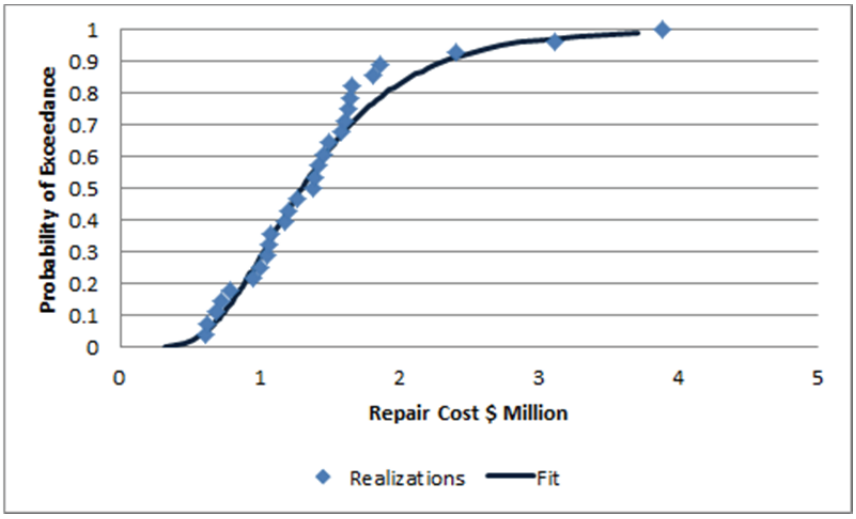

Figure 7-6 Sample repair cost loss curve.

Any value of total loss can also be de-aggregated into performance group losses as shown in Figures 7-7, by summing up, on a realization basis, the sources of the loss, in this case, repair costs. Results for other consequences are similar. Casualties can be deaggregated into those due to collapse in different modes and those caused by various non-collapse hazards associated with performance groups.

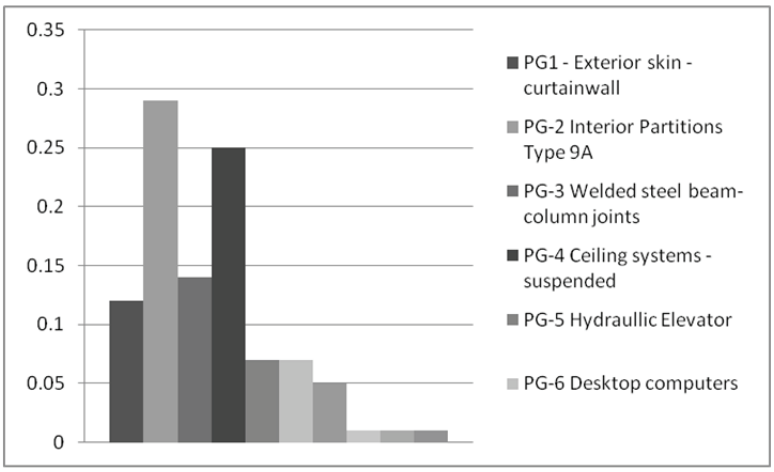

Figure 7-7 Sample repair cost deaggregation by performance group.

7.7 Time-Based Assessments

Time-based assessment produces a loss curve of the type shown in Figure 7-8, which plots the total repair cost (or other consequence measure), as a function of the annual rate of exceeding these losses. The curve shown in Figure 7-8 is constructed using the results of a series of intensity-based assessments and a site seismic hazard curve.

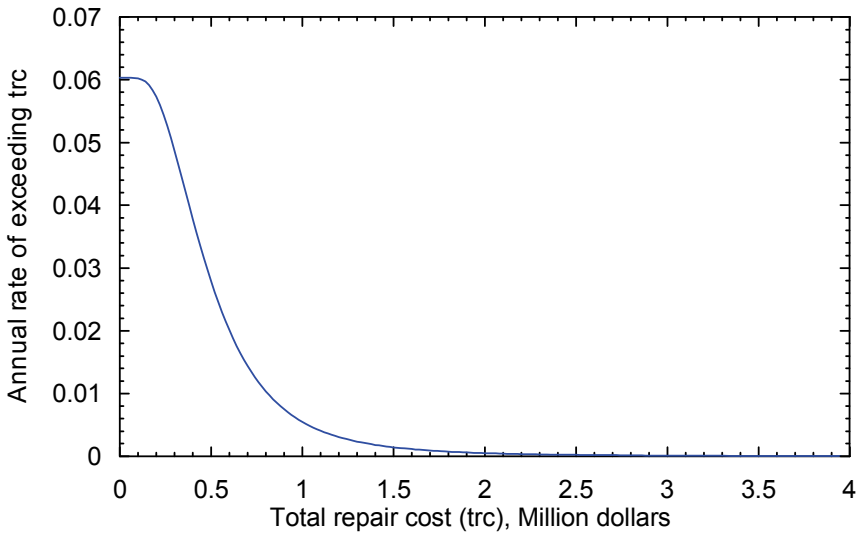

Figure 7-8 Distribution of mean annual total repair cost.

Figure 7-9 shows a representative seismic hazard curve, where the annual frequency of exceeding earthquake intensity, $\lambda(e)$, is plotted against the earthquake intensity, e. Typically, earthquake intensity is measured as spectral acceleration at the building's first mode period.

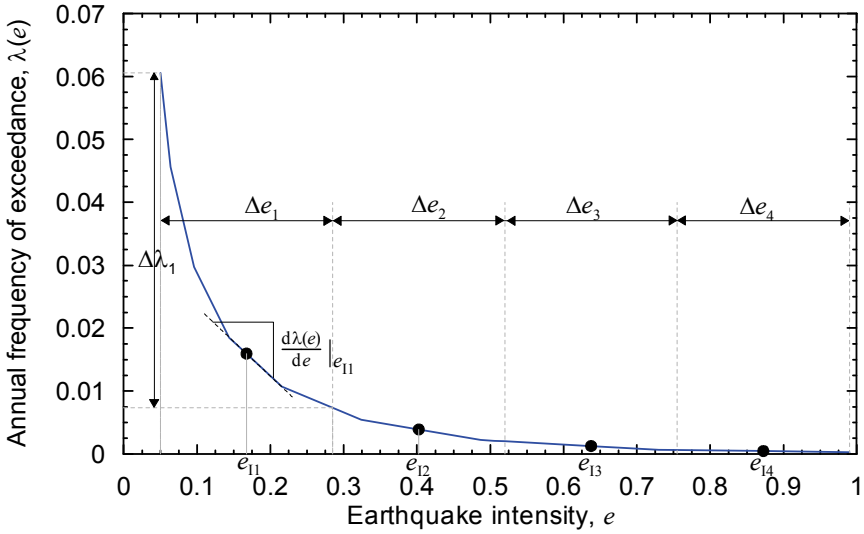

Figure 7-9 Seismic hazard curve and time-based loss calculations.

The hazard curve for the building's site is used together with Equation (7-1) to calculate the annual probability that the loss L will exceed a value l:

$$P(L > l) = \int_{\lambda} P(L > l \,|\, E = e)\, d\lambda(e) \qquad (7\text{-}1)$$

where the term $P(L > l \,|\, E = e)$ is the loss curve obtained from an intensity based assessment for intensity e. Equation 7-1 is solved by numerical integration.

To perform this numerical integration, the spectral range of interest is divided into n intervals, Δe_i. The spectral range of interest will typically range from a very low intensity that results in no damage to a very large intensity that produces a high probability of collapse. The midpoint intensity in each interval is e_{Ii}, and the annual frequency of earthquake intensity in the range Δe_i is $\Delta\lambda_i$ where the parameters Δe_i, e_{Ii} and $\Delta\lambda_i$ are defined in Figure 7-9 for a sample hazard curve using $n = 4$. This small value for n is chosen for clarity. In real time-based assessments, a larger number, n, of intensities will typically be necessary.

An intensity-based assessment is performed at each of the n midpoint intensities, e_{I1} through e_{In}. The number, n, of intensities required to implement this process will vary from structure to structure, and will depend on the steepness of the hazard curve and the ability of the structure to survive

a wide range of ground shaking intensities. Earthquake intensity at intensity e_{I1} is assumed to represent all shaking in the interval Δe_1. The product of the *n* intensity-based assessments is *n* loss curves of the type shown in Figure 7-10. The annual probability of shaking of intensity e_{Ij}, $\Delta\lambda_i$, is calculated directly from the seismic hazard curve as the difference in annual exceedance frequencies at the beginning and end of each intensity segment. Figure 7-9 illustrates the calculation of $\Delta\lambda_i$ for intensity segment 1. Figure 7-10 is constructed by: (1) multiplying each loss curve by the annual frequency of shaking in the interval of earthquake intensity used to construct the loss curve; and (2) summing the annual frequencies for a given value of the loss.

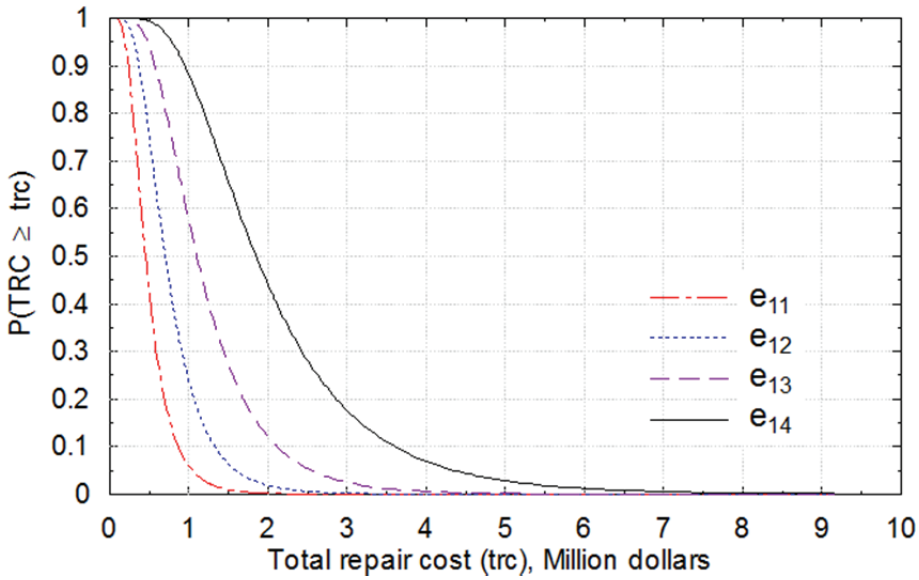

Figure 7-10 Example cumulative probability loss distributions for a hypothetical building at four ground motion intensities.

Chapter 8
Decision Making

8.1 Introduction

Performance assessment can provide useful information for many decisions associated with real property. These include:

- demonstrating equivalence of alternative design approaches;
- selecting appropriate design criteria for new buildings;
- determining if existing buildings constitute an acceptable risk for a particular planned use;
- determining if an existing building should be upgraded, and if so, to what level; and
- determining whether insurance is a cost-effective risk management technique.

This chapter illustrates how data obtained from performance assessments can be used as an aid to making such decisions.

8.2 Code Equivalence

For many years the building codes have permitted building officials to accept alternative designs and construction techniques that do not conform to the code's prescriptive criteria. This permission is subject to the building official's satisfaction that the proposed design or construction is capable of providing performance equivalent to that expected of code-conforming buildings. The performance assessment process can be used to directly indicate whether an alternative design is capable of providing equivalent performance.

Commentary to ASCE/SEI 7-10, *Minimum Design Loads for Buildings and Other Structures* (ASCE, 2010), Section 1.3 establishes the intended minimum safety-related seismic performance of building structures conforming to any of four Risk (or Occupancy) Categories. This performance is quantified in terms of limiting acceptable probabilities of collapse, given that the structure is subjected to Maximum Considered Earthquake (MCE) shaking. The procedures of Chapter 6 can be used to

Under ASCE/SEI 7-10, Occupancy Category I and II buildings should have less than a 10% chance of collapse given MCE shaking, Occupancy Category III buildings a 6% chance of collapse, and Occupancy Category IV buildings a 3% chance of collapse.

develop a collapse fragility and to determine directly, the probability of collapse for MCE shaking, individual scenarios, or on a time-basis.

Future building codes will likely include quantitative criteria that address performance issues in both a broader and more direct manner. Rather than considering the probability of collapse, future codes will likely set safety-related performance goals in terms of the risk of life loss, rather than collapse. Additional performance measures likely to be considered and quantified by future codes and standards include the potential for loss of beneficial use and for damage of critical function-related equipment. Intensity-based assessment procedures can be used to indicate probable building performance for Design Earthquake shaking or MCE shaking, as defined in the building code, or for any other response spectrum.

8.3 Scenario-Based Assessments

Scenario-based assessments can be useful for decision makers with buildings located close to major active faults.

Scenario-based assessments can be useful for decision makers with buildings that are located close to a major active fault, and who believe that a particular magnitude earthquake may occur on this fault within a time-horizon that is meaningful to them, often ranging from 10 to 30 years.

Scenario-based assessments will provide direct information as to the probable repair costs for such an occurrence, the potential for life loss, and the potential for long term loss of use. Scenario-based assessments quantify these impacts in the form of performance curves that indicate the probability that loss will exceed a certain value, over the full range of possible values. Many decision-makers are unable to use this probabilistic information and want a specific answer to the question: How bad will the loss be? It is probably best to provide this answer in the form of an expected performance together with upper and lower bounds.

Expected performance can be mathematically derived from the performance curve through numerical integration. Figure 8-1 illustrates this process. The figure shows a scenario-based performance curve for an unidentified performance-measure. In Figure 8-1, the performance curve has been divided into 5 equal stripes, each stripe having a probability of occurrence of 20%, conditioned on the occurrence of the earthquake scenario. Also identified in the figure is a central value of the performance measure for each stripe. The value of the mean performance measure is given by the formula:

$$\overline{PM} = \sum_{i=1}^{k} P(i)\, PM_i \qquad (8\text{-}1)$$

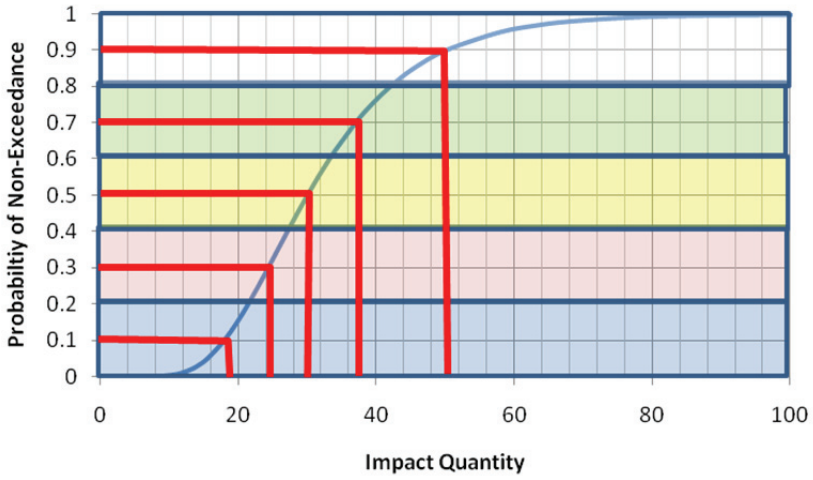

Figure 8-1 Hypothetical Peformance Function for building illustrating calculation of the mean value of a performance measure.

where, $\overline{PM}$ is the mean value of the performance measure; *P(i)* is the probability of occurrence of a value of the performance measure within stripe "*i*"; PM_i is the central value of the performance measure for stripe "*i*"; and *k* is the number of stripes. For the case illustrated in the figure, in which performance measures within each stripe have a probability of occurrence of 0.2, given that the scenario earthquake occurs, the mean value is given by 0.2 (19 + 24 +30 + 38 + 50) = 32. It should be noted that this is slightly greater than the median value, which in this case has a value of 30. As the distribution's skew increases, so too does the difference between the median and mean values, with the mean being larger than the median. Any number of stripes can be used in this integration process and the stripes do not need to be of uniform size. As the number of stripes used in the integration is increased, the accuracy of the integration will also increase.

An alternative means of finding the mean value is to assume that the performance curve is approximated by a lognormal distribution, with median value, PM_{50}, and dispersion, β. The median value is the value exceeded 50% of the time, which in the case of the figure, is a value of 30, as previously stated. The dispersion can be approximated as:

$$\beta = 0.43\left(\frac{PM_{50}}{PM_{10}} - .782\right) \qquad (8\text{-}2)$$

where, PM_{50} and PM_{10} are the 50th and 10th percentile values read off the loss curve. The mean value can be determined as:

$$\overline{PM} = PM_{50}e^{\beta^2/2} \qquad (8\text{-}3)$$

where all terms have been previously defined. For the example loss curve of Figure 8-1, these equations provide a value of β of 0.34 and a value of the mean of 31.8, which compares well with the value of 32 computed by numerical integration, and which is also approximate.

It is also important to specify bounds on this performance for decision-makers wanting to use mean performance measures, so that they have some understanding of the chance that performance will either be superior or inferior to the mean. Often the PM_{10} (value of the performance measure not exceeded 10% of the time) and PM_{90} (value of the performance measure not exceeded 90% of the time) values are appropriate bounds for this purpose.

8.4 Time-Based Assessments

Time-based assessments provide the average annual value of a performance measure, which is useful in cost-benefit analyses.

Time-based assessments can be used to provide the average annual value of a performance measure. The average annual value of a performance measure is useful in cost-benefit analyses and also for determining a reasonable insurance premium for a property.

The average annual value is the mean value obtained from a time-based performance curve, such as that shown in Figure 2-7. It can be obtained by numerical integration, in the same way mean values are obtained from scenario-based performance curves as described in the previous section. Figure 8-2 illustrates this process for a hypothetical annual performance curve. For this example, the computed mean annual value is 0.2 (0.05 + 0.07 + 0.1 + 0.14 + 0.19) = 0.11 per year. If the performance measure selected is casualty, this would indicate an average annual casualty rate of 0.11. If the performance measure selected is repair cost, in millions of dollars, this would indicate an annual average repair cost of $110,000.

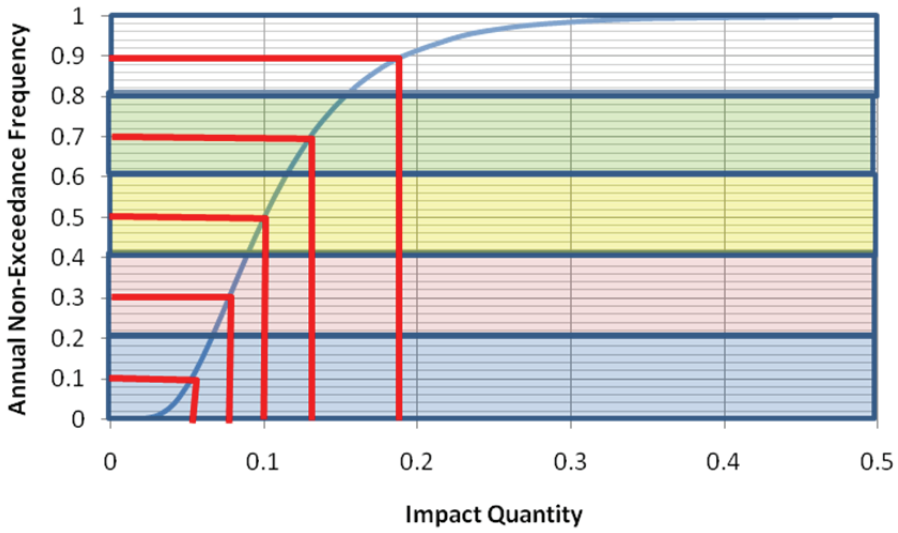

Figure 8-2 Hypothetical annual performance function for building illustrating calculation of mean annual value of performance measure.

Of course, earthquake losses do not really occur in annual increments. However, over a period of many years, the average annual loss should approximate the total loss well in that period of time, divided by the number of years in that period. As such, when the performance measure is repair cost, the average annual value of repair cost is a reasonable measure of the insurance premium that one should be willing to pay to insure against possible future repair costs. If the performance measure is expanded to include the probable costs associated with loss of use, this can also indicate the reasonable value of insurance premiums to cover occupancy interruption costs.

Average annual repair costs are a good measure of the insurance premium a person should be willing to pay.

The average annual performance measure can also be used as an input to cost-benefit studies that are useful in deciding how much should be invested to provide seismic resistance in a building, over and above any legal requirements. Essentially this process is performed by evaluating the present value of the average annual costs associated with future earthquake damage that is avoided by enhanced resistance, against the present value of the costs associated with enhanced seismic resistance. The net present value of a stream of equal annual future expenditures is given by the formula:

$$NPV = A\left[\frac{1-\frac{1}{(1+i)^t}}{i}\right] \qquad (8\text{-}4)$$

where *NPV* is the net present value of a stream of equal annual expenditures (or avoided expenditures), *A*, conducted over a period of *t* years. The variable, "*i*," in this equation is variously called the internal rate of return, or the interest rate. It represents either the amount of interest one would expect to incur if one borrowed money from others, or the amount of return on one's investment one expects to make.

For decisions associated with property with an anticipated life of more than 40 years, the annual average cost or saving can be considered an annuity of infinite term. In this case, Equation 8-4 reduces to the simpler form:

$$NPV = \frac{A}{i} \tag{8-5}$$

As an example of the use of this analysis, consider a hypothetical company (ACME) with operations in a single building in an earthquake-prone region. A performance assessment of the building indicates negligible risk of life endangerment; however, it does indicate an annual average repair cost of $150,000 and average annual repair times of 5 days. ACME estimates that each day of downtime costs the company $100,000 in profit. ACME's engineer has determined that a seismic upgrade of the building will reduce the average annual repair cost to $50,000 and the average annual repair time to 3 days. The estimated cost of the upgrade, including design fees and ACME's internal costs is $3,000,000. ACME uses an internal rate of return for their investments of 7%. If ACME expects to remain in the building for 10 years should they invest in the upgrade? If ACME expects to remain in the building indefinitely, should they invest in the upgrade?

The average annual benefit of performing the upgrade is the avoided average annual repair cost ($150,000 - $50,000 = $100,000) and the avoided lost profit per year ((5 days - 3 days) x ($100,000) = $200,000) for a total reduction in average annual loss of $300,000.

The Net Present Value of the avoided average annual loss for 10-year and an indefinite period is given by:

$$NPV_{10\,years} = \$300,000\left[\frac{1-\frac{1}{1.07^{10}}}{.07}\right] = \$2,108,000$$
$$NPV_{indefinite} = \frac{\$300,000}{.07} = \$4,290,000 \tag{8-6}$$

Since the Net Present Value of the avoided annual average loss over a 10-year period is less than the cost of the upgrade, it would not make economic

sense for the company to invest in this upgrade if it expects to remain in the building only 10 years. However, if the company anticipates remaining in this building indefinitely, there would be a net benefit to investing in the upgrade.

While cost benefit analyses of this type are useful tools for some decision-makers, not all decision makers prefer this approach. In the above example, it is possible, though unlikely, that within 10 years of the date that the company elects not to upgrade their building, an earthquake actually occurs resulting in real cost to the company that is substantially in excess of the $3,000,000 upgrade cost. In this unlikely, but possible scenario, the company would have been economically better off if they had invested in the seismic upgrade than not.

Time-based assessments provide a convenient means to determine the maximum loss likely in a specified return period, a useful tool for some risk-adverse decision makers.

Some decision-makers, who are risk-adverse, would want to avoid the realistic possibility of such a scenario. These risk-adverse decision-makers would prefer basing decisions on a loss with a specific anticipated probability of occurrence, or return period, such as 10-year, 50-year or 100-year losses. Time-based assessments can also be used to provide this type of information.

Return period is the reciprocal of the annual frequency of exceedance. Thus, if one were interested in a 50-year loss, one could enter the time-based performance curve for the loss at an annual probability of exceedance of 2% (1/50) and determine the loss directly at this level. A risk-adverse decision maker, with a risk tolerance of 50-years, might be willing to spend as much as the amount of this projected loss, but not more, to avoid incurring the loss.

8.5 Probable Maximum Loss

Many commercial lenders and real estate investors use a measure of seismic risk known as Probable Maximum Loss (PML). Many such investors will either not make an investment in a property, or require the purchase of earthquake insurance, when the projected PML exceeds a threshold value, often 20%.

Intensity-based assessments directly provide Scenario Expected Loss, Scenario Upper Bound Loss, and Probable Loss values as defined in ASTM E-2026 and ASTM E-2557.

ASTM E-2026, *Standard Guide for Seismic Risk Assessment of Buildings* (ASTM, 2007a) and ASTM E-2557, *Standard Practice for Probable Maximum Loss (PML) Evaluations for Earthquake Due-Diligence Assessments* (ASTM, 2007b) set standard procedures for seismic evaluations and the development of PMLs for use by the financial industry. These standards define several types of PML including:

- **Scenario Expected Loss** represents the mean repair cost, expressed as a percentage of building replacement value, for a particular intensity of

ground motion, typically defined as that ground motion having a 475-year return period.

- **Scenario Upper Loss** represents the 90th percentile repair cost, expressed as a percentage of building replacement value, for a particular intensity of ground motion, typically defined as that ground motion having a 475-year return period.
- **Probable Loss** represents that amount of loss, having a specific probability of exceedance, over a specified number of years.

Both the Scenario Expected Loss and Scenario Upper Loss values can be determined by performing intensity-based assessments for response spectra having the specified return period. The Scenario Expected Loss is obtained by computing the mean repair cost for the assessment. The Scenario Upper Loss is determined directly from the performance curve for repair cost at the 90th percentile.

Probable loss can be derived directly from a time-based assessment using an appropriate return period for the assessment. The return period for a loss, P_R, can be derived from the desired probability of exceedance, P_{EY} in Y years, using the formula:

$$P_R = \frac{-Y}{ln\left(1 - P_{EY}\right)} \tag{8-7}$$

Once the return period for the loss is known, it is possible to determine the annual frequency of exceedance of the loss, as $1/P_R$, and then read the corresponding loss directly from the performance curve, such as that shown in Figure 8-2.

Appendix A
Probability, Statistics, and Distributions

A.1 Introduction

This appendix provides a brief tutorial on probability and statistics including methods of expressing probabilities in the form of statistical distributions. It is intended to provide readers unfamiliar with these topics the basic information necessary for understanding the process used to account for uncertainties in performance assessment. Interested readers can obtain additional information in textbooks on probability and statistics, and on structural reliability theory. Benjamin and Cornell (1970) is one such example.

A.2 Statistical Distributions

Statistical distributions are mathematical representations of the probability of encountering a specific outcome given a set of possible outcomes. The set representing all possible outcomes is termed a population. There are generally two broad types of populations considered in statistical studies. The first of these is a finite population of outcomes, where each possible outcome has a discrete value representing one of the finite number of possible outcomes. The second of these is an infinite population of possible outcomes. Each is discussed separately, below.

A.2.1 Finite Populations and Discrete Outcomes

Consider the classic case of a coin thrown in the air to determine an outcome. One of two possible outcomes will occur each time the coin is tossed. One potential outcome is that the coin will land "heads-up" and the other that it will land "heads-down." Which way the coin will land on a given toss is a function of a number of factors including which way the coin is held before the toss, the technique used to toss the coin, how hard or high the coin is tossed, how much rotation it is given, and how it lands. We could never hope to precisely simulate each of these factors, and therefore, the occurrence of a "heads-up" or "heads-down" outcome in a given coin toss appears to be a random phenomena, that is not predictable. There is an equal chance that

the coin will land "heads-up" or "heads-down," and we cannot know before tossing the coin, which way it will land.

If we toss a coin in the air one time there are two possible outcomes. These two outcomes – coin lands "heads-up" and coin lands "heads-down" completely define all possibilities for one coin toss and therefore, the probability that the coin will land either heads-up or heads-down is 100%. In essence, this illustrates the total probability theorem, that is, that the sum of the probabilities of all possible outcomes will be 100%, which can also be expressed as 1.0.

The probability that the coin will land "heads-up" is 50%, or 0.5. The probability that it will land "heads-down" is the inverse of this, calculated as one minus the probability of "heads-up," 1 – 0.5 = 0.5, or 50%.

If we toss the coin in the air many times, we would expect that we would get a "heads-up" outcome in half of these tosses and "heads-down" outcome in the other half. This does not mean that every second toss of the coin will have a "heads-up" outcome. We might obtain several successive "heads-up" outcomes or several successive "heads-down" outcomes; however, over a large number of tosses, we should have approximately the same number of each possible outcome.

A.2.2 Combined Probabilities

A combined probability is the probability of experiencing a specific combination of two or more independent outcomes. We can calculate the combined probability of two independent events as the product of the probability of outcome 1 and the probability of outcome 2. That is:

$$P(A+B) = P(A) * P(B) \qquad \text{(A-1)}$$

To illustrate this, if we toss the coin into the air two times, there is a 50% chance, each time, that the coin will land "heads-up." The chance that the coin will land "heads-up" both times is calculated, using Equation A-1, as the probability of landing "heads-up" the first time (0.5) multiplied by the probability that it will land "heads-up" the second time (0.5), or (0.5 x 0.5) = 0.25, or 25%.

This probability means that if we toss a coin into the air twice in succession, a large number of times, and record the number of "heads-up" outcomes, in each pair of tosses, approximately 25% of the total number of pairs of tosses will have two successive heads-up outcomes. This does not mean that every fourth time we make a pair of coin tosses we will get two successive heads-up outcomes. There is some possibility that we will get two successive

heads-up outcomes several times in a row and there is also a possibility that we will have to make more than four pairs of coin tosses to obtain an outcome of two heads-up in any of the pairs of tosses. However, over a very large number of pairs of tosses, 25% of the pairs should be successive heads-up outcomes.

If we toss the coin into the air three times, there is again a 50% chance on each toss that the coin will land "heads-up." The probability that the coin will land "heads-up" all three times is given by the probability that it will land "heads-up" the first two times (25%) multiplied by the probability that it will land "heads-up" the third time (50%), or (0.25 x 0.5) = 0.125, or 12.5%. If we repeat this exercise with 4 coin tosses, the probability that all four will land "heads-up" will be the probability that the first three tosses will land "heads-up" (12.5%) times the probability that the fourth toss will land "heads-up" or (0.125 x 0.5 = 0.0625) or 6.25%. That is, there is approximately a 6% chance that we will have two successive pairs of coin tosses both having two heads-up outcomes.

A.2.3 Mass Distributions

A probability mass distribution is a plot of the probability of occurrence of each of the possible outcomes in a finite population of discrete outcomes, such as a coin landing either "heads-up" or "heads-down" a specified number of times in *N* throws.

Consider the case of four coin tosses. As shown in the previous section, there is a 6.25% chance that all four coin tosses will land "heads-up." There is also a 6.25% chance that all four coin tosses will land "heads-down" or that none of the coin tosses will land "heads-up." The chance that three of the four coin tosses will land "heads-up" is equal to the combined chance of any of the following outcomes: "T, H, H, H"; "H, T, H, H"; "H, H, T, H" or "H, H, H, T," where "H" indicates "heads-up" and "T" "heads-down ." The chance of each of these outcomes is the same as having all four tosses landing "heads-up" or 6.25%. Therefore, the chance of exactly three out of four tosses landing "heads-up" is equal to 6.25% for the "T, H, H, H" combination, plus 6.25% for the "H, T, H, H" combination, plus 6.25% for the "H, H, T, H" combination, plus 6.25% for the "H, H, H, T" combination, or 6.25% + 6.25% + 6.25% +6.25% = 25%. Similarly, the probability that exactly three of the four tosses will be "heads-down," or that only one of the tosses will land "heads-up," is 25%. We can use similar approaches, to show the probability that exactly half of the tosses will land "heads-up" is 37.5%.

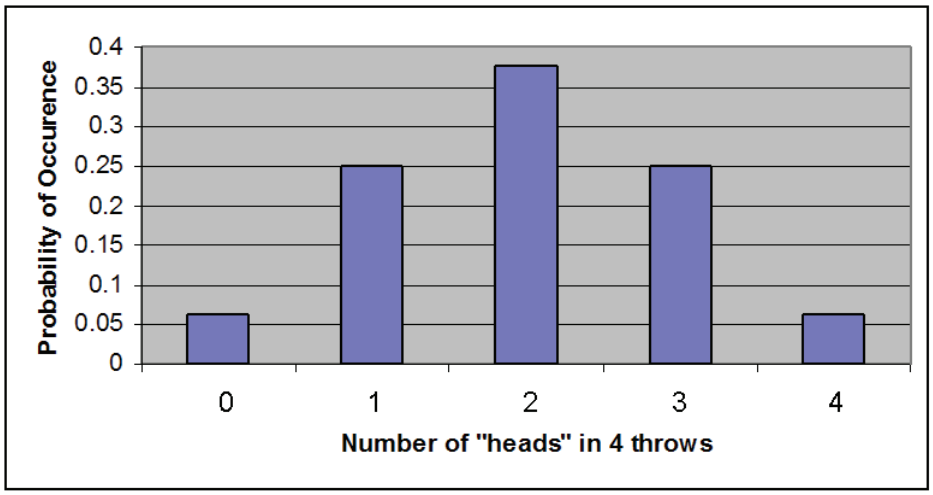

Figure A-1 Probability mass function indicating the probability of the number of "heads-up" outcomes in four successive coin tosses.

Figure A-1 is a plot that shows the probability of obtaining zero, one, two, three, or four "heads-up" outcomes from four coin tosses. Plots of this type are termed probability mass distributions. By entering the plot along the horizontal axis, at a particular outcome, for example one "heads-up" out of four throws, we can read vertically to see the probability of that outcome, which is 25%. The probability of having not more than one "heads-up" outcome in four tosses, is calculated as the sum of the probability of no "heads-ups", which is 6.25% plus the probability of one "heads-up" which is 25%, for a cumulative probability of 31.25%. Another way to say this is that the probability of non-exceedance for one "heads-up" in four coin tosses is 31.25%. The inverse of this is the cumulative probability of more than one "heads-up," which is 1 – 0.3125 = 68.75%. This could also be called the probability of exceedance of one "heads-up" in four tosses."

A.2.4 Continuous Distributions

The distribution of possible "heads-up" throws in a finite number of coin tosses is an example of a discrete distribution. That is, there are only a finite number of possible outcomes, and these have discrete values. In the example above, these values are 0, 1, 2, 3 or 4 "heads-up" outcomes in 4 coin tosses.

For many situations, the possible outcomes are not a finite number of discrete possibilities but rather a continuous range of possibilities. An example of such a continuous distribution is the possible compressive strengths obtained from concrete cylinder compression tests, where all cylinders are from concrete using the same mix design. Such a distribution will have the form shown in Figure A-2, where the dispersion in strength is due to minor variability in the amount of cement, amount of water, strength of aggregates,

cylinder-casting technique, curing technique, and other factors. There are an infinite number of possible outcomes for the strength of any particular cylinder test. The plot shown in Figure A-2 is termed a probability density function.

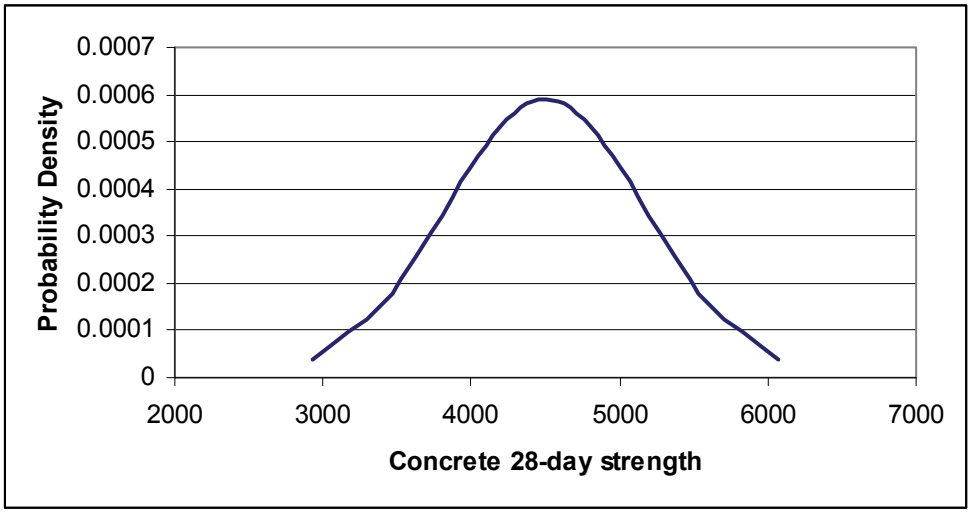

Figure A-2 Probability density function of possible concrete cylinder strengths for a hypothetical mix design.

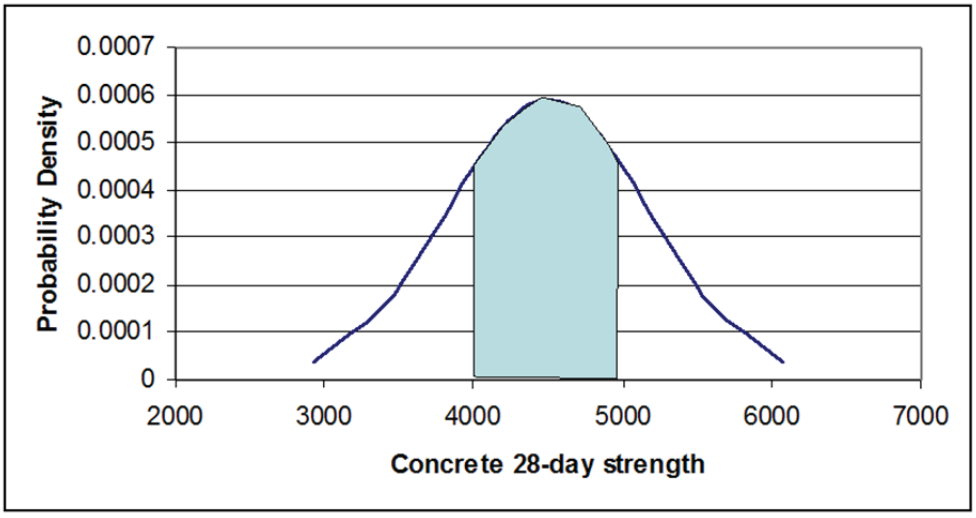

Figure A-3 Calculation of probability that a member of the population will have a value within a defined range.

The area under the curve of a probability density function between any two points along the horizontal axis gives the probability that the value of any member of the population will be within the range defined by the two values. In Figure A-3, the probability that a single cylinder test will have strength that is greater than 4,000 psi but less than or equal to 5,000 psi is given by the area under the curve between the two strength values, which in this case has a calculated probability of 54%. That is, there is a 54% chance that any

cylinder test in this population will have strength between 4,000 psi and 5,000 psi.

A.3 Common Forms of Distributions

A.3.1 Normal Distributions

The probability density function illustrated in Figure A-2 has a special set of properties known as a normal distribution. In a normal distribution the "median" outcome, which is the outcome that is exceeded 50% of the time, is also equal to the average or "mean" outcome, which is the total value of all possible outcomes, divided by the number of possible outcomes. In the example above, the median outcome is a compressive strength of 4,500 psi. The average strength of all cylinders tested is also 4,500 psi.

Normal distributions are also symmetric. That is, there is an equal probability of having a value at a defined measure above the average (e.g., 1,000 psi above the mean, or 5,500 psi), as there is of having a value at the same defined measure below the average (e.g., 1,000 psi below the mean, or 3,500 psi).

Two parameters are used to uniquely specify the characteristics of a normal distribution, namely, the mean value $\bar{x}$ and standard deviation, σ. Equation A-2 and Equation A-3, define these values for a random variable x (e.g., compressive strength of concrete as measured by cylinder testing) and a sample of size N:

$$\bar{x} = \frac{\sum_{i=1}^{N} x_i}{N} \tag{A-2}$$

$$\sigma = \sqrt{\frac{1}{N-1}\sum_{i=1}^{N}\left(x_i - \bar{x}\right)^2} \tag{A-3}$$

where N is the size of the population. If a parameter is normally distributed, that is, its population of possible outcomes is represented by a normal distribution, having mean value $\bar{x}$ and standard deviation σ, it is possible to determine the value x of an outcome that has a specific probability of exceedance, based on the number of standard deviations that the value x lies away from the mean, $\bar{x}$. For example, there is a 97.7% chance that the value of any single outcome x will be greater than $\bar{x} - 2\sigma$, an 84.1% chance that the value of any single outcome x will be greater than $\bar{x} - \sigma$, a 50% chance it will be greater than $\bar{x}$, a 15.8% chance it will exceed $\bar{x} + \sigma$ and a 2.3% chance that it will be greater than $\bar{x} + 2\sigma$. Standard tables that are available in most texts on probability theory provide the probability that the

value of any outcome in a normally distributed population of potential outcomes will exceed a value that is a defined number of standard deviations from the mean. The number of standard deviations above or below the mean that will have a specified probability of exceedance is sometimes termed the Gaussian variate, and the probability tables that give these values are called Gaussian tables. Table A-1 indicates some representative values of the Gaussian variate for several commonly referenced probabilities.

Table A-1 Values of the Gaussian Variate in Normal Distributions for Common Probabilities

Probability of Non Exceedance	Number of Standard Deviations below Mean		Probability of Non Exceedance	Number of Standard Deviations Above Mean
.02	-2.0		.60	.25
.05	-1.64		.70	.52
.10	-1.28		.80	.84
.158	-1.0		.84	1.0
.20	-.84		.90	1.28
.30	-.52		.95	1.64
.40	-.25		.98	2.0
.50	0			

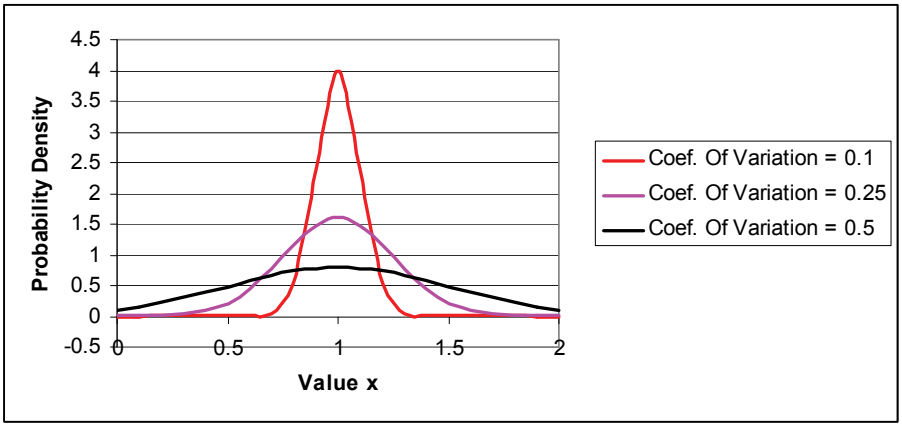

Figure A-4 Probability density function plots of normal distributions with a mean value of 1.0 and coefficients of variation of 0.1, 0.25, and 0.5.

A.3.2 Cumulative Probability Functions

Figure A-4 shows probability density functions for different coefficients of variation. An alternative means of plotting probability distributions is the form of a cumulative probability function. A cumulative probability function plot shows the probability that an outcome in the population of possible outcomes will have a value that is less than or equal to the specified value *x*.

This probability is sometimes termed the probability of non-exceedance. Cumulative density plots are obtained by integrating over the probability density function to determine the area under the curve between the lowest possible value of x and any other value of x. Figure A-5 presents cumulative probability plots for the same normally distributed populations shown in Figure A-4. From both series of plots, it is possible to observe that the larger the coefficient of variation becomes, the greater the amount of scatter in the values of the possible outcomes.

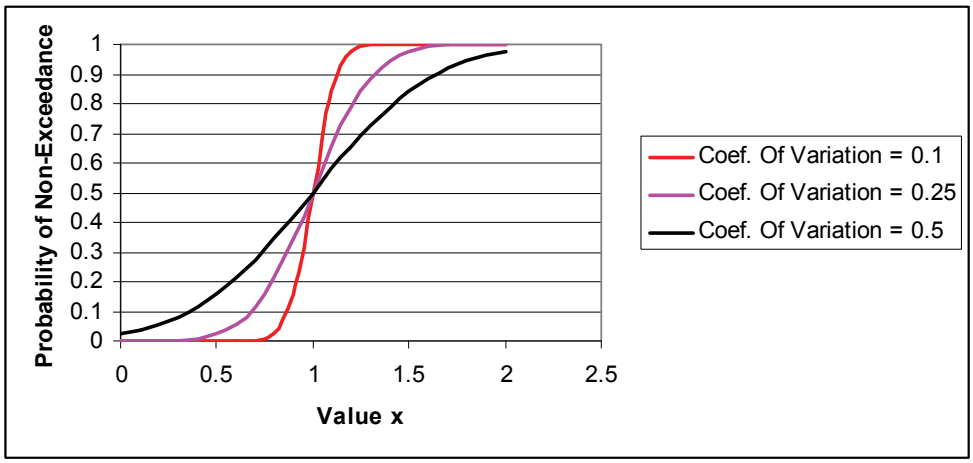

Figure A-5 Cumulative probability plots of normal distributions with a mean value of 1.0 and coefficients of variation of 0.1, 0.25, and 0.5.

A.3.3 Lognormal Distributions

Although normal distributions represent some random variables well, they do not represent all variables well. Some variables have skewed distributions. In skewed distributions, the mean value, $\overline{x}$, will be greater than or less than the median value. In structural reliability applications, such as performance assessment, it is common to use a specific type of skewed distribution known as a lognormal distribution. This is because the skew inherent in lognormal distributions can reasonably represent the distributions observed in many structural engineering phenomena, such as the distribution of strength in laboratory specimens.

The lognormal distribution has the property that the natural logarithm of the values of the population, $\ln(x)$, are normally distributed. The mean and the median of the natural logarithms of the population have the same value, equal to $\ln(\theta)$, where θ is the median value. The standard deviation of the natural logarithms of the values, $\sigma_{\ln(x)}$, is called the dispersion, and is denoted by the symbol, β. For relatively small values of dispersion, the value of β is approximately equal to the coefficient of variation for x.

Together, the values of θ and β completely define the lognormal distribution for a population.

Figure A-6 plots probability density functions for three lognormally-distributed populations having a median value of 1.0 and dispersions of 0.1, 0.25 and 0.5. Figure A-7 plots this same data in the form of cumulative probability functions.

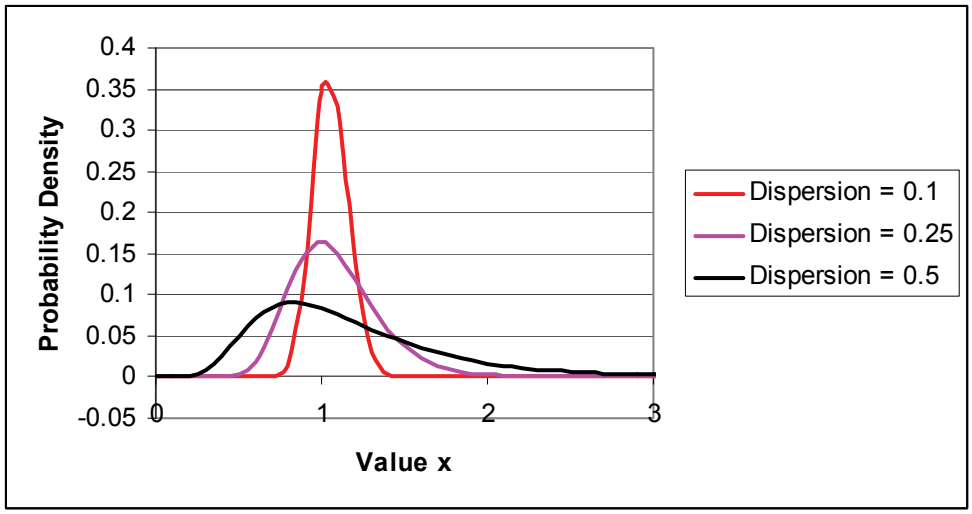

Figure A-6 Probability density function plots of lognormal distributions with a median value of 1.0 and dispersions of 0.1, 0.25, and 0.5.

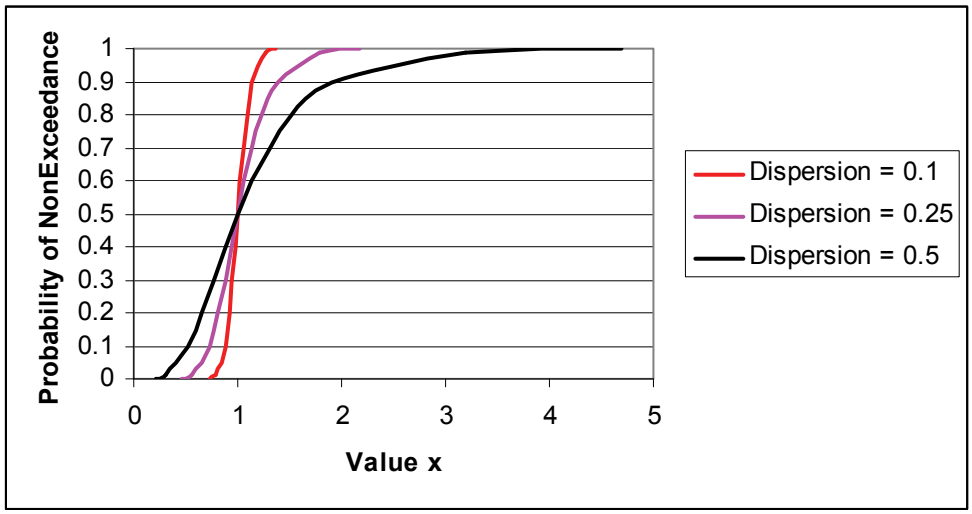

Figure A-7 Cumulative probability plots of lognormal distributions with a median value of 1.0 and dispersions of 0.1, 0.25, and 0.5.

As can be seen from the plots, for small values of the dispersion, the distribution approaches the shape of the normal distribution, but as the dispersion increases in value, the distribution becomes more and more skewed. This skew is such that there is zero probability of incurring a negative value in the distribution (because the logarithm of a negative

number is positive) and extreme values above the median are substantially more probable than extreme values below the median.

Consider the distribution of possible actual yield strengths of various steel parts, all conforming to a specific ASTM specification and grade. Since this variable (yield strength) cannot take on values of less than zero, the lognormal distribution could be used to describe the variation in possible steel strength using a median value and dispersion. In this example, the median value will be substantially higher than the minimum specified value, which is intended to have a very low probability of non-exceedance by any steel conforming to the specification.

The seismic performance assessment methodology uses lognormal distributions to represent many uncertain factors that affect performance including: (1) the distributions of intensity for a scenario earthquake; (2) the values of response parameters given an intensity; (3) the probability of incurring a damage state as a function of response parameter, herein termed a fragility; and (4) the probability of incurring a specific level of casualties, repair costs, repair time or other impacts, given a damage state. These lognormal distributions are derived in a variety of ways:

- Intensity distributions are obtained based on statistical analysis of actual ground motion data recorded from past earthquakes, and represented in the form of equations known as attenuation relationships or ground motion prediction equations.
- Response parameter distributions are obtained by performing suites of structural analyses using multiple ground motion recordings and varying the strength, stiffness, damping, and ductility capacity of the structural elements.
- Fragility distributions are obtained primarily through laboratory testing or observation of actual damage in past earthquakes.
- Loss distributions are obtained through performing multiple calculations of loss, varying the factors that affect the loss, such as contractor efficiency, and number of persons likely to be occupying a building at the time of the earthquake.

Regardless of how these distributions are derived, they are represented by two variables including the median value, θ, and dispersion, β.

The mean m_Y and standard deviation, σ_Y, of a lognormal distribution, Y, can be calculated from θ_Y and β_Y as follows:

$$m_Y = \theta_Y \exp\left(\frac{\beta_Y^2}{2}\right) \quad \text{(A-4)}$$

$$\sigma_Y^2 = m_Y^2\left[\exp\left(\beta_Y^2\right) - 1\right] \quad \text{(A-5)}$$

The coefficient of variation, ν_Y, is given by

$$\nu_Y = \frac{\sigma_Y}{m_Y} = \sqrt{\exp(\beta_Y^2) - 1} \quad \text{(A-6)}$$

Many common spreadsheet applications have embedded functions that will automatically solve lognormal distribution problems. For example, in Excel, the LOGNORMDIST function will determine the cumulative probability of non-exceedance of any value in a population *Y*, based on input of the value, *y*, the natural logarithm of the median, $\ln\theta_Y$, and the dispersion, β_Y. The Excel input is of the form =LOGNORMDIST (*y,* $\ln\theta_Y$, β_Y). Similarly, the LOGINV function can be used to determine the value of *y*, at a given cumulative probability of non-exceedance, based on the desired probability, *p*, which must be less than 1.0, the natural logarithm of the median $\ln\theta_Y$ and the dispersion, β_Y. The Excel input is of the form =LOGINV(*p,* $\ln\theta_Y$, β_Y).

A.4 Probabilities over Time

Sometimes it is convenient to express the probability of the occurrence of an event conditioned on a specific period of time, such as a single year, the length of a lease, or the length of a mortgage loan. The probability that an event will occur in a single year is termed the annual probability. If the annual probability of the occurrence of an event, P_1, is known, it is possible to convert this into the probability, P_N, of the event occurring over any arbitrary length of time, *N*, using the formula:

$$P_N = 1 - \left(1 - P_1\right)^N \quad \text{(A-7)}$$

Appendix B
Ground Shaking Hazards

B.1 Scope

This appendix presents supplemental information on characterization of ground shaking hazards and an alternate procedure for scaling ground motions for scenario-based assessments.

B.2 Ground Motion Prediction Models

Ground motion prediction models, sometimes termed attenuation relationships, relate ground motion parameters to the magnitude of an earthquake, site distance from the fault rupture, and other parameters such as soil type, rupture directivity, etc. Models have been established for many ground motion parameters including peak horizontal acceleration , velocity and displacement, and corresponding spectral terms.

Ground motion prediction models are developed primarily by statistical evaluation of large sets of ground motion data. Relationships have been developed for different regions of the United States (and other countries) and different fault types (i.e., strike-slip, dip-slip and subduction).

Chapter 4 presents the basic construction of ground motion predictive models. These models generally return a geometric mean[1] of two horizontal spectral ordinates.

Table B-1 presents selected North American ground motion prediction models. These models all use moment magnitude M_W to define earthquake magnitude but use different definitions of site-to-source distance and other parameters. Figure B-1 defines some of the distance parameters used.

[1] For a given pair of horizontal earthquake histories, the geometric mean ($\overline{S}_g$) of the spectral ordinates of the two components (S_x and S_y) is generally used to characterize the pair of histories: $\overline{S}_g = \sqrt{S_x S_y}$. Since the functional form of the attenuation relationship involves the natural log of the ground motion parameter, the geometric mean of the ordinates (which is equivalent to the arithmetic mean of the logs of the ordinates) is used instead of the arithmetic mean.

Table B-1 Ground Motion Prediction Models

Model	Calculated[1]	Site Conditions[2]	Variables[3]	Ranges		
				T_n (secs)	r (km)	M_W[4]
Western North America (WNA)						
Abrahamson and Silva, 2008	PHA, PHV, Sah	$180 \le V_{S30} \le 2000$[5]	M, r_{rup}, r_{jb}, V_{S30}, F, H, B	0-10	0-200	5-8.5
Boore and Atkinson, 2008	PHA, PHV, Sah	$180 \le V_{S30} \le 1300$	M, r_{jb}, V_{S30}, F			5-8
Campbell and Bozorgnia, 2008	PHA, PHV, Sah	$150 \le V_{S30} \le 1500$	M, r_{rup}, r_{jb}, V_{S30}, F, H, B			4-8.5 (s) 4-8 (r) 4-7.5 (n)
Chiou and Youngs, 2008	PHA, PHV, Sah	$150 \le V_{S30} \le 1500$	M, r_{rup}, r_{jb}, V_{S30}, F, H, B			4-8.5 (s) 4-8 (r&n)
Idriss, 2008	PHA, Sah	$V_{S30} > 900$, $450 \le V_{S30} \le 900$	M, r_{rup}, F			4.5-8[5]
Central and Eastern North America (CENA)						
Atkinson & Boore, 1997	PHA, Sah	Rock	M, r_{hypo}	0-2	10-300	4-9.5
Campbell, 2003	PHA, Sah	Hard rock	M, r_{rup}	0-4	1-1000	5-8.2
Toro et al., 1997	PHA, Sah	Rock	M, r_{jb}	0-2	1-100	5-8
Subduction Zones						
Atkinson & Boore, 2003	PHA, Sah	Rock to poor soil	M, r_{hypo}, +	0-3	10-300	5.5-8.3
Youngs et al., 1997	PHA, Sah	Rock, Soil	M, r_{rup}, F, H	0-4	0-100	4-9.5

1. PHA = peak horizontal ground acceleration, PHV = peak horizontal ground velocity, Sah = horizontal spectral acceleration
2. V_{S30} = Average shear wave velocity in the upper 30 meters of sediments, unit: m/s
3. r_{rup} = closest distance to the rupture surface, r_{jb} = closest horizontal distance to the vertical projection of the rupture, r_{hypo} = hypocentral distance, M = magnitude, F = fault type, H = hanging wall, B = 3-D basin response.
4. s = strike-slip faulting, r = reverse faulting, n = normal faulting.
5. Ranges are not specified (Abrahamson and Silva 2008; Idriss 2008) but are estimated based on the datasets.

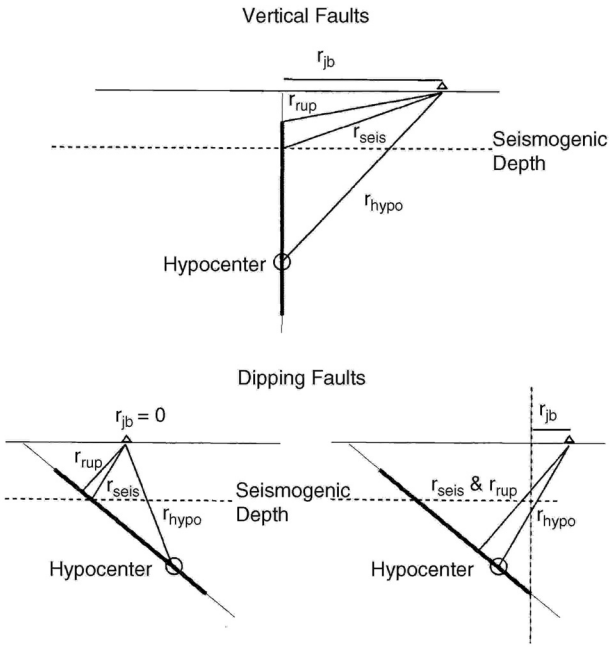

Figure B-1 Site-to-source distance definitions (Abrahamson and Shedlock, 1997).

B.3 Fault Rupture Directivity and Maximum Direction Shaking

Rupture directivity causes spatial variation in the amplitude and duration of ground motions in the regions surrounding faults. Propagation of rupture towards a site produces larger amplitudes of shaking at periods longer than 0.6 second and shorter strong-motion durations than for average directivity conditions.

Somerville et al. (1997) developed modifications to the Abrahamson and Silva (1997) ground motion prediction model to account for these variations. This and other models of that time were constructed from strong motion databases that included few near-fault records and so could not adequately represent the spectral demands associated with near-fault shaking.

Somerville (1997) identified fault rupture directivity parameters θ and X for strike-slip faults and ϕ and Y for dip slip faults as shown in Figure B-2; and developed three ground motion parameters to characterize directivity: (1) *Amplitude factor*: bias in average horizontal response spectrum acceleration with respect to Abrahamson and Silva (1997) and (2) *Fault-normal/Average amplitude*: ratio of fault normal to average (directivity) horizontal response spectrum acceleration. Bounds were set on the range of applicability of the directivity model.

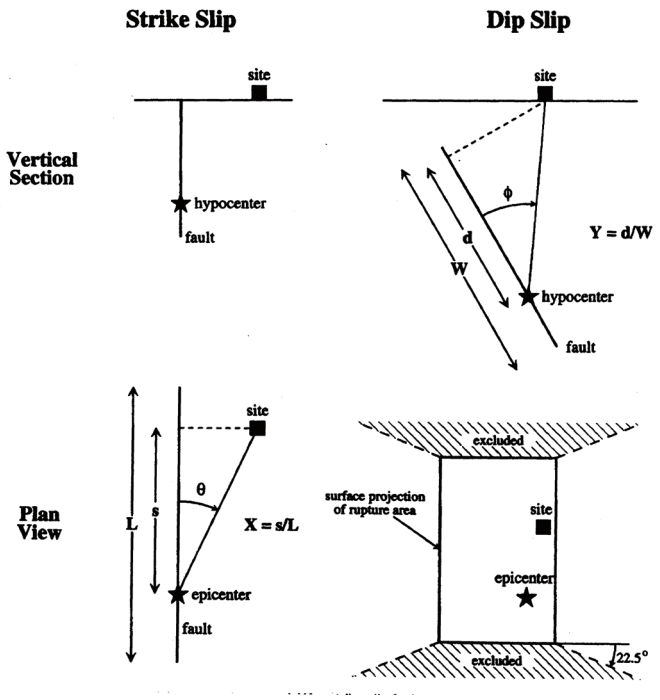

Figure B-2 Fault rupture directivity parameters (Somerville et al., 1997).

The recently developed Next-Generation Attenuation relationships for the Western United States were developed using a database that included many near-fault ground motion recordings. These relationships predict geomean spectral demand of recorded near-fault motions (i.e., average directivity) well with little bias (Huang et al. 2008a, 2008b). Huang et al. also report the median and 84th percentile ratios of maximum and minimum direction spectral demand to Next-Generation Attenuation -calculated geomean spectral demand for average directivity (i.e., all near-fault records) and the forward directivity region.

B.4 Probabilistic Seismic Hazard Assessment

B.4.1 Introduction

Performance-assessment will often utilize site-specific characterization of the ground shaking associated with different probabilities of exceedance or return periods. Such characterizations are routinely performed using Probabilistic Seismic Hazard Assessment. The following subsections provide introductory information on this technique, drawing substantially from Kramer (1996), McGuire (2004) and Bozorgnia and Bertero (2004).

B.4.2 Probabilistic Seismic Hazard Assessment Calculations

General

In this technique, probability distributions are determined for the magnitude of each possible earthquake on each source, $f_M(m)$, the location of each earthquake in or along each source, $f_R(r)$, and the prediction of the response parameter of interest $P(\text{pga} > \text{pga}' | m, r)$. Kramer describes this as a four-step process enumerated below and depicted in Figure B-3.

1. Identify and characterize (geometry and potential M_W) of all earthquake sources capable of generating significant shaking (say $M_W \geq 4.5$) at the site. Develop the probability distribution of rupture locations within each source. Combine this distribution with the source geometry to obtain the probability distribution of source-to-site distance for each source.
2. Develop a distribution of earthquake occurrence for each source using a recurrence relationship. This distribution can be random or time-dependent.
3. Using predictive models determine the ground motion produced at the building site (including the uncertainty) by earthquakes of any possible size or magnitude occurring at any possible point in each source zone.
4. Combine the uncertainties in earthquake location, size, and ground motion prediction to obtain the probability that the chosen ground motion parameter (e.g., peak horizontal ground acceleration, spectral acceleration at a specified frequency) will be exceeded in a particular time period (say 10% in 50 years).

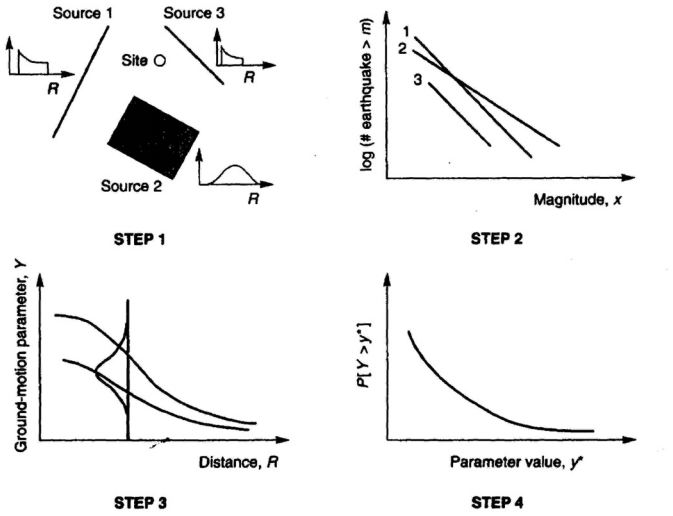

Figure B-3 Steps in probabilistic seismic hazard assessment (Kramer, 1996).

The sections below present summary information on parts of each step in this process. Kramer (1996) and McGuire (2004) provide much additional information.

Earthquake Source Characterization

Characterization of an earthquake source (there can be a number of sources for some sites) requires consideration of the spatial characteristics of the source, the distribution of earthquakes within that source, the distribution of earthquake size within that source, and the distribution of earthquakes with time. Each of these characteristics involves some degree of uncertainty, which is explicitly addressed by the process.

Spatial Uncertainty

Earthquake source geometries are typically characterized, as shown in Figure B-4 from Kramer (1996) a) as *point sources* (e.g., volcanoes); b) two-dimensional *areal sources* (e.g., a well-defined fault plane); and, c) three-dimensional *volumetric sources* (e.g., areas where earthquake mechanisms are poorly defined such as the Central and Eastern USA). These representations can have varying level of accuracy.

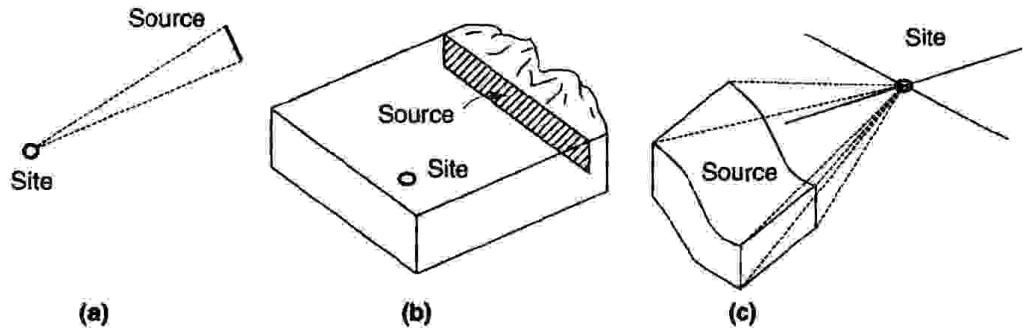

Figure B-4 Source zone geometries (Kramer, 1996).

Since attenuation relationships and other predictive models express ground motion parameters in terms of a measure of the source-to-site distance, the spatial uncertainty must be described with respect to the appropriate distance parameter. The uncertainty in source-to-site distance can be described by a probability density function as shown in Figure B-5.

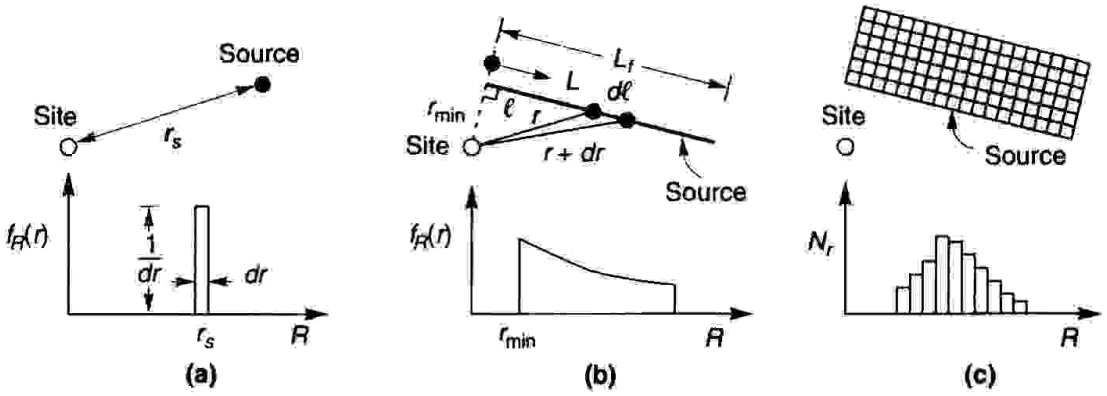

Figure B-5 Variations in site-to-source distance for three source zone geometries (Kramer, 1996).

As shown in Figure B-5, for the point source, the distance *R* is r_S; the probability that $R = r_s$ is 1.0 and that $R \neq r_s$ is 0. For more complex source zones, it is easier to evaluate $f_R(r)$ by numerical integration. For example, the source zone of part c of the figure above is broken up into a large number of discrete elements of the same area. A histogram that approximates $f_R(r)$ can be constructed by tabulating the values of *R* that correspond to the center of each element.

Size Uncertainty

Recurrence laws describe the distribution of probable earthquake sizes over a period of time. One basic assumption is that past recurrence rates for a source are appropriate for the prediction of future seismicity. The best known recurrence law is that of Gutenberg and Richter (1944), who collected data from Southern Californian earthquakes over a period of years and plotted the data according to the number of earthquakes that exceeded different magnitudes during that period. The number of exceedances of each magnitude was divided by the length of the time period used to assemble the data to define a *mean annual rate of exceedance* λ_m of an earthquake of magnitude *m*. The reciprocal of the mean annual rate of exceedance of a particular magnitude is termed the return period of earthquakes exceeding that magnitude. Guttenberg-Richter plotted the logarithm of the annual rate of exceedance (of earthquakes in Southern California) against earthquake magnitude and obtained the linear regression relationship:

$$\log \lambda_m = a - bm \tag{B-1}$$

where λ_m is defined above, 10^a is the mean yearly number of earthquakes of magnitude greater than or equal to magnitude *m*, and *b* describes the relative likelihood of large and small earthquakes. As the value of *b* increases, the number of larger magnitude earthquakes relative to smaller magnitude

earthquakes decreases. The mean rate of small earthquakes is often under-predicted because historical records are often used to supplement the instrumental records and only the larger magnitude events from part of the historical record.

The Guttenberg-Richter law was originally developed from regional data and not for specific source zones. Paleoseismic studies over the past 30 years have indicated that individual points on faults (or fault segments) tend to move by approximately the same distance in successive earthquakes, suggesting that individual faults repeatedly generate earthquakes of a similar (with 0.5 magnitude unit) size, known as *characteristic earthquakes* at or near their maximum capable magnitude. Geological evidence indicates that characteristic earthquakes occur more frequently than would be implied by extrapolation of the law from high exceedance rates (of low magnitude events) to low exceedance rates (of high magnitude), resulting in a more complex recurrence law than that given by equation B-1.

Attenuation Relationships

Scatter or randomness in the results obtained from predictive models is inevitable because of differences in site condition, travel path and fault rupture mechanics associated with the data set and a lack of certainty as to the precise values of these parameters for any specific stie. The scatter can be characterized by confidence limits or by the standard deviation of the predicted parameter.

The probability that a ground motion parameter Y exceeds a certain value y for an earthquake of magnitude m, occurring at a distance r is given by

$$P[Y > y | m, r] = 1 - F_y(y) \tag{B-2}$$

$$P[Y > y | m, r] = 1 - F_y(y) = 1 - \Phi\left(\frac{\ln y - \ln \theta}{\beta}\right)$$

where $F_Y(y)$ is the value of the cumulative distribution function of Y at m and r, which is assumed to be lognormal in form; θ is the median value of Y and β is the dispersion. Figure B-6 illustrates the conditional probability of exceeding a particular value of a ground motion parameter for a given combination of m and r.

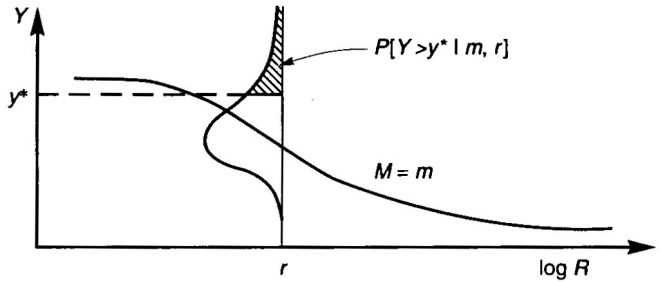

Figure B-6 Conditional probability calculation (Kramer, 1996).

Temporal Uncertainty

The distribution of earthquake occurrence with time must be computed or assumed to calculate the probabilities of different earthquake magnitudes occurring in a given time period. Earthquakes are assumed to occur randomly with time and the assumption of random occurrence permits the use of simple probability models.

The temporal occurrence of earthquakes is commonly described as a *Poisson* process: one that yields values of a random variable describing the number of occurrences of a particular event during a given time interval (or spatial region). In a Poisson process: (a) the number of occurrences in one time interval are independent of the number that occur in any other time interval; (b) the probability of occurrence during a very short time interval is proportional to the length of the time interval; and (c) the probability of more than one occurrence in a very short time interval is negligible. Events in a Poisson process occur randomly, with no memory of the time, size or location of any preceding events. Cornell (1988) showed that the Poisson model is useful for probabilistic hazard analysis unless the hazard is dominated by a single source zone that produces characteristic earthquakes and the time since the previous significant event exceeds the average inter-event time.

For a Poisson process, the probability of a random variable N, representing the number of occurrences of a particular event in a given time period is given by

$$P[N = n] = \frac{\mu^n e^{-\mu}}{n!} \qquad \text{(B-3)}$$

where μ is the average number of occurrences of the event in the time period. To characterize the temporal distribution of earthquake recurrence for probabilistic seismic hazard analsyis, the Poisson probability is normally expressed as

$$P[N = n] = \frac{(\lambda t)^n e^{-\lambda t}}{n!} \quad \text{(B-4)}$$

where λ is the average rate of recurrence of the event and *t* is the time period. When the event is the exceedance of a particular earthquake magnitude, the Poisson model can be combined with a suitable recurrence law to predict the probability of at least one exceedance in a period of *t* years by

$$P[N \geq 1] = 1 - e^{-\lambda_m t} \quad \text{(B-5)}$$

Probability Computations and Seismic Hazard Curves

S*eismic hazard curves* identify the annual frequency of exceedance of different values of a selected ground motion parameter. Development of these curves involves probabilistic calculations that combine the uncertainties in earthquake size, location and frequency for each potential earthquake source that could impact shaking at the site under study.

The seismic hazard curve calculations are straightforward once the uncertainties in earthquake size, location and frequency are established but much bookkeeping is involved. The probability of exceeding a particular value *y* of a ground motion parameter *Y* is calculated for one possible source location and then multiplied by the probability of that magnitude earthquake occurring at that particular location. The calculation is then repeated for all possible magnitudes and locations and the probabilities of each are summed to compute the $P[Y > y]$ at the site. A summary of this process is presented below. Kramer (1996) and McGuire (2004) provide much additional information.

For a given earthquake occurrence, the probability that a ground motion parameter *Y* will exceed a particular value *y* can be computed using the total probability theorem (Cornell and Benjamin, 1968) as:

$$P[Y > y] = P[Y > y|\mathbf{X}]P[\mathbf{X}] = \int P[Y > y|\mathbf{X}] f_x(\mathbf{X})\, dx \quad \text{(B-6)}$$

where $\mathbf{X}$ is a vector of random variables that influence *Y*. In most cases, the quantities in $\mathbf{X}$ are limited to the magnitude *M* and distance *R*. Assuming that *M* and *R* are independent, the probability of exceedance can be written as

$$P[Y > y] = \iint P[Y > y|m,r] f_M(m) f_R(r)\, dm\, dr \quad \text{(B-7)}$$

where $P[Y > y|m,r]$ is obtained from the predictive relationship and $f_M(m)$ and $f_R(r)$ are the probability density functions for magnitude and distance, respectively.

If the building site is in a region of N_s potential earthquake sources, each of which has an average rate of threshold exceedance $\nu_i = \exp(\alpha_i - \beta_i m)$, the total average exceedance rate for the region is given by the equation:

$$\lambda_y = \sum_{i=1}^{N_s} P[Y > y | m, r] f_{Mi}(m) f_{Ri}(r) \, dm \, dr \tag{B-8}$$

This equation is typically solved by numerical integration. One simple approach described by Kramer is to divide the possible ranges of magnitude and distance into N_M and N_R segments, respectively. The average exceedance rate can then be calculated using the multi-level summation:

$$\begin{aligned} \lambda_y &= \sum_{i=1}^{N_s} \sum_{j=1}^{N_m} \sum_{k=1}^{N_R} \nu_i P[Y > y | m_j, r_k] f_{Mi}(m_j) f_{Ri}(r_k) \Delta m \Delta r \\ &= \sum_{i=1}^{N_s} \sum_{j=1}^{N_m} \sum_{k=1}^{N_R} \nu_i P[Y > y | m_j, r_k] P[M = m_j] P[R = r_k] \end{aligned} \tag{B-9}$$

where the terms are $m_j = m_0 + (j - 0.5)(m_{\max} - m_0)/N_M$, $\Delta r = (r_{\max} - r_{\min})/N_r$, $r_k = r_{\min} + (k - 0.5)(r_{\max} - r_{\min})/N_R$ and $\Delta m = (m_{\max} - m_0)/N_M$. The above statement is equivalent to assuming that each source is capable of generating only N_M different earthquakes of magnitude m_j at only N_R different source-to-site distances of r_k. The accuracy of this method increases with smaller segments and thus larger values of N_M and N_R.

Figure B-7 presents a sample seismic hazard curve for peak ground acceleration at a site in Berkeley, California (McGuire, 2004). The figure shows the contributions to the annual frequency of exceedance from 9 different seismic sources.

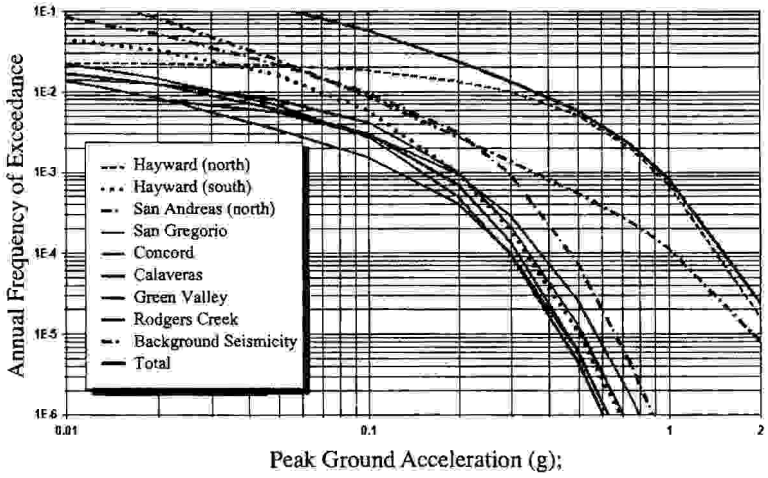

Figure B-7 Seismic hazard curve for Berkeley, California (McGuire, 2004).

Exceedance probabilities in a selected time period can be computed using seismic hazard curves combined with the Poisson model. The probability of exceedance of y in a time period T is

$$P[Y_T > y] = 1 - e^{-\lambda_y T} \tag{B-10}$$

As an example, the probability that a peak horizontal ground acceleration of 0.10 g will be exceeded in a 50-year time period for the site characterized by the hazard curve above is:

$$P[\text{PHA} > 0.1g \text{ in 50 years}] = 1 - e^{-\lambda_y T} = 1 - e^{-(0.060)(50)} = 0.950 = 95\% \tag{B-11}$$

An alternate, often made, computation is the value of the ground motion parameter corresponding to a particular probability of exceedance in a given time period. For example, the acceleration that has a 10% probability of exceedance in a 50-year period would be that with an annual rate of exceedance, calculated by re-arranging the second-to-last equation, namely

$$\lambda_y = -\frac{\text{In}(1 - P[Y_T > y])}{T} = -\frac{\text{In}(1 - 0.10)}{50} = 0.00211 \tag{B-12}$$

Using the hazard curve from Figure B-7 for all nine sources, the corresponding zero-period spectral acceleration is approximately 0.75 g.

Hazard curves can be developed for specific oscillator periods (0.2 second and 1.0 second are widely used) and the above calculations of probability of exceedance can be extended across the spectral domain. This permits development of probabilistic estimates of spectral demands for different probabilities of exceedance or return periods. Hazard curves have been developed for many different response quantities and characterizations of earthquake ground motion.

B.4.3 Inclusion of Rupture Directivity Effects

If the building site is located within 20 *km* of an active fault capable of generating an M_w 6.5 earthquake or greater, rupture directivity effects should be considered.

Average rupture directivity effects can be included directly in probabilistic seismic hazard analysis if the attenuation relationships are either a) constructed using a database of recorded ground motions that include directivity effects (i.e., the NGA relationships described previously), or b) corrected to account for rupture directivity in a manner similar to that described by Somerville et al. (1997) and Abrahamson (2000). Note that the ratio of median maximum demand to geomean demand in the near-fault

region is period-dependant and can be as great as 2 (Huang et al. 2008a, 2008b).

B.4.4 Deaggregation of Seismic Hazard Curves and Epsilon

Probabilistic seismic hazard analysis enables calculation of annual rates of exceedance of ground motion parameters (e.g., spectral acceleration at a selected period) at a particular site based on aggregating the risks from all possible source zones. Therefore, the computed rate of exceedance for a given parametric intensity value is not associated with any particular earthquake magnitude *m* or distance *r*.

For a given building site and hazard curve, it is possible to establish the combinations of magnitude, distance and source that contribute most to particular values of an intensity. This process is termed de-aggregation (or disaggregation). Hazard deaggregation requires expression of the mean annual rate of exceedance as a function of magnitude and distance of the form:

$$\lambda_y(m_j, r_k) = P[M = m_j]P[R = r_k]\sum_{i=1}^{N_s} \nu_i P[Y > y | m_j, r_k] \qquad \text{(B-13)}$$

McGuire (2004) provides detailed information on hazard deaggregation.

Figure B-8 shows sample deaggregation results for horizontal spectral acceleration at periods of 0.2 second and 1.0 second for a site in the Western United States, for a 2% probability of exceedance in 50 years. Consider the 1-second deaggregation data of part b of Figure B-8. The plot shows the contribution to the 1-second uniform hazard spectral ordinate as a function of moment magnitude and distance. The figure shows that approximately 50% of the total 1-second seismic demand can be ascribed to a moment magnitude 7.8 earthquake at a distance of 14 *km*–the [*M*, *r*] pair that dominates the 1-second spectral demand at this site is [7.8, 14].

This figure also introduces another important ground motion variable, epsilon, ε . One straightforward definition of ε is:

$$\varepsilon = \frac{\ln S_a - \ln \theta}{\beta} \qquad \text{(B-14)}$$

where all variables vary as a function of period, and S_a is the computed spectral acceleration for a given probability (e.g., 2%) of exceedance in a specified time period (e.g., 50 years) and equal to 0.829*g* in this instance at a period of 1 second; θ is the median value of spectral acceleration computed by an appropriate attenuation relationship(s) for the dominant [*M*, *r*] pair (equal to [7.8, 14] in this instance), and β is the dispersion in the attenuation

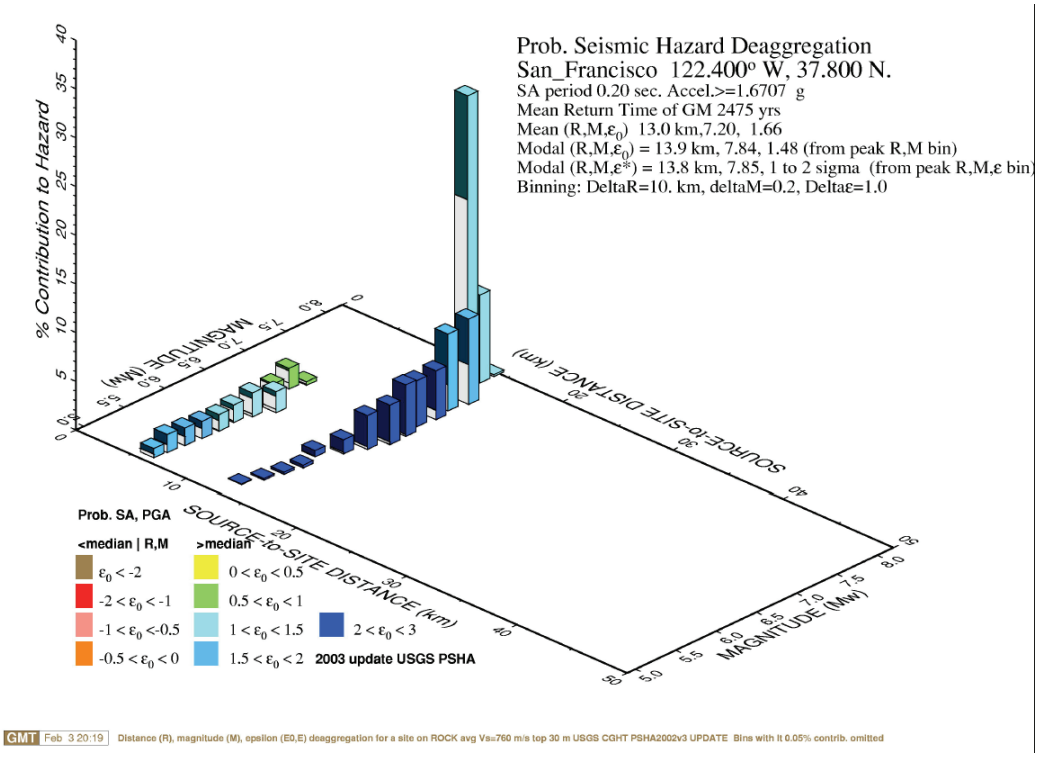

a. 0.2 second deaggregation

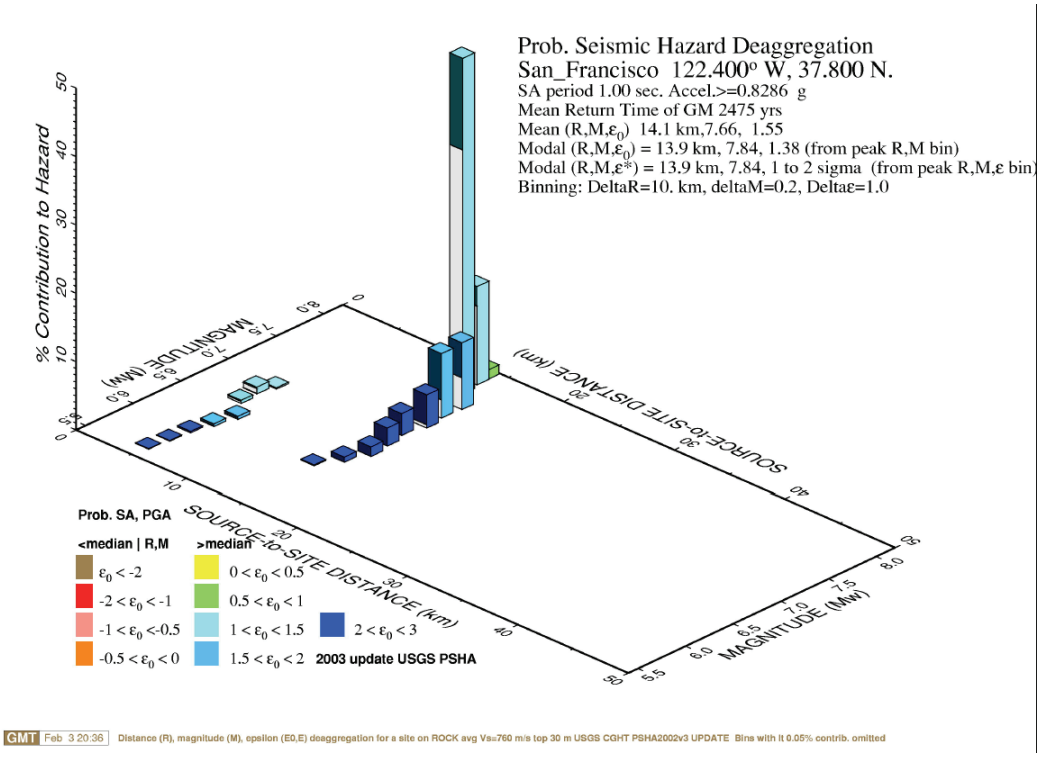

b. 1.0 second deaggregation

Figure B-8 Sample de-aggregation of a hazard curve (from www.usgs.gov).

relationship. In this example, and using the modal [M, r, ε] triple, we see that ε ranges between 1 and 2, meaning that less than 15% of moment magnitude 7.8 earthquakes at a distance of 14 *km* would produce *geomean* spectral demands in excess of 0.829 *g*.

Baker and Cornell (2005, 2006) observed that ε is an indicator of spectral shape, with a positive (negative) value of ε at a given period tending to indicate a relative peak (valley) in the acceleration response spectrum at that period. Figure B-9 illustrates these trends using six bins of 20 ground motions defined by $\varepsilon \geq 2.25$, $-0.06 \leq \varepsilon \leq 0.06$ and $\varepsilon \leq -2.25$, respectively, at periods of 0.8 (Figure B-9a) and 0.3 second (Figure B-9b). The relative peak (valley) in the spectra for the $+\varepsilon$ ($-\varepsilon$) bin of motions at the two periods is clearly evident. No relative peak or valley at the reference periods is associated with the ε -neutral bin.

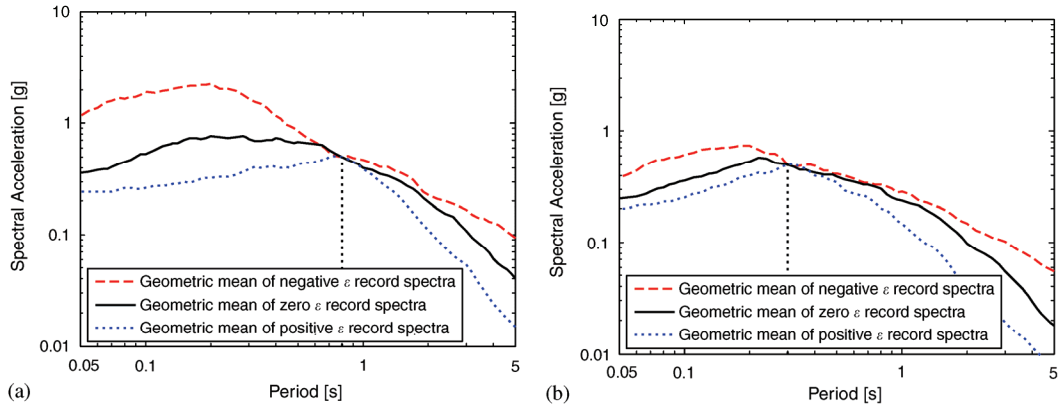

Figure B-9 Sample geometric-mean response spectra for negative-, zero- and positive-ε record sets with each record in the sets scaled to a) $S_a(0.8s) = 0.5\ g$ and b) $S_a(0.3s) = 0.5\ g$ (Baker and Cornell 2006).

B.4.5 Conditional Mean Spectrum and Spectral Shape

Chapter 4 introduced Probabilistic Seismic Hazard Assessment and the development of Uniform Hazard Spectra and noted that the ordinates of Uniform Hazard Spectra are each associated with the same annual frequency of exceedance.

Building code and seismic design standard provisions for nonlinear response history analysis recommend scaling ground motions to match a target uniform hazard spectrum over a wide period range. Although convenient for design and likely conservative, such scaling procedures ignore the following:

- If the spectral ordinates of the uniform hazard spectrum are governed by multiple scenario events, the spectral shape will not represent that for any

of the governing events, regardless of the return period (Baker and Cornell, 2006).

- For long-return-period earthquake shaking, the spectral ordinates of Uniform Hazard spectra are typically associated with a high value (greater than 1) of ε across a wide range of period (Harmsen 2001). For the case where the geomean spectral ordinate of a ground motion pair attains the uniform hazard spectrum ordinate at a given period, the geomean spectrum of the pair is unlikely to have ordinates as large as those of the uniform hazard spectrum at other periods. The geomean spectra for the $+\varepsilon$ record sets in Figure B-9 support this observation.

Baker and Cornell (2005, 2006) introduced the Conditional Mean Spectrum which considers the correlation of spectral demands (represented by values of ε) at different periods, to address these two issues. Conditional Mean Spectra estimate the median geomean spectral acceleration response of a pair of ground motions given an [*M*, *r*] pair and a target spectral ordinate, $\overline{S}_a(T_1)$ (from which ε_{T_1} is back-calculated using an appropriate attenuation relationship). Baker and Cornell (2005) used the following equation to generate conditional mean spectra:

$$CMS_{\overline{S}_a(T_1)}(T_2) = \theta(M,r,T_2) \cdot \exp\left[\beta(M,r,T_2) \cdot \rho_{\varepsilon(T_1),\varepsilon(T_2)} \cdot \varepsilon_{T_1}\right] \qquad \text{(B-15)}$$

where $CMS_{\overline{S}_a(T_1)}(T_2)$ is the ordinate of the spectrum at period T_2 given that the spectral demand at T_1 is $\overline{S}_a(T_1)$; $\theta(M,r,T_2)$ and $\beta(M,r,T_2)$ are the median and logarithmic standard deviation of spectral acceleration at T_2 computed using a ground motion attenuation relationship for the [*M*, *r*] pair of interest; ε_{T_1} is the value of ε associated with $\overline{S}_a(T_1)$; and $\rho_{\varepsilon(T_1),\varepsilon(T_2)}$ is the correlation coefficient for ε between T_1 and T_2.

Baker and Jayaram (2008) developed a model for $\rho_{\varepsilon(T_1),\varepsilon(T_2)}$ using the Next Generation Attenuation ground motion database (www.peer.berkeley.edu) :

$$\begin{aligned}
&\text{if } T_{\max} < 0.109 && \rho_{\varepsilon(T_1),\varepsilon(T_2)} = C_2 \\
&\text{else if } T_{\min} > 0.109 && \rho_{\varepsilon(T_1),\varepsilon(T_2)} = C_1 \\
&\text{else if } T_{\max} < 0.109 && \rho_{\varepsilon(T_1),\varepsilon(T_2)} = \min(C_2, C_4) \\
&\text{else} && \rho_{\varepsilon(T_1),\varepsilon(T_2)} = C_4
\end{aligned} \qquad \text{(B-16)}$$

where $T_{\min} = \min(T_1, T_2)$, $T_{\max} = \max(T_1, T_2)$ and

$$C_1 = 1 - \cos\left(\frac{\pi}{2} - 0.366 \ln\left(\frac{T_{\max}}{\max(T_{\min}, 0.11)}\right)\right) \qquad \text{(B-17)}$$

$$C_2 = \begin{cases} 1 - 0.105\left(1 - \dfrac{1}{1+e^{100T_{\max}-5}}\right)\left(\dfrac{T_{\max}-T_{\min}}{T_{\max}-0.01}\right) & \text{if } T_{\max} < 0.2\,\text{sec} \\ 0 & \text{otherwise} \end{cases} \quad \text{(B-18)}$$

$$C_3 = \begin{cases} C_2 \text{ if } T_{\max} < 0.11\,\text{sec} \\ C_1 \text{ if } T_{\max} \geq 0.11\,\text{sec} \end{cases} \quad \text{(B-19)}$$

$$C_4 = C_1 + 0.5(\sqrt{C_3} - C_3)\left(1 + \cos\left(\frac{\pi T_{\min}}{0.11}\right)\right) \quad \text{(B-20)}$$

Conditioinal Mean Spectra can be constructed using the following procedure:

1. Determine the value of $\overline{S}_a(T_1)$ from the probabilistic seismic hazard analysis at the desired mean annual frequency of exceedance.
2. De-aggregate the hazard at $\overline{S}_a(T_1)$ and identify the modal [*M*, *r*, ε] triple.
3. Select an appropriate ground motion attenuation relationship.
4. Generate the spectrum using (E-15) through (E-20) and the selected attenuation relationship for the [*M*, *r*, ε] triple of Step 2.
5. Amplitude scale the spectrum to recover $\overline{S}_a(T_1)$.

To illustrate this procedure, consider the deaggregation results of Figure B-8b for a site in San Francisco. As presented in Figure B-8b, the value of $\overline{S}_a(T_1)$ is 0.83 *g* for a return period of 2475 years and the modal [*M*, *r*, ε] triple for the hazard is [7.8, 14 *km*, 1 to 2]. A value of $\varepsilon = 1.5$ (midpoint of 1 and 2) was used for this example. In this example, the Chiou-Youngs NGA relationship was selected. Figure B-10 presents the results of Steps 4 and 5 using dotted and solid lines, respectively. (If $\varepsilon = 2$ is used in Step 4, the scale factor for Step 5 is 1.) The figure also presents the uniform hazard spectrum for this site at a return period of 2475 years. Except at period, T_1, the ordinates of the uniform hazard spectrum are greater than those of the scaled conditional mean spectrum.

The Conditional Mean Spectrum can be refined to also consider uncertainty in each spectral acceleration value at periods other than $S_a(T_1)$. This is done because the probabilities associated with the target spectrum are associated only with $S_a(T_1)$, and real ground motions with the target $S_a(T_1)$ also have variability. Baker and Cornell (2005) computed the conditional standard deviation of spectral accelerations as follows:

$$\beta_{\overline{S}_a(T_1)=x}(T_2) = \beta(M, r, T_2)\sqrt{1 - \rho^2_{\varepsilon(T_1),\varepsilon(T_2)}} \quad \text{(B-21)}$$

where $\beta_{\overline{S_a(T_1)}=x}(T_2)$ is the conditional dispersion in $S_a(T_2)$ given $S_a(T_1)$ and the other variables are as defined above. The target spectrum computed using Equations B-15 and B-20 has been termed a Conditional Spectrum (Abrahamson and Al Atik 2010), as unlike the CMS it is not just a mean value. Figure B-11 shows the Conditional Spectrum corresponding to the CMS plotted in Figure B-10. While less simple than selecting and scaling ground motions to match the mean spectrum only, methods and software tools are available to find ground motions that match a target mean and standard deviation (Jayaram et al. 2011).

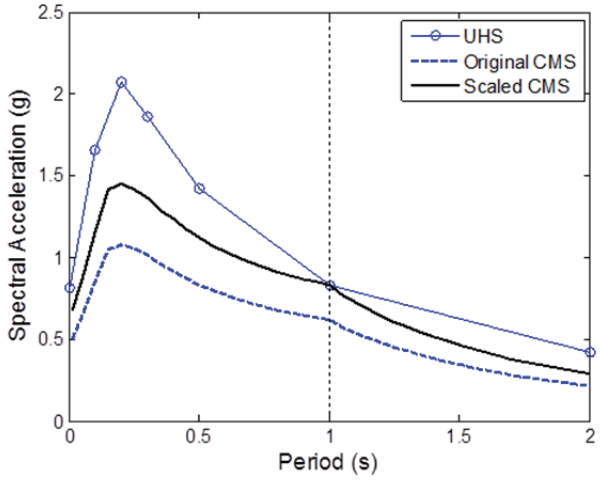

Figure B-10 UHS for a 2% probability of exceedance in 50 years and original and scaled CMS for a rock site in San Francisco.

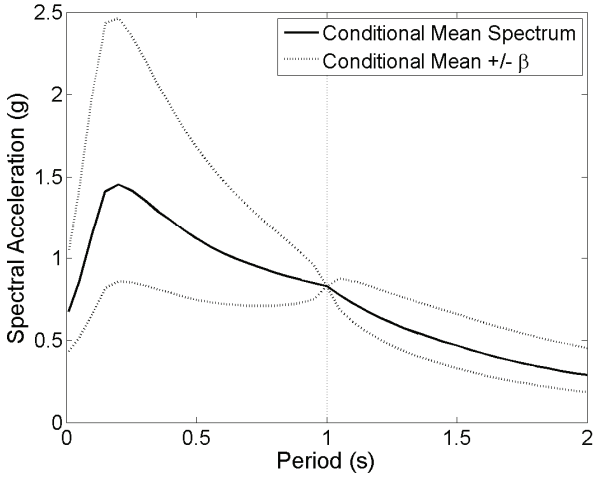

Figure B-11 Conditional Spectrum for Sa(1s) with 2% probability of exceedance in 50 years for a rock site in San Francisco.

B.5 Vertical Earthquake Shaking

B.5.1 Introduction

Vertical response spectra can be generated by using ground motion prediction models for vertical ground shaking parameters and probabilistic seismic hazard analysis to determine ordinates of spectral response at the desired annual frequencies of exceedance. Gülerce (2011) provides discussion of this technique.

This section presents simplified procedures that can be used to generate vertical response spectra from horizontal spectra for the same site using approximate relationships between typical vertical and horizontal spectra. These procedures, extracted from BSSC (2009) can be used for most buildings, where important vertical periods of response are less than or equal to 1.0 second. For buildings with important natural periods of vertical response in excess of 1.0 second, site-specific analysis should be conducted.

B.5.2 Procedure for Site Classes A, B and C

For structural periods less than or equal to 1.0 second, the vertical response spectrum can be constructed by scaling the corresponding ordinates of the horizontal response spectrum, S_a, as follows.

For periods less than or equal to 0.1 second, the vertical spectral acceleration, S_v, can be taken as

$$S_v = S_a \tag{B-21}$$

For periods between 0.1 and 0.3 second, the vertical spectral acceleration S_v, can be taken as

$$S_v = (1 - 1.048[\log(T) + 1])S_a \tag{B-22}$$

For periods between 0.3 and 1.0 second, the vertical spectral acceleration, S_v, can be taken as

$$S_v = 0.5S_a \tag{B-23}$$

B.5.3 Procedure for Site Classes D and E

For structural periods less than or equal to 1.0 second, the vertical response spectrum can be constructed by scaling the corresponding ordinates of the horizontal response spectrum, S_a, as follows.

For periods less than or equal to 0.1 second, the vertical spectral acceleration, S_v, can be taken as

$$S_v = \eta S_a \tag{B-24}$$

For periods between 0.1 and 0.3 second, the vertical spectral acceleration, S_v, can be taken as

$$S_v = (\eta - 2.1(\eta - 0.5)[\log(T) + 1])S_a \quad \text{(B-25)}$$

For periods between 0.3 and 1.0 second, the vertical spectral acceleration, S_v, can be taken as

$$S_v = 0.5S_a \quad \text{(B-26)}$$

In equations (B-24) through (B-26), η can be taken as 1.0 for $S_s \le 0.5g$; 1.5 for $S_s \le 1.5g$; and $(1 + 0.5(S_s - 0.5))$ for $0.5g \le S_s \le 1.5g$.

B.6 Soil-Foundation-Structure Interaction

B.6.1 General

Structural response to earthquake shaking is affected by the dynamic properties of the three components of the soil-foundation-structure system and the interactions between these components. Soil-foundation-structure interaction analysis involves either direct or indirect analysis of the three-component system to prescribed free-field inputs, which are typically imposed as bedrock motions.

Traditional structural analysis neglects soil-foundation-structure interaction. As illustrated in Figure B-12, such analysis assumes the base of the structure is rigid (components fixed at their base) and the input motions at the base of the foundation are derived assuming one of the standard soil categories described in the building code and its referenced standards. The use of such fixed base models is inappropriate for structural framing systems that incorporate stiff vertical components for lateral resistance (e.g., reinforced concrete shear walls, steel braced frames) because the response of such systems can be sensitive to small base rotations and translations that are neglected by the fixed base assumption. Relatively flexible lateral framing systems such as moment-resisting frames are often not significantly affected by soil-foundation-structure interaction effects.

B.6.2 Direct Soil-Foundation-Structure-Interaction Analysis

Soil-foundation-structure interaction can be directly analyzed using finite-element models that represent the soil as discretized solid finite elements. Soil elements can either use equivalent linear properties, or full nonlinear representation. Such direct analysis can address the three key effects of soil-foundation-structure interaction: foundation flexibility, kinematic effects, and foundation damping. Solution of the kinematic interaction problem is often difficult without customized finite element codes because typical finite

element codes cannot account for wave inclination and wave incoherence effects, both of which can be important.

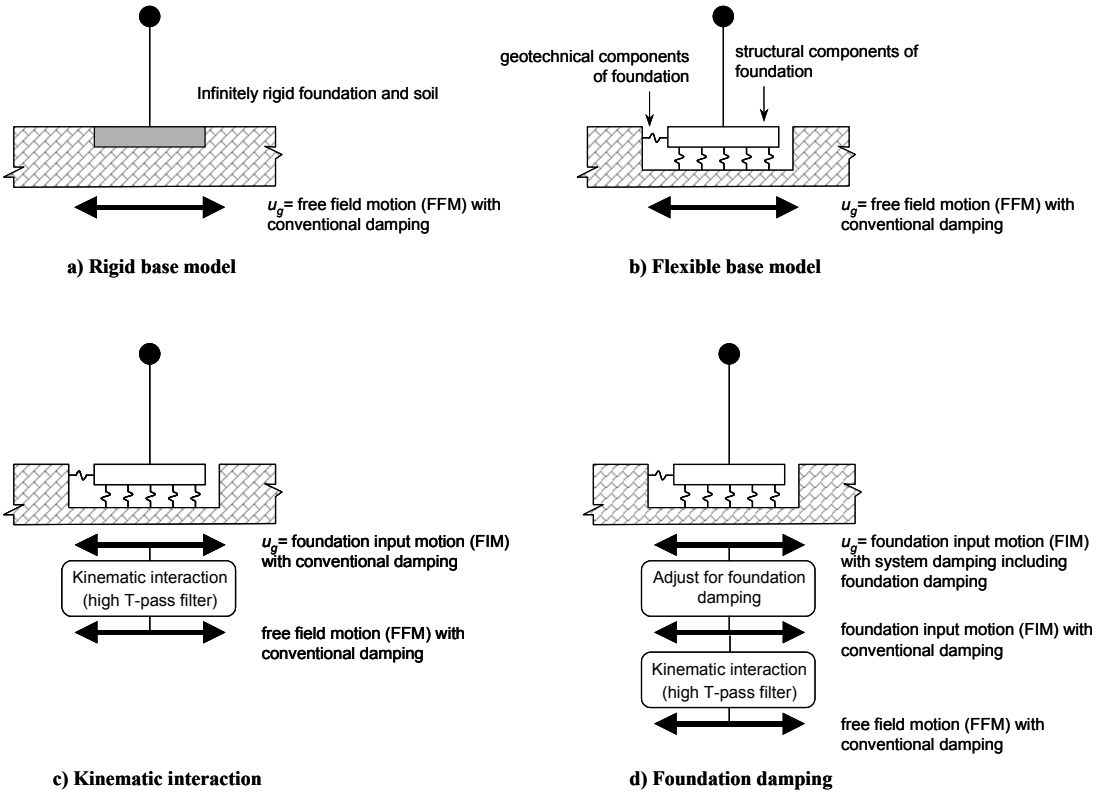

Figure B-12 Analysis for soil foundation structure interaction (FEMA, 2005)

Response-history analysis requires the development of a three-dimensional numerical model of the soil-foundation-structure system. Stress-strain or constitutive models (linear, nonlinear or equivalent linear) for the soils in the model should be developed based on test data. Appropriate and consistent frequency-dependant stiffness and damping matrices should be developed for the edges or boundaries of the soil in the numerical model.

B.6.3 Simplified Soil-Foundation-Structure-Interaction Analysis

Simplified Procedures

This section presents simplified procedures for including the effects of soil-foundation-structure interaction in response analysis. The procedures are based on those presented in FEMA 440 (FEMA, 2005). More rigorous procedures are available in Appendix A of FEMA 440.

For the discussion below, soil-foundation-structure interaction is parsed into three key effects:

- foundation flexibility

- kinematic effects (filtering of the ground shaking to the building)
- foundation damping (dissipation of energy from the soil structure system through radiation and hysteretic soil damping).

Figure B-12b illustrates the incorporation of foundation flexibility into the numerical model of a building frame. Current analysis procedures in guidelines such as ASCE 41 (ASCE, 2006) and ATC 40 (ATC, 1996) partially address the flexible foundation effect by providing guidance on the stiffness and strength of the geotechnical (soil) components of the foundation in the structural analysis model. However, these analysis procedures do not characterize the reduction of the shaking demand on the structural framing system relative to the free-field motion due to kinematic interaction or the foundation damping effect, both of which are described below. Guidance on including these effects in a simplified manner for nonlinear dynamic response analysis is provided below. Numerical simulation using models like that illustrated in Figure B-12b predicts global response that includes elastic and inelastic deformations in the structural and geotechnical parts of the foundation system. These deformations are sometimes referred to as an *inertial soil-structure-interaction effect*. The inclusion of foundation flexibility in the numerical model can provide significantly different and more accurate response predictions than those computed assuming a fixed base (Figure B-12a). Further, foundation response and failures (e.g., rocking, soil bearing failure, pier/pile slip) can be explicitly evaluated using this approach.

Kinematic soil-structure interaction (Figure B-12c) results from the presence of relatively stiff foundation elements atop or within soil that causes the foundation motions to deviate from free-field motions. Base slab averaging and embedment are two kinematic effects. Ground motion shaking is spatially variable (i.e., in the absence of a foundation, each point beneath a building footprint, would experience somewhat different shaking at the same instant in time). Placement of a structure and foundation across these spatially variable motions produces an averaging effect and the weighted or overall motion experienced by the building is less than the localized maxima that would have occurred in the free-field, particularly at short period. The embedment effect is associated with the reduction of ground motion with depth into a soil deposit. Both base slab averaging[2] and embedment[3] affect

[2] Base slab averaging occurs to some extent in virtually all buildings. The slab averaging effect occurs at the foundation level for mats or spread footings interconnected by either grade beams or reinforced concrete slabs. Even if a laterally stiff foundation system is not present, the averaging can occur at the first elevated level of buildings with rigid diaphragms. The

the characteristics of the foundation-level motion (sometimes called the foundation input motion) in a manner that is independent of the superstructure (i.e., the portion of the structure above the foundation) with one exception. The effects are strongly period dependent, being maximized at short periods. The effects can be visualized as a filter applied to the high-frequency components of the free-field ground motion. The impact of those effects on superstructure response will tend to be greatest for short-period buildings. A simplified procedure to reduce the free field motion to a foundation input motion is presented below. The foundation input motion can be applied to a fixed base model or combined with a flexible base model. Kinematic effects tend to be important for buildings with relatively short fundamental periods (e.g., less than 0.5 second), large plan dimensions and basements embedded 10 feet or more in soil materials.

Figure B-11d illustrates foundation damping effects that are another result of *inertial soil-structure interaction*. Foundation damping results from the relative movements of the foundation and free-field soil. It is associated with radiation of energy away from the foundation and hysteretic damping within the soil. The result is an effective decrease in the spectral ordinates of ground motion experienced by the structure. Foundation damping effects tend to be greatest for stiff structural framing systems (e.g., reinforced concrete shear walls, steel braced frames) and relatively soft foundation soils (e.g., Site Classes D and E per ASCE-7-10). Simplified procedures for incorporating foundation damping in a numerical model analysis are described below.

Simplified Procedure for Kinematic Interaction

A ratio-of-response-spectra factor can be used to represent kinematic interaction effects. This is the ratio of the response spectral ordinates imposed on the foundation (i.e., the foundation input motion, FIM) to the free-field spectral ordinates. Two phenomena should be considered in evaluating the ratio: base-slab averaging and foundation embedment. Foundation embedment effects should be considered for buildings with basements. The simplified procedure of Chapter 8 of FEMA 440 (FEMA, 2005) can be used for assessment of kinematic interaction. The following information is needed for such assessment: dominant building period (as measured by % mass participating in the elastic base shear computation),

only case where base slab averaging effects should be neglected is for buildings without a laterally connected foundation system and with flexible floor and roof diaphragms.

[3] Embedment effects should not be considered for buildings without basements, even if the footings are embedded. Embedment effects tend to be significant when the depth of basements is greater than about 10 feet.

building foundation plan dimension, foundation embedment, peak horizontal ground acceleration, and shear wave velocity. Section 8 of FEMA 440 specifies limitations on the applicability of the simplified procedure Figures B-13a and B-13b (from FEMA 440) provide summary information on the reductions in spectral demand due to base-slab averaging and embedment. The 5% damped free-field spectrum is multiplied by the product of the period-dependant reduction factors for base-slab averaging and embedment to derive the foundation input motion spectrum. Since the embedment computation is dependant on the peak horizontal ground acceleration, the computation must be repeated for every level of hazard considered for the performance and loss assessment.

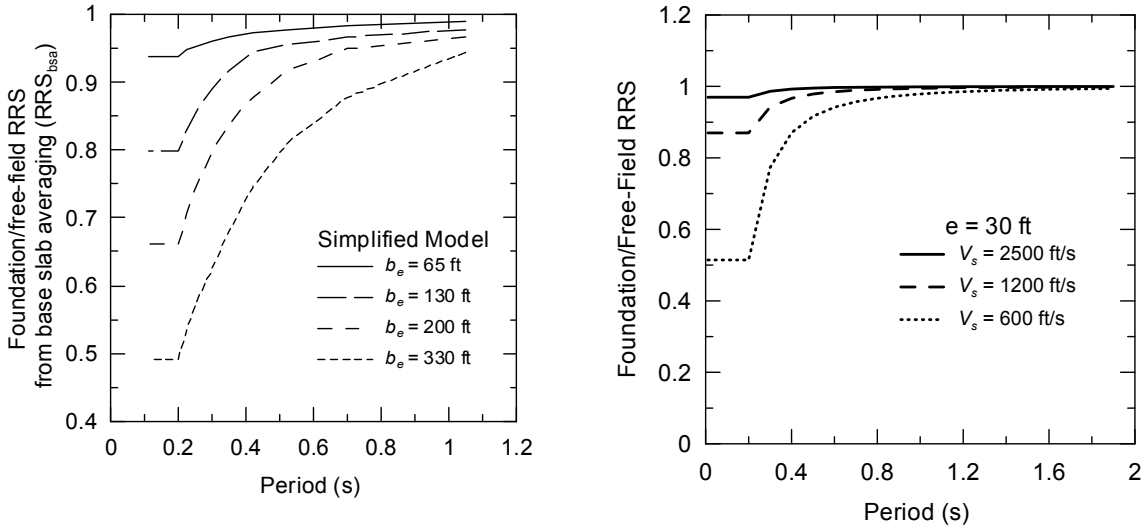

a. base slab averaging b. embedment

Figure B-13 Reductions in spectral demand due to kinematic interaction.

Simplified Procedure for Foundation Damping

Soil-foundation interaction can significantly increase the effective damping in associated with a structure's dynamic response to earthquake shaking.

The simplified procedure of FEMA 440 can be used for assessment of foundation damping. In this procedure foundation radiation damping effects reduce the ordinates of the 5% damped acceleration response spectrum, typically used as the basis for selecting and scaling ground motions used in analysis. Hysteretic damping in the soil should be captured directly through the use of nonlinear soil springs. The following information is needed for such an assessment: dominant (first mode) building period (as measured by % mass participating in the elastic base shear computation), T_1; first modal mass; building foundation plan dimension; building height; foundation embedment; strain-degraded soil shear modulus and soil Poisson's ratio.

Section 8 of FEMA 440 presents limitations on the use of the simplified procedure. The 5% damped free-field spectrum is modified in the period range $T \geq 0.75T_1$.

B.7 Alternate Procedure for Hazard Characterization for Scenario-Based Assessment Using Nonlinear Response-History Analysis

Scenario-based assessments consider uncertainty in spectral demand. Ground motion intensity is assumed to be lognormally distributed with median value θ, and dispersion, β.

Eleven values of spectral acceleration at each user-selected period are used to characterize the distribution of seismic demand for scenario-assessments as follows:

$$S_{ai} = \theta e^{\beta \eta_i} \qquad i = 1, 11 \tag{B-27}$$

where S_{ai} is the i^{th} target spectral acceleration at a given period and values of η_i are listed in Table B-2.

Table B-2 Values of η_i for Generating a Distribution of $S_{ai}(T)$

i	η_i	*I*	η_i	*i*	η_i
1	-1.69	5	-0.23	9	0.75
2	-1.10	6	0	10	1.10
3	-0.75	7	0.23	11	1.69
4	-0.47	8	0.47		

Figure B-14 illustrates this process for a scenario earthquake having median spectral acceleration of 0.3 *g* and dispersion equal to 0.4. The figure shows the cumulative probability distribution represented by this median and dispersion. Horizontal lines across the plot divide the distribution into eleven striped-regions, each having a probability of occurrence of 9.09%. For each stripe, the central or midpoint value of the probability of exceedance is shown by × with values of 4.55%, 13.64%, 22.73%, 31.82%, 40.91%, 50%, 59.09%, 68.18%, 77.27%, 86.36% and 95.45%. A dashed horizontal line is drawn across the plot from the vertical axis to intersect the cumulative distribution function and dropped vertically to the horizontal axis, where spectral acceleration values of .153 *g*, .193 *g*, .222 *g*, 0.248 *g*, 0.274 *g*, 0.300 *g*, 0.329 *g*, 0.362 *g*, 0.405 *g*, 0.465 *g* and 0.590 *g*, respectively, are read off.

The values of spectral acceleration, S_{a1} to S_{a11}, characterize the distribution of spectral acceleration shown in the figure and can be obtained from the following equation:

$$S_{ai} = \theta \cdot e^{\beta \cdot \Phi^{-1}(P_i)} \tag{B-28}$$

where Φ^{-1} is the inverse standardized normal distribution and P_i is the midpoint cumulative probability for region *i*. The values for η_i in Table B-2 are calculated from $\Phi^{-1}(P_i)$ for 11 target spectral accelerations. Alternatively, these values can be generated using an Excel spreadsheet and the function LOGINV (p, $\ln\theta$, β), where values of p = (0.04545 ….. 0.9545), $\ln\theta$ (ln(0.3)=-1.204) is the mean, and β (=0.4) is the dispersion.

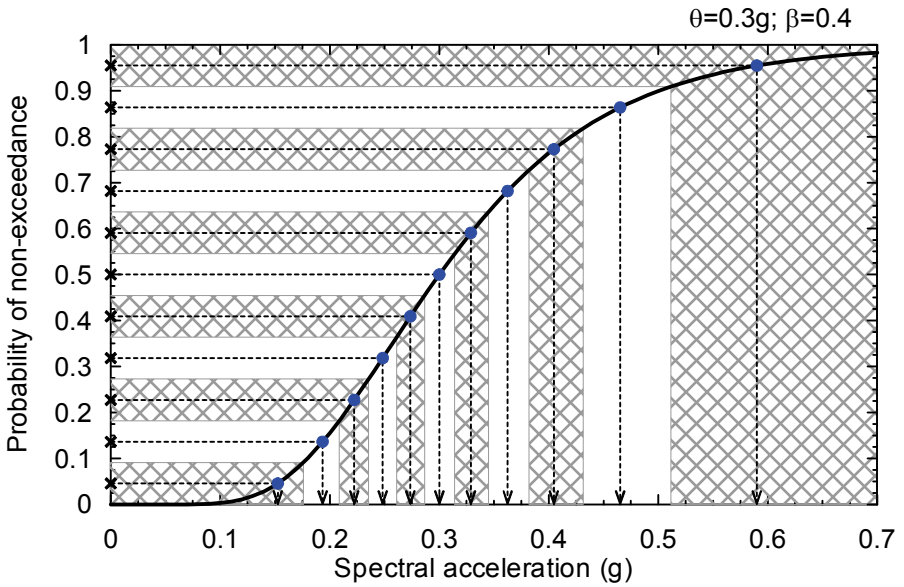

Figure B-14 Calculation of spectral accelerations given a lognormal distribution.

Identical to the procedures of Section B.4 involving the Uniform Hazard Spectrum, the user must specify a period range (T_{max}, T_{min}) for scaling pairs of ground motions. The characterization of the earthquake hazard can involve the following steps:

1. Select the magnitude and site-to-source distance for the scenario event
2. Select an appropriate attenuation relationship(s) for the region, site soil type and source characteristics
3. Establish the period range (T_{max}, T_{min}) for scaling pairs of ground motions

4. Determine the median spectral acceleration demands, θ, and the corresponding dispersions, β, in the period range ($T_{\max}$, $T_{\min}$) using the attenuation relationship(s) of step 2
5. Establish 11 target spectra, $S_{ai}(T), i = 1, 11$, using the medians and dispersions from step 4 and equation (B-28) in the period range ($T_{\max}$, $T_{\min}$)
6. Select 11 pairs of ground motions
7. Construct a geomean spectrum for each pair of ground motions
8. For each target spectrum of step 5, scale a pair of motions such that for each period in the range ($T_{\max}$, $T_{\min}$), the geomean spectrum matches the response spectrum $S_{ai}(T)$
9. Repeat step 8 for the remaining 10 spectra.

This procedure will result in 11 pairs of earthquake histories to represent the potential range of intensities associated with the scenario.

Step 8 in this procedure requires the selection of pairs of motions in step 6 with geomean spectra in the period range ($T_{\max}$, $T_{\min}$) that are similar in shape to the target spectra of step 5. If appropriate pairs of motions are unavailable, an alternative to steps 7, 8 and 9 is to spectrally match pairs of motions to the target spectra of step 5, with each component in a pair matched to the same target spectrum.

A refinement to the above 9-step procedure involves the use of Conditional Mean Spectra and the effective fundamental period $\overline{T}$ as defined in Section 5.6.1. Steps 4 through 9 above are altered as follows:

4. Determine the median spectral acceleration demand, θ, and the corresponding dispersion, β, at effective fundamental period $\overline{T}$, using the attenuation relationship(s) of step 2
5. Compute 11 target values of spectral acceleration, $S_{ai}(\overline{T}), i = 1, 11$, using the medians and dispersions from step 3
6. Generate Conditional Mean Spectra (CMS_i) for the 11 target values of $S_{ai}(\overline{T})$ given magnitude and distance from step 1 and η from Section B-7
7. Select 11 pairs of ground motions, $p_i, i = 1,11$ such that the shape of the geomean spectrum for p_i is similar to that of the CMS_i of step 5 over a user-specified range of period, which must include T_1^X and T_1^Y
8. Amplitude scale the geomean spectral acceleration of the two components of p_i to $S_{ai}(\overline{T})$

9. Repeat step 8 for the remaining 10 spectra.

Similar to the first procedure presented in this section, spectral matching of pairs of motions can be used in lieu of selecting pairs of ground motions with geomean spectral shapes that are similar to CMS_i .

Appendix C
Residual Drift

C.1 Introduction

Residual (permanent) drift is an important consideration in judging a structure's post-earthquake safety and the economic feasibility of repair. Modest amounts of residual drift may require costly and difficult adjustments to nonstructural components, such as re-plumbing of elevator rails and adjustments to building facades, and can also lead to judgments that a building is unsafe during post-earthquake inspections. Larger residual drifts may require straightening of the structural frame or alternative measures to strengthen the frame for stability. Residual drifts may become large enough to seriously jeopardize structural stability in earthquake aftershocks and render the building uneconomical to repair, in which case the cost of repair becomes comparable to complete building replacement.

Research has shown that residual drifts predicted by nonlinear response-history analysis are highly variable and sensitive to the assumed modeling features including the post-yield hardening/softening slope and unloading response and that residual drift may be larger under near-fault records with forward directivity pulses or under long-duration records that cause many cycles of significant response. Accurate statistical simulation of residual drifts requires advanced nonlinear response-history analyses, with a large number of ground motions and with careful attention paid to cyclic hysteretic response of the models and numerical accuracy of the solution. Since the requirements for direct simulation of residual drifts are computationally complex for general implemenation, equations are provided to estimate residual drifts as a function of the peak transient response.

C.2 Prediction of Residual Drift

Analytical studies by Riddell and Newmark (1979) and Mahin and Bertero (1981) first identified some of the key behavioral aspects associated with calculating residual drifts. More recent studies (including MacRae and Kawashima (1997), MacRae (1994), Christopoulos et al. (2003), Christopoulos and Pampanin (2004), Pampanin et al. (2003), and Ruiz-Garcia and Miranda (2005 and 2006)) have confirmed that residual drifts are

largely dependent on the following parameters: (1) magnitude of peak transient inelastic drifts; (2) lateral strength of the structure relative to the earthquake demand; (3) inelastic post-yield stiffness; (4) cyclic unloading response; (5) pulses in the ground motions; and (6) duration of ground shaking. In many respects, these parameters are all inter-related and affect transient and residual drifts. Some of these factors are implicitly accounted for in the story drift assessment. It is desirable that analytical models account for variations in post-yield stiffness and the cyclic unloading response since these parameters are structural parameters that can be influenced by design. For example, the residual drift assessment should differentiate between conventional structures and ones that employ self-centering features that are designed to minimize residual drifts.

Figure C-1 presents a schematic plot relating predicted peak transient and residual drift under increasing earthquake intensity. Point "a" corresponds to the onset of inelastic response, prior to which residual drifts cannot occur. Point "c" corresponds to the collapse point, where residual and transient response converges and point "b" corresponds to regions between these two limits, where the residual drifts represent some fraction of the story drift. As this figure clearly indicates, the ratio of residual to transient drifts is not constant but it may be reasonable to treat the ratio as a constant. Much of the existing literature has evaluated residual drifts at intermediate levels of response, sometimes distinguishing between the degree of inelasticity by varying the strength of the structure, either adjusting the strength using a response modification factor or by adjusting the transient story ductility demand.

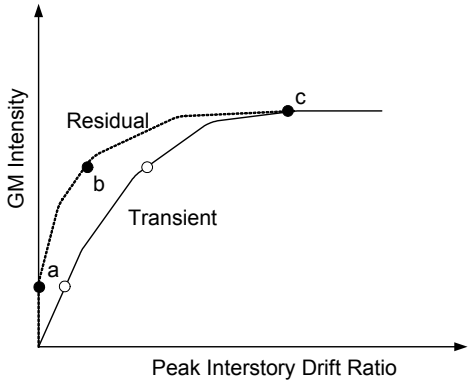

Figure C-1 Idealized incremental dynamic analysis presenting transient and residual story drifts.

A structure's unloading characteristics are significant behavioral effects that impact residual displacements. Figure C-2 presents load versus deflection plots representing the basic aspects of unloading response that have been

identified as important in prior research. These studies have consistently shown that residual displacements are largest in elastic-plastic (EP) systems, due to their tendency to preserve the inelastic displacements upon unloading. This is in contrast to general inelastic (GI) response, where pinching or other effects lead to smaller unloading stiffness. Most recently, researchers have been examining the benefits of so-called self-centering (SC) systems that are specifically designed with unloading characteristics that are intended to minimize (or potentially eliminate) residual displacements. There are also behavioral effects, such as foundation rocking, which have natural self-centering tendencies.

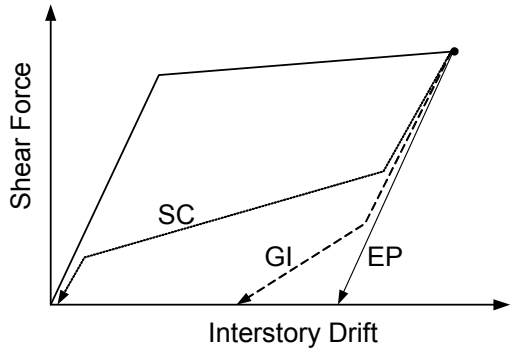

Figure C-2 Idealized response characteristics for elastic-plastic (EP), general inelastic (GI) and self-centering (SC) systems.

Due to the variety of approaches and parameters addressed by various researchers, it is difficult to generalize the results of previous research. However, in the interest of developing a simplified model, the following discussion summarizes some overall results and observations from published analytical studies.

MacRae and Kawashima (1997) investigated residual displacements in single degree-of-freedom bilinear oscillators with a focus on bridge design, where the presence of residual displacements was cited as a major factor in bridge closures and replacement. They proposed a model to estimate residual displacements as a function of the peak inelastic displacement, unloading properties of the inelastic oscillator, and a statistical coefficient based on inelastic response history analyses. In an illustrative example, they predicted residual displacements equal to about 0.16 times the maximum transient displacement. According to their proposed model, the residual displacement ratio could be disaggregated into the following product, $0.16 = 0.67 \times 0.9 \times 0.27$, where 0.67 is the ratio of plastic to total drift (equal to the sum of the elastic and plastic drift), 0.9 reflects the effect of the reduced unloading stiffness, and 0.27 is a statistical parameter accounting for inelastic dynamic response. The specific value of 0.27 represents the mean

plus standard deviation from a range of analyses for systems with modest strain hardening and a ductility demand ratio of 4.

Christopoulos et al. (2003) conducted analyses of single-degree of freedom models with the primary emphasis on characterizing the effect of post-yield hardening stiffness and hysteretic unloading behavior on response. The models were generally representative of modern ductile moment frame buildings, ranging in height from 4 to 20 stories designed with base shear yield ratios (V_y / W) ranging from 0.26 to 0.11, respectively. They applied ground motions to represent both design and maximum earthquakes. Maximum drift ratios observed in their analyses were in the range of 2% to 3%. Analyses of elastic-plastic (EP) models with zero hardening had residual displacements ranging from 0.1 to 0.4 times the peak inelastic transient displacements. These ratios reduced to 0.1 to 0.2 for systems with 5% strain hardening and increased up to 0.7 for systems with 5% strain softening (-5% hardening). The largest residual displacements and peak transient ductility (up to 5 times yield) were observed in the 4-story (period approximately equal to1 second) building with strain softening. Comparable analyses run with a general inelastic model (the Takeda model) had significantly smaller residual drifts, ranging between 7 to 12% of the peak transient drifts for systems with zero or positive strain hardening and 10 to 15% for systems with strain softening. In related studies of multi-degree-of-freedom models (Pampanin et al., 2003) the researchers reported residual drifts equal to 0.05 to 0.25 times the total transient drift, depending on the hardening and hysteretic model.

Ruiz-Garcia and Miranda (2005 and 2006) conducted an extensive parametric study of single and multi degree-of-freedom systems with the goal to characterize probabilistic residual drift hazard curves. They generally expressed their results in terms of a parameter, C_r, which related residual drifts to elastic spectral displacement. Thus, for consistency with the previous studies, this parameter would need to be modified to account for the difference between peak inelastic transient displacement and the elastic spectral displacement. Presumably, this adjustment is close to unity where the equal displacement rule applies (long period single mode dominated systems under small to moderate displacements). For elastic-plastic models with periods greater than 1 second and elastic demand to yield strength ratios of R = 1.5 to 6, they reported median values of C_r = 0.25 to 0.5. This ratio increased to C_r = 0.8 for oscillators with period between 0.5 and 1 second, and became even larger for smaller periods. Since the ratio is conditioned on elastic spectral displacement, the large amplification at small periods probably reflects the amplification between elastic and inelastic transient

displacements. For stiffness degrading systems, the median value coefficient reduced to C_r = 0.1 to 0.3. They also reported dispersion in C_r of about 0.8, which was fairly constant across various periods and building strengths.

C.3 Model to Calculate Residual Drift

Prior studies have indicated that for ductility demands of about 4, residual drifts were on the order of 0.15 to 0.30 times the peak transient drifts. Using this as a guide, a set of equations are proposed to relate residual story drift, Δ_r, to story drift, Δ:

$$\begin{aligned} \Delta_r &= 0 && \Delta \le \Delta_y \\ \Delta_r &= 0.3\left(\Delta - \Delta_y\right) && \Delta_y < \Delta \le 4\Delta_y \\ \Delta_r &= \left(\Delta - 3\Delta_y\right) && 4\Delta y < \Delta \end{aligned} \qquad \text{(C-1)}$$

where Δ_y is the story drift at yield. Figure C-3 illustrates these equations.

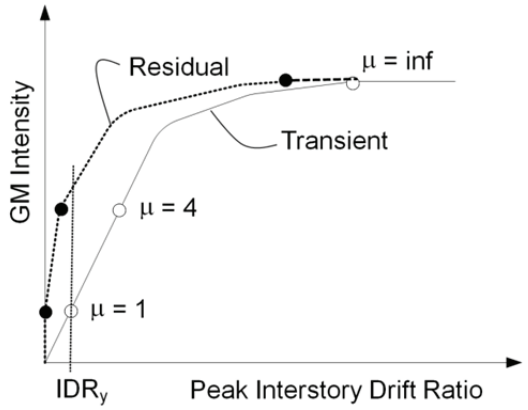

Figure C-3 Idealized model to estimate residual drift from story drift.

These equations are calibrated such that at a story ductility ratio of 4, the ratio of residual to peak transient drift is 0.23. At ductility ratios of 2 and 6, the ratios of residual to peak transient drift are 0.15 and 0.5, respectively. Ultimately, as the collapse point is reached the residual drift will approach the story drift. As an example, consider a steel moment frame with a yield drift ratio of 1%. At 3% total drift, the predicted residual drift ratio would be 0.6%, or about 0.20 times the peak transient. At 5% total drift, the predicted residual would be about 1.9%, or about 0.38 times the peak transient. At 7% total drift (approaching the collapse point), the residual drift would be about 3.9%, or 0.56 times the peak transient.

The proposed equations apply to typical building systems and do not distinguish between many of the behavioral effects that are known to affect residual drifts. For example, whereas previous studies of idealized models

have shown a correlation between post-yield stiffness and residual drifts, this is not reflected in the equations except insofar as the post-yield stiffness affects story drift. The equations are presented in this simple format owing to the lack of physical data to validate modeling of residual displacements and due to the complexity of obtaining significant improvements in the residual drift estimates.

Per Ruiz-Garcia and Miranda, the dispersion for residual drift estimates is about 0.8. Two alternative ways to consider this in the assessment would be to either: (1) calculate the median residual drift demand fragility using Equation C-1 based on the median transient and yield drift ratios, and then apply a dispersion of 0.8; or (2) calculate the residual drift probability based on the integration of the conditional probability of residual drift and the transient drift. In this case, the dispersion on the conditional probability of residual drift should be reduced by the record-to-record variability in the transient drift.

C.4 Proposed Damage States for Residual Drift

Table C-1 proposes four damage states associated with residual drift, ranging from the onset of damage to nonstructural components to near-collapse. The proposed median story drifts (residual drift as a percentage of story height) are approximate and based on a combination of judgment and limits that have been previously suggested in FEMA 356, *Prestandard and Commentary for the Seismic Rehabilitation of Buildings* (FEMA, 2000), Table C1-3. For damage state 4, the limits on the residual drifts that are expressed in terms of the design shear force are intended to cover cases in regions of low seismicity where the destabilizing effects of $P-\Delta$ may dominate at smaller drift ratios than the values noted.

Further work remains to establish appropriate parameters to describe the uncertainty in these limits and loss functions to define the direct economic loss and downtime losses associated with these damage states. For example, damage state 1 may require repairs to nonstructural components that may not otherwise be damaged, except for the need to realign components. Similarly, depending on the type of system, damage state 2 may require extensive structural repairs beyond those evident from the assessment of structural component damage.

The relationship between transient and residual drift demands, per Equation C-1, can be combined with the information in Table C-1 to relate these damage states to the story drifts. Through the yield drift, the relationship between the residual drift damage states and peak transient drift will depend

on the stiffness of the system. A few example relationships are summarized in Table C-2, which are based on the assumed yield drift ratios noted in the table.

Table C-1 Damage States for Residual Story Drifts

Damage State	Description	Residual story drift[1] Δ/h
DS1	No structural realignment is necessary for structural stability; however, the building may require adjustment and repairs to nonstructural and mechanical components that are sensitive to building plumb (e.g., elevator rails, curtain walls, doors).	0.2% (equal to the maximum out of plumb typically permitted in new construction)
DS2	Realignment of structural frame and related structural repairs required to both maintain permissible drift limits for nonstructural and mechanical components and to limit degradation in structural stability (collapse safety)	0.5%
DS3	Major structural realignment is required to restore safety margin for lateral stability; however, the required realignment and repair of the structure may not be economically and practically feasible (i.e., the structure might be at total economic loss).	1%
DS4	Residual drift is sufficiently large that the structure is in danger of collapse from earthquake aftershocks. For this reason the performance point might be considered as equal to collapse, albeit with greater uncertainty.	High Ductility Systems $4\% < 0.5V_{design}/W$ Moderate Ductility Systems $2\% < 0.5V_{design}/W$ Limited Ductility Systems $1\% < 0.5V_{design}/W$

1. h is the story height

Table C-2 Sample Transient Story Drift, Δ / h, Associated with the Residual Story Drift Damage States of Table C-1

		Δ / h			
Sample framing system	Δ_y / h	**DS1**[1]	**DS2**[1]	**DS3**[1]	**DS4**[2]
Steel ductile moment resisting frame	1%	1.5%	2.7%	4.1%	7.1%
Reinforced concrete wall	0.5%	1%	2.2%	2.6%	3.6%
Timber shear wall	1%	1.5%	2.7%	4.1%	5.1%

1. Δ_r / h = 0.2%, 0.5% and 1.0% for DS1, DS2 and DS3, respectively.

2. Δ_r / h = 4%, 2% and 2% for steel moment resisting frames, reinforced concrete walls, and timber shear walls, respectively.

Appendix D

Component Fragility Specifications

D.1 Provided Specifications

Table D-1 provides a summary listing of structural and nonstructural component fragility specifications provided as part of the methodology. The table is organized by general system type, and includes the fragility group classification number, a description of the type of components included in the fragility group, and the number of sub-categories available for each component type. The fragility classification numbers are based on NISTIR 6389, *UNIFORMAT II Elemental Classification for Building Specifications, Cost Estimating and Cost Analysis* (NIST, 1999). The sub-categories have been developed to differentiate between components with:

- Different vulnerability to damage (e.g., braced versus unbraced ceiling systems, and anchored versus unanchored mechanical equipment).
- Different repair, life-safety, or occupancy consequences associated with damage (e.g., gypsum wallboard repairs consisting of patch and paint versus replacement of wallboard).

Sub-categories developed based on differences in consequence functions are generally related to repair costs, which are a function of the quantity of material damaged. For instance, fragility specifications for low aspect ratio concrete shear walls include sub-categories for the following wall thicknesses:

- less than 8 inches thick
- 8 to 16 inches thick
- 16 to 24 inches thick

For each of these wall thicknesses, additional sub-categories are provided to account for differences related to panel height, including heights that are:

- Less than 15 feet tall
- 16 to 24 feet tall

- 25 to 40 feet tall

This categorization system expands the database to more than 700 individual fragility specifications. Each fragility specification includes a description of the component, a description of the possible damage states, the logical interrelationship between the damage states, the demand parameter used to determine damage state occurrence, the consequence functions associated with each damage state, and a quality rating for the specification. The quality rating is an indication of the reliability of the data and procedures used in the development of the fragility.

The *Volume 2 – Implementation Guide* describes the procedures for selecting appropriate fragility specifications for individual building assessments and procedures for creating user-defined, building-specific fragility specifications. Details on the specific attributes of each fragility specification are provided in *Volume 3 – Supporting Electronic Materials*, accessible through the Fragility Manager in the *Performance Assessment Calculation Tool* (PACT), the Fragility Database, or the Fragility Specification PDF file.

Table D-1 List of Provided Fragility Specifications

General System Description	Fragility Classification Number	Component Description	Number of Sub-Categories
Miscellaneous Structural Steel Components/Connections	B1031.001	Bolted shear tab gravity connections	1
	B1031.011	Steel column base plates	3
	B1031.021	Welded column splices	3
Structural Steel Special Concentric Braced Frame	B1033.001	Special Concentric Braced Frame with WF braces, balanced design criteria, Chevron Brace	3
	B1033.002	Special Concentric Braced Frame with Wide Flange (WF) braces, balanced design criteria, Single Diagonal Brace	3
	B1033.003	Special Concentric Braced Frame with WF braces, balanced design criteria, X Brace	3
	B1033.011	Special Concentric Braced Frame with Hollow Structural Section (HSS) braces, balanced design criteria, Chevron Brace	3
	B1033.012	Special Concentric Braced Frame with HSS braces, balanced design criteria, Single Diagonal Brace	3
	B1033.013	Special Concentric Braced Frame with HSS braces, balanced design criteria, X Brace	3
	B1033.021	Special Concentric Braced Frame with HSS braces, tapered gusset plates & design to AISC minimum standard, Chevron Brace	3
	B1033.022	Special Concentric Braced Frame with HSS braces, tapered gusset plates & design to AISC minimum standard, Single Diagonal Brace	3
	B1033.023	Special Concentric Braced Frame with HSS braces, tapered gusset plates & design to AISC minimum standard, X Brace	3

Table D-1 List of Provided Fragility Specifications (continued)

General System Description	Fragility Classification Number	Component Description	Number of Sub-Categories
Structural Steel Special Concentric Braced Frame (continued)	B1033.031	Special Concentric Braced Frame, design to AISC minimum standards, Chevron Brace	3
	B1033.032	Special Concentric Braced Frame, design to AISC minimum standards, Single Diagonal Brace	3
	B1033.033	Special Concentric Braced Frame, design to AISC minimum standards, X Brace	3
	B1033.041	Special Concentric Braced Frame with double angle braces, Chevron Brace	3
	B1033.042	Special Concentric Braced Frame with double angle braces, Single Diagonal Brace	3
	B1033.043	Special Concentric Braced Frame with double angle braces, X Brace	3
Structural Steel Concentric Braced Frame	B1033.051	Ordinary Concentric Braced Frame with compact braces, Chevron Brace	3
	B1033.052	Ordinary Concentric Braced Frame with compact braces, Single Diagonal Brace	3
	B1033.053	Ordinary Concentric Braced Frame with compact braces, X Brace	3
	B1033.061	Ordinary Concentric Braced Frame, braces design to ductile slenderness limits, Chevron Brace	3
	B1033.062	Ordinary Concentric Braced Frame, braces design to ductile slenderness limits, Single Diagonal Brace	3
	B1033.063	Ordinary Concentric Braced Frame, braces design to ductile slenderness limits, X Brace	3
	B1033.071	Braced frame, design for factored loads, no additional seismic detailing, Chevron Brace	3

Table D-1 List of Provided Fragility Specifications (continued)

General System Description	Fragility Classification Number	Component Description	Number of Sub-Categories
Structural Steel Concentric Braced Frame (continued)	B1033.072	Braced frame, design for factored loads, no additional seismic detailing, Single Diagonal Brace	3
	B1033.073	Braced frame, design for factored loads, no additional seismic detailing, X Brace	3
Structural Steel Moment Frame	B1035.001	Post-Northridge Reduced Beam Section (RBS) connection with welded web, beam one side	2
	B1035.011	Post-Northridge RBS connection with welded web, beams both sides	2
	B1035.021	Post-Northridge welded steel moment connection other than RBS, beam one side	2
	B1035.031	Post-Northridge welded steel moment connection other than RBS, beams both sides	2
	B1035.041	Pre-Northridge Welded Unreinforced Flange-Bolted (WUF-B) beam-column joint, beam one side	2
	B1035.051	Pre-Northridge WUF-B beam-column joint, beam both sides	2
Reinforced Concrete Special Moment Frame	B1041.001a	ACI 318 Special Moment Frame (SMF), beam one side	3
	B1041.001b	ACI 318 SMF, beam both sides	3
	B1041.011a	MF with SMF-conforming beam and column flexural and confinement reinforcement but weak joints, beam one side	3
	B1041.011b	Moment Frame (MF) with SMF-conforming beam and column flexural and confinement reinforcement but weak joints, beam both sides	3

Table D-1 List of Provided Fragility Specifications (continued)

General System Description	Fragility Classification Number	Component Description	Number of Sub-Categories
Reinforced Concrete Intermediate Moment Frame	B1041.021a	ACI 318 Intermediate Moment Frame (IMF), beam one side	3
	B1041.021b	ACI 318 IMF, beam both sides	3
Reinforced Concrete Ordinary Moment Frame	B1041.031a	ACI 318 Ordinary Moment Frame (OMF) with weak joints and beam flexural response, beam one side	3
	B1041.031b	ACI 318 OMF with weak joints and beam flexural response, beam both sides	3
	B1041.041a	ACI 318 OMF with weak joints and column flexural response, beam one side	3
	B1041.041b	ACI 318 OMF with weak joints and column flexural response, beam both sides	3
	B1041.051a	ACI 318 OMF with weak beams and weak joints, beam flexural or shear response, beam one side	3
	B1041.051b	ACI 318 OMF with weak beams and weak joints, beam flexural or shear response, beam both sides	3
	B1041.061a	ACI 318 OMF with weak columns, beam one side	3
	B1041.061b	ACI 318 OMF with weak columns, beam both sides	3
	B1041.071a	ACI 318 OMF with weak columns and high axial load, beam one side	3
	B1041.071b	ACI 318 OMF with weak columns and high axial load, beam both sides	3
Reinforced Concrete Non-conforming Moment Frame	B1041.081a	Non-conforming MF with weak joints and beam flexural response, beam one side	3
	B1041.081b	Non-conforming MF with weak joints and beam flexural response, beam both sides	3

Table D-1 List of Provided Fragility Specifications (continued)

General System Description	Fragility Classification Number	Component Description	Number of Sub-Categories
Reinforced Concrete Non-conforming Moment Frame (continued)	B1041.091a	Non-conforming MF with weak joints and column flexural response, beam one side	3
	B1041.091b	Non-conforming MF with weak joints and column flexural response, beam both sides	3
	B1041.101a	Non-conforming MF with weak beams and strong joints, beam one side	3
	B1041.101b	Non-conforming MF with weak beams and strong joints, beam both sides	3
	B1041.111a	Non-conforming MF with weak columns, beam one side	3
	B1041.111b	Non-conforming MF with weak columns, beam both sides	3
	B1041.121a	Non-conforming MF with weak columns and strong joints, beam both sides	3
	B1041.121b	Non-conforming MF with weak columns and strong joints, beam one side	3
	B1041.131a	Non-conforming MF with inadequate development of reinforcing, beam one side	3
	B1041.131b	Non-conforming MF with inadequate development of reinforcing, beam both sides	3
Reinforced Concrete Low Aspect Ratio Planar Wall	B1044.001	Rectangular low aspect ratio concrete walls, 8" or less thick	3
	B1044.011	Rectangular low aspect ratio concrete walls, 8" to 16"	3
	B1044.021	Rectangular low aspect ratio concrete walls, 18" to 24" thick	3

Table D-1 List of Provided Fragility Specifications (continued)

General System Description	Fragility Classification Number	Component Description	Number of Sub-Categories
Reinforced Concrete Low-rise Wall	B1044.031	Low-rise reinforced concrete walls with return flanges, less than 8" thick	3
	B1044.041	Low-rise reinforced concrete walls with return flanges, 8" to 16" thick	3
	B1044.051	Low-rise reinforced concrete walls with return flanges, 17" to 24" thick	3
	B1044.061	Low rise reinforced concrete walls with boundary columns, less than 8" thick	3
	B1044.071	Low rise reinforced concrete walls with boundary columns, 8" to 16" thick	3
	B1044.081	Low rise reinforced concrete walls with boundary columns, 17" to 24" thick	3
Reinforced Concrete Flat Slab	B1049.001	Reinforced concrete flat slabs - joints without shear reinforcing	6
	B1049.011	Reinforced concrete flat slabs - joints with shear reinforcing	2
	B1049.021	Post-tensioned concrete flat slabs - joints without shear reinforcing	4
	B1049.031	Post-tensioned concrete flat slabs - joints with shear reinforcing	2
	B1049.041	Reinforced concrete flat slabs drop panel or drop capital - joints without shear reinforcing	4
Reinforced Masonry Ordinary Wall	B1051.001	Ordinary reinforced masonry walls with partially grouted cells, 4" to 6" thick, shear dominated	2
	B1051.003	Ordinary reinforced masonry walls with partially grouted cells, 4" to 6" thick, flexure dominated	2
	B1051.011	Ordinary reinforced masonry walls with partially grouted cells, 8" to 12"' thick, shear dominated	2

Table D-1 List of Provided Fragility Specifications (continued)

General System Description	Fragility Classification Number	Component Description	Number of Sub-Categories
Reinforced Masonry Ordinary Wall (continued)	B1051.013	Ordinary reinforced masonry walls with partially grouted cells, 8" to 12" thick, flexure dominated	2
	B1051.021	Ordinary reinforced masonry walls with partially grouted cells, 16" thick, shear dominated	2
	B1051.023	Ordinary reinforced masonry walls with partially grouted cells, 16" thick, flexure dominated	2
Reinforced Masonry Special Wall	B1052.001	Special reinforced masonry walls with fully grouted cells, 8" or 12" thick, shear dominated	2
	B1052.003	Special reinforced masonry walls with fully grouted cells, 8" to 12" thick, flexure dominated	2
	B1052.011	Special reinforced masonry walls with fully grouted cells, 16" thick, shear dominated	2
	B1052.013	Special reinforced masonry walls with fully grouted cells, 16" thick, flexure dominated	2
Light-framed Wood Wall	B1071.001	Light framed wood walls with structural panel sheathing, gypsum wallboard	2
	B1071.002	Light framed wood walls with structural panel sheathing, stucco	2
	B1071.031	Wood walls with diagonal let-in bracing	1
Precast Concrete Wall Panels	B2010.201	User Specified in-plane and out-of-plane wall panel connection capacity	2
Exterior Windows	B2022.001	Curtain Walls and Storefronts	48
Tile Roof	B3011.011	Concrete tile roof, tiles secured and compliant with UBC94	1
	B3011.012	Clay tile roof, tiles secured and compliant with UBC94	1

Table D-1 List of Provided Fragility Specifications (continued)

General System Description	Fragility Classification Number	Component Description	Number of Sub-Categories
Tile Roof (continued)	B3011.013	Concrete tile roof, unsecured tiles	1
	B3011.014	Clay tile roof, unsecured tiles	1
Masonry Chimneys	B3031.001	Replacement with our without masonry (codes may no longer permit)	6
Masonry Parapet	B3041.001	Unreinforced and unbraced	1
Stairs	C2011.001	Prefabricated Steel and Concrete and Cast-in-place concrete	10
Wall Partition	C1011.001	Wall Partition, Type: Gypsum	6
	C3011.001	Wall Partition, Type: Gypsum + Wallpaper	3
	C3011.002	Wall Partition, Type: Gypsum + Ceramic Tile	3
	C3011.003	Wall Partition, Type: High End Marble or Wood Panel	3
Raised Access Floors	C3027.001	Not seismically rated and seismically rated	2
Ceilings	C3032.001	Suspended Ceiling	16
Recessed Lighting in Suspended Ceilings	C3032.001	With and without support wires	2
Independent Pendant Lighting	C3034.001	Not seismically rated and seismically rated	2
Elevators	D1014.010	Traction elevator	2
	D1014.021	Hydraulic elevator	2
Piping	D2021.011	Domestic Cold Water Piping	4
	D2022.011	Domestic Hot Water Piping	8
	D2031.001	Sanitary Waste Piping - flexible coupling	4

Table D-1 List of Provided Fragility Specifications (continued)

General System Description	Fragility Classification Number	Component Description	Number of Sub-Categories
Piping (continued)	D2031.002	Sanitary Waste Piping - bell & spigot coupling	4
	D2051.011	Chilled Water Piping	8
	D2061.011	Steam Water Piping	8
	C3021.001	Floor flooding	16
Chillers	D3031.011a	Chiller - Anchorage fragility only	8
	D3031.011e	Chiller - Equipment fragility only	8
	D3031.011i	Chiller - Combined anchorage & equipment fragility	8
Cooling Towers	D3031.021a	Cooling Tower - Anchorage fragility only	8
	D3031.021e	Cooling Tower - Equipment fragility only	8
	D3031.021i	Cooling Tower - Combined anchorage & equipment fragility	8
Compressors	D3032.011a	Compressor - Anchorage fragility only	8
	D3032.011e	Compressor - Equipment fragility only	8
	D3032.011i	Compressor - Combined anchorage & equipment fragility	8
HVAC Distribution	D3041.001	HVAC Fan In Line Fan, Fan independently supported and vibration isolators	4
	D3041.002	HVAC Fan In Line Fan, Fan independently supported but not on vibration isolators	4
	D3041.011	HVAC Galvanized Sheet Metal Ducting	8
	D3041.021	HVAC Stainless Steel Ducting	8

Table D-1 List of Provided Fragility Specifications (continued)

General System Description	Fragility Classification Number	Component Description	Number of Sub-Categories
HVAC Distribution (continued)	D3041.031	HVAC Drops / Diffusers in suspended ceilings	2
	D3041.032	HVAC Drops / Diffusers without ceilings	4
	D3041.041	Variable Air Volume (VAV) box with in-line coil	2
	D3041.101a	HVAC Fan - Anchorage fragility only	2
	D3041.101b	HVAC Fan - Equipment fragility only	2
	D3041.101c	HVAC Fan - Combined anchorage & equipment fragility	2
Packaged Air Handling Unit	D3063.011a	Packaged Air Handling Unit - Anchorage fragility	8
	D3063.011e	Packaged Air Handling Unit - Equipment fragility only	8
	D3063.011i	Packaged Air Handling Unit - Combined anchorage & equipment fragility	8
Control Panel	D3067.011a	Control panel - Anchorage fragility only	1
	D3067.011b	Control panel - Equipment fragility only	2
	D3067.011c	Control panel - Combined anchorage & equipment fragility	1
Fire Sprinkler Water Piping	D4011.001	Fire Sprinkler Water Piping - Horizontal Mains and Branches - New Style Vitaulic / Threaded Steel	4
	D4011.002	Fire Sprinkler Water Piping - Horizontal Mains and Branches - Old Style Vitaulic	4

Table D-1 List of Provided Fragility Specifications (continued)

General System Description	Fragility Classification Number	Component Description	Number of Sub-Categories
Fire Sprinkler Drop	D4011.031	Fire Sprinkler Drop Standard Threaded Steel - Dropping into unbraced lay-in tile SOFT ceiling	2
	D4011.012	Fire Sprinkler Drop Standard Threaded Steel - Dropping into unbraced lay-in tile HARD ceiling	2
	D4011.013	Fire Sprinkler Drop Standard Threaded Steel - Dropping into braced lay-in tile SOFT ceiling	2
	D4011.014	Fire Sprinkler Drop Standard Threaded Steel - Dropping into braced lay-in tile HARD ceiling	2
	D4011.015	Fire Sprinkler Drop Standard Threaded Steel - No Ceiling	4
Motor Control Center	D5010.011a	Motor control center - Anchorage fragility only	1
	D5010.011b	Motor control center - Equipment fragility only	2
	D5010.011c	Motor control center - Combined anchorage & equipment fragility	1
Transformer/Primary Service	D5011.011a	Transformer/Primary Service - Anchorage fragility only	8
	D5011.011e	Transformer/Primary Service - Equipment fragility only	8
	D5011.011i	Transformer/Primary Service - Combined anchorage & equipment fragility	8
Low Voltage Switchgear	D5012.021a	Low voltage switchgear - Anchorage fragility only	8
	D5012.021e	Low voltage switchgear - Equipment fragility only	8
	D5012.021i	Low voltage switchgear - Combined anchorage & equipment fragility	8

Table D-1 List of Provided Fragility Specifications (continued)

General System Description	Fragility Classification Number	Component Description	Number of Sub-Categories
Distribution Panel	D5012.031a	Distribution panel - Anchorage fragility only	8
	D5012.031e	Distribution panel - Equipment fragility only	8
	D5012.031i	Distribution panel - Combined anchorage & equipment fragility	8
Battery Rack	D5092.011a	Battery Rack - Anchorage fragility only	2
	D5092.011b	Battery Rack - Equipment fragility only	2
	D5092.011c	Battery Rack - Combined anchorage & equipment fragility	2
Battery Charger	D5092.021a	Battery Charger - Anchorage fragility only	2
	D5092.021b	Battery Charger - Equipment fragility only	2
	D5092.021c	Battery Charger - Combined anchorage & equipment fragility	2
Diesel Generator	D5092.031a	Diesel generator - Anchorage fragility only	8
	D5092.031e	Diesel generator - Equipment fragility only	8
	D5092.031i	Diesel generator - Combined anchorage & equipment fragility	8
Miscellaneous Contents	E2022.001	Modular Workstation	1
	E2022.010	Unsecured fragile objects on shelves	4
	E2022.020	Home entertainment equipment	4
	E2022.102	Bookcase	10
	E2022.112	Vertical Filing Cabinet	4
	E2022.124	Lateral Filing Cabinet	4

Appendix E
Population Models

E-1 Population Models

Population models are used to determine the distribution of people within a building envelope, and the variability of this distribution over time of day and day of the year. Table E-1 presents a series of population models for different occupancies, and Table E-2 presents the monthly variation of occupancy, relative to peak, for these occupancies. Figure E-1 plots the variation of population versus time of day, as depicted in Table E-1. Peak population values are defined Chapter 3. In this appendix, population models are provided for the following occupancies:

- Commercial office
- Education (K-12) – typical elementary, middle school, and high school classrooms
- Healthcare – general in-patient hospitals
- Hospitality – hotels and motels
- Multi-Unit Residential – also applicable to single-family detached housing, with some modification
- Research
- Retail – shopping malls and department stores
- Warehouse

Table E-1 Default Variation in Population by Time of Day and Day of Week, Relative to Expected Peak Population for Different Occupancies

	Commercial Office		Education - Elementary Schools		Education - Middle Schools		Education - High Schools		Healthcare	
Time of Day	Week-days	Week-ends	Week-days	Week-ends	Week-days	Week-ends	Week-days	Week-ends	Week-days	Week-ends
12:00 AM	0%	0%	0%	0%	0%	0%	0%	0%	40%	40%
1:00 AM	0%	0%	0%	0%	0%	0%	0%	0%	40%	40%
2:00 AM	0%	0%	0%	0%	0%	0%	0%	0%	40%	40%
3:00 AM	0%	0%	0%	0%	0%	0%	0%	0%	40%	40%
4:00 AM	0%	0%	0%	0%	0%	0%	0%	0%	40%	40%
5:00 AM	0%	0%	0%	0%	0%	0%	0%	0%	40%	40%
6:00 AM	0%	0%	0%	0%	5%	0%	5%	0%	40%	40%
7:00 AM	25%	0%	5%	0%	50%	0%	50%	0%	40%	40%
8:00 AM	50%	5%	100%	2%	100%	2%	100%	2%	40%	40%

Table E-1 Default Variation in Population by Time of Day and Day of Week, Relative to Expected Peak Population for Different Occupancies (continued)

	Commercial Office		Education - Elementary Schools		Education - Middle Schools		Education - High Schools		Healthcare	
Time of Day	Week-days	Week-ends	Week-days	Week-ends	Week-days	Week-ends	Week-days	Week-ends	Week-days	Week-ends
9:00 AM	75%	5%	100%	2%	100%	2%	100%	2%	60%	50%
10:00 AM	100%	5%	100%	2%	100%	2%	100%	2%	80%	65%
11:00 AM	100%	5%	100%	2%	100%	2%	100%	2%	100%	80%
12:00 PM	50%	5%	100%	2%	100%	2%	100%	2%	100%	80%
1:00 PM	50%	5%	100%	2%	100%	2%	100%	2%	100%	80%
2:00 PM	100%	5%	100%	2%	100%	2%	100%	2%	100%	80%
3:00 PM	100%	5%	50%	2%	100%	2%	100%	2%	100%	80%
4:00 PM	75%	5%	5%	2%	50%	2%	50%	2%	100%	80%
5:00 PM	50%	5%	5%	2%	25%	2%	25%	2%	100%	80%
6:00 PM	25%	0%	5%	0%	5%	0%	5%	0%	100%	80%
7:00 PM	0%	0%	0%	0%	0%	0%	0%	0%	100%	80%
8:00 PM	0%	0%	0%	0%	0%	0%	0%	0%	80%	65%
9:00 PM	0%	0%	0%	0%	0%	0%	0%	0%	60%	50%
10:00 PM	0%	0%	0%	0%	0%	0%	0%	0%	40%	40%
11:00 PM	0%	0%	0%	0%	0%	0%	0%	0%	40%	40%

	Hospitality		Multi-Unit Residential		Research Laboratories		Retail		Warehouse	
Time of Day	Week-days	Week-ends	Week-days	Week-ends	Week-days	Week-ends	Week-days	Week-ends	Week-days	Week-ends
12:00 AM	100%	100%	100%	100%	10%	10%	0%	0%	0%	0%
1:00 AM	100%	100%	100%	100%	10%	10%	0%	0%	0%	0%
2:00 AM	100%	100%	100%	100%	10%	10%	0%	0%	0%	0%
3:00 AM	100%	100%	100%	100%	10%	10%	0%	0%	0%	0%
4:00 AM	100%	100%	100%	100%	10%	10%	0%	0%	0%	0%
5:00 AM	100%	100%	100%	100%	10%	10%	0%	0%	0%	0%
6:00 AM	100%	100%	80%	100%	25%	25%	0%	0%	0%	0%
7:00 AM	80%	100%	60%	100%	25%	25%	0%	0%	25%	0%
8:00 AM	70%	100%	40%	100%	50%	25%	5%	5%	50%	2%
9:00 AM	50%	75%	20%	75%	75%	25%	10%	10%	100%	2%
10:00 AM	50%	50%	20%	50%	100%	25%	20%	25%	100%	2%
11:00 AM	50%	25%	20%	50%	100%	25%	40%	50%	100%	2%
12:00 PM	50%	25%	20%	50%	50%	25%	60%	75%	100%	2%
1:00 PM	50%	25%	20%	50%	50%	25%	60%	100%	100%	2%
2:00 PM	50%	25%	25%	50%	100%	25%	60%	100%	100%	2%
3:00 PM	50%	25%	30%	50%	100%	25%	60%	100%	100%	2%
4:00 PM	50%	25%	35%	50%	75%	25%	60%	100%	100%	2%
5:00 PM	50%	25%	50%	50%	50%	25%	60%	100%	100%	2%
6:00 PM	50%	25%	67%	50%	25%	25%	60%	75%	50%	0%
7:00 PM	50%	25%	84%	50%	25%	25%	60%	50%	25%	0%
8:00 PM	50%	50%	100%	50%	10%	10%	40%	25%	0%	0%
9:00 PM	50%	50%	100%	75%	10%	10%	20%	10%	0%	0%
10:00 PM	100%	100%	100%	100%	10%	10%	5%	5%	0%	0%
11:00 PM	100%	100%	100%	100%	10%	10%	0%	0%	0%	0%

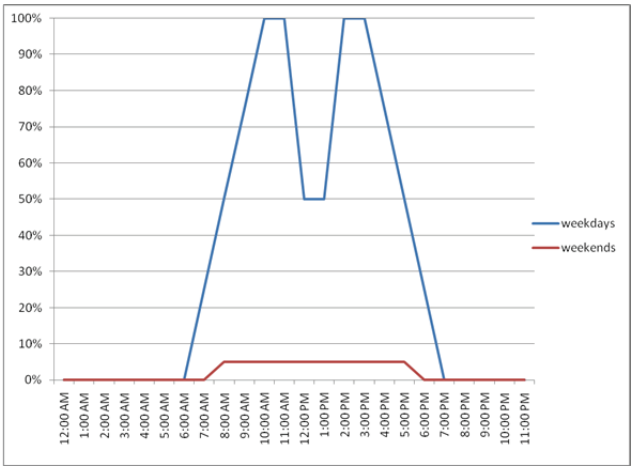

(a) Commercial office

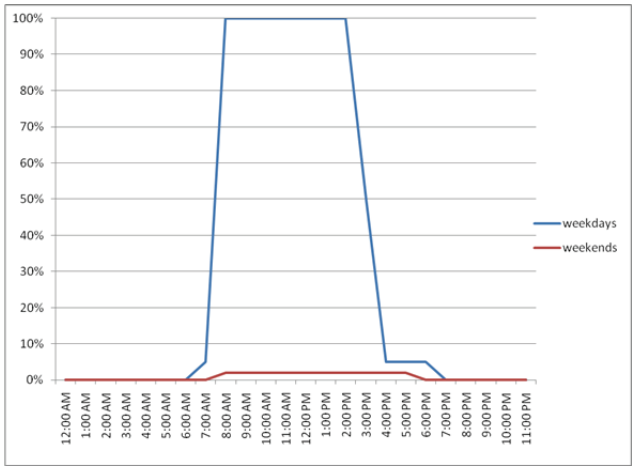

(b) Education – elementary school

Figure E-1 Plot of default variation in population (relative to expected peak population) by time of day for: (a) Commercial office; and (b) Education – elementary school occupancies.

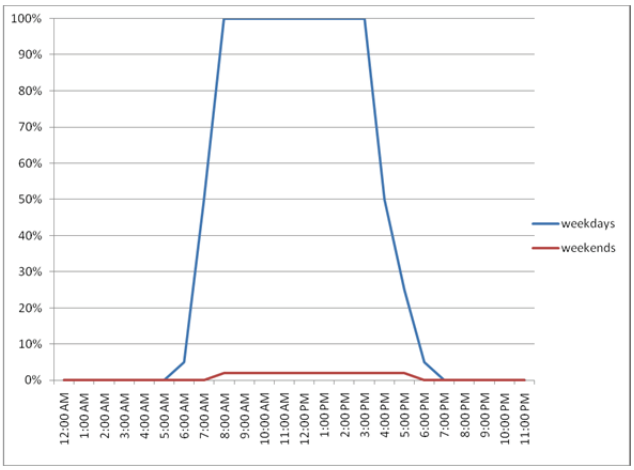

(a) Education – middle school

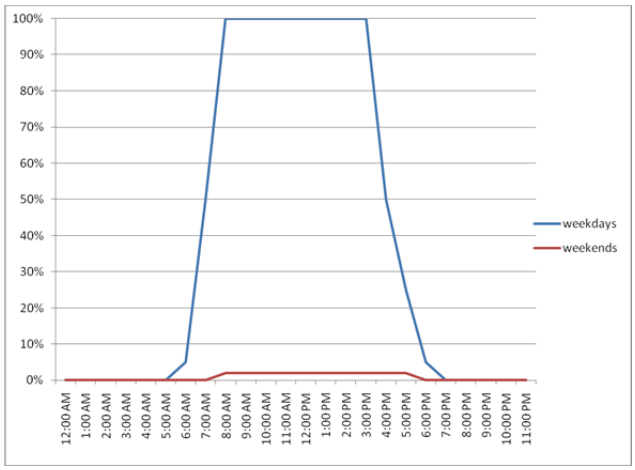

(b) Education – high school

Figure E-2 Plot of default variation in population (relative to expected peak population) by time of day for: (a) Education – middle school; and (b) Education – high school occupancies.

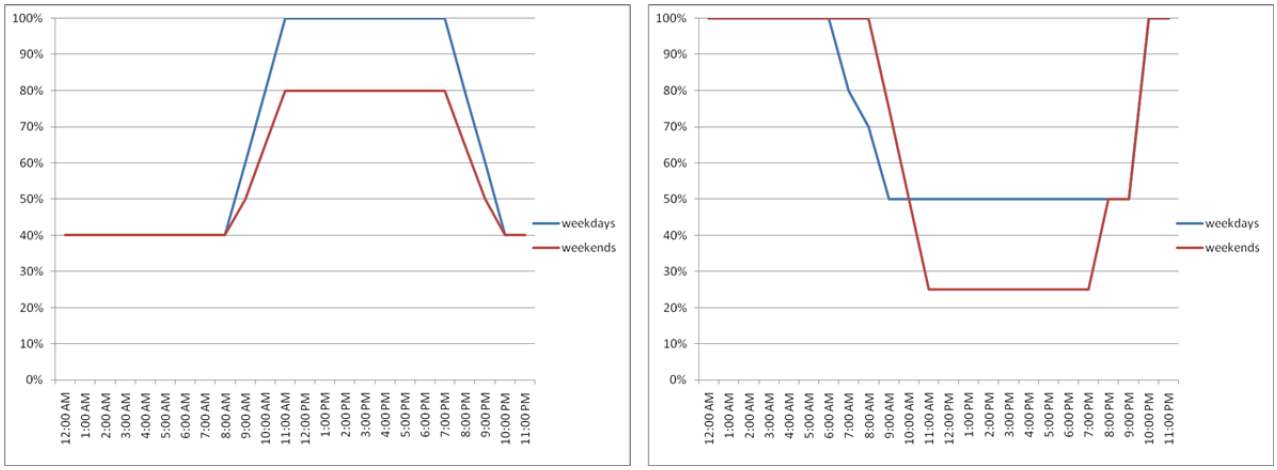

(a) Healthcare (b) Hospitality

Figure E-3 Plot of default variation in population (relative to expected peak population) by time of day for: (a) Healthcare; and (b) Hospitality occupancies.

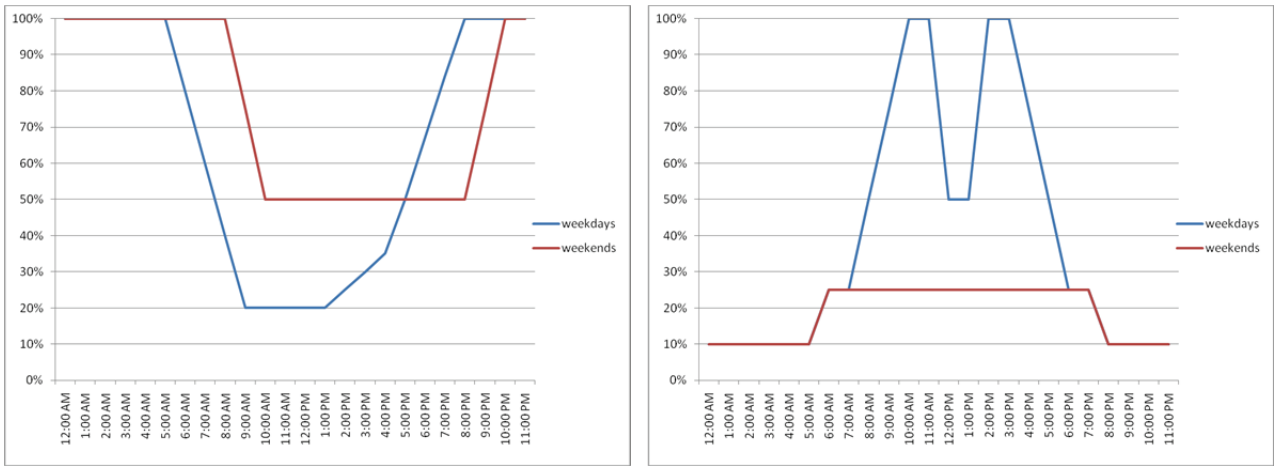

(a) Multi-Unit Residential (b) Research

Figure E-4 Plot of default variation in population (relative to expected peak population) by time of day for: (a) Multi-Unit Residential; and (b) Research occupancies.

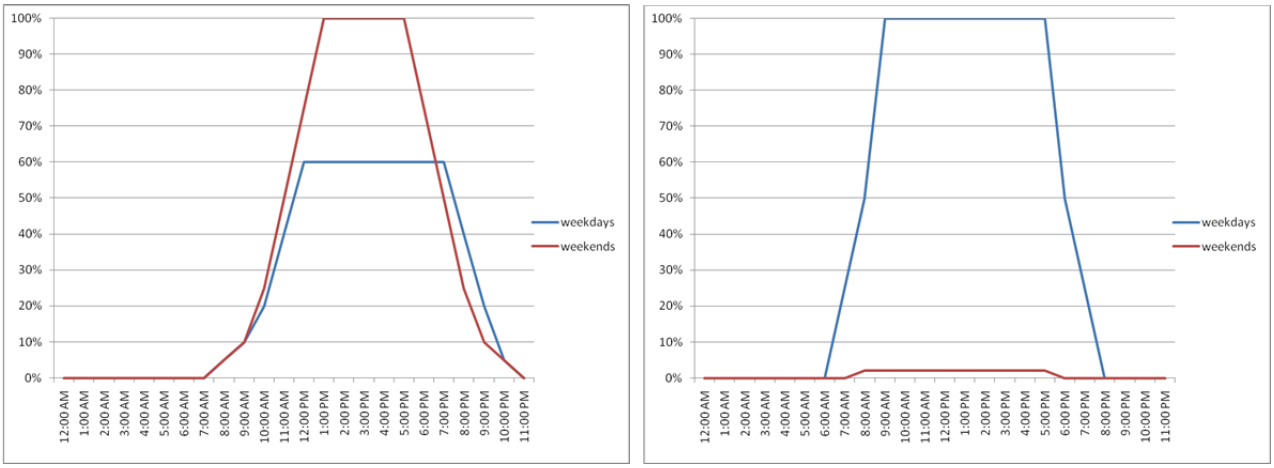

(a) Retail (b) Warehouse

Figure E-5 Plot of default variation in population (relative to expected peak population) by time of day for: (a) Retail; and (b) Warehouse occupancies.

Table E-2 Default Variation in Population by Month, Relative to Expected Peak Population for Different Occupancies

	Commercial Office		Education - Elementary Schools		Education - Middle Schools		Education - High Schools		Healthcare	
Month	Week-day	Week-end	Week-day	Week-end	Week-day	Week-end	Week-day	Week-end	Week-day	Week-end
Jan.	91%	100%	73%	100%	73%	100%	73%	100%	100%	100%
Feb.	95%	100%	90%	100%	90%	100%	90%	100%	100%	100%
March	100%	100%	100%	100%	100%	100%	100%	100%	100%	100%
April	100%	100%	77%	100%	77%	100%	77%	100%	100%	100%
May	95%	100%	95%	100%	95%	100%	95%	100%	100%	100%
June	100%	100%	77%	100%	77%	100%	77%	100%	100%	100%
July	95%	100%	0%	100%	0%	100%	0%	100%	100%	100%
Aug.	100%	100%	0%	100%	0%	100%	0%	100%	100%	100%
Sept.	95%	100%	95%	100%	95%	100%	95%	100%	100%	100%
Oct.	100%	100%	95%	100%	95%	100%	95%	100%	100%	100%
Nov.	95%	100%	81%	100%	81%	100%	81%	100%	100%	100%
Dec.	95%	100%	64%	100%	64%	100%	64%	100%	100%	100%
	Hospitality		Multi-Unit Residential		Research Laboratories		Retail		Warehouse	
Month	Week-day	Week-end	Week-day	Week-end	Week-day	Week-end	Week-day	Week-end	Week-day	Week-end
Jan.	100%	100%	100%	100%	91%	100%	95%	100%	91%	100%
Feb.	100%	100%	100%	100%	95%	100%	100%	100%	95%	100%
March	100%	100%	100%	100%	100%	100%	100%	100%	100%	100%
April	100%	100%	100%	100%	100%	100%	100%	100%	100%	100%
May	100%	100%	100%	100%	95%	100%	100%	100%	95%	100%
June	100%	100%	100%	100%	100%	100%	100%	100%	100%	100%
July	100%	100%	100%	100%	95%	100%	95%	100%	95%	100%
Aug.	100%	100%	100%	100%	100%	100%	100%	100%	100%	100%
Sept.	100%	100%	100%	100%	95%	100%	100%	100%	95%	100%
Oct.	100%	100%	100%	100%	100%	100%	100%	100%	100%	100%
Nov.	100%	100%	100%	100%	95%	100%	95%	100%	95%	100%
Dec.	100%	100%	100%	100%	95%	100%	95%	100%	95%	100%

Appendix F

Normative Quantities

F-1 Normative Quantities

Normative quantities can be used to provide an approximate inventory of the type and quantity of typical components found in buildings. Values for 10th, 50th, and 90th percentile quantities were developed based on data from surveys of typical buildings of specific occupancies. The units of measurement are consistent with quantities used in the fragility specifications to determine repair cost and repair time consequences. Tables F-1 through F-8 provide normative quantity information for the following occupancies:

- Commercial office
- Education (K-12) – typical elementary, middle school, and high school classrooms
- Healthcare – general in-patient hospitals, medical equipment excluded
- Hospitality – hotels and motels
- Multi-Unit Residential – also applicable to single-family detached housing, with some modification
- Research – special purpose laboratory equipment excluded
- Retail – shopping malls and department stores
- Warehouse – inventory excluded

Table F-1 Normative Quantities for Commercial Office Occupancies

Component Type	Unit of Measurement	10th Percentile Quantity	50th Percentile Quantity	90th Percentile Quantity
Gross Area	SF	10,000	85,000	1,103,000
Volume	CF per 1 gsf	10.300	13.600	18.000
Cladding				
Gross Wall Area	SF per 1 gsf	0.380	0.645	1.200
Windows or Glazing Area	100 SF per 1 gsf	8.0E-04	3.0E-03	6.0E-03
Roof Area - Total	SF per 1 gsf	0.025	0.270	1.300
Interior Partition Length	100 LF per 1 gsf	7.0E-04	1.0E-03	1.2E-03
Ceramic tile floors	SF per 1 gsf	0.020	0.042	0.104
Ceramic tile walls	100 LF per 1 gsf	3.6E-05	7.6E-05	1.9E-04
Ceilings				
Ceiling - Lay in tile percentage	%		90%	
Ceiling - Gypsum board percentage	%		5%	
Ceiling - Exposed percentage	%		3%	
Ceiling - Other (high end) percentage	%		2%	
Stairs	FL per 1 gsf	8.0E-05	1.0E-04	1.2E-04
Elevators	EA per 1 gsf	1.5E-05	2.8E-05	7.9E-05
Plumbing				
Plumbing Fixtures	EA per 1 gsf	5.0E-04	1.1E-03	2.6E-03
Piping				
Cold Domestic Water Piping - 2 ½ inch diameter or smaller	1,000 LF per 1 gsf	2.0E-05	4.2E-05	1.0E-04
Cold Domestic Water Piping – greater than 2 ½ diameter	1,000 LF per 1 gsf	1.0E-05	1.5E-05	2.0E-05
Hot Domestic Water Piping - 2 ½ inch diameter or smaller	1,000 LF per 1 gsf	4.0E-05	8.4E-05	2.1E-04
Hot Domestic Waster Piping – greater than 2 ½ diameter	1,000 LF per 1 gsf	2.0E-05	3.0E-05	4.0E-05
Gas supply piping	1,000 LF per 1 gsf	1.0E-05	1.5E-05	2.0E-05
Sanitary Waste Piping	1,000 LF per 1 gsf	3.0E-05	5.7E-05	1.2E-04
HVAC				
Chiller capacity	TN per 1 gsf	2.5E-03	2.9E-03	3.3E-03
Cooling Tower capacity	TN per 1 gsf	2.5E-03	2.9E-03	3.3E-03
Boiler capacity	BTU per 1 gsf	30.000	45.000	60.000

Table F-1 Normative Quantities for Commercial Office Occupancies (continued)

Component Type	Unit of Measurement	10th Percentile Quantity	50th Percentile Quantity	90th Percentile Quantity
Air Handling Units	CFM per 1 gsf	0.500	0.700	0.900
Fans	CFM per 1 gsf	0.000	0.000	0.000
HVAC Ducts – 6 sq. feet for larger	1,000 LF per 1 gsf	1.5E-05	2.0E-05	2.5E-05
HVAC Ducts – less than 6 sq. feet	1,000 LF per 1 gsf	5.0E-05	7.5E-05	9.0E-05
HVAC in-line Drops & Diffusers	EA per 1 gsf	6.0E-03	9.0E-03	2.0E-02
HVAC in-line Coils	EA per 1 gsf	3.0E-03	5.0E-03	6.0E-03
VAV Boxes	EA per 1 gsf	1.0E-03	2.0E-03	4.0E-03
Piping				
Steam & Chilled Water Piping - 2 ½ inch diameter or smaller	1,000 LF per 1 gsf	0.0E+00	0.0E+00	5.0E-06
Steam & Chilled Water Piping – greater than 2 ½ diameter	1,000 LF per 1 gsf	0.0E+00	0.0E+00	5.0E-06
Heating Water Piping - 2 ½ inch diameter or smaller	1,000 LF per 1 gsf	0.0E+00	5.0E-06	1.0E-05
Heating Water Piping – greater than 2 ½ diameter	1,000 LF per 1 gsf	0.0E+00	5.0E-06	1.0E-05
Electrical				
Electrical Load	W per 1 gsf	6.000	16.200	27.000
Electrical Distribution conduits	LF per 1 gsf	7.0E-02	2.0E-01	4.0E-01
Electrical Distribution – cable trays	LF per 1 gsf	0.0E+00	2.0E-02	5.0E-02
Wall mounted switchgear	EA per 1 gsf	1.0E-04	1.5E-04	2.0E-04
Lighting Fixtures – Lay in fluorescent	EA per 1 gsf	1.0E-02	1.5E-02	2.0E-02
Lighting Fixtures – Stem hung fluorescent	EA per 1 gsf	1.0E-02	1.5E-02	2.0E-02
Standby generators	KVA per 1 gsf	0.0E+00	0.0E+00	0.0E+00
Fire Protection				
Sprinkler Piping	20 LF per 1 gsf	8.5E-03	1.0E-02	1.1E-02
Sprinkler Drops	EA per 1 gsf	7.0E-03	9.0E-03	1.2E-02

Table F-2 Normative Quantities for Education (K-12) Occupancies

Component Type	Unit of Measurement	10th Percentile Quantity	50th Percentile Quantity	90th Percentile Quantity
Gross Area	SF	3,100	36,400	218,900
Volume	CF per 1 gsf	10.400	13.370	19.200
Cladding				
Gross Wall Area	SF per 1 gsf	0.380	0.750	1.700
Windows or Glazing Area	100 SF per 1 gsf	3.0E-04	1.1E-03	2.9E-03
Roof Area - Total	SF per 1 gsf	0.150	0.680	1.280
Interior Partition Length	100 LF per 1 gsf	3.0E-04	5.6E-04	9.8E-04
Ceramic tile floors	SF per 1 gsf	0.024	0.079	0.166
Ceramic tile walls	100 LF per 1 gsf	4.4E-05	1.4E-04	3.0E-04
Ceilings				
Ceiling - Lay in tile percentage	%		95%	
Ceiling - Gypsum board percentage	%		3%	
Ceiling - Exposed percentage	%		2%	
Ceiling - Other (high end) percentage	%		0%	
Stairs	FL per 1 gsf	6.0E-05	7.0E-05	9.0E-05
Elevators	EA per 1 gsf	9.0E-06	2.0E-05	1.3E-04
Plumbing				
Plumbing Fixtures	EA per 1 gsf	6.1E-04	2.0E-03	4.2E-03
Piping				
Cold Domestic Water Piping - 2 ½ inch diameter or smaller	1,000 LF per 1 gsf	2.0E-05	3.0E-05	4.0E-05
Cold Domestic Water Piping – greater than 2 ½ diameter	1,000 LF per 1 gsf	1.0E-05	1.5E-05	2.0E-05
Hot Domestic Water Piping - 2 ½ inch diameter or smaller	1,000 LF per 1 gsf	4.0E-05	6.0E-05	8.0E-05
Hot Domestic Waster Piping – greater than 2 ½ diameter	1,000 LF per 1 gsf	2.0E-05	3.0E-05	4.0E-05
Gas supply piping	1,000 LF per 1 gsf	2.0E-05	4.0E-05	4.5E-05
Sanitary Waste Piping	1,000 LF per 1 gsf	3.0E-05	4.5E-05	6.0E-05
HVAC				
Chiller capacity	TN per 1 gsf	0.0E+00	0.0E+00	2.5E-03
Cooling Tower capacity	TN per 1 gsf	0.0E+00	0.0E+00	2.5E-03
Boiler capacity	BTU per 1 gsf	30.000	45.000	60.000
Air Handling Units	CFM per 1 gsf	0.000	0.000	0.600

Table F-2 Normative Quantities for Education (K-12) Occupancies (continued)

Component Type	Unit of Measurement	10th Percentile Quantity	50th Percentile Quantity	90th Percentile Quantity
HVAC Ducts – 6 sq. feet for larger	1,000 LF per 1 gsf	0.0E+00	0.0E+00	1.5E-05
HVAC Ducts – less than 6 sq. feet	1,000 LF per 1 gsf	0.0E+00	5.0E-05	8.0E-05
HVAC in-line Drops & Diffusers	EA per 1 gsf	0.0E+00	5.0E-03	8.0E-03
HVAC in-line Coils	EA per 1 gsf	0.0E+00	0.0E+00	1.5E-03
VAV Boxes	EA per 1 gsf	0.0E+00	0.0E+00	1.5E-03
Fan Coil Units	EA per 1 gsf	2.0E-03	4.0E-03	0.0E+00
Piping				
Steam & Chilled Water Piping - 2 ½ inch diameter or smaller	1,000 LF per 1 gsf	0.0E+00	0.0E+00	5.0E-06
Steam & Chilled Water Piping – greater than 2 ½ diameter	1,000 LF per 1 gsf	0.0E+00	5.0E-06	1.0E-05
Heating Water Piping - 2 ½ inch diameter or smaller	1,000 LF per 1 gsf	0.0E+00	2.5E-05	4.0E-05
Heating Water Piping – greater than 2 ½ diameter	1,000 LF per 1 gsf	0.0E+00	5.0E-06	1.0E-05
Electrical				
Electrical Load	W per 1 gsf	7.000	18.800	23.000
Electrical Distribution conduits	LF per 1 gsf	1.0E-01	2.0E-01	3.0E-01
Electrical Distribution – cable trays	LF per 1 gsf	0.0E+00	0.0E+00	0.0E+00
Wall mounted switchgear	EA per 1 gsf	1.0E-04	1.5E-04	2.0E-04
Lighting Fixtures – Lay in fluorescent	EA per 1 gsf	1.0E-02	1.5E-02	1.7E-02
Lighting Fixtures – Stem hung fluorescent	EA per 1 gsf	1.0E-02	1.5E-02	1.7E-02
Standby generators	KVA per 1 gsf	0.0E+00	0.0E+00	0.0E+00
Fire Protection				
Sprinkler Piping	20 LF per 1 gsf	7.5E-03	9.0E-03	1.0E-02
Sprinkler Drops	EA per 1 gsf	6.0E-03	8.0E-03	1.0E-02
Gross Area	SF	20,000	127,700	1,515,000
Volume	CF per 1 gsf	13.000	15.750	18.000
Cladding				
Gross Wall Area	SF per 1 gsf	0.260	0.500	1.000
Windows or Glazing Area	100 SF per 1 gsf	4.0E-04	1.4E-03	3.1E-03
Roof Area - Total	SF per 1 gsf	0.090	0.290	1.050
Interior Partition Length	100 LF per 1 gsf	7.5E-04	1.1E-03	1.4E-03
Ceramic tile floors	SF per 1 gsf	0.035	0.071	0.159

Table F-3 Normative Quantities for Healthcare Occupancies

Component Type	Unit of Measurement	10th Percentile Quantity	50th Percentile Quantity	90th Percentile Quantity
Ceramic tile walls	100 LF per 1 gsf	6.2E-05	1.3E-04	2.9E-04
Ceilings				
Ceiling - Lay in tile percentage	%		80%	
Ceiling - Gypsum board percentage	%		8%	
Ceiling - Exposed percentage	%		8%	
Ceiling - Other (high end) percentage	%		4%	
Stairs	FL per 1 gsf	7.0E-05	8.0E-05	1.0E-04
Elevators	EA per 1 gsf	1.2E-05	2.8E-05	9.8E-05
Plumbing				
Plumbing Fixtures	EA per 1 gsf	1.2E-03	2.4E-03	5.3E-03
Piping				
Cold Domestic Water Piping - 2 ½ inch diameter or smaller	1,000 LF per 1 gsf	8.0E-05	1.1E-04	1.3E-04
Cold Domestic Water Piping – greater than 2 ½ diameter	1,000 LF per 1 gsf	3.0E-05	4.0E-05	5.0E-05
Hot Domestic Water Piping - 2 ½ inch diameter or smaller	1,000 LF per 1 gsf	1.6E-04	2.2E-04	2.6E-04
Hot Domestic Waster Piping – greater than 2 ½ diameter	1,000 LF per 1 gsf	6.0E-05	8.0E-05	1.0E-04
Gas supply piping	1,000 LF per 1 gsf	5.0E-06	1.0E-05	1.5E-05
Sanitary Waste Piping	1,000 LF per 1 gsf	1.1E-04	1.5E-04	1.8E-04
Process Piping - 2 ½ inch diameter or smaller	1,000 LF per 1 gsf	1.2E-04	1.6E-04	2.0E-04
Process Piping – greater than 2 ½ diameter	1,000 LF per 1 gsf	4.0E-05	6.0E-05	7.0E-05
Acid Waste Piping	1,000 LF per 1 gsf	4.0E-05	6.0E-05	7.0E-05
HVAC				
Chiller capacity	TN per 1 gsf	2.9E-03	3.3E-03	3.7E-03
Cooling Tower capacity	TN per 1 gsf	2.9E-03	3.3E-03	3.7E-03
Boiler capacity	BTU per 1 gsf	40.000	50.000	65.000
Air Handling Units	CFM per 1 gsf	0.800	1.000	1.250
Fans	CFM per 1 gsf	0.800	1.000	1.250
HVAC Ducts – 6 sq. feet for larger	1,000 LF per 1 gsf	2.5E-05	3.5E-05	4.0E-05
HVAC Ducts – less than 6 sq. feet	1,000 LF per 1 gsf	5.0E-05	7.5E-05	9.0E-05

Table F-3 Normative Quantities for Healthcare Occupancies (continued)

Component Type	Unit of Measurement	10th Percentile Quantity	50th Percentile Quantity	90th Percentile Quantity
HVAC in-line Drops & Diffusers	EA per 1 gsf	1.6E-02	2.0E-02	2.2E-02
HVAC in-line Coils	EA per 1 gsf	3.0E-03	5.0E-03	6.0E-03
VAV Boxes	EA per 1 gsf	3.0E-03	5.0E-03	6.0E-03
Piping				
Steam & Chilled Water Piping - 2 ½ inch diameter or smaller	1,000 LF per 1 gsf	0.0E+00	2.0E-05	1.5E-05
Steam & Chilled Water Piping – greater than 2 ½ diameter	1,000 LF per 1 gsf	2.0E-05	3.0E-05	2.5E-05
Heating Water Piping - 2 ½ inch diameter or smaller	1,000 LF per 1 gsf	6.0E-05	8.0E-05	1.0E-04
Heating Water Piping – greater than 2 ½ diameter	1,000 LF per 1 gsf	2.0E-05	3.0E-05	3.5E-05
Electrical				
Electrical Load	W per 1 gsf	14.000	23.100	35.600
Electrical Distribution conduits	LF per 1 gsf	3.0E-01	5.0E-01	6.0E-01
Electrical Distribution – cable trays	LF per 1 gsf	0.0E+00	4.0E-02	7.5E-02
Wall mounted switchgear	EA per 1 gsf	2.0E-04	4.0E-04	5.0E-04
Lighting Fixtures – Lay in fluorescent	EA per 1 gsf	1.0E-02	1.5E-02	1.7E-02
Lighting Fixtures – Stem hung fluorescent	EA per 1 gsf	1.0E-02	1.5E-02	1.7E-02
Standby generators	KVA per 1 gsf	3.5E-03	5.0E-03	1.5E-02
Fire Protection				
Sprinkler Piping	20 LF per 1 gsf	1.0E-02	1.1E-02	1.3E-02
Sprinkler Drops	EA per 1 gsf	1.0E-02	1.2E-02	1.4E-02

Table F-4 Normative Quantities for Hospitality Occupancies

Component Type	Unit of Measurement	10th Percentile Quantity	50th Percentile Quantity	90th Percentile Quantity
Gross Area	SF			
Volume	CF per 1 gsf	9.000	11.000	14.000
Cladding				
Gross Wall Area	SF per 1 gsf	0.300	0.350	0.500
Windows or Glazing Area	100 SF per 1 gsf	7.0E-04	1.2E-03	1.7E-03
Roof Area - Total	SF per 1 gsf	0.600	0.200	0.060
Interior Partition Length	100 LF per 1 gsf	5.5E-04	6.0E-04	8.0E-04
Ceramic tile floors	SF per 1 gsf	0.120	0.160	0.240
Ceramic tile walls	100 LF per 1 gsf	2.2E-04	2.9E-04	4.3E-04
Ceilings				
Ceiling - Lay in tile percentage	%		15%	
Ceiling - Gypsum board percentage	%		70%	
Ceiling - Exposed percentage	%		8%	
Ceiling - Other (high end) percentage	%		7%	
Stairs	FL per 1 gsf	9.0E-05	1.1E-04	1.2E-04
Elevators	EA per 1 gsf	1.4E-05	1.5E-05	4.0E-05
Plumbing				
Plumbing Fixtures	EA per 1 gsf	3.0E-03	4.0E-03	6.0E-03
Piping				
Cold Domestic Water Piping - 2 ½ inch diameter or smaller	1,000 LF per 1 gsf	6.0E-05	8.0E-05	1.2E-04
Cold Domestic Water Piping – greater than 2 ½ diameter	1,000 LF per 1 gsf	1.0E-05	1.5E-05	2.0E-05
Hot Domestic Water Piping - 2 ½ inch diameter or smaller	1,000 LF per 1 gsf	1.2E-04	1.6E-04	2.4E-04
Hot Domestic Waster Piping – greater than 2 ½ diameter	1,000 LF per 1 gsf	2.0E-05	3.0E-05	4.0E-05
Gas supply piping	1,000 LF per 1 gsf	2.0E-05	4.0E-05	4.5E-05
Sanitary Waste Piping	1,000 LF per 1 gsf	7.0E-05	9.5E-05	1.4E-04
HVAC				
Chiller capacity	TN per 1 gsf	0.0E+00	0.0E+00	2.0E-03
Cooling Tower capacity	TN per 1 gsf	0.0E+00	0.0E+00	2.0E-03
Boiler capacity	BTU per 1 gsf	30.000	45.000	50.000
Air Handling Units	CFM per 1 gsf	0.000	0.000	0.600

Table F-4 Normative Quantities for Hospitality Occupancies (continued)

Component Type	Unit of Measurement	10th Percentile Quantity	50th Percentile Quantity	90th Percentile Quantity
HVAC Ducts – 6 sq. feet for larger	1,000 LF per 1 gsf	0.0E+00	0.0E+00	1.5E-05
HVAC Ducts – less than 6 sq. feet	1,000 LF per 1 gsf	0.0E+00	5.0E-05	8.0E-05
HVAC in-line Drops & Diffusers	EA per 1 gsf	4.0E-03	8.0E-03	1.2E-02
HVAC in-line Coils	EA per 1 gsf	0.0E+00	0.0E+00	1.5E-03
VAV Boxes	EA per 1 gsf	0.0E+00	0.0E+00	1.5E-03
Fan Coil Units	EA per 1 gsf	4.0E-03	6.0E-03	0.0E+00
Piping				
Steam & Chilled Water Piping - 2 ½ inch diameter or smaller	1,000 LF per 1 gsf	0.0E+00	0.0E+00	5.0E-06
Steam & Chilled Water Piping – greater than 2 ½ diameter	1,000 LF per 1 gsf	0.0E+00	0.0E+00	5.0E-06
Heating Water Piping - 2 ½ inch diameter or smaller	1,000 LF per 1 gsf	0.0E+00	5.0E-06	1.0E-05
Heating Water Piping – greater than 2 ½ diameter	1,000 LF per 1 gsf	0.0E+00	5.0E-06	1.0E-05
Electrical				
Electrical Load	W per 1 gsf	6.000	11.000	15.000
Electrical Distribution conduits	LF per 1 gsf	0.0E+00	2.0E-01	3.0E-01
Electrical Distribution – cable trays	LF per 1 gsf	0.0E+00	0.0E+00	0.0E+00
Wall mounted switchgear	EA per 1 gsf	1.0E-04	1.5E-04	2.0E-04
Lighting Fixtures – Lay in fluorescent	EA per 1 gsf	0.0E+00	0.0E+00	4.0E-03
Lighting Fixtures – Stem hung fluorescent	EA per 1 gsf	0.0E+00	0.0E+00	4.0E-03
Standby generators	KVA per 1 gsf	0.0E+00	0.0E+00	0.0E+00
Fire Protection				
Sprinkler Piping	20 LF per 1 gsf	1.0E-02	1.1E-02	1.3E-02
Sprinkler Drops	EA per 1 gsf	1.0E-02	1.2E-02	1.4E-02

Table F-5 Normative Quantities for Multi-Unit Residential Occupancies

Component Type	Unit of Measurement	10th Percentile Quantity	50th Percentile Quantity	90th Percentile Quantity
Gross Area	SF	5,000	34,000	582,200
Volume	CF per 1 gsf	7.440	10.460	14.500
Cladding				
Gross Wall Area	SF per 1 gsf	0.320	0.770	1.300
Windows or Glazing Area	100 SF per 1 gsf	6.0E-04	1.5E-03	3.0E-03
Roof Area - Total	SF per 1 gsf	0.090	0.320	1.000
Interior Partition Length	100 LF per 1 gsf	7.0E-04	1.2E-03	1.6E-03
Ceramic tile floors	SF per 1 gsf	0.108	0.212	0.340
Ceramic tile walls	100 LF per 1 gsf	1.9E-04	3.8E-04	6.1E-04
Ceilings				
Ceiling - Lay in tile percentage	%		0%	
Ceiling - Gypsum board percentage	%		95%	
Ceiling - Exposed percentage	%		5%	
Ceiling - Other (high end) percentage	%		0%	
Stairs	FL per 1 gsf	1.0E-04	1.2E-04	1.4E-04
Elevators	EA per 1 gsf	7.0E-06	3.4E-05	8.0E-05
Plumbing				
Plumbing Fixtures	EA per 1 gsf	2.7E-03	5.3E-03	8.5E-03
Piping				
Cold Domestic Water Piping - 2 ½ inch diameter or smaller	1,000 LF per 1 gsf	5.4E-05	1.1E-04	1.7E-04
Cold Domestic Water Piping – greater than 2 ½ diameter	1,000 LF per 1 gsf	1.0E-05	1.5E-05	2.0E-05
Hot Domestic Water Piping - 2 ½ inch diameter or smaller	1,000 LF per 1 gsf	1.1E-04	2.1E-04	3.4E-04
Hot Domestic Waster Piping – greater than 2 ½ diameter	1,000 LF per 1 gsf	2.0E-05	3.0E-05	4.0E-05
Gas supply piping	1,000 LF per 1 gsf	2.0E-05	4.0E-05	4.5E-05
Sanitary Waste Piping	1,000 LF per 1 gsf	6.4E-05	1.2E-04	1.9E-04
HVAC				
Chiller capacity	TN per 1 gsf	0.0E+00	0.0E+00	2.0E-03
Cooling Tower capacity	TN per 1 gsf	0.0E+00	0.0E+00	2.0E-03
Boiler capacity	BTU per 1 gsf	30.000	45.000	60.000
Air Handling Units	CFM per 1 gsf	0.000	0.000	0.600

Table F-5 Normative Quantities for Multi-Unit Residential Occupancies (continued)

Component Type	Unit of Measurement	10th Percentile Quantity	50th Percentile Quantity	90th Percentile Quantity
HVAC Ducts – 6 sq. feet for larger	1,000 LF per 1 gsf	0.0E+00	0.0E+00	1.5E-05
HVAC Ducts – less than 6 sq. feet	1,000 LF per 1 gsf	0.0E+00	5.0E-05	8.0E-05
HVAC in-line Drops & Diffusers	EA per 1 gsf	4.0E-03	8.0E-03	1.2E-02
HVAC in-line Coils	EA per 1 gsf	0.0E+00	0.0E+00	1.5E-03
VAV Boxes	EA per 1 gsf	0.0E+00	0.0E+00	1.5E-03
Fan Coil Units	EA per 1 gsf	2.0E-03	4.0E-03	0.0E+00
Piping				
Steam & Chilled Water Piping - 2 ½ inch diameter or smaller	1,000 LF per 1 gsf	0.0E+00	0.0E+00	5.0E-06
Steam & Chilled Water Piping – greater than 2 ½ diameter	1,000 LF per 1 gsf	0.0E+00	0.0E+00	5.0E-06
Heating Water Piping - 2 ½ inch diameter or smaller	1,000 LF per 1 gsf	0.0E+00	5.0E-06	1.0E-05
Heating Water Piping – greater than 2 ½ diameter	1,000 LF per 1 gsf	0.0E+00	5.0E-06	1.0E-05
Electrical				
Electrical Load	W per 1 gsf	8.300	11.400	19.500
Electrical Distribution conduits	LF per 1 gsf	0.0E+00	2.0E-01	3.0E-01
Electrical Distribution – cable trays	LF per 1 gsf	0.0E+00	0.0E+00	0.0E+00
Wall mounted switchgear	EA per 1 gsf	1.0E-04	1.5E-04	2.0E-04
Lighting Fixtures – Lay in fluorescent	EA per 1 gsf	0.0E+00	0.0E+00	4.0E-03
Lighting Fixtures – Stem hung fluorescent	EA per 1 gsf	0.0E+00	0.0E+00	4.0E-03
Standby generators	KVA per 1 gsf	0.0E+00	0.0E+00	0.0E+00
Fire Protection				
Sprinkler Piping	20 LF per 1 gsf	1.0E-02	1.1E-02	1.3E-02
Sprinkler Drops	EA per 1 gsf	1.0E-02	1.2E-02	1.4E-02

Table F-6 Normative Quantities for Research Occupancies

Component Type	Unit of Measurement	10th Percentile Quantity	50th Percentile Quantity	90th Percentile Quantity
Gross Area	SF	35,000	96,000	330,000
Volume	CF per 1 gsf	13.000	16.000	20.000
Cladding				
Gross Wall Area	SF per 1 gsf	0.400	0.520	1.100
Windows or Glazing Area	100 SF per 1 gsf	7.0E-04	1.5E-03	4.3E-03
Roof Area - Total	SF per 1 gsf	1.050	0.245	0.110
Interior Partition Length	100 LF per 1 gsf	6.0E-04	8.5E-04	1.1E-03
Ceramic tile floors	SF per 1 gsf	0.010	0.028	0.080
Ceramic tile walls	100 LF per 1 gsf	1.8E-05	5.0E-05	1.4E-04
Ceilings				
Ceiling - Lay in tile percentage	%		85%	
Ceiling - Gypsum board percentage	%		5%	
Ceiling - Exposed percentage	%		8%	
Ceiling - Other (high end) percentage	%		2%	
Laboratory Casework	LF per 1 gsf	0.0E+00	2.2E-02	4.0E-02
Fume Hoods	EA per 1 gsf	0.0E+00	9.0E-04	1.9E-03
Stairs	FL per 1 gsf	8.0E-05	1.0E-04	1.2E-04
Elevators	EA per 1 gsf	1.3E-05	1.7E-05	1.0E-04
Plumbing				
Plumbing Fixtures				
Domestic	EA per 1 gsf	2.5E-04	7.0E-04	2.0E-03
Lab	EA per 1 gsf	7.0E-05	2.7E-04	3.0E-03
Piping				
Cold Domestic Water Piping - 2 ½ inch diameter or smaller	1,000 LF per 1 gsf	4.0E-05	6.0E-05	8.0E-05
Cold Domestic Water Piping – greater than 2 ½ diameter	1,000 LF per 1 gsf	1.0E-05	2.0E-05	3.0E-05
Hot Domestic Water Piping - 2 ½ inch diameter or smaller	1,000 LF per 1 gsf	8.0E-05	1.2E-04	1.6E-04
Hot Domestic Waster Piping – greater than 2 ½ diameter	1,000 LF per 1 gsf	2.0E-05	4.0E-05	6.0E-05
Gas supply piping	1,000 LF per 1 gsf	5.0E-06	1.0E-05	1.5E-05
Sanitary Waste Piping	1,000 LF per 1 gsf	5.0E-05	8.0E-05	1.1E-04
Process Piping - 2 ½ inch diameter or smaller	1,000 LF per 1 gsf	3.0E-04	4.0E-04	5.0E-04

Table F-6 Normative Quantities for Research Occupancies (continued)

Component Type	Unit of Measurement	10th Percentile Quantity	50th Percentile Quantity	90th Percentile Quantity
Process Piping – greater than 2 ½ diameter	1,000 LF per 1 gsf	1.0E-04	1.5E-04	1.8E-04
Acid Waste Piping	1,000 LF per 1 gsf	1.0E-04	1.5E-04	1.8E-04
HVAC				
Chiller capacity	TN per 1 gsf	2.9E-03	3.3E-03	3.7E-03
Cooling Tower capacity	TN per 1 gsf	2.9E-03	3.3E-03	3.7E-03
Boiler capacity	BTU per 1 gsf	55.000	65.000	75.000
Air Handling Units	CFM per 1 gsf	1.000	1.250	1.500
Fans	CFM per 1 gsf	1.000	1.250	1.500
HVAC Ducts – 6 sq. feet for larger	1,000 LF per 1 gsf	3.5E-05	5.0E-05	7.0E-05
HVAC Ducts – less than 6 sq. feet	1,000 LF per 1 gsf	8.0E-05	1.0E-04	1.2E-04
HVAC in-line Drops & Diffusers	EA per 1 gsf	1.3E-02	1.6E-02	2.0E-02
HVAC in-line Coils	EA per 1 gsf	1.3E-03	2.0E-03	2.5E-03
VAV Boxes	EA per 1 gsf	0.0E+00	3.0E-04	5.0E-04
Pressure Dependent Air Valves (Phoenix type boxes)	EA per 1 gsf	6.0E-03	1.0E-02	1.2E-02
Piping				
Steam & Chilled Water Piping - 2 ½ inch diameter or smaller	1,000 LF per 1 gsf	0.0E+00	1.0E-05	1.5E-05
Steam & Chilled Water Piping – greater than 2 ½ diameter	1,000 LF per 1 gsf	1.5E-05	2.0E-05	2.5E-05
Heating Water Piping - 2 ½ inch diameter or smaller	1,000 LF per 1 gsf	6.0E-05	8.0E-05	1.0E-04
Heating Water Piping – greater than 2 ½ diameter	1,000 LF per 1 gsf	2.0E-05	3.0E-05	3.5E-05
Electrical				
Electrical Load	W per 1 gsf	14.500	22.800	48.800
Electrical Distribution conduits	LF per 1 gsf	3.0E-01	5.0E-01	6.0E-01
Electrical Distribution – cable trays	LF per 1 gsf	0.0E+00	4.0E-02	7.5E-02
Wall mounted switchgear	EA per 1 gsf	1.0E-03	3.0E-03	4.0E-03
Lighting Fixtures – Lay in fluorescent	EA per 1 gsf	1.0E-02	1.5E-02	1.7E-02
Lighting Fixtures – Stem hung fluorescent	EA per 1 gsf	1.0E-02	1.5E-02	1.7E-02
Standby generators	KVA per 1 gsf	3.5E-03	5.0E-03	1.5E-02

Table F-6 Normative Quantities for Research Occupancies (continued)

Component Type	Unit of Measurement	10th Percentile Quantity	50th Percentile Quantity	90th Percentile Quantity
Fire Protection				
Sprinkler Piping	20 LF per 1 gsf	9.0E-03	1.0E-02	1.1E-02
Sprinkler Drops	EA per 1 gsf	8.0E-03	1.0E-02	1.3E-02

Table F-7 Normative Quantities for Retail Occupancies

Component Type	Unit of Measurement	10th Percentile Quantity	50th Percentile Quantity	90th Percentile Quantity
Gross Area	SF	25,000	40,000	90,000
Volume	CF per 1 gsf	18.000	20.000	23.000
Cladding				
Gross Wall Area	SF per 1 gsf	0.250	0.300	0.400
Windows or Glazing Area	100 SF per 1 gsf	4.0E-04	6.0E-04	8.0E-04
Roof Area - Total	SF per 1 gsf	0.700	0.500	0.300
Interior Partition Length	100 LF per 1 gsf	6.0E-05	1.0E-04	1.2E-04
Ceramic tile floors	SF per 1 gsf	0.040	0.060	0.072
Ceramic tile walls	100 LF per 1 gsf	7.2E-05	1.1E-04	1.3E-04
Ceilings				
Ceiling - Lay in tile percentage	%		90%	
Ceiling - Gypsum board percentage	%		3%	
Ceiling - Exposed percentage	%		2%	
Ceiling - Other (high end) percentage	%		5%	
Stairs	FL per 1 gsf	5.0E-05	1.0E-04	1.2E-04
Elevators	EA per 1 gsf	5.0E-05	1.0E-04	1.2E-04
Plumbing				
Plumbing Fixtures	EA per 1 gsf	1.0E-03	1.5E-03	1.8E-03
Piping				
Cold Domestic Water Piping - 2 ½ inch diameter or smaller	1,000 LF per 1 gsf	2.0E-05	3.0E-05	4.0E-05
Cold Domestic Water Piping – greater than 2 ½ diameter	1,000 LF per 1 gsf	1.0E-05	1.5E-05	2.0E-05
Hot Domestic Water Piping - 2 ½ inch diameter or smaller	1,000 LF per 1 gsf	4.0E-05	6.0E-05	8.0E-05
Hot Domestic Waster Piping – greater than 2 ½ diameter	1,000 LF per 1 gsf	2.0E-05	3.0E-05	4.0E-05
Gas supply piping	1,000 LF per 1 gsf	2.0E-05	4.0E-05	4.5E-05

Table F-7 Normative Quantities for Retail Occupancies (continued)

Component Type	Unit of Measurement	10th Percentile Quantity	50th Percentile Quantity	90th Percentile Quantity
Sanitary Waste Piping	1,000 LF per 1 gsf	3.0E-05	4.5E-05	6.0E-05
HVAC				
Chiller capacity	TN per 1 gsf	0.0E+00	0.0E+00	2.5E-03
Cooling Tower capacity	TN per 1 gsf	0.0E+00	0.0E+00	2.5E-03
Boiler capacity	BTU per 1 gsf	30.000	45.000	60.000
Air Handling Units	CFM per 1 gsf	0.000	0.000	0.600
Fans	CFM per 1 gsf	0.000	0.000	15.000
HVAC Ducts – 6 sq. feet for larger	1,000 LF per 1 gsf	0.0E+00	5.0E-05	8.0E-05
HVAC Ducts – less than 6 sq. feet	1,000 LF per 1 gsf	0.0E+00	5.0E-06	8.0E-06
HVAC in-line Drops & Diffusers	EA per 1 gsf	0.0E+00	0.0E+00	1.5E-03
HVAC in-line Coils	EA per 1 gsf	0.0E+00	0.0E+00	1.5E-03
VAV Boxes	EA per 1 gsf	2.0E-03	4.0E-03	0.0E+00
Piping				
Steam & Chilled Water Piping - 2 ½ inch diameter or smaller	1,000 LF per 1 gsf	0.0E+00	0.0E+00	5.0E-06
Steam & Chilled Water Piping – greater than 2 ½ diameter	1,000 LF per 1 gsf	0.0E+00	5.0E-06	1.0E-05
Heating Water Piping - 2 ½ inch diameter or smaller	1,000 LF per 1 gsf	0.0E+00	2.5E-05	4.0E-05
Heating Water Piping – greater than 2 ½ diameter	1,000 LF per 1 gsf	0.0E+00	5.0E-06	1.0E-05
Electrical				
Electrical Load	W per 1 gsf	7.000	18.800	23.000
Electrical Distribution conduits	LF per 1 gsf	1.0E-01	2.0E-01	3.0E-01
Electrical Distribution – cable trays	LF per 1 gsf	0.0E+00	0.0E+00	0.0E+00
Wall mounted switchgear	EA per 1 gsf	1.0E-04	1.5E-04	2.0E-04
Lighting Fixtures – Lay in fluorescent	EA per 1 gsf	1.0E-02	1.5E-02	1.7E-02
Lighting Fixtures – Stem hung fluorescent	EA per 1 gsf	1.0E-02	1.5E-02	1.7E-02
Standby generators	KVA per 1 gsf	0.0E+00	0.0E+00	0.0E+00
Fire Protection				
Sprinkler Piping	20 LF per 1 gsf	7.5E-03	9.0E-03	1.0E-02
Sprinkler Drops	EA per 1 gsf	6.0E-03	8.0E-03	1.0E-02

Table F-8 Normative Quantities for Warehouse Occupancies

Component Type	Unit of Measurement	10th Percentile Quantity	50th Percentile Quantity	90th Percentile Quantity
Gross Area	SF			
Volume	CF per 1 gsf	20.000	28.000	40.000
Cladding				
Gross Wall Area	SF per 1 gsf	0.200	0.220	0.300
Windows or Glazing Area	100 SF per 1 gsf	0.0E+00	1.0E-05	2.0E-05
Roof Area - Total	SF per 1 gsf	1.000	1.000	1.000
Interior Partition Length	100 LF per 1 gsf	3.0E-05	3.0E-05	4.0E-05
Ceramic tile floors	SF per 1 gsf	0.001	0.002	0.004
Ceramic tile walls	100 LF per 1 gsf	2.2E-06	4.3E-06	7.2E-06
Ceilings				
Ceiling - Lay in tile percentage	%		5%	
Ceiling - Gypsum board percentage	%		5%	
Ceiling - Exposed percentage	%		90%	
Ceiling - Other (high end) percentage	%		0%	
Stairs	FL per 1 gsf	0.0E+00	0.0E+00	0.0E+00
Elevators	EA per 1 gsf	0.0E+00	0.0E+00	0.0E+00
Plumbing				
Plumbing Fixtures	EA per 1 gsf	3.0E-05	6.0E-05	1.0E-04
Piping				
Cold Domestic Water Piping - 2 ½ inch diameter or smaller	1,000 LF per 1 gsf	2.4E-06	4.8E-06	8.0E-06
Cold Domestic Water Piping – greater than 2 ½ diameter	1,000 LF per 1 gsf	1.0E-05	1.5E-05	2.0E-05
Hot Domestic Water Piping - 2 ½ inch diameter or smaller	1,000 LF per 1 gsf	4.8E-06	9.6E-06	1.6E-05
Hot Domestic Waster Piping – greater than 2 ½ diameter	1,000 LF per 1 gsf	2.0E-05	3.0E-05	4.0E-05
Gas supply piping	1,000 LF per 1 gsf	1.0E-05	1.5E-05	2.0E-05
Sanitary Waste Piping	1,000 LF per 1 gsf	1.2E-05	2.0E-05	2.8E-05
HVAC				
Chiller capacity	TN per 1 gsf	0.0E+00	0.0E+00	2.0E-03
Cooling Tower capacity	TN per 1 gsf	0.0E+00	0.0E+00	2.0E-03
Boiler capacity	BTU per 1 gsf	10.000	15.000	20.000
Air Handling Units	CFM per 1 gsf	0.000	0.200	0.400
Fans	CFM per 1 gsf	0.000	0.000	0.300

Table F-8 Normative Quantities for Warehouse Occupancies (continued)

Component Type	Unit of Measurement	10th Percentile Quantity	50th Percentile Quantity	90th Percentile Quantity
HVAC Ducts – 6 sq. feet for larger	1,000 LF per 1 gsf	0.0E+00	0.0E+00	1.0E-05
HVAC Ducts – less than 6 sq. feet	1,000 LF per 1 gsf	0.0E+00	4.0E-05	6.0E-05
HVAC in-line Drops & Diffusers	EA per 1 gsf	2.0E-03	3.0E-03	5.0E-03
HVAC in-line Coils	EA per 1 gsf	0.0E+00	0.0E+00	1.0E-03
VAV Boxes	EA per 1 gsf	0.0E+00	0.0E+00	1.0E-03
Piping				
Steam & Chilled Water Piping - 2 ½ inch diameter or smaller	1,000 LF per 1 gsf	0.0E+00	0.0E+00	5.0E-06
Steam & Chilled Water Piping – greater than 2 ½ diameter	1,000 LF per 1 gsf	0.0E+00	0.0E+00	5.0E-06
Heating Water Piping - 2 ½ inch diameter or smaller	1,000 LF per 1 gsf	0.0E+00	5.0E-06	1.0E-05
Heating Water Piping – greater than 2 ½ diameter	1,000 LF per 1 gsf	0.0E+00	5.0E-06	1.0E-05
Electrical				
Electrical Load	W per 1 gsf	4.000	6.000	12.000
Electrical Distribution conduits	LF per 1 gsf	2.0E-02	1.0E-01	1.5E-01
Electrical Distribution – cable trays	LF per 1 gsf	0.0E+00	0.0E+00	0.0E+00
Wall mounted switchgear	EA per 1 gsf	5.0E-05	8.0E-05	1.0E-03
Lighting Fixtures – Lay in fluorescent	EA per 1 gsf	0.0E+00	0.0E+00	0.0E+00
Lighting Fixtures – Stem hung fluorescent	EA per 1 gsf	1.0E-02	1.5E-02	2.0E-02
Standby generators	KVA per 1 gsf	0.0E+00	0.0E+00	0.0E+00
Fire Protection				
Sprinkler Piping	20 LF per 1 gsf	4.5E-03	5.5E-03	6.5E-03
Sprinkler Drops	EA per 1 gsf	6.0E-03	8.0E-03	1.0E-02

Appendix G
Generation of Simulated Demands

G.1 General

As described in Chapter 7, this methodology uses a Monte Carlo procedure to determine the distribution of probable losses for each ground motion intensity or earthquake scenario evaluated. In this process, a large number of earthquake realizations (hundreds to thousands) are developed; each realization representing one possible outcome of the building's response to the particular motion intensity or scenario. Each realization requires a unique set of demands (peak floor accelerations, story drift ratios, story velocities, etc.) to determine component damage states. Rather than requiring a large number of structural analyses to develop these demands, the results from a limited suite of analyses in the case of nonlinear response history analysis, or a single analysis in the case of the simplified procedure, are mathematically transformed into a large series of simulated demands sets.

This appendix describes the algorithms used to transform the demands developed from a limited number of structural analyses into the large number of simulated demands used to determine performance. Section G.2 presents the algorithm used when demands are obtained from nonlinear response-history analysis. Section G.3 presents the algorithm used with the simplified analysis procedure.

G.2 Nonlinear Response-History Analysis

G.2.1 Introduction

When nonlinear response history analysis is used, the results of the structural analyses are assembled into a matrix with each row representing the peak values of demand obtained from a particular analysis, and each column containing the peak value of a particular demand parameter, e.g. floor acceleration at the 3rd level in the east-west direction; obtained from the suite of analyses. This demand matrix is considered to be representative of a jointly lognormal distribution. Mathematical manipulation is performed to determine a median value for each parameter based on the analysis results, and also a covariance matrix that indicates the relationship of each parameter

to the others. Then a large number of simulated demand vectors are mathematically generated using a random number selection process, the median values and covariance matrix. The minimum number of nonlinear analyses required depends on many parameters, including the required accuracy of the loss calculation; the building's dynamic properties and number of stories; and, the properties of the ground motion. In this Appendix, 11 analyses are assumed for purposes of illustration.

G.2.2 Algorithm

Yang (Yang, 2006; Yang et al., 2009) developed the original algorithm used to generate simulated demands. Huang et al. (2008) extended the algorithm to address the effects of modeling uncertainty, β_m and ground motion uncertainty, β_{gm} on demand distribution.

Let *m* represent the number of response analyses performed at an intensity level, or scenario. For each analysis, the peak absolute value of each demand parameter (e.g., third story drift ratio, roof acceleration) is assembled into a row vector with *n* entries, where *n* is the number of demand parameters. The *m* row vectors are catenated to form an $m \times n$ matrix (*m* rows × *n* columns; analyses × demand parameters)–each column presents *m* values of one demand parameter.

Denote the matrix of demand parameters, $\mathbf{X}$. The entries in $\mathbf{X}$ are assumed to be jointly lognormal. The natural logarithm of each entry in $\mathbf{X}$ is computed to form an $m \times n$ matrix $\mathbf{Y}$. The entries in $\mathbf{Y}$ are assumed to be jointly normal and can be characterized by a $1 \times n$ mean vector, $\mathbf{M}_\mathbf{Y}$, containing the means of the natural logarithms of each demand and an $n \times n$ covariance matrix, $\Sigma_{\mathbf{YY}}$.

A vector of natural logarithm of demand parameters, $\mathbf{Z}$, can be generated with the same statistical distribution as $\mathbf{Y}$ using a vector of uncorrelated standard normal random variables, $\mathbf{U}$, with a mean of $\mathbf{0}$, that is vector of 0s, and a covariance of $\mathbf{I}$ as shown in Eqn G-1 where $\mathbf{A}$ and $\mathbf{B}$ are matrices of constant coefficients that linearly transforms $\mathbf{U}$ to $\mathbf{Z}$.

$$\mathbf{Z} = \mathbf{AU} + \mathbf{B} = \mathbf{L}_{np}\mathbf{D}_{pp}\mathbf{U} + \mathbf{M}_\mathbf{Y} \tag{G-1}$$

In Eqn G-1, *p* is the rank of the covariance matrix $\Sigma_{\mathbf{YY}}$ and is obtained by counting the number nonzero eigenvalues of $\Sigma_{\mathbf{YY}}$. If $\Sigma_{\mathbf{YY}}$ is full-rank, then $p = n$. The rank of $\Sigma_{\mathbf{YY}}$ may not be full (i.e., $p \leq n$) for two reasons: (1) Number of analyses *m* is less than or equal to the number of demand variables *n*, a common situation; and, (2) one or more vectors of peak demands obtained from analyses are a linear combination of other analysis vectors . In either

case, a non-full-rank covariance matrix can be interpreted as a condition of insufficient data for generating the covariance matrix. For example using 11 analyses (m = 11) to assess to develop simulated demands for an 8-story plane frame building would result in 11 demand vectors, each having 8 entries representing peak story drift ratios and 9 entries representing peak accelerations at the building's levels (1st floor, 2nd floor, … 8th floor, roof) resulting in a 17×17 (n = 8 + 9 = 17) covariance matrix that is not-full-rank with p = 10.

PACT utilizes Eq. G-1 to generate the demand parameters vector, $\mathbf{Z}$. This equation can handle both full-rank and non-full-rank $\Sigma_{\mathbf{YY}}$. In Eq. G-1, $\mathbf{D}_{pp}$ is a $p \times p$ matrix obtained by partitioning the square-root of eigenvalues of covariance matrix $\Sigma_{\mathbf{YY}}$, denoted as $\mathbf{D}_{\mathrm{Y}}$, which is an $n \times n$ matrix. As mentioned earlier, p is the rank of $\Sigma_{\mathbf{YY}}$, therefore, if $\Sigma_{\mathbf{YY}}$ is full rank, $p = n$; and if $\Sigma_{\mathbf{YY}}$ is not-full-rank, then $p < n$. Similarly, matrix $\mathbf{L}_{np}$ is an $n \times p$ matrix obtained by partitioning the $n \times n$ eigenvector matrix of $\Sigma_{\mathbf{YY}}$, denoted as $\mathbf{L}_{\mathrm{Y}}$.

The effect of modeling uncertainty, represented by β_m and β_{gm}, in estimation of losses is implemented in the process for estimation of $\mathbf{Z}$. Once the covariance matrix of observations, $\Sigma_{\mathbf{YY}}$, is generated, it is decomposed into two matrices: a variance matrix and a correlation coefficient matrix. The variance matrix consists of variance of each demand parameter and is inflated with β_m and β_{gm} using a square root sum of squares technique to incorporate the modeling uncertainty. A new covariance matrix is assembled using the original correlation coefficient matrix and the inflated variance matrix. The process of estimation of $\mathbf{Z}$ using Eq. G-1 continues as further described below.

One simulated demand is generated by 1) computing $\mathbf{M}_{\mathbf{Y}}$, and $\Sigma_{\mathbf{YY}}$ from the matrix of the logarithms of the analysis results $\mathbf{Y}$; 2) updating $\Sigma_{\mathbf{YY}}$ for modeling uncertainty, 3) populating $\mathbf{U}$ by random sampling each demand parameter on a distribution with a mean of $\mathbf{0}$ and a covariance matrix of $\mathbf{I}$; 4) computing $\mathbf{Z}$ per (G-1); and 5) taking the exponential of every entry in $\mathbf{Z}$ to recover the vector of simulated demand parameters $\mathbf{W}$. N vectors of $\mathbf{U}$ are required for the N simulations: one vector per simulation. The process is computationally efficient because $\mathbf{M}_{\mathbf{Y}}$, $\Sigma_{\mathbf{YY}}$ are computed just once for each intensity of shaking. The process is illustrated in Figure G-1, below.

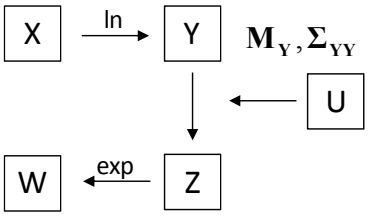

Where:
X – is the matrix of analytically determined demands (observations)
Y – is the natural logarithm of X
$\mathbf{M}_Y$ – is the mean demand vector
$\mathbf{\Sigma}_{YY}$ – is the covariance matrix of demand vector
Z – is the natural logarithm of realizations
W – is the matrix of statistically determined demands

Figure G-1 Generation of simulated vectors of correlated demand parameters .

G.2.3 Sample Application of the Algorithm

G.2.3.1 Description

This section illustrates the process described above for a sample 3-story, planar building. For this sample application, Seven demand parameters, 3 story drift ratios (δ_1, δ_2, δ_3) and 4 floor accelerations (a_1, a_2, a_3, a_4) ($n = 7$) are used to assess performance N, is selected as 10000. Eleven analyses ($m = 11$) are performed. Residual drift ratio and floor velocities are not considered in this example, but are included in the actual implementation. Table G-1 presents demand parameter matrix $\mathbf{X}$ 11 rows (one per analysis) × 7 columns (one per demand parameter) for this example. Modeling uncertainty, record-to-record variability and ground motion variability are set aside here to simplify the presentation. In this example as $m > n$, the covariance matrix of observations is full-rank, therefore $p = n = 7$. Section G2.3.2 presents details of the calculations.

Section G.2.3.3 illustrates the same example, however, only the results from the first five analysis are used ($m = 5$) as observations. In this case $m < n$, therefore the covariance matrix of observations is not-full-rank and $p = 4$. Calculations are provided in detail such that the process for implementation of (G-1) is thoroughly illustrated.

To visually illustrate the process of drawing realizations using observed data; consider the matrix $\mathbf{X} = [\mathbf{X}_1, \mathbf{X}_2 ..... \mathbf{X}_7]$ in Table G-1, below, with: 7 column vectors of demand, with 11 entries per vector. Joint probability distributions can be developed for pairs of vectors, for examples, between a) $\mathbf{X}_1$ (first story drift ratio) and $\mathbf{X}_3$ (third story drift ratio), and b) $\mathbf{X}_4$ (ground floor acceleration) and $\mathbf{X}_7$ (roof acceleration). The black solid circles in Figure G-2 below presents the relationships between $\mathbf{X}_1$ & $\mathbf{X}_3$, and $\mathbf{X}_4$ & $\mathbf{X}_7$

constructed using the data of Table G-1: $\mathbf{X}_1$ & $\mathbf{X}_3$ are weakly correlated and $\mathbf{X}_4$ & $\mathbf{X}_7$ are strongly correlated.

Table G-1 Matrix of Analytically Determined Demand Parameters, $\mathbf{X}$

	Δ_1(%)	Δ_2 (%)	Δ_3 (%)	a_1 (g)	a_2 (g)	a_3 (g)	a_r (g)
1	1.26	1.45	1.71	0.54	0.87	0.88	0.65
2	1.41	2.05	2.43	0.55	0.87	0.77	0.78
3	1.37	1.96	2.63	0.75	1.04	0.89	0.81
4	0.97	1.87	2.74	0.55	0.92	1.12	0.75
5	0.94	1.8	2.02	0.40	0.77	0.74	0.64
6	1.73	2.55	2.46	0.45	0.57	0.45	0.59
7	1.05	2.15	2.26	0.38	0.59	0.49	0.52
8	1.40	1.67	2.1	0.73	1.50	1.34	0.83
9	1.59	1.76	2.01	0.59	0.94	0.81	0.72
10	0.83	1.68	2.25	0.53	1.00	0.9	0.74
11	0.96	1.83	2.25	0.49	0.90	0.81	0.64

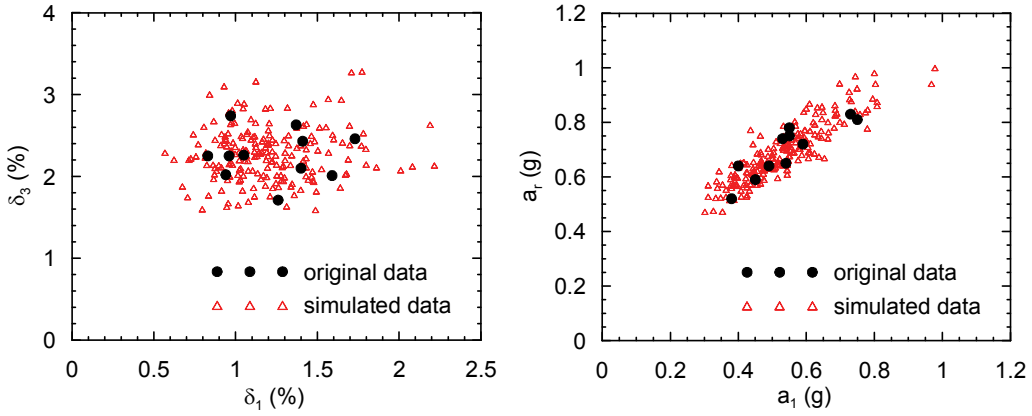

a. $\mathbf{X}_1$ and $\mathbf{X}_3$ b. $\mathbf{X}_4$ and $\mathbf{X}_7$

Figure G-2 Relationships between demand parameters.

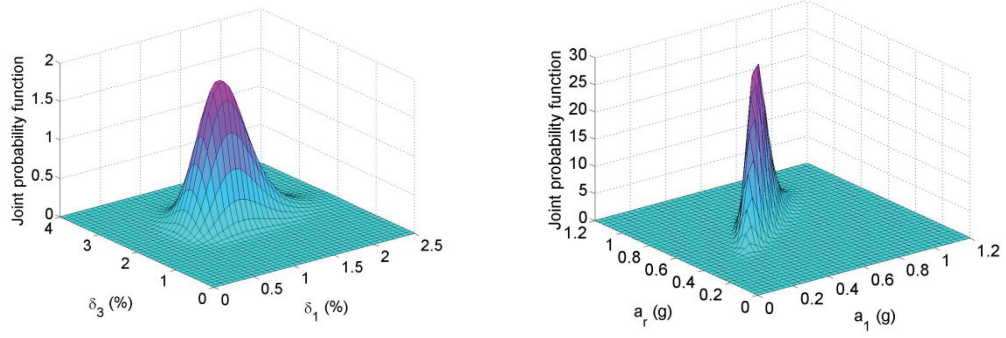

joint pdf for $\mathbf{X}_1$ & $\mathbf{X}_3$ joint pdf for $\mathbf{X}_4$ & $\mathbf{X}_7$

Figure G-3 Joint probability density functions.

A joint probability density function of the type shown in Figure G-3 can be constructed for any pair of vectors given two means, two variances, a

covariance and type of distribution (normal, log-normal). This figure presents the joint probability density functions for $\mathbf{X}_1$ & $\mathbf{X}_3$, and $\mathbf{X}_4$ & $\mathbf{X}_7$ constructed using the data of Table G-2, termed the *original* data hereafter.G2.3.2

Analysis for full-rank covariance matrix

The entries in matrix $\mathbf{X}$ are assumed to be jointly lognormal. The log of each entry in $\mathbf{X}$ is used to construct the entries in matrix $\mathbf{Y}$, which are now assumed to be jointly normal. Table G-2 below presents the entries in $\mathbf{Y}$; the last row in the table contains the mean of each column vector in $\mathbf{Y}$ representing the mean vector $\mathbf{M}_\mathbf{Y}$ of Eq. G-1. Table G-3 presents the covariance matrix $\Sigma_{\mathbf{YY}}$ of Y. Table G-4 presents the diagonal matrix of square root of eigenvalues of $\Sigma_{\mathbf{YY}}$, denoted as $\mathbf{D}_\mathbf{Y}$. All diagonal terms in $\mathbf{D}_\mathbf{Y}$ are positive, showing that $\Sigma_{\mathbf{YY}}$ is full-rank.

Table G-2 Natural Logarithm of Demand Parameters, Y

	δ_1	δ_2	δ_3	a_1	a_2	a_3	a_r
1	0.231	0.372	0.536	-0.616	-0.139	-0.128	-0.431
2	0.344	0.718	0.888	-0.598	-0.139	-0.261	-0.248
3	0.315	0.673	0.967	-0.288	0.039	-0.117	-0.211
4	-0.030	0.626	1.008	-0.598	-0.083	0.113	-0.288
5	-0.062	0.588	0.703	-0.916	-0.261	-0.301	-0.446
6	0.548	0.936	0.900	-0.799	-0.562	-0.799	-0.528
7	0.049	0.765	0.815	-0.968	-0.528	-0.713	-0.654
8	0.336	0.513	0.742	-0.315	0.405	0.293	-0.186
9	0.464	0.565	0.698	-0.528	-0.062	-0.211	-0.329
10	-0.186	0.519	0.811	-0.635	0.000	-0.105	-0.301
11	-0.041	0.604	0.811	-0.713	-0.105	-0.211	-0.446
μ_y	0.179	0.625	0.807	-0.634	-0.131	-0.222	-0.370

Table G-3 Covariance Matrix of Demand Parameters Y, $\Sigma_{\mathbf{YY}}$

	1	2	3	4	5	6	7
1	0.059	0.012	-0.001	0.020	-0.001	-0.015	0.005
2	0.012	0.022	0.013	-0.011	-0.025	-0.034	-0.008
3	-0.001	0.013	0.018	0.004	-0.003	-0.003	0.004
4	0.020	-0.011	0.004	0.046	0.048	0.049	0.027
5	-0.001	-0.025	-0.003	0.048	0.070	0.078	0.033
6	-0.015	-0.034	-0.003	0.049	0.078	0.099	0.037
7	0.005	-0.008	0.004	0.027	0.033	0.037	0.021

Table G-4 Matrix $\mathbf{D}_Y$ for the Sample Problem

0.007	0.000	0.000	0.000	0.000	0.000	0.000
0.000	0.046	0.000	0.000	0.000	0.000	0.000
0.000	0.000	0.060	0.000	0.000	0.000	0.000
0.000	0.000	0.000	0.070	0.000	0.000	0.000
0.000	0.000	0.000	0.000	0.169	0.000	0.000
0.000	0.000	0.000	0.000	0.000	0.273	0.000
0.000	0.000	0.000	0.000	0.000	0.000	0.471

Table G-5 Matrix $\mathbf{L}_Y$ for the Sample Problem

-0.209	0.026	0.098	0.329	-0.294	0.866	-0.026
0.639	0.104	0.487	0.066	0.490	0.230	-0.216
-0.578	0.150	-0.122	0.121	0.778	0.087	-0.019
0.316	0.262	-0.551	-0.472	0.140	0.369	0.386
-0.266	0.078	0.654	-0.434	-0.032	0.030	0.552
0.191	0.202	-0.037	0.679	0.028	-0.185	0.652
0.081	-0.922	-0.071	0.014	0.216	0.131	0.271

All of the matrices required to generate the correlated vectors have been constructed. The next step in the process is to compute the 7×1 vector $\mathbf{U}$ of uncorrelated standard normal random variables, with a mean of **0** and a ovariance matrix of **I**. The Matlab **randn** function is used for this purpose in this example, but any random generation algorithm can be used. This process is repeated 9999 times to construct the 10000 simulations. The next step involves taking the exponential of each value in the 7×10000 matrix to recover the demand parameters. Table G-6 presents the first 10 simulations of the 10000.

As a last step, the statistics of the simulated demands should be compared with those of the demands calculated by response-history analysis. A rigorous comparison of the analytical and simulated demands is achieved by computing the ratios of the mean vectors and the covariance matrices. Table G-7 presents ratios of elements of mean simulated response vector to elements of mean response-history response vector—all values are close to 1.0. Table G-8 presents similar ratios of elements covariance matrices obtained from realizations and observations covariance matrices—all values are close to 1.0. The data of Tables G-7 and G-8 indicate that the *simulated* vectors of demand have the same underlying statistics as those of the *original* demand vectors.

Table G-6 Matrix of Simulated Demand Parameters (first 10 vectors of 10000)

	δ_1 (%)	δ_2 (%)	δ_3 (%)	a_1 (g)	a_2 (g)	a_3 (g)	a_r (g)
1	0.886	1.927		0.282	0.528	0.435	0.464
2	1.259	1.992	2.614	0.585	0.860	0.841	0.765
3	1.373	1.784	2.019	0.612	1.172	0.918	0.698
4	1.136	2.394	2.989	0.461	0.661	0.645	0.716
5	1.428	1.518	1.699	0.491	0.779	0.831	0.691
6	1.019	1.782	2.358	0.553	0.929	0.891	0.710
7	1.441	2.141	2.307	0.501	0.786	0.644	0.620
8	1.032	1.720	1.967	0.449	0.892	0.842	0.671
9	0.993	1.766	2.316	0.501	0.936	0.991	0.758
10	1.513	2.039	2.071	0.460	0.691	0.590	0.615

Table G-7 Ratio of Simulated to Original Logarithmic Means

δ_1	δ_2	δ_3	a_1	a_2	a_3	a_r
0.9895	0.9967	0.9977	1.0001	0.9836	0.9913	0.9991

Table G-8 Ratio of Entries in Simulated and Original Σ_{YY} Matrices

0.999	1.022	0.718	1.000	1.058	1.044	1.008
1.022	1.006	1.015	0.973	0.993	0.997	0.955
0.718	1.015	1.016	1.047	0.975	0.947	1.064
1.000	0.973	1.047	0.996	0.993	0.986	0.991
1.058	0.993	0.975	0.993	0.989	0.989	0.986
1.044	0.997	0.947	0.986	0.989	0.993	0.983
1.008	0.955	1.064	0.991	0.986	0.983	0.991

G2.3.3 Analysis covariance matrix with less than full rank

This section illustrates the process and approximations involved with a case where the covariance matrix of demand parameters is not-full-rank, using the same example considered in the previous section. In this illustration, it is assumed that only five analyses ($m = 5$) are performed. Table G-9 shows the natural logarithm of these five observations, which are the first five out of eleven observations used in the previous example in Table G-2. This matrix of demand parameters is denoted as $\mathbf{Y}'$ .The last row in Table G-2 tabulates the

mean of each column vector in $\mathbf{Y}'$ representing the mean vector $\mathbf{M}_{\mathbf{Y}'}$ of Eq. G-1. Table G-10 presents the covariance matrix $\Sigma_{\mathbf{Y}'\mathbf{Y}'}$ of $\mathbf{Y}'$. Table G-11 presents the diagonal matrix $\mathbf{D}_{\mathbf{Y}'}$ of square root of eigenvalues of $\Sigma_{\mathbf{Y}'\mathbf{Y}'}$,. Only the last four diagonal terms in $\mathbf{D}_{\mathbf{Y}}$ are positive, showing that $\Sigma_{\mathbf{Y}'\mathbf{Y}'}$ is not-full-rank and $p = 4$. The matrix $\mathbf{D}_{pp}$ in Eq. G-1, in this example is a 4×4 matrix, is shaded with gray color in Table G-11 and separately illustrated in Table G-12. In the same fashion, the matrix of eigenvectors of $\Sigma_{\mathbf{Y}'\mathbf{Y}'}$, denoted as $\mathbf{L}_{\mathbf{Y}'}$, is shown in Table G-13, where the shaded area corresponds to matrix $\mathbf{L}_{np}$ in (G-1) and is separately shown in Table G-14. The matrix $\mathbf{L}_{np}$ in this example is a 7×4 matrix.

Table G-9 Natural Logarithm of Demand Parameters, $\mathbf{Y}'$

	δ_1	δ_2	δ_3	a_1	a_2	a_3	a_r
1	0.231	0.372	0.536	-0.616	-0.139	-0.128	-0.431
2	0.344	0.718	0.888	-0.598	-0.139	-0.261	-0.248
3	0.315	0.673	0.967	-0.288	0.039	-0.117	-0.211
4	-0.030	0.626	1.008	-0.598	-0.083	0.113	-0.288
5	-0.062	0.588	0.703	-0.916	-0.261	-0.301	-0.446
μ_y	0.159	0.595	0.820	-0.603	-0.117	-0.139	-0.325

Table G-10 Covariance Matrix of Demand Parameters $\mathbf{Y}'$, $\Sigma_{\mathbf{Y}'\mathbf{Y}'}$

	1	2	3	4	5	6	7
1	0.037	0.004	0.001	0.029	0.011	-0.008	0.011
2	0.004	0.018	0.022	0.008	0.004	-0.002	0.011
3	0.001	0.022	0.039	0.022	0.013	0.015	0.018
4	0.029	0.008	0.022	0.049	0.024	0.015	0.019
5	0.011	0.004	0.013	0.024	0.012	0.009	0.009
6	-0.008	-0.002	0.015	0.015	0.009	0.026	0.005
7	0.011	0.011	0.018	0.019	0.009	0.005	0.012

Table G-11 Matrix $\mathbf{D}_{\mathbf{Y}'}$ for the Sample Problem

0.000	0.000	0.000	0.000	0.000	0.000	0.000
0.000	0.000	0.000	0.000	0.000	0.000	0.000
0.000	0.000	0.000	0.000	0.000	0.000	0.000
0.000	0.000	0.000	0.056	0.000	0.000	0.000
0.000	0.000	0.000	0.000	0.176	0.000	0.000
0.000	0.000	0.000	0.000	0.000	0.222	0.000
0.000	0.000	0.000	0.000	0.000	0.000	0.331

Table G-12 Matrix $\mathbf{D}_{pp}$ for the Sample Problem

0.056	0.000	0.000	0.000
0.000	0.176	0.000	0.000
0.000	0.000	0.222	0.000
0.000	0.000	0.000	0.331

Table G-13 Matrix $\mathbf{L}_{Y'}$ for the Sample Problem

0.215	-0.154	0.034	-0.577	0.180	-0.667	0.345
-0.152	-0.267	-0.696	0.002	0.560	0.241	0.223
0.485	0.118	0.414	-0.081	0.294	0.532	0.450
0.072	0.402	-0.278	0.472	-0.281	-0.242	0.629
-0.135	-0.808	0.287	0.346	-0.178	-0.030	0.308
-0.043	-0.110	-0.278	-0.533	-0.658	0.387	0.207
-0.818	0.254	0.327	-0.188	0.157	0.058	0.309

Table G-14 Matrix $\mathbf{L}_{np}$ for the Sample Problem

-0.577	0.180	-0.667	0.345
0.002	0.560	0.241	0.223
-0.081	0.294	0.532	0.450
0.472	-0.281	-0.242	0.629
0.346	-0.178	-0.030	0.308
-0.533	-0.658	0.387	0.207
-0.188	0.157	0.058	0.309

Given matrices $\mathbf{D}_{pp}$, $\mathbf{L}_{np}$, and $\mathbf{M}_{Y'}$, Eq. G-1 is used to generate realizations based on the five analyses. In this process $\mathbf{U}$ is a 4×1 vector of uncorrelated standard normal random variables, with a mean of $\mathbf{0}$ and a covariance matrix of $\mathbf{I}$. The fact that only a vector of 4 random numbers are used to draw a vector of seven demand parameters for one realization vector shows how insufficient observed data affects drawing realizations. By repeating this exercise 9999 times, 10000 realizations are generated as per (G-1) to create the 7×10000 matrix $\mathbf{Z}$. Finally, the exponential of $\mathbf{Z}$ is obtained as $\mathbf{W}$. Table G-15 presents the first 10 simulations of $\mathbf{W}$.

Tables G-16 and G-17 presents ratios of mean simulated response to mean response-history response, and ratios of the simulated to response-history

covariance matrix elements. The data of Tables G-16 and G-17 indicate that the *simulated* vectors of demand have similar underlying statistics as those of the *original* demand vectors, however, with less precision then when a larger number of analyses were performed, as in the first example, where $m = 11$.

Table G-15 Matrix of Simulated Demand Parameters (first 10 vectors of 10000)

	δ_1 (%)	δ_2 (%)	δ_3 (%)	a_1 (g)	a_2 (g)	a_3 (g)	a_r (g)
1	1.122	1.751	2.185	0.582	0.926	0.845	0.703
2	0.981	1.979	2.578	0.478	0.849	0.907	0.727
3	1.409	1.798	2.106	0.590	0.903	0.778	0.734
4	1.024	2.147	3.374	0.694	1.043	1.119	0.839
5	1.287	1.661	2.169	0.590	0.915	0.988	0.729
6	1.808	2.159	2.812	0.726	0.982	0.878	0.897
7	1.190	1.668	1.855	0.490	0.832	0.744	0.660
8	1.014	1.790	2.505	0.530	0.895	1.069	0.728
9	1.092	1.748	1.928	0.427	0.781	0.737	0.653
10	0.890	2.006	2.745	0.479	0.863	0.968	0.729

Table G-16 Ratio of Simulated to Original Logarithmic Means

δ_1	δ_2	δ_3	a_1	a_2	a_3	a_r
1.003	1.000	0.999	1.001	1.003	1.005	1.001

Table G-17 Ratio Of Entries in Simulated and Original $\Sigma_{Y'Y'}$ Matrices

1.001	0.925	0.662	0.991	0.986	1.013	0.983
0.925	0.982	0.981	0.958	0.964	0.980	0.976
0.662	0.981	0.977	0.956	0.961	0.964	0.970
0.991	0.958	0.956	0.979	0.976	0.942	0.972
0.986	0.964	0.961	0.976	0.975	0.951	0.970
1.013	0.980	0.964	0.942	0.951	0.967	0.944
0.983	0.976	0.970	0.972	0.970	0.944	0.973

G.2.4 Matlab Code

The Matlab macro below can be used to generate correlated simulated vectors of demand parameters. The vectors of demand parameters established by response-history analysis, EDP.txt file, should have the same construction

as Table G-1, that is, one demand parameter per column, one analysis per row. The file beta.txt includes a $2 \times n$ matrix where the values in the two rows are for β_m and β_{gm}, respectively, and those in each column are for each demand parameter.

For intensity- and time-based assessments and for scenario-based assessments the user should input dispersions for analysis and modeling for each demand parameter and set the dispersion for ground motion equal to zero. For scenario-based assessment using the procedures of Chapter 5, the user should input for dispersions for analysis, modeling and ground motion for each demand parameter.

Example Matlab Code:

```
% Develop underlying statistics of the response-history analysis
clear;
num_realization = 10000;

% loading information: EDP, epistemic variability,
EDPs =load('EDP.txt');
B=load('beta.txt');%matrix for dispersions βm and βgm ,

% taking natural logarithm of the EDPs. Calling it lnEDPs
lnEDPs=log(EDPs);     % Table G-2, or Table G-9
[num_rec num_var]=size(lnEDPs);

% finding the mean matrix of lnEDPs. Calling it lnEDPs_mean
 lnEDPs_mean=mean(lnEDPs); % last row in Table G-2, or Table G-9
 lnEDPs_mean=lnEDPs_mean';

% finding the covariance matrix of lnEDPs. Calling it lnEDPs_cov
 lnEDPs_cov=cov(lnEDPs); % Table G-3, or Table G-10

% finding the rank of covariance matrix of lnEDPs. Calling it
% lnEDPs_cov_rank
 lnEDPs_cov_rank=rank(lnEDPs_cov);

 % inflating the variances with epistemic variability
sigma = sqrt(diag(lnEDPs_cov)); % sqrt first to avoid under/overflow
 R = lnEDPs_cov ./ (sigma*sigma');
B=B';
sigma=sigma+(B(:,1).* B(:,1)); % Inflating variance for βm
sigma=sigma+(B(:,2).* B(:,2)); % Inflating variance for βgm
sigma2=sigma*sigma';
 lnEDPs_cov_inflated=R.*sigma2;
```

```
% finding the eigenvalues eigenvectors of the covariance matrix. Calling
% them D2_total and L_total
[L_total D2_total]=eig(lnEDPs_cov_inflated);  % Table G-5, Table G-13
 D2_total=eig(lnEDPs_cov_inflated);

% Partition L_total to L_use. L_use is the part of eigenvector matrix
% L_total that corresponds to positive eigenvalues
 if lnEDPs_cov_rank >= num_var
    L_use =L_total; % Table G-5
else
    L_use =(L_total(:,num_var- lnEDPs_cov_rank+1:num_var)); %Table G-13
end
% Partition the D2_total to D2_use. D2_use is the part of eigenvalue
%vector D2_total that corresponds to positive eigenvalues
if lnEDPs_cov_rank >= num_var
   D2_use =D2_total;
else
   D2_use =D2_total(num_var- lnEDPs_cov_rank+1:num_var);
end

% Find the square root of D2_use and call is D_use.
 D_use =diag((D2_use).^0.5); %Table G-4, or Table G-12

% Generate Standard random numbers
if lnEDPs_cov_rank >= num_var
    U = randn(num_realization,num_var) ;
else
    U = randn(num_realization, lnEDPs_cov_rank) ;
end
U = U' ;

% Create Lambda = D_use . L_use
Lambda = L_use * D_use ;

% Create realizations matrix
Z = Lambda * U + lnEDPs_mean * ones(1,num_realization) ;

lnEDPs_sim_mean=mean(Z');
lnEDPs_sim_cov=cov(Z');

A=lnEDPs_sim_mean./lnEDPs_mean'; %Table G-7, or Table G-16
B=lnEDPs_sim_cov./lnEDPs_cov; %Table G-8, or Table G-17

W=exp(Z);

%end
```

G.3 Simplified Analysis

When the simplified analysis procedure is used, only a single analysis is performed for each intensity level or scenario. The results of this analysis are transformed into estimated median demands, which are then associated with a judgmentally determined dispersion for use in simulated demand generation.

For assessment using the simplified method of analysis PACT internally generates a set of N statistically consistent demand vectors, given the single column vector of demand parameters, $\{\theta\}$ and a value of the dispersion, β, using the following two-step procedure: 1) randomly generate N values of z, where z is normally distributed with a mean of 0 and a standard deviation of 1.0; and 2) compute $\{\theta\}\exp(z\beta)$ for each value of z. Each vector computed using step 2 is used to generate one value of loss.

Appendix H
Fragility Development

H.1 Introduction

H.1.1 Purpose

This appendix provides guidelines for development of building component fragility functions. It may be used for either structural or nonstructural components, elements or systems.

H.1.2 Fragility Function Definition

Fragility functions are probability distributions used to indicate the probability that a component, element or system will be damaged to a given or more severe damage state as a function of a single predictive demand parameter such as story drift or floor acceleration. Here, fragility functions take the form of lognormal cumulative distribution functions, having a median value θ and logarithmic standard deviation, or dispersion, β. The mathematical form for such a fragility function is:

$$F_i(D) = \Phi\left(\frac{\ln\left(D/\theta_i\right)}{\beta_i}\right) \quad \text{(H-1)}$$

where: $F_i(D)$ is the conditional probability that the component will be damaged to damage state "i" or a more severe damage state as a function of a demand parameter, D; Φ denotes the standard normal (Gaussian) cumulative distribution function, θ_i denotes the median value of the probability distribution, and β_i denotes the logarithmic standard deviation. Both θ and β are established for each component type and damage state using one of the methods presented in Section H.2.

For sequential damage states, as described in Chapter 3, the conditional probability that a component will be damaged to damage state "i" and not to a more or less severe state, given that it experiences demand, D is given by:

$$P\left[i\middle|D\right] = F_{i+1}\left(D\right) - F_i\left(D\right) \quad \text{(H-2)}$$

where $F_{i+1}(D)$ is the conditional probability that the component will be damaged to damage state "i+1" or a more severe state and $F_i(D)$ is as previously defined. Note that, when β_{i+1} is greater than β_i, Equation H-2 can

produce a meaningless negative probability at some levels of *D*. Section H.3.4 addresses this case.

Figure H-1 (a) shows the form of a typical lognormal fragility function when plotted in the form of a cumulative distribution function and (b) the calculation of the probability that a component will be in damage state "i" at a particular level of demand, *d*.

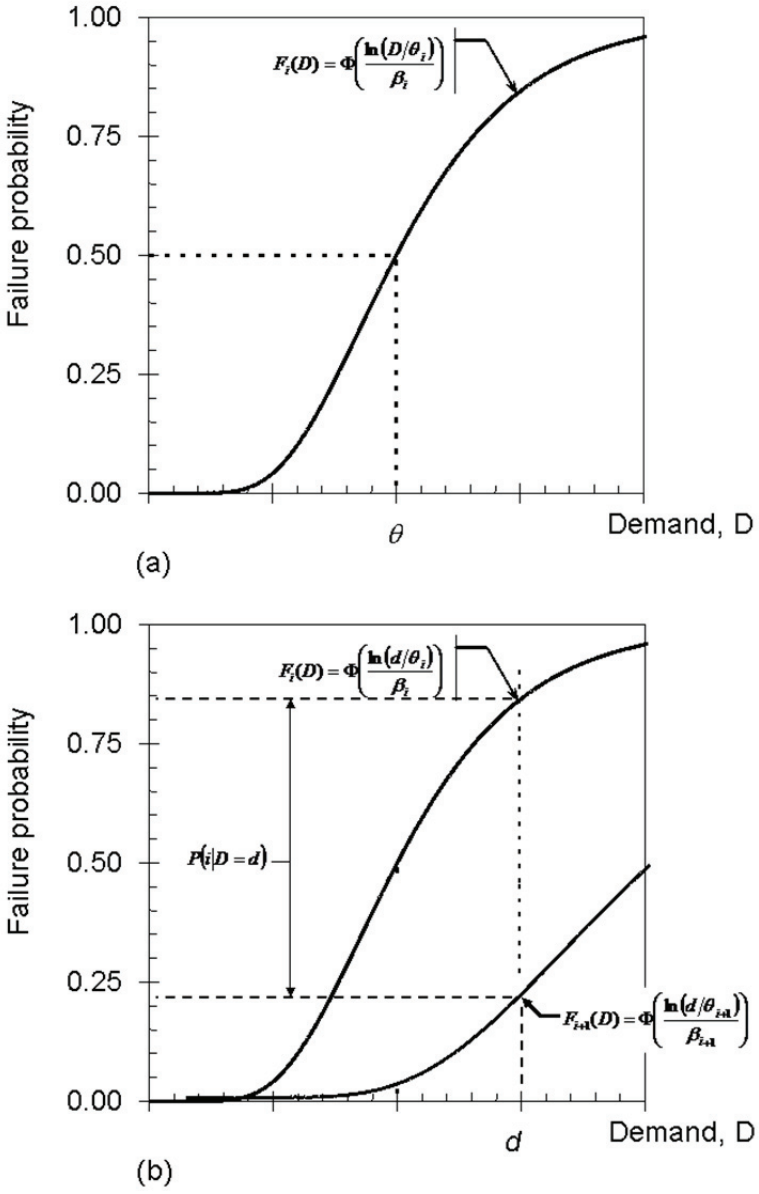

Figure H-1 Illustration of (a) fragility function, and (b) evaluating individual damage-state probabilities.

The dispersion, β, represents uncertainty in the actual value of demand, *D*, at which a damage state is likely to initiate in a component . This uncertainty is a result of variability in the quality of construction and installation of the

components in the building, as well as variability in the loading history that the component may experience before it fails. When fragility parameters are determined on the basis of a limited set of test data, two components of the dispersion should be considered. The first of these, termed herein β_r, represents the random variability that is observed in the available test data from which the fragility parameters are determined. The second portion, β_u, represents uncertainty that the tests represent the actual conditions of installation and loading that a real component in a building will experience, or that the available test data is an inadequate sample to accurately represent the true random variability. The dispersion parameter β, is computed as:

$$\beta = \sqrt{\beta_r^2 + \beta_u^2} \quad \text{(H-3)}$$

The following minimum values of the uncertainty parameter β_u are recommended:

A minimum value of 0.25 should be used if any of the following apply:

- Test data are available for five (5) or fewer specimens
- In an actual building, the component can be installed in a number of different configurations, however, all specimens tested had the same configuration.
- All specimens were subjected to the same loading protocol
- Actual behavior of the component is expected to be dependent on two or more demand parameters, e.g. simultaneous drift in two orthogonal directions, however, specimens were loaded with only one of these parameters.

If none of the above conditions apply, a value of β_u of 0.10 may be used.

H.1.3 Derivation Methods

Fragility functions can best be derived when there is a large quantity of appropriate test data available on the behavior of the component of interest at varying levels of demand. *FEMA 461* provides recommended protocols for performing such tests and recording the data obtained. Since testing is expensive and time consuming, there is not a great body of test data presently available to serve as the basis for determining fragility functions for many building components. Therefore, these guidelines provide procedures for developing the median (θ) and dispersion (β) values for a fragility under five different conditions of data. These are:

a. Actual Demand Data: When test data is available from *m* individual specimen tests and each tested component actually experienced the damage state of interest at a known value of demand, *D*.

b. Bounding Demand Data: When test data or earthquake experience data are available from *m* individual specimen tests, however, the damage state of interest only occurred in some specimens. For the other specimens, testing was terminated before the damage state occurred or the test did not damage the specimens. The value of the maximum demand, D_i, to which each specimen was subjected is known for each specimen. This maximum demand need not necessarily be the demand at which the damage state initiated.

c. Capable Demand Data: When test data or earthquake experience data are available from *m* specimen tests, however, the damage state of interest did not occur in any of the specimens. The maximum value of demand, D_i, to which each specimen was subjected is known.

d. Derivation (analysis): When no test data are available, however, it is possible to model the behavior and estimate the level of demand at which the damage state of interest will occur.

e. Expert Opinion: When no data are available and analysis of the behavior is not feasible, however, one or more knowledgeable individuals can offer an opinion as to the level of demand at which damage is likely to occur, based either on experience or judgment.

In addition, a procedure is presented for updating existing fragility functions as more data become available, for example from additional testing. Section C2.6 provides this guidance.

H.1.4 Documentation

Each fragility function should be accompanied by documentation of the sources of data and procedures used to establish the fragility parameters in sufficient detail that others may evaluate the adequacy of the process and findings. As a minimum, it is recommended that the documentation include the following:

1. *Description of applicability.* Describe the type of component that the fragility function addresses including any limitations on the type of installation to which the fragility applies.

2. *Description of specimens*. Describe the specimens used to establish the fragility including identifying the number of specimens examined, their

locations, and the specific details of the specimen fabrication/construction, mounting and installation.

3. *Demands and Load Application*. Detail the loading protocol or characteristics of earthquake motion applied to each specimen. Identify the demand parameters examined that might be most closely related to failure probability and define how demand is calculated or inferred from the loading protocol or excitation. Indicate whether the reported demand quantities are the value at which damage occurred (Method A data) or the maximum to which each specimen was subjected.

4. *Damage state.* Fully describe each damage state for which fragilities are developed including the kinds of physical damage observed and any force-deformation quantities recorded. Define damage states quantitatively in terms of the repairs required or potential downtime or casualty consequences.

5. *Observation summary, analysis method, and results.* Present a tabular or graphical listing of specimens, demand parameters, and damage states. Identify the method(s) used to derive the fragility parameters per Section H.2 of this Appendix. Present resulting fragility function parameters θ and β and results of tests to establish fragility function quality (discussed below). Provide sample calculations.

H.2 Fragility Parameter Derivation

H.2.1 Actual Demand Data

When data is available from a suitable series of tests and for each tested specimen, the damage state of interest was initiated at a known value of the demand, d_i, the median value of the demand at which the damage state is likely to initiate, θ, is given by the equation:

$$\theta = e^{\left(\frac{1}{M}\sum_{i=1}^{M}\ln d_i\right)} \tag{H-4}$$

where:

M = total number of specimens tested

d_i = demand in test "i" at which the damage state was first observed to occur.

The value of the random dispersion, β_r, is given by:

$$\beta_r = \sqrt{\left(\frac{1}{M-1}\sum_{i=1}^{M}\left(\ln\left(d_i/\theta\right)\right)^2\right)^2} \tag{H-5}$$

where M, d_i and θ are as defined above.

If one or more of the d_i values appear to lie far from the bulk of the data, either above or below, apply the procedure specified in Section H3.2. Finally, test the resulting fragility parameters using the Lilliefors goodness-of-fit test (Section H3.3). If it passes at the 5% significance level, the fragility function may be deemed acceptable.

Example: Determine the parameters θ and β, from a series of 10 tests, all of which produced the damage state of interest. Demands at which the damage state initiated are respectively story drifts of: 0.9, 0.9, 1.0, 1.1, 1.1, 1.2, 1.3, 1.4, 1.7, and 2 percent.

Test #	Demand di	ln(di)	ln(di/θi)	ln(di/θi)^2
1	0.9	-0.10536	-0.30384	0.092321
2	0.9	-0.10536	-0.30384	0.092321
3	1	0	-0.19848	0.039396
4	1.1	0.09531	-0.10317	0.010645
5	1.1	0.09531	-0.10317	0.010645
6	1.2	0.182322	-0.01616	0.000261
7	1.3	0.262364	0.063881	0.004081
8	1.4	0.336472	0.137989	0.019041
9	1.7	0.530628	0.332145	0.11032
10	2	0.693147	0.494664	0.244692
Σ		1.984833		0.623723

$$\theta = e^{\left(\frac{1}{M}\sum_{i=1}^{M}\ln d_i\right)} = e^{\left(\frac{1}{10}(1.9848)\right)} = 1.22$$

$$\beta_r = \sqrt{\frac{1}{M-1}\sum_{i=1}^{M}\left(\ln\left(d_i/\theta\right)\right)^2} = \sqrt{\frac{1}{(10-1)}(0.6237)} = 0.26$$

H.2.2 Bounding Demand Data

When data are available from a suitable series of specimen; however, the damage state of interest was initiated in only some of the specimens, the procedures of this section can be used to derive fragility parameters. For each specimen "i", it is necessary to know the maximum value of the demand, d_i to which the specimen was subjected, and whether or not the damage state of interest occurred in the specimen.

Divide the data into a series of N bins. It is suggested, but not essential, that N be taken as the largest integer that is less than or equal to the square root of M, where M is the total number of specimens available, as this will usually result in an appropriate number of approximately equally sized sets.

In order to divide the specimens into the several bins, sort the specimen data in order of ascending maximum demand value, d_i, for each test, then divide

the list into N groups of approximately equal size. Each group "j" will have M_j specimens, where:

$$\sum_{i=1}^{N} M_j = M \tag{H-6}$$

Next, determine the average value of the maximum demand for each bin of specimens:

$$\overline{d}_j = \frac{1}{M_j}\sum_{k=1}^{M_j} d_k \tag{H-7}$$

and x_j, the natural logarithm of d_j (i.e., $\ln(d_j)$). Also determine the number of specimens within each bin, m_j, in which the damage state of interest was achieved and the inverse standard normal distribution, y_j, of the failed fraction specimens in the bin:

$$y_j = \Phi^{-1}\left(\frac{m_j + 1}{M_j + 1}\right) \tag{H-8}$$

That is, determine the number of standard deviations, above the mean that the stated fraction lies, assuming a mean value, μ=0 and a standard deviation, σ=1. This can be determined using the "normsinv" function on a Microsoft Excel spreadsheet or by referring to standard tables of the normal distribution. Next, fit a straight line to the data points, x_j, y_j, using a least-squares approach. The straight line will have the form:

$$y = bx + c \tag{H-9}$$

where, b is the slope of the line and c is the y intercept. The slope b is given by:

$$b = \frac{\sum_{i=1}^{M}\left(x_j - \overline{x}\right)\left(y_j - \overline{y}\right)}{\sum_{i=1}^{M}\left(x_j - \overline{x}\right)^2} \tag{H-10}$$

$$\overline{x} = \frac{1}{M}\sum_{j=1}^{M} x_j \tag{H-11}$$

$$\overline{y} = \frac{1}{M}\sum_{j=1}^{M} y_j \tag{H-12}$$

Determine the value of the random dispersion, β_r as:

$$\beta_r = \frac{1}{b} = \frac{\sum_{i=1}^{M}\left(x_j - \bar{x}\right)}{\sum_{i=1}^{M}\left(x_j - \bar{x}\right)\left(y_j - \bar{y}\right)} \tag{H-13}$$

The value of the median, θ, is taken as:

$$\theta = e^{-c\beta_r} = e^{\left(\bar{x} - \bar{y}\beta_r\right)} \tag{H-14}$$

Example: Consider the damage statistics shown in the figure below. The figure depicts the hypothetical performance of motor control centers (MCCs) observed after various earthquakes in 45 facilities. Each box represents one specimen. Several damage states are represented. Crosshatched boxes represent MCCs that experienced a noticeable earthquake effect such as shifting but that remained operable. Black boxes represent those that were found to be inoperable following the earthquake. Each stack of boxes represents one facility. Calculate the fragility function using *PGA* as the demand parameter, binning between halfway points between *PGA* values shown in the figure.

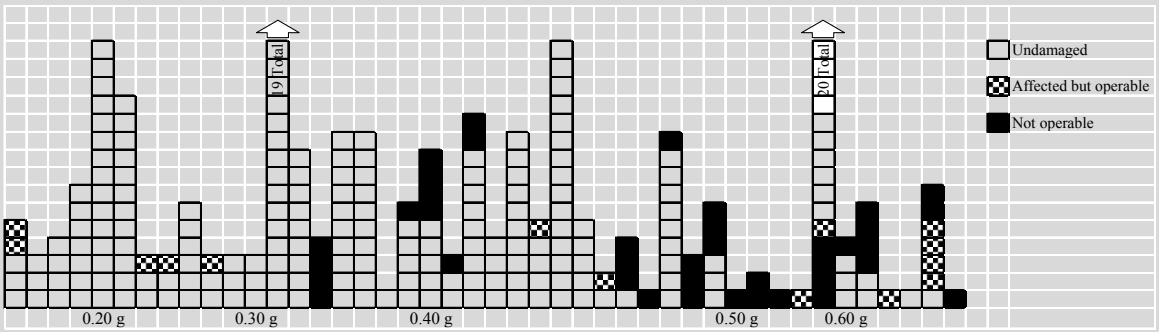

Hypothetical observed earthquake damage data for motor control centers

The number of bins, *N*, and the lower demand bounds a_j, are dictated by the available data: *N* is taken as 5 with lower bounds, a_j of 0.15g, 0.25g, 0.35g, 0.45g, and 0.55g respectively. The damage state of interest is loss of post-earthquake functionality (black boxes in figure). The values of M_j and m_j are found by counting all boxes and black boxes, respectively, in the figure in each bin, and are shown in the table below. The value of *M* is found by summing: $M = \Sigma M_j = 260$. Values x_j and y_j are calculated as $x_j = \ln(\bar{r}_i)$, and $y_j = \Phi^{-1}((m_j+1)/(M_j+1))$. Average values are calculated as shown: $\bar{x} = -0.99$, $\bar{y} = -1.05$, according to Equations H-11 and H-12. For each bin, the values of $x_i - \bar{x}$ and $y_i - \bar{y}$ are calculated as shown.

Table of Example Solution Data

j	$a_j(g)$	$\overline{r}_j(g)$	M_j	m_j	x_j	y_j	$x_j-\overline{x}$	$y_j-\overline{y}$	$(x_j-\overline{x})^2$	$(x_j-\overline{x})(y_j-\overline{y})$
1	0.15	0.2	52	0	-1.61	-2.08	-0.623	-1.031	0.388	0.642
2	0.25	0.3	48	4	-1.20	-1.27	-0.217	-0.223	0.047	0.049
3	0.35	0.4	84	8	-0.92	-1.25	0.070	-0.202	0.005	-0.014
4	0.45	0.5	35	15	-0.69	-0.14	0.294	0.907	0.086	0.266
5	0.55	0.6	41	12	-0.51	-0.50	0.476	0.549	0.226	0.261
$\sum=$			**260**		**-4.93**	**-5.23**			**0.753**	**1.204**
		Average=			-0.99	-1.05				

Then, β and θ are calculated as:

$$\beta_r = \frac{\sum_{j=1}^{N}\left(x_j-\overline{x}\right)^2}{\left(x_j-\overline{x}\right)\left(y_j-\overline{y}\right)} = \frac{0.753}{1.204} = 0.63$$

$$\theta = e^{\left(\overline{x}-\overline{y}\beta_r\right)} = e^{\left(-0.99+1.05(0.63)\right)} = e^{(-0.329)} = 0.72g$$

H.2.3 Capable Demand Data

When data is available from a suitable series of specimen tests, however, the damage state of interest was not initiated in any of the specimens the procedures of this section may be used to estimate fragility functions. For each available specimen, "*i*," the maximum demand "d_i" at which the specimen was loaded, , and whether or not the specimen experienced any distress or damage must be known.

From the data for the *M* specimen tests, determine the maximum demand experienced by each specimen, d_{max}, and the minimum demand for any of the specimens that exhibited any distress or damage, d_{min}. Determine d_a as the smaller of d_{min} or $0.7d_{max}$. Determine M_A as the number of specimens that did not exhibit distress or damage, but that were loaded with demands, $d_i \geq d_a$; M_B as the number of specimens that exhibited distress or damage, but which did not appear to be initiating or on the verge of initiating the damage state of interest; and M_C as the number of specimens appeared to be on the verge of initiating the damage state of interest.

If none of the specimens in any of the tests exhibited any sign of distress or damage, take the value of d_m as d_{max}. If one or more of the specimens exhibited distress or damage of some type, take d_m as:

$$d_m = \frac{d_{\max} + d_a}{2} \tag{H-15}$$

Determine the subjective failure probability S at d_m as:

$$S = \frac{0.5M_C + 0.1M_B}{M_A + M_B + M_C} \tag{H-16}$$

Take the logarithmic standard deviation, β, as having a value of 0.4. Determine the median, θ, as:

$$\theta = d_m e^{-0.4z} \tag{H-17}$$

where, z is determined from Table H-1 based on the value of M_A and S.

Table H-1 Values of z

Conditions	*Z*
$M_A \geq 3$ and $S = 0$	-2.326
$M_A < 3$ and $S \leq 0.075$	-1.645
$0.075 < S \leq 0.15$	-1.282
$0.15 < S \leq 0.3$	-0.842
$S > 0.3$	-0.253

Example: Determine the parameters θ and β, from tests of 10 specimens. Five of the specimens had maximum imposed drift demands of 1% with no observable signs of distress. Three of the specimens had maximum imposed drift demands of 1.5% and exhibited minor distress, but did not appear to be at or near the initiation of the damage state of interest. Two of the specimens had maximum imposed drift demands of 2%, did not enter the damage state of interest during the test, but appeared to be about to sustain such damage. From the given data determine: $d_{max} = 2\%$, $d_{min} = 1.5\%$. d_a is the smaller of $0.7d_{max}$ or d_{min} and therefore, is $0.7(2\%) = 1.4\%$. $M_A = 0$, M_B=3, and M_C=2.

$$d_m = \frac{d_{\max} + d_a}{2} = \frac{2\% + 1.4\%}{2} = 1.7\%$$

$$S = \frac{0.5M_C + 0.1M_B}{M_A + M_B + M_C} = \frac{0.5(2) + 0.1(3)}{0 + 3 + 2} = 0.26$$

From Table 2-1, z is taken as -0.842. Therefore,

$$\theta = d_m e^{-0.4z} = 1.7\% e^{-0.4(-0.842)} = 2.4\%$$

and β is taken as 0.4.

H.2.4 Derivation

There are two methods available for analytical derivation of fragility parameters. The first of these uses a single calculation of the probable capacity and a default value of the logarithmic standard deviation. The second method uses Monte Carlo analysis to explore the effect of variation in material strength, construction quality and other random variables.

Single calculation

Calculate the capacity of the component, Q in terms of a demand parameter, d, using average material properties and dimensions and estimates of workmanship. Resistance factors should be taken as unity and any conservative bias in code equations, if such equations are used, should be removed. The logarithmic standard deviation, β, is taken as having a value of 0.4. The median capacity θ is taken as:

$$\theta = 0.92Q \qquad \text{(H-18)}$$

Monte Carlo simulation

Identify all those factors, important to predicting the capacity that are uncertain including material strength, cross section dimensions, member straightness, workmanship. Estimate a median value and dispersion for each of these random variables. Conduct sufficient analyses, randomly selecting the values of each of these random variables in accordance with their estimated distribution properties, each time calculating the capacity. Determine the median value of the capacity as that capacity exceeded in 50% of the calculations. Determine the random logarithmic standard deviation, β_r, as the standard deviation of the natural logarithm of the calculated capacity values. Use equation 1-3 to determine the total logarithmic standard deviation, β, assuming a value of β_u of 0.25.

H.2.5 Expert Opinion

Select one or more experts with professional experience in the design or post-earthquake damage observation of the component of interest. Solicit their advice using the format shown in Figure H-2. Note the suggested inclusion of representative images, which should be recorded with the responses. If an expert refuses to provide estimates or limits them to certain conditions, either narrow the component definition accordingly and iterate, or ignore that expert's response and analyze the remaining ones.

Calculate the median value, θ, as:

$$\theta = \frac{\sum_{i=1}^{N} w_i^{1.5} \theta_i}{\sum_{i=1}^{N} w_i^{1.5}} \tag{H-19}$$

where, N is the number of experts providing an opinion; θ_i is expert "i's" opinion as to the median value, and w_i is expert "i's" level of expertise, on a 1-5 scale.

Calculate the lower bound value for the capacity as:

$$d_l = \frac{\sum_{i=1}^{N} w_i^{1.5} d_{li}}{\sum_{i=1}^{N} w_i^{1.5}} \tag{H-20}$$

where, d_{li} is expert "i's" opinion as to the lower bound value and other terms are as previously defined. The value of the logarithmic standard deviation, β, is taken as:

$$\beta = \frac{\ln(\theta / d_l)}{1.28} \tag{H-21}$$

If this calculation produces an estimate of β that is less than 0.4, either justify the β, or take β as having a value of 0.4 and recalculate θ as:

$$\theta = 1.67 d_l \tag{H-22}$$

H.2.6 Updating

This section addresses procedures for re-evaluating fragility parameters for a building component as additional data become available. The pre-existing and updated fragility parameters are respectively termed θ, β, θ', and β'. The additional data are assumed to be a set of M specimens with known maximum demand and damage states. It is not necessary that any of the specimens experienced damage.

Calculate the revised median, θ' and logarithmic standard deviation β' as follows:

$$\theta' = e^{\sum_{j=1}^{5} w'_j \ln(d_j)} \tag{H-23}$$

$$\beta' = \sum_{j=1}^{5} w'_j \beta_j \tag{H-24}$$

Example Form for Expert Opinion:

Objective. This form solicits your judgment about the values of a demand parameter (*D*) at which a particular damage state occurs to a particular building component. Judgment is needed because the component may contribute significantly to the future earthquake repair cost, fatality risk, or post-earthquake operability of a building, and because relevant empirical and analytical data are currently impractical to acquire. Your judgment is solicited because you have professional experience in the design or post-earthquake damage observation of the component of interest.

Definitions. Please provide judgment on the damageability of the following component and damage state. Images of a representative sample of the component and damage state may be attached. It is recognized that other demand parameters may correlate better with damage, but please consider only the one specified here.

Component name: _____
Component definition:_____
Damage state name: _____
Damage state definition: ___
_____
Relevant Demand Parameter_
Definition of *Demand Parameter*_____
_____

Uncertainty; no personal stake. Please provide judgment about this general class of components, not any particular instance, and not one that you personally designed, constructed, checked, or otherwise have any stake in. There is probably no precise threshold level of demand that causes damage, because of variability in design, construction, installation, inspection, age, maintenance, interaction with nearby components, etc. Even if there were such a precise level, nobody might know it with certainty. To account for these uncertainties, **please provide two values of demand at which damage occurs: median and lower bound.**

Estimated median capacity _____ *Definition*. Damage would occur at this level of demand in 5 cases out of 10, or in a single instance, you judge there to be an equal chance that your median estimate is too low or too high.

Estimated lower-bound capacity _____*Definition*. Damage would occur at this level of demand in 1 case in 10. In a single case, you judge there to be a 10% chance that your estimate is too high. *Judge the lower bound carefully*. Make an initial guess, then imagine all the conditions that might make the actual threshold demand lower, such as errors in design, construction or installation, substantial deterioration, poor maintenance, more interaction with nearby components, etc. Revise accordingly and record your revised estimate. Research shows that without careful thought, expert judgment of the lower bound tends to be too close to the median estimate, so think twice and do not be afraid of showing uncertainty.

On a 1-to-5 scale, please judge your expertise with this component and damage state, where 1 means "no experience or expertise" and 5 means "very familiar or highly experienced."
Your level of expertise:_____

Your name:_____ Date: _____

Figure H-2 Example form for soliciting expert opinion on component fragility.

where:

$$w'_j = \frac{w_j \prod_{i=1}^{M} L(i,j)}{\sum_{j=1}^{5} w_j \prod_{i=1}^{M} L(i,j)} \qquad \text{(H-25)}$$

Π denotes the product of the terms that come after it, and

$L(i,j) = 1 - \Phi\left(\frac{\ln\left(d_i / x_j\right)}{0.707 s \beta_j}\right)$ if specimen "i" did not experience the damage state of interest, and

$L(i,j) = \Phi\left(\frac{\ln\left(d_i / x_j\right)}{0.707 s \beta_j}\right)$ if specimen "i" did experience the damage state of interest, or a more severe state. and

$x_1 = x_4 = x_5 = \theta$

$x_2 = \theta e^{-1.22\beta}$

$x_3 = \theta e^{1.22\beta}$

$\beta_1 = \beta_2 = \beta_3 = \beta$

$\beta_4 = 0.64\beta$

$\beta_5 = 1.36\beta$

$w_1 = 1/3$

$w_2 = w_3 = w_4 = w_5 = 1/6$

H.3 Assessing Fragility Function Quality

The quality of fragility parameters can be assessed using the procedures of this Section.

H.3.1 Competing Demand Parameters

The behavior of some components may be dependent on several types of demands, for example in-plane and out-of-plane drift, or both drift and acceleration. It may not be clear which demand is the best single predictor of component damage. Assuming that data are available to create fragility functions for each possibly relevant demand, do so. Choose the fragility function that has the lowest β.

H.3.2 Dealing with Outliers using Pierce's Criterion

When fragilities are determined on the basis of actual demand data (Section C2.1), it is possible that one or more tests reported spurious values of demand, d_i, and reflect experimental errors rather than the true demands at which the specimens failed. In cases where one or more d_i values in the data set are obvious outliers from the bulk of the data, investigate whether the data reflects real issues in the damage process that may recur, especially where $d_i << \theta$ for these outliers. If there is no indication that these data reflect a real recurring issue in the damage process, apply the following

procedure (Peirce's criterion) to test and eliminate doubtful observations of d_i.

1. Calculate $\ln(\theta)$ and β of the complete data set.
2. Let D denote the number of doubtful observations, and let R denote the maximum distance of an observation from the body of the data, defined as:

$$R = \frac{\left|\ln(d) - \ln\theta\right|}{\beta} \quad \text{(H-26)}$$

where θ, β, and M are as previously defined, d is a measured demand value, and R is as shown above. Assume $D = 1$ first, even if there appears to be more than one doubtful observation.

3. Calculate the maximum allowable deviation: $|\ln(d) - \ln(\theta)|_{max}$. Note that this can include $d >> \theta$ and $d << \theta$.
4. For any suspicious measurement d_i, obtain $|\ln(d_i) - \ln(\theta)|$.
5. Eliminate the suspicious measurements if: $\left|\ln(d_i) - \ln(\theta)\right| > \left|\ln(d) - \ln(\theta)\right|_{max}$
6. If this results in the rejection of one measurement, assume D=2, keeping the original values of θ and β, and go to step 8.
7. If more than one measurement is rejected in the above test, assume the next highest value of doubtful observations. For example, if two measurements are rejected in step 5, assume the case of $D = 3$, keeping the original values of θ, and β, as the process is continued.
8. Repeat steps 2 – 5, sequentially increasing D until no more data measurements are eliminated.
9. Obtain θ and β of the reduced data set as for the original data.

H.3.3 Goodness of Fit Testing

Fragility parameters that are developed based on actual demand data (Section H2.1) should be tested for goodness of fit in accordance with this section. Calculate

$$D = \max_x \left|F_i(d) - S_M(d)\right| \quad \text{(H-27)}$$

where $S_M(d)$ denotes the sample cumulative distribution function

$$S_M(d) = \frac{1}{M}\sum_{i=1}^{M} H\left(d_i - d\right) \quad \text{(H-28)}$$

and H is taken as:

- 1.0 if $d_i - d$ is positive
- ½ if $d_i - d$ is zero
- 0 if $d_i - d$ is negative.

Table H-2 Parameters for Applying Peirce's Criterion

M	*D*=1	*D*=2	*D*=3	*D*=4	*D*=5	*D*=6	*D*=7	*D*=8	*D*=9
3	1.1960								
4	1.3830	1.0780							
5	1.5090	1.2000							
6	1.6100	1.2990	1.0990						
7	1.6930	1.3820	1.1870	1.0220					
8	1.7630	1.4530	1.2610	1.1090					
9	1.8240	1.5150	1.3240	1.1780	1.0450				
10	1.8780	1.5700	1.3800	1.2370	1.1140				
11	1.9250	1.6190	1.4300	1.2890	1.1720	1.0590			
12	1.9690	1.6630	1.4750	1.3360	1.2210	1.1180	1.0090		
13	2.0070	1.7040	1.5160	1.3790	1.2660	1.1670	1.0700		
14	2.0430	1.7410	1.5540	1.4170	1.3070	1.2100	1.1200	1.0260	
15	2.0760	1.7750	1.5890	1.4530	1.3440	1.2490	1.1640	1.0780	
16	2.1060	1.8070	1.6220	1.4860	1.3780	1.2850	1.2020	1.1220	1.0390
17	2.1340	1.8360	1.6520	1.5170	1.4090	1.3180	1.2370	1.1610	1.0840
18	2.1610	1.8640	1.6800	1.5460	1.4380	1.3480	1.2680	1.1950	1.1230
19	2.1850	1.8900	1.7070	1.5730	1.4660	1.3770	1.2980	1.2260	1.1580
20	2.2090	1.9140	1.7320	1.5990	1.4920	1.4040	1.3260	1.2550	1.1900
>20	$a\ln M + b$								
a	0.4094	0.4393	0.4565	0.4680	0.4770	0.4842	0.4905	0.4973	0.5046
b	0.9910	0.6069	0.3725	0.2036	0.0701	-0.0401	-0.1358	-0.2242	-0.3079

If $D > D_{crit}$ from Table H-3, the fragility function fails the goodness of fit test. This result is used in assigning a quality level to the fragility function. Use $\alpha = 0.05$.

Table H-3 Critical Values for the Lilliefors Test

Significance Level	D_{crit}
$\alpha = 0.15$	$0.775 / (M^{0.5} - 0.01 + 0.85M^{-0.5})$
$\alpha = 0.10$	$0.819 / (M^{0.5} - 0.01 + 0.85M^{-0.5})$
$\alpha = 0.05$	$0.895 / (M^{0.5} - 0.01 + 0.85M^{-0.5})$
$\alpha = 0.025$	$0.995 / (M^{0.5} - 0.01 + 0.85M^{-0.5})$

H.3.4 Fragility Functions that Cross

Some components will have two or more possible damage states, with a defined fragility function for each. For any two (cumulative lognormal) fragility functions i and j with medians $\theta_j > \theta_i$ and logarithmic standard deviations $\beta_i \neq \beta_j$, the fragility functions will cross at extreme values. In such a case, adjust the fragility functions by one of the following two methods;

Method 1: adjust the fragility functions such that.

$$F_i(D) = \max_j \left\{ \Phi\left(\frac{\ln(D/\theta_i)}{\beta_i} \right) \right\} \quad \text{for all } j \geq i \tag{H-29}$$

This has the effect that for the damage state with the higher median value, the probability of failure, $F_i(D)$ is never taken as less than the probability of failure for a damage state with a lower median value.

Method 2: First establish θ and β values for the various damage states independently. Next calculate the average of the dispersion values for each of the damage states with crossing fragility curves as:

$$\beta_i' = \frac{1}{N} \sum_{i=1}^{N} \beta_i \tag{H-30}$$

This average logarithmic standard deviation is used as a replacement for the independently calculated values. An adjusted median value must be calculated for each of the crossing fragilities as:

$$\theta_i' = e^{\left(1.28(\beta' - \beta_i) + \ln \theta_i\right)} \tag{H-31}$$

H.3.5 Assigning a Single Quality Level to a Fragility Function

Assign each fragility function a quality level of high, medium, or low, as shown in Table H-4.

Table H-4 Fragility Function Quality Level

Quality	Method	Peer reviewed*	Number of specimens	Other
High	A	Yes	≥ 5	Passes Lilliefors test at 5% significance level. Examine and justify (a) differences of greater than 20% in θ or β, compared with past estimates, and (b) any case of $\beta < 0.2$ or $\beta > 0.6$.
	B	Yes	≥ 20	Examine and justify (a) differences of greater than 20% in θ or β, compared with past estimates, and (b) any case of $\beta < 0.2$ or $\beta > 0.6$.
	U	Yes	≥ 6	Prior was at least moderate quality
Moderate	A		≥ 3	Examine and justify any case of $\beta < 0.2$ or $\beta > 0.6$.
	B		≥ 16	Examine and justify any case of $\beta < 0.2$ or $\beta > 0.6$.
	C	Yes	≥ 6	
	D	Yes		
	E	Yes		At least 3 experts with $w \geq 3$
	U		≥ 6	or prior was moderate quality
Low				All other cases

* Data and derivation published in a peer-reviewed archival journal.

Appendix I
Rugged Components

I.1 Rugged Components

Rugged components are components that are not subject to shaking-induced damage, or have very high thresholds for damage. High thresholds for damage include shaking intensities that are not likely to be encountered in typical structures. Since rugged components are not directly damaged by earthquake shaking, they are not explicitly included in the building performance model. Estimates of building replacement cost and replacement time, however, must consider the presence of rugged components. If a fragility specification associated with a component is omitted from a building performance model, it has the same effect as considering that component rugged for the purposes of that assessment.

Table I-1 provides a list of structural and nonstructural components identified as rugged. This list was developed based on post-earthquake investigations and laboratory testing. The table is organized by general system description and classification number, which is the same classification system used for fragility specifications.

If items identified in Table I-1 are determined to be vulnerable to damage (i.e., not rugged) in the case of a particular building or assessment, user-defined fragilities must be developed to assess their impact on performance.

Table I-1 List of Rugged Components

General System Description	NISTIR Classification Number	Component Description
Foundations	A10	Spread footings, mat foundations, grade beams
Basement Construction	A20	Basement walls and slabs
Floor Construction	B101	Gravity-framed components of floor systems that do not participate in lateral-resistance. This includes most floor framing and sheathing other than concrete slab-column frames
Roof Construction	B102	Gravity-framed components of roof systems that do not participate in lateral-resistance. This includes most roof framing other than concrete slab-column frames. This also includes most diaphragm sheathing.
Structural Steel	B103	Simple beam framing
Reinforced Concrete	B104	Floor and roof framing other than slab-column frames and beam-column frames
Cold-Formed Steel	B106	Horizontal floor and roof framing.
Light-framed Wood	B107	Horizontal floor and roof framing.
Roof Coverings	B301	Composite and built-up roofing systems other than tile roofing on sloped surfaces, including flashing and insulation.
Roof Openings	B302	Roof hatches and skylights
Floor Finishes	C302	Floor finishes, including carpeting, except when water leaks occur
Plumbing Fixtures	D201	Toilets, sinks, tubs, urinals
Rain Water Drainage	D204	Rain water leaders and gutters
Electrical Distribution Systems	D304	Conduits and raceways
Standpipes	D402	Wet and dry standpipes
Other Fire Protection Systems	D409	Smoke detectors, heat detectors, and alarm control systems
Lighting & Branch Wiring	D502	Lighting panels and wiring
Communications and Security	D503	Communications and security equipment
Commercial Equipment	E101	Commercial equipment

Appendix J
Collapse Fragility Development Using Incremental Dynamic Analysis

J.1 Introduction

This appendix describes the use of Incremental Dynamic Analysis for collapse fragility development. FEMA P-695, *Quantification of Building Seismic Performance Factors* (FEMA, 2009b), provides additional information on the Incremental Dynamic Analysis technique.

J.2 Basic Procedure

The basic steps in the procedure are:

1. Construct a mathematical model to represent the structure. Three-dimensional models are recommended.
2. Select an appropriate suite of ground motion pairs that represent scenario events likely to result in collapse of the structure, considering the site seismic hazard
3. Scale the ground motion suite such that the geomean spectral acceleration at the structure's effective first mode period $S_a\left(\overline{T}\right)$ for each pair is at a value where inelastic response is negligible.
4. Analyze the mathematical for each scaled ground motion pair and determine the maximum value of story drift.
5. Increment the intensity of the effective first mode spectral response acceleration, $S_a\left(\overline{T}\right)$, to which each ground motion pair is scaled.
6. Analyze the structure for each incrementally scaled ground motion pair and record the maximum value of story drift.
7. Repeat steps 5, and 6 above for each ground motion pair until analysis using the pair either:
    a. Produces a very large increase in drift for a small increment in the value of intensity, indicating the onset of instability
    b. Results in numerical instability suggesting collapse

c. Results in predicted demands on gravity load bearing elements that exceed their reliable gravity load carrying capacities

d. Predicts drift that exceeds the range of modeling validity.

8. Determine the value of spectral acceleration, $S_a\left(\overline{T}\right)$ at which 50% of the ground motion pairs produce predictions of collapse. This value of $S_a(\overline{T})$ is taken as the median collapse capacity $\hat{S}_a\left(\overline{T}\right)$.

9. Determine a dispersion for the collapse fragility

Figure J-1 illustrates this process.

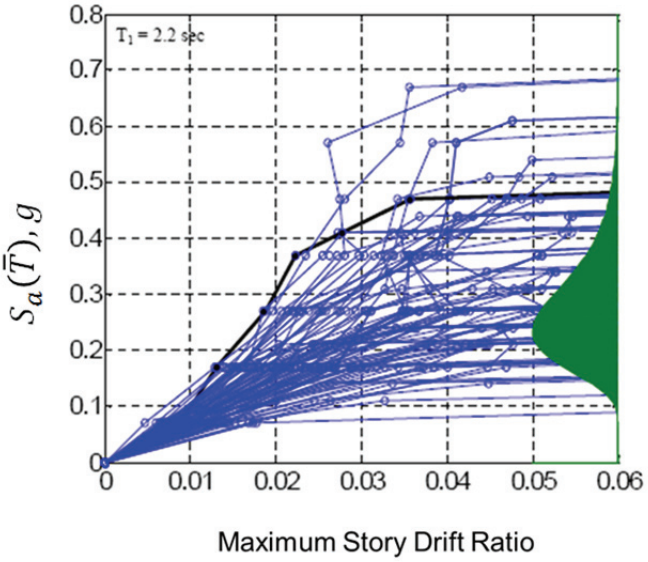

Figure J-1 Sample Results of Incremental Dynamic Analysis for a Hypothetical Building

J.3 Mathematical Models

Section 5.2.2 and Section 6.2.4 describe modeling considerations. Three dimensional mathematical models should be used unless structural response is truly independent in each of two orthogonal directions.

J.4 Ground Motion Selection and Scaling

Two different methods for selecting and scaling ground motions for use in this procedure are presented below. One uses uniform hazard spectra and the other, conditional mean spectra, both of which are described in Appendix B. In both procedures, a sufficient number of ground motions should be used to provide stable estimates of the median collapse capacity. In limited studies, the use of 11 pairs of motions, each rotated 90 degrees to produce a total of 22 motion sets have been found to be sufficient for this purpose. For some

structures, stable prediction of median collapse capacity may be possible with a smaller number of motions. Ground motions generated for response-history analysis at an intensity approximately equal to the median collapse capacity, $\hat{S}_a(\overline{T})$ as described in Chapter 4, can be used.

Method A – Uniform Hazard Spectrum:

1. Estimate the median collapse capacity, $\hat{S}_a(\overline{T})$, and the mean annual frequency of exceedance of $\hat{S}_a(\overline{T})$ For typical structures conforming to the detailing criteria contained in recent editions of ASCE-7, $\hat{S}_a(\overline{T})$ can be estimated as being approximately 3 times the value of the design shaking spectral ordinate at period, $\overline{T}$.
2. Develop a Uniform Hazard Spectrum consistent with the mean annual frequency of exceedance for $\hat{S}_a(\overline{T})$ estimated in Step 1
3. Select an appropriate suite of ground motion pairs with geometric mean spectra that have a similar shape to the Uniform Hazard Spectrum of Step 2

If the estimate of median collapse capacity in Step 1 is significantly larger or smaller than the value computed using the suite of records and incremental dynamic analysis, a new Uniform Hazard Spectrum should be determined for the mean annual frequency of exceedance corresponding with the value of $\hat{S}_a(\overline{T})$ determined by the analysis. If the shape is significantly different from that developed in Step 2, a new suite of motions should be selected per Step 3 to match the new spectrum and the analysis repeated.

Method B – Conditional Mean Spectrum:

1. Estimate the median collapse capacity, $\hat{S}_a(\overline{T})$, and the mean annual frequency of exceedance of $\hat{S}_a(\overline{T})$ as described above for Method A.
2. Deaggregate the seismic hazard at this annual frequency of exceedance (refer to Appendix B) to determine the magnitude and distance of characteristic events that dominate the hazard at this probability.
3. Generate a Conditional Mean Spectrum at period $\overline{T}$ per Appendix B for the $[M, r, \varepsilon]$ of the events selected in Step 2 using an appropriate attenuation function. Normalize the Conditional Mean Spectrum so that the peak ordinate is equal to 1.0
4. Select an appropriate suite of ground motions with geometric mean spectra that have a similar shape and period at peak spectral response to the Conditional Mean Spectrum.

As with the Uniform Hazard Spectrum procedure, if the estimate of median collapse capacity in Step 1 is significantly higher or lower than that determined by incremental dynamic analysis, using this suite of motions, a new annual exceedance frequency should be determined for the value of $\hat{S}_a(\overline{T})$ determined from analysis, and a new Conditional Mean Spectrum generated. If the shape of the spectrum has changed significantly, a new suite of ground motions should be selected and the analysis repeated.

J.5 Collapse Fragility Development

Regardless of the method used to select ground motion pairs, the amplitude of each ground motion pair should be incremented, and nonlinear response history analysis performed until either numerical instability occurs in the analysis, indicating collapse, story drift or forces producing non-simulated collapse modes are predicted, or predicted drifts become larger than the valid range of modeling. The value of $S_a(\overline{T})$ at which any of these occur should be noted. If numerical instability or a non-simulated collapse mode is not predicted, the analysis should be repeated, with an incremented amplitude for the ground motion pair until a small increment in the value of $S_a(\overline{T})$ produces a large change in the maximum predicted story drift, numerical instability occurs, or demands associated with non-simulated modes are predicted. In this case, the value of $S_a(\overline{T})$ at which this occurs should be taken as the collapse capacity for this ground motion pair.

The median collapse capacity is taken as that value of $S_a(\overline{T})$ at which 50% of the ground motion pairs produce either:

1. Numerical instability or simulated collapse,
2. Predicted response that would result in non-simulated collapse,
3. Large increment in story drift for small increase in $S_a(\overline{T})$

Figure J-2 presents a collapse fragility plot constructed using the median and dispersion values obtained from Figure J-1 and the assumption of a lognormal distribution. Note that the dispersion in Figure J-2, which is based on analysis of a mathematical model constructed using *best estimate* mechanical properties, does not include all sources of uncertainty. These additional sources of uncertainty, identified below, must also be considered in developing the collapse fragility dispersion.

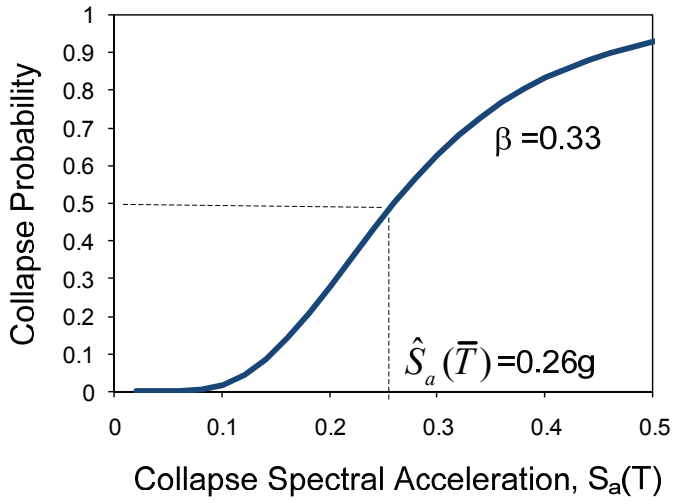

Figure J-2 Transforming results of IDA to a collapse fragility curve

Collapse fragility dispersion should account for three sources of uncertainty:

1. Variation in collapse capacity among different ground motion records, $\beta_{a\Delta}$, (also termed record-to-record uncertainty);
2. Variations due to building definition and construction quality assurance, β_c; and,
3. Uncertainty associated with the quality and completeness of the nonlinear analysis model, β_q.

Chapter 5 provides recommendations for the second and third sources of uncertainty and groups these together as modeling uncertainty, β_m. Total dispersion can be estimated using equation (J-1) and the information presented below. Alternately, a default dispersion value of 0.6 can be used.

$$\beta = \sqrt{\beta_{a\Delta}^2 + (\beta_c^2 + \beta_q^2)} = \sqrt{\beta_{a\Delta}^2 + \beta_m^2} \qquad \text{(J-1)}$$

a. *Record-to-record uncertainty.* The record to record dispersion in collapse capacity, $\beta_{a\Delta}$, can either be selected from the values presented as a function of structural period and geographic region in column 3 of Table 5-6, or taken as 0.45.

b. *Building definition and construction quality assurance.* Table 5-1 provides default values for β_c.

c. *Model quality and completeness:* Table 5-2 provides default values for β_q. Given that few models account for strength and stiffness deterioration through component failure have been validated by large-size experimentation, β_q should typically have a value between 0.3 and 0.5.

Appendix K

Sliding and Overturning

K.1 Introduction

This appendix provides the derivation and assumptions that underlie procedures for calculation of fragility functions related to overturning and sliding of anchored and unanchored components. Note that these procedures address only the probability that sliding or overturning will occur, not the consequences of such behavior. For sliding behaviors, users must determine a sliding displacement, δ, at which the component is likely to become damaged either by falling off a bearing surface or impacting an adjacent object. For both sliding and overturning behaviors, users must determine the extent of damage that results from the behavior, and the consequences thereof.

The procedures for development of sliding and overturning fragility parameters are based on Section 7.1, A.2 and Appendix B of ASCE 43-05.

K.2 Overturning

Fragility functions for overturning use peak total floor velocity V_{PT} as the demand parameter. Functions are expressed in the form of a median value, $\hat{V}_{PT}$ and dispersion, β.

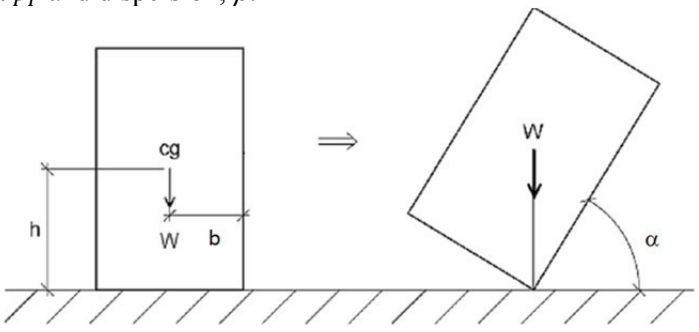

Figure K-1 Overturning of unanchored object.

The procedure assumes that unanchored objects subject to ground shaking will exhibit an oscillatory rocking behavior until a critical displacement of the center of mass is reached at which point the object becomes unstable and topples. As shown in Figure K-1, the critical displacement is represented in

the form of a tipping angle, α, at which the component's center of mass is directly aligned with the edge about which it can overturn.

The procedure uses spectral characteristics of the motion at the component's base, either the ground or floor that supports the object, and estimates of the component's rocking frequency f_r and effective damping ratio, β_r, to express the probability of overturning occurrence as a function of V_{PT}. Housner (1963) developed a reference for overturning failure of unanchored objects as a function of peak ground velocity as:

$$PGV = 2gR\sqrt{(1-\cos\alpha)} \tag{K-1}$$

where, PGV is the peak ground velocity at which overturning initiates, $R = \sqrt{b^2 + h^2}$ and the quantities α, b and h are as defined in Figure K-1. The procedure presented here, adapted from *ASCE 43-05*, reflects a more detailed understanding of the dynamics associated with overturning instability and provides general corroboration with Housner's equation for aspect ratios of typical concern.

The procedure adopts the following assumptions:

1. The relationships between peak ground velocity PGV and object rocking frequencies and damping are valid for use on elevated floors, with V_{PT} substituted for peak ground velocity.
2. Overturning about only one axis is considered. Simultaneous rocking about two axes is neglected as are the effects of vertical shaking.
3. The unanchored component's weight, W, is uniformly distributed.
4. The component has a rectangular shape with height $2h$ and width $2b$.

From simple geometry, the critical tipping angle at which the component will become unstable is given by geometry and the equation:

$$\alpha = \arctan\left(\frac{b}{h}\right) \tag{K-1}$$

The horizontal spectral acceleration that will tip the component to the critical angle, α, can be determined from the formula:

$$S_{aO} = \frac{2B}{\alpha} \tag{K-2}$$

where B is given by the equation:

$$B = \cos(\alpha) + \frac{b}{h}\sin(\alpha) - 1 \tag{K-3}$$

A value of S_{aO} that is greater than the static coefficient of friction between the component and the surface it is mounted on, μ_S, indicates the object will likely slide rather than overturn, while a value less than μ_S indicates the object will overturn.

The component's effective rocking frequency, f_r and effective rocking damping ratio, β_r are determined respectively from equations K-4 and K-5:

$$f_r = \frac{1}{2\pi}\sqrt{\frac{2gB}{C_3\alpha^2 h}} \tag{K-4}$$

$$\beta_r = \frac{\gamma}{\sqrt{4\pi^2 + \gamma^2}} \tag{K-5}$$

where:

$$C_3 = \frac{4}{3}\left(1 + \left(\frac{b}{h}\right)^2\right) \tag{K-6}$$

$$C_R = 1 - \frac{2\left(\frac{b}{h}\right)^2}{C_3} \tag{K-7}$$

$$\gamma = -2\ln\left(C_R\right) \tag{K-8}$$

Spectral floor velocity, as a function of damping, β, is represented by the equation:

$$S_v\left(\beta\right) = V_{PT} D_{amp} \tag{K-9}$$

Spectral relative velocity can be related to pseudo spectral acceleration using the relationship:

$$S_v\left(\beta\right) = \frac{S_a\left(f_r, \beta\right)}{2\pi f_r} \tag{K-10}$$

The spectral amplification factor is derived from Table 2 of Newmark and Hall (1982) assuming that f_r falls within the constant velocity domain of the shaking spectrum. This yields:

$$D_{amp} = 2.31 - 0.41 ln\left(100\beta_r\right) \tag{K-11}$$

Equating $S_a(f_r, \beta)$ in equation K-10 to S_{ao} obtained from equation K-2, and equating equations K-9 and K-10, equation K-12 is obtained:

$$\hat{V}_{PT} = \frac{S_{ao} g}{2\pi f_r D_{amp}} \tag{K-12}$$

Due to the considerable uncertainty associated with the assumptions underlying this derivation, a dispersion of 0.5 is recommended.

K.3 Sliding

Unanchored objects resting on surfaces with static coefficient of friction less than the horizontal spectral acceleration overturning capacity S_{aO} are likely to slide rather than overturn. This procedure provides an estimate of the median peak total floor velocity at which the sliding displacement of an unanchored object will equal or exceed a user-defined distance.

Peak sliding displacement, δ is a function of the square of V_{PT} and the dynamic coefficient of friction, μ_D at the object's base. The procedure for estimating median V_{PT} is based on the reserve energy approach described in Section 7.1, A.1 and Appendix B of ASCE 43-05. The approach relies on the observation that peak sliding displacements tend to be related to the frequency associated with 10%-damped spectral velocity ordinates that are equal to or greater than twice the dynamic coefficient of friction μ_D. As with overturning fragility it is assumed that the spectral characteristics of motion at elevated floors can be used in a manner similar to shaking at the ground, as characterized by response spectra and that the assumed relationship between critical sliding frequencies, 10% damped spectral velocity ordinates and V_{PT} are valid.

The procedure additionally assumes the following:

1. The object's aspect ratio and the coefficient of friction at its base are such that sliding, rather than overturning will occur. Section K.2 above presents procedures for confirming this condition.

5. Vertical seismic motion is neglected.

6. For any floor response spectrum, the frequency at which the 10% damped spectral acceleration equals or exceeds $2\mu_D$ is within the constant velocity domain of the spectrum

7. Damping associated with sliding can be approximated as 10% of critical and the corresponding spectral velocity amplification factor, D_{amp} for 10% damped behavior has a value of 1.37.

The sliding frequency f_s in the constant velocity domain of the response spectrum is related to spectral acceleration by the equation:

$$S_a = 2\pi f_s S_v \tag{K-13}$$

Substituting $2\mu_D$ for the critical value of spectral acceleration at which sliding occurs and using the relationship of equation K-9, it follows that:

$$2\mu_D = 2\pi f_s S_v = 2\pi f_s \left(1.37 V_{PT}\right) \quad \text{(K-14)}$$

and:

$$2\pi f_s = \frac{2\mu_D g}{V_{PT}} \quad \text{(K-15)}$$

From ASCE 43.05, sliding displacement can be approximated by:

$$\delta = \frac{2\mu g}{\left(2\pi f_s\right)^2} \quad \text{(K-16)}$$

Substituting for $2\pi f_s$ using the expression of equation K-15 yields:

$$\delta = 2\mu_D g \left(\frac{1.37 V_{PT}}{2\mu_D g}\right)^2 \quad \text{(K-17)}$$

Solving for V_{PT}:

$$\hat{V}_{PT} = \frac{\sqrt{2\mu_D g \delta}}{1.37} \quad \text{(K-18)}$$

As with overturning, a dispersion value of 0.5 is recommended.

Glossary

Definitions

Annual frequence of exceedance. The average number of times per year that an event having magnitude larger than a reference value is likely to occur (typically less than 1).

Annualized loss. The average value of loss per year over a period of many years.

Casualties. Loss of life, or serious injury requiring hospitalization.

Component. One of many parts, both structural and nonstructural, that together comprise a building.

Conditional probability. The probability that an outcome will occur, given that a particular event occurs or condition exists.

Consequences. The losses resulting from earthquake damage in terms of potential casualties, repair and replacement costs, repair time, and unsafe placarding.

Consequence function. A relationship that indicates the potential distribution of losses as a function of damage state.

Correlation. A mathematical relationship that defines the extent to which the value of one parameter is dependent on the value of one or more other parameters.

Damage state. For a particular component, or the building as a whole, a range of damage conditions associated with unique consequences.

Decision-maker(s). An individual or group responsible for selecting the performance objectives for a performance-based design.

Demand. A parameter that is predictive of component or building damage states, including peak floor (or ground) acceleration, peak component deformation, peak (or residual) story drift, peak floor (or ground) velocity, or peak component force (or stress).

Discount rate. A factor used to indicate the time-value of money in economic analyses.

Distribution. A mathematical function describing the statistical probability that elements in a set will have specific values.

Dispersion. A measure of uncertainty associated with prediction of the true value of a random, or otherwise uncertain, behavior.

Earthquake scenario. A specific earthquake event, defined by a magnitude and geographic location relative to a building site.

Floor acceleration. At a floor level, the acceleration of the center of mass relative to a fixed point in space.

Floor velocity. At a floor level, the velocity of the center of mass relative to a fixed point in space.

Fragility function. A mathematical relationship that defines the probability of incurring a damage state conditioned on the value of a single demand parameter.

Fragility group. A set of similar building components having the same potential damage characteristics in terms of fragility and consequence functions.

Fragility specification. A detailed description of potential component damage states, fragility functions, and consequence functions.

Geometric mean (geomean). In characterization of ground motion intensity, the square root of the product of the value of a ground motion parameter in each of two orthogonal directions (i.e., $\sqrt{xy}$).

Intensity. The severity of ground shaking as represented by a 5%-damped, elastic acceleration response spectrum, or the 5% damped spectral response acceleration at a specific natural period of vibration.

Intensity-based assessment. An assessment of the probable performance of a building subjected to a ground motion of a specified intensity.

Lognormal distribution. A distribution of values, characterized by a median value and dispersion, with the property that the natural logarithm of the values is normally distributed.

Median. The value of an uncertain parameter (or population of values) that will be exceeded 50% of the time.

Mean. The average value of a parameter (or population of values). If the population of values is normally distributed, the mean will be equal to the median. If the distribution is skewed, the mean may be less than or greater than the median.

Mean recurrence interval. The average amount of time between expected repeat occurrences of an event (e.g., an earthquake scenario or loss), typically expressed in years.

Mutually exclusive damage states. A series of related damage states in which the occurrence of any one type of damage will prevent the occurrence of another type of damage.

Net present value. For a particular discount rate, the present value of benefits that will be received in the future, less the associated costs of these benefits, considering the time-dependent value of money.

Normal distribution. A symmetric distribution completely described by a mean value and standard deviation. When plotted as a probability density function, a normal distribution has the shape of a bell curve.

Nonstructural component. A building component that is not part of the structural system.

Performance. The probable damage and resulting consequences of a building's response to earthquake shaking or other hazards.

Performance group. A set of components described by a single fragility group that will experience the same demand in response to earthquake shaking.

Performance objective. An expectation as to the probable damage state and resulting consequences that a building may experience in future earthquakes.

Period. The time, in seconds, necessary for a structure to complete one cycle of motion in free vibration.

Probable Maximum Loss. The probable cost of repairing earthquake damage expressed as percentage of building replacement cost with a particular confidence of non-exceedance, conditioned on a particular earthquake return period.

Realization. One possible performance outcome for a particular earthquake scenario or intensity comprising a unique set of demands, damage states, and consequences.

Repair cost. The cost, in present dollars, necessary to restore a building to its pre-earthquake condition, or in the case of total loss, to replace the building with a new structure of similar construction.

Repair time. The time, in weeks, necessary to repair a damaged building to its pre-earthquake condition.

Replacement cost. The cost, in present dollars, necessary to replace a building that has been damaged beyond the point of practicable repair, including costs associated with demolition and removal of debris.

Replacement time. The time, in weeks, necessary to replace a building that has been damaged beyond the point of practicable repair, including time associated with demolition and removal of debris.

Residual drift. The difference in permanent displacement between the center of mass of two adjacent floors as a result of earthquake shaking.

Residual drift ratio. Residual drift divided by story height.

Return on investment. The annual income that can be derived from an investment divided by the present value of the investment.

Return period. See mean recurrence interval.

Scenario-based assessment. An assessment of the probable performance of a building subjected to a specified earthquake scenario.

Scenario Expected Loss. A probable maximum loss with mean chance of occurrence.

Scenario Upper Loss. A probable maximum loss with a 10% chance of exceedance.

Seismic hazard curve. A plot of the annual frequency of exceedance of the possible values of a ground shaking intensity parameter.

Sequential damage states. A series of related component damage states such that after the occurrence of an initial damage state, one or more additional damage states can occur in sequence.

Simulated demands. A vector set of demands representing the building response in a particular realization.

Simultaneous damage states. A series of unrelated component damage states that can occur, but need not necessarily occur, at the same time.

Stakeholder(s). An individual or group affected by the performance of a building, including building owners, lenders, insurers, tenants, and the general public.

Story drift. The instantaneous difference in lateral displacement between the center of mass of two adjacent floors.

Story drift ratio. Story drift divided by story height.

Structural component. A building component that is part of the intended gravity or seismic-force-resisting system, or that provides measurable resistance to earthquake shaking.

Structural system. A collection of structural components acting together in resisting gravity forces, seismic forces, or both.

Time-based assessment. An assessment of the probable performance of a building, considering all earthquake scenarios and the associated probability of occurrence of each, over a specified period of time.

Unsafe placarding. A post-earthquake inspection rating that deems a building, or portion of a building, damaged to the point that entry, use, or occupancy poses immediate risk to safety. Unsafe placards are typically colored red.

Yield drift. The value of drift at which a structure reaches its effective yield strength.

Yield story drift. The value of story drift at which a story in a structure reaches its effective yield strength

Yield story drift ratio. Yield story drift divided by story height.

Symbols

Notation

a_i^* in the simplified analysis method, estimated median peak floor acceleration at level "i"

b the slope of a straight line fit to a series of data having x and y values

c the y intercept of a straight line fit to a series of data having x and y values

d_i the value of the demand at which a particular damage state was first observed to occur in specimen "i" in a series of m tests, or the maximum value of demand to which a specimen was subjected without occurrence of the damage state

$\overline{d}_j$ the maximum demand experienced by a series of test specimens in bin "j"

d_{max} the maximum demand, d, experienced by a specimen in a series of tests

d_{min} for a series of tests of specimens, the minimum value of demand, d, at which any specimen exhibited damage or distress

e_i in time-based assessment the mid-range intensity within an incremental range of intensities, Δe_i

f_r rocking frequency of an unanchored object (hz)

f_s frequency associated with sliding of an unanchored object (hz)

h building height

h_j in the simplified procedure, the height of level "j" above the building base

i interest rate, or expected rate of return on money

k in the simplified procedure, a coefficient used to account for nonlinear mode shape

m_j the number of specimens in bin "j" for which damage conforming to a particular damage state is observed

pga peak ground acceleration

t a period of years over which an investment decision is amortized

v_i^* in the simplified analysis method, estimated median peak floor velocity at level "i"

v_{si} a reference floor velocity parameter used to determine estimated peak floor velocity in the simplified analysis procedure

w_j in simplified analysis, weight lumped at a structure's level "*j*"

x_j the natural logarithm of $\overline{d}_j$

$\overline{x}$ the mean value of a series of values, x_j

y_j the inverse lognormal distribution value for the number of specimen tests that experienced a damage state in a bin "j" of specimen tests

$\overline{y}$ the mean of the values of y_j

A an amount of money that is earned or expended each year over a period of several years

B a parameter used to calculate the critical tipping demand on an unanchored object

C_1 in the simplified analysis procedure, a coefficient used to account for the difference in displacement response between elastic and inelastic structures, assuming non-degrading inelastic behavior

C_2 in the simplified analysis procedure, a coefficient used to account for the effects of stiffness degradation on displacement response

C_3 a coefficient used to determine the rocking capacity of an unanchored object

C_R a coefficient used to determine the rocking capacity of an unanchored object

C_{sm} a coefficient used to derive an approximate estimate of the fraction of the structure's total mass effective in first mode response

C_q a coefficient that adjusts computed median strength capacity for construction quality

C_{vx} in the simplified analysis procedure, the fraction of the total pseudo lateral force, applied to level "*x*"

D_{amp} spectral velocity amplification factor

F_x in the simplified analysis procedure, the pseudo lateral force applied to level "*x*"

H in the simplified analysis procedure, total building height above the base

M the total number of test specimens for which test data is available and for which the damage state of interest occurred

M_A in a series of M tests, the number of specimens that did not experience any damage or distress but which experienced demands greater than or equal to a reference value, d_a

M_B in a series of M tests, the number of specimens that experienced some damage or distress but which did not experience the damage state of interest

M_j the number of test specimens in a bin "j" of a series of tests

NPV the net present value of a future stream of incomes or expenditures

PGV Peak ground velocity in units of in/sec

PM_{10} that value of a performance measure, for example, repair cost that has a 10% chance of exceedance.

PM_{50} the median value of a performance measure, for example, repair time that has a 50% of exceedance.

PM_{90} that value of a performance measure, for example, casualties, that has a 90% chance of exceedance.

$\overline{PM}$ the mean, value of a performance measure, sometimes also termed the expected value or average value.

$P(C)$ the conditional probability of building collapse, given an intensity of shaking

$P(U_i)$ the probability, for a given intensity or scenario, that damage sustained by components in performance group "i" will result in an unsafe placard.

$P(U_T)$ the total conditional probability, given a specific intensity of motion or earthquake scenario, that a building will receive an unsafe placard

P_{EY} Probability of exceedance of an event in Y years

P_R Mean return period for an event

R_n nominal resistance in accordance with an appropriate LRFD design specification

S in the simplified analytical procedure, the ratio of elastic base shear force to the structure's yield shear strength

$S_a(T)$ spectral response acceleration at period T.

S_a^{min} for time-based assessment, the minimum spectral response acceleration, in units of "g" at which performance is assessed

S_a^{max} for time-based assessment, the maximum spectral response acceleration, in units of "g" at which performance is assessed

S_{aO} spectral acceleration that will produce tipping of an unanchored object to a critical value at which instability will occur (g)

$S_v(1)$ spectral velocity at a period of 1 second

T period of structural response, i.e. the amount of time, typically in seconds, a structure in free vibration will take to make one complete cycle of motion

T_1 period of fundamental mode of vibration

T_1^X period of fundamental mode of vibration in the "X" horizontal direction

T_1^Y period of fundamental mode of vibration in the "Y" horizontal direction

$\overline{T}$ the average of the periods of the fundamental translation modes about each of two orthogonal building axes

T_{min} the minimum period in a range of periods, used to scale ground motions for nonlinear response history analysis

T_{max} the maximum period in a range of periods, used to scale ground motions for nonlinear response history analysis

T_1^X the fundamental period of translational vibration in the first of two orthogonal directions of a structure's dynamic response

T_1^Y the fundamental period of translational vibration in the second of two orthogonal directions of a structure's dynamic response

V in the simplified analysis procedure, a pseudo lateral force used to estimate story drifts

V_s average shear wave velocity of soil soil in the upper 100 feet (30 meters)

V_{PT} peak total floor velocity at a floor level (in/sec)

V_{yt} a structure's effective yield strength in first mode response.

W_1 in simplified analysis, the weight effective in the structure's first mode response

Y a number of years considered in a time-based assessment

α α for an unanchored object, the critical tip angle at which the object will become unstable and overturn (radians)

β a measure of uncertainty in the true value of a random parameter, also called dispersion.

β_a uncertainty associated with record to record response variability

$\beta_{a\Delta}$ record to record variability (dispersion) associated with story drift response

β_{aa} record to record variability (dispersion) associated with floor acceleration response

β_c modeling uncertainty associated with lack of definition of the way a building has actually been constructed

β_r in a series of data used to establish fragility functions, the random variability evident in the data

β_u a measure of uncertainty that represents the probability that conditions inherent in a data set used to establish fragility do not represent actual conditions a real component in a building will experience

β_{gm} dispersion accounting for uncertainty in ground motion intensity as reflected in attenuation relationships

β_a modeling uncertainty associated with inaccuracies in the structural model associated with imperfect hysteretic models, estimates of damping, and failure to include all elements in the model

β_m modeling dispersion, representing the uncertainty in the predicted response obtained from structural modeling and analysis.

β_r damping ratio (fraction of critical) for a rocking object

β_C uncertainty associated with the quality of installation or construction of a component

β_D uncertainty associated with the ability of a design equation to predict actual behavior when material strength is defined

β_M uncertainty in material strength

β_{SD} in the simplified procedure, the total dispersion associated with story drift

δ a sliding displacement that will cause an unanchored component to hit another object, resulting in damage

δ_t peak displacement of floor "i" relative to the base

δ_r peak displacement of the roof relative to the base

δ_y component deformation at yield

γ	factor used to determine effective damping for a rocking component
Δ_i	in the simplified procedure, the uncorrected story drift at level "*i*"
Δ_i^*	estimated median peak story drift at story "*i*"
Δ_r	estimated median residual story drift ratio
Δe_i	in time-based assessments an incremental range of earthquake intensities
$\Delta\lambda_i$	in time-based assessments the probability of occurrence, in a period of time, of earthquake intensity with range Δe_i
Δ_y	estimated story drift at development of yield strength
ϕ	resistance factor as specified by an LRFD design specification
ϕ_{j1}	in simplified analysis, the ordinate of the first mode deflection at floor level "*j*"
λ	mean annual frequency of exceedance of a ground motion parameter
μ	the ratio of component deformation at the onset of damage to component deformation at yield
μ_D	the kinetic coefficient of friction between an unanchored object and its resting surface
μ_S	the static coefficient of friction between an unanchored object and its resting surface

References

Abrahamson, N.A., 2000, "State of the practice of seismic hazard evaluation," *Proceedings*, GeoEng2000, Melbourne, Australia.

Abrahamson, N.A. and Al Atik, L., 2010, "Scenario spectra for design ground motions and risk calculation," *Proceedings*, 9th US National and 10th Canadian Conference on Earthquake Engineering, Toronto, Canada.

Abrahamson, N.A. and Shedlock, K., 1997, "Overview," *Seismological Research Letters*, Vol. 68, No. 1, pp. 9-23.

Abrahamson, N. and Silva, W., 1997, "Empirical response spectral attenuation relations for shallow crustal earthquakes," *Seismological Research Letters*, Vol. 68, pp. 94-127.

ACI, 2011, *Building Code Requirements for Structural Concrete and Commentary*, ACI 318-11, American Concrete Institute, Farmington Hills, Michigan.

AISC, 2010, *Specification for Structural Steel Buildings*, ANSI/AISC 360-10, American Institute of Steel Construction, Chicago, Illinois.

ASCE, 2003, *Seismic Evaluation of Existing Buildings*, ASCE/SEI 31-03, American Society of Civil Engineers, Reston, Virginia.

ASCE, 2005, *Seismic Design Criteria for Structures, Systems, and Components in Nuclear Facilities,* ASCE/SEI 43-05, American Society of Civil Engineers, Reston, Virginia.

ASCE, 2007, *Seismic Rehabilitation of Existing Buildings*, ASCE/SEI 41-06, American Society of Civil Engineers, Reston, Virginia.

ASCE, 2010, *Minimum Design Loads for Buildings and Other Structures,* ASCE/SEI 7-10, American Society of Civil Engineers, Reston, Virginia.

ASTM, 2007a, *Standard Guide for Seismic Risk Assessment of Buildings*, ASTM E2026-07, American Society of Testing and Materials, West Conshohocken, Pennsylvania.

ASTM, 2007b, *Standard Practice for Probable Maximum Loss (PML) Evaluations for Earthquake Due-Diligence Assessments*, ASTM E2557-

07, American Society of Testing and Materials, West Conshohocken, Pennsylvania.

ATC, 1992, *Guidelines for Cyclic Seismic Testing of Components of Steel Structures,* ATC-24 Report, Applied Technology Council, Redwood City, California.

ATC, 1996, *Seismic Evaluation and Retrofit of Concrete Buildings,* ATC-40 Report, Applied Technology Council, Redwood City, California.

ATC, 2002, *Proceedings of: FEMA-Sponsored Workshop on Communicating Earthquake Risk*, Applied Technology Council, Redwood City, California.

ATC, 2010, *Modeling and Acceptance Criteria for Seismic Design and Analysis of Tall Buildings*, PEER/ATC-72-1 Report, prepared by Applied Technology Council for Pacific Earthquake Engineering Research Center, Redwood City, California.

Baker, J. and Cornell, C.A., 2005, "A vector-valued ground motion intensity measure consisting of spectral acceleration and epsilon," *Earthquake Engineering and Structural Dynamics*, Vol. 34, No. 10, pp. 1193-1217.

Baker, J. and Cornell, C.A., 2006, "Spectral shape, epsilon and record selection," *Earthquake Engineering and Structural Dynamics*, Vol. 35, No. 9, pp. 1077-1095.

Benjamin, J. and Cornell, C.A., 1970, *Probability, Statistics, and Decision for Civil Engineers*, McGraw Hill, New York, New York.

Bozorgnia, Y. and Bertero, V.V., 2004, "Earthquake Engineering: From Engineering Seismology to Performance-Based Earthquake Engineering," CRC Press.

Christopoulos, C., Pampanin, S., and Priestley, M.J.N., 2003, "Performance-based seismic response of frame structures including residual deformations, Part I: single degree of freedom systems," *Journal of Earthquake Engineering*, Vol. 7, No. 1, pp. 97-118.

Christopoulos, C. and Pampanin, S., 2004, "Towards performance-based design of MDOF structures with explicit consideration of residual deformations," Invited Paper, *Indian Society for Earthquake Technologies (ISET) Journal of Earthquake Technology*, Special Issue on Performance-Based Design, Vol. 41, pp. 172-193.

Cornell, C.A. and Winterstein, S.R., 1988, "Temporal and magnitude dependence in earthquake recurrence models," *Bulletin of the Seismological Society of America*, Vol. 78, No. 4, pp. 1522-1537.

FEMA, 1997, *NEHRP Guidelines for the Seismic Rehabilitation of Buildings*, FEMA 273, prepared by the Applied Technology Council for the Building Seismic Safety Council, funded and published by the Federal Emergency Management Agency, Washington, DC.

FEMA, 2000, *Prestandard and Commentary for the Seismic Rehabilitation of Buildings*, FEMA 356, prepared by American Society of Civil Engineers for the Federal Emergency Management Agency, Washington D.C.

FEMA, 2005, *Improvement of Nonlinear Static Seismic Analysis Procedures*, FEMA 440, prepared by Applied Technology Council for the Federal Emergency Management Agency, Washington, D.C.

FEMA, 2007, *Interim Testing Protocols for Determining the Seismic Performance Characteristics of Structural and Nonstructural Components*, FEMA 461, prepared by Applied Technology Council for Federal Emergency Management Agency, Washington, D.C.

FEMA, 2009a, *NEHRP Recommended Seismic Provisions for New Buildings and Other Structures,* FEMA P-750, prepared by Building Seismic Safety Council for Federal Emergency Management Agency, Washington, D.C.

FEMA, 2009b, *Quantification of Building Seismic Performance Factors*, FEMA P-695 Report, prepared by Applied Technology Council for Federal Emergency Management Agency, Washington, D.C.

FEMA, 2009c, *Effects of Strength and Stiffness Degradation on Seismic Response*, FEMA P-440A Report, prepared by Applied Technology Council for Federal Emergency Management Agency, Washington, D.C.

Gülerce, Z. and Abrahamson, N.A., 2011, "Site-specific design spectra for vertical ground motion," *Earthquake Spectra*, Vol. 27, No. 4, pp. 1023-1047.

Gutenberg, R. and Richter, C.F., 1944, "Frequency of earthquakes in California," *Bulletin of the Seismological Society of America*, Vol. 34, pp. 185-188.

Harmsen, S.C., 2001, "Mean and modal ε in the deaggregation of probabilistic ground motion," *Bulletin of the Seismologic Society of America*, Vol. 91, No. 6, pp. 1537-1552.

Housner, G.W., 1963, "The behavior of inverted pendulum structures during earthquakes," *Bulletin of the Seismological Society of America*, Vol. 53, No. 2, pp. 403-417.

Huang, Y.-N. and Whittaker, A.S., 2012, "Calculation of peak ground velocity from 1-second spectral velocity," ATC-58-1 Project Report, Applied Technology Council, Redwood City, California.

Huang, Y., Whittaker, A.S., and Luco, N., 2008, "Maximum spectral demands in the near-fault region," *Earthquake Spectra*, Vol. 24, No. 1, pp. 319-341.

Huang, Y.-N., Whittaker, A.S., and Luco, N., 2008, "Performance assessment of conventional and base-isolated nuclear power plants for earthquake and blast loadings," Technical Report MCEER-08-0019, Multidisciplinary Center for Earthquake Engineering Research, University at Buffalo, Buffalo, New York.

Huang, Y.-N., Whittaker, A.S., Luco, N., and Hamburger, R.O., 2011, "Selection and scaling of earthquake ground motions in support of performance-based design," *Journal of Structural Engineering*, Vol. 137, No. 3, pp. 311-321.

Ibarra, L.F. and Krawinkler, H.K., 2005, *Global Collapse of Frame Structures under Seismic Excitations,* PEER 2005/06 Report, Pacific Earthquake Engineering Research Center, Berkeley, California.

Jayaram, N., Lin, T., and Baker, J.W., 2011, "A computationally efficient ground-motion selection algorithm for matching a target response spectrum mean and variance," *Earthquake Spectra*, Vol. 27, No. 3, pp. 797-815.

Kramer, S.L., 1996, *Geotechnical Earthquake Engineering*, Prentice Hall, Upper Saddle River, New Jersey.

Liel, A., Haselton, C., Deierlein, G., and Baker, J., 2009, "Incorporating modeling uncertainties in the assessment of seismic collapse risk of buildings," *Structural Safety*, Vol. 31, No. 2, pp. 197-211.

MacRae, G.A., 1994, "P-delta effects on single-degree-of-freedom structures in earthquakes," *Earthquake Spectra*, Vol. 10, No. 3, pp. 539-568.

MacRae, G.A. and Kawashima, K., 1997, "Post-earthquake residual displacements of bilinear oscillators," *Earthquake Engineering & Structural Dynamics*, Vol. 26, No. 7, pp. 701-716.

Mahin, S.A. and Bertero, V.V., 1981, "An evaluation of inelastic seismic design spectra," *Journal of the Structural Division*, ASCE, Vol. 107, No. 9, pp. 1777-1795.

McGuire, R., 2004, *Seismic Hazard and Risk Analysis,* EERI Monograph, Earthquake Engineering Research Institute, Oakland, California.

Moehle, J. and Deierlein, G., 2004, "A Framework Methodology for Performance-Based Earthquake Engineering," *Proceedings*, 13th World Conference on Earthquake Engineering, Vancouver, British Columbia, Paper No. 679.

Newmark, N.M. and Hall, W.J., 1982, *Earthquake Spectra and Design*, Earthquake Engineering Research Institute, Oakland, California.

NIST, 1999, *UNIFORMAT II Elemental Classification for Building Specifications, Cost Estimating and Cost Analysis*, NISTIR 6389 Report, National Institute of Standards and Technology, Gaithersburg, Maryland.

NIST, 2010, *Nonlinear Structural Analysis for Seismic Design: A Guide for Practicing Engineers*, GCR 10-917-5, prepared by the NEHRP Consultants Joint Venture, a partnership of the Applied Technology Council and the Consortium of Universities for Research in Earthquake Engineering, for the National Institute of Standards and Technology, Gaithersburg, Maryland.

NIST, 2011, *Selecting and Scaling Earthquake Ground Motions for Performing Response-History Analyses*, GCR 11-917-15, prepared by the NEHRP Consultants Joint Venture, a partnership of the Applied Technology Council and the Consortium of Universities for Research in Earthquake Engineering, for National Institute of Standards and Technology, Gaithersburg, Maryland.

NIST, 2012, *Soil-Structure Interaction for Building Structures*, GCR 12-917-21, prepared by the NEHRP Consultants Joint Venture, a partnership of the Applied Technology Council and the Consortium of Universities for Research in Earthquake Engineering, for the National Institute of Standards and Technology, Gaithersburg, Maryland.

Pampanin, S., Christopoulos, C., and Priestley, M.J.N., 2003, "Performance-based seismic response of frame structures including residual

deformations, Part II: multidegree of freedom systems," *Journal of Earthquake Engineering*, Vol. 7, No. 1, pp. 119-147.

Riddell, R. and Newmark, N.M., 1979, Statistical Analysis of the Response of Nonlinear Systems Subjected to Earthquakes, Structural Research Series No. 468 Technical report, Illinois University, Urbana-Campaign, Illinois.

Ross, S.M., 2003, "Peirce's criterion for the elimination of suspect experimental data," *Journal of Engineering Technology*, Vol. 20, No 2, pp. 38-41.

Ruiz-Garcia, J. and Miranda, E., 2005, "Performance-based assessment of existing structures accounting for residual displacements," No. 153. Technical Report, The John A. Blume Earthquake Engineering Center, Stanford University, Stanford, California.

Ruiz-Garcia, J. and Miranda, E., 2006, "Direct estimation of residual displacement from displacement spectral ordinates," *Proceedings of 8th U.S. National Conference on Earthquake Engineering*, Paper No. 1101, 10 pp.

Somerville, P.G., Smith, N.F., Graves, R.W., and Abrahamson, N.A., 1997, "Modification of empirical strong ground motion attenuation relations to include the amplitude and duration effects of rupture directivity," *Seismological Research Letters*, Vol. 68, No. 1, pp. 199-222.

Vamvatsikos, D. and Cornell, C.A., 2006, "Direct estimation of the seismic demand and capacity of oscillators with multi-linear static pushovers through IDA," *Earthquake Engineering and Structural Dynamics*, Vol. 35, Issue 9, pp. 1097-1117.

Yang, T.Y., Moehle, J., Stojadinovic, B., Der Kiureghian, A., 2006, "An Application of PEER Performance-Based Earthquake Engineering Methodology," *Proceedings*, 8th US National Conference on Earthquake Engineering, San Francisco, California, Paper No. 1448.

Yang, T.Y., Moehle, J., Stojadinovic, B., and Der Kiureghian, A., 2009, "Seismic performance evaluation of facilities: methodology and implementation," *Journal of Structural Engineering*, Vol. 135, No. 10, pp. 146-1154.

Project Participants

ATC Management and Oversight

Christopher Rojahn (Project Executive Director)
Project Executive Director
Applied Technology Council
201 Redwood Shores Parkway, Suite 240
Redwood City, California 94065

Jon A. Heintz (Project Manager)
Applied Technology Council
201 Redwood Shores Parkway, Suite 240
Redwood City, California 94065

Ayse Hortacsu
Applied Technology Council
201 Redwood Shores Parkway, Suite 240
Redwood City, California 94065

FEMA Oversight

Mike Mahoney (Project Officer)
Federal Emergency Management Agency
500 C Street, SW, Room 416
Washington, DC 20472

Robert D. Hanson (Technical Monitor)
Federal Emergency Management Agency
2926 Saklan Indian Drive
Walnut Creek, California 94595

Project Management Committee

Ronald O. Hamburger
(Project Technical Director)
Simpson Gumpertz & Heger
The Landmark @ One Market, Suite 600
San Francisco, California 94105

John Gillengerten
Office of Statewide Health
Planning and Development
1600 9th Street, Room 420
Sacramento, California 95814

William T. Holmes (ex-officio)
Rutherford & Chekene
55 Second Street, Suite 600
San Francisco, California 94105

Peter J. May
University of Washington
3630 Evergreen Point Road
Medina, Washington 98039

Jack P. Moehle
University of California, Berkeley
3444 Echo Springs Road
Lafayette, California 94549

Maryann T. Phipps (ATC Board Contact)
Estructure
8331 Kent Court, Suite 100
El Cerrito, California 94530

Steering Committee

William T. Holmes (Chair)
Rutherford & Chekene
55 Second Street, Suite 600
San Francisco, California 94105

Roger D. Borcherdt
U.S. Geological Survey
345 Middlefield Road, MS977
Menlo Park, California 94025

Anne Bostrom
University of Washington
Parrington Hall, Room 327
Seattle, Washington 98195

Bruce Burr
Burr & Cole Consulting Engineers
3485 Poplar Avenue, Suite 200
Memphis, Tennessee 38111

Kelly Cobeen
Wiss, Janney, Elstner Associates, Inc.
2200 Powell Street, Suite 925
Emeryville, California 94608

Anthony B. Court
A.B. Court & Associates
4340 Hawk Street
San Diego, California 92103

Terry Dooley
Morley Builders
2901 28th Street, Suite 100
Santa Monica, California 90405

Dan Gramer
Turner Construction Company
830 4th Avenue South, Suite 400
Seattle, Washington 98134

Michael Griffin
CCS Group, Inc.
1415 Elbridge Payne Road, Suite 265
Chesterfield, Missouri 63017

R. Jay Love
Degenkolb Engineers
300 Frank H Ogawa Plaza, Suite 450
Oakland, California 94612

David Mar
Tipping-Mar & Associates
1906 Shattuck Avenue
Berkeley, California 94704

Steven McCabe
National Institute of Standards and Technology
100 Bureau Drive, MS 8630
Gaithersburg, Maryland 20899

Brian J. Meacham
Worcester Polytechnic Institute
Dept. of Fire Protection Engineering
100 Institute Road
Worcester, Massachusetts 01609

William J. Petak
University of Southern California
School of Policy Planning and Development
MC 0626
Los Angeles, California 90089

Risk Management Products Team

John D. Hooper (Co-Team Leader)
Magnusson Klemencic Associates
1301 Fifth Avenue, Suite 3200
Seattle, Washington 98101

Craig D. Comartin (Co-Team Leader)
Comartin Engineers
7683 Andrea Avenue
Stockton, California 95207

Mary Comerio
University of California, Berkeley
Dept. of Architecture
232 Wurster Hall
Berkeley, California 94720

Allin Cornell (deceased)
Stanford University
110 Coquito Way
Portola Valley, California 94028

Mahmoud Hachem
Degenkolb Engineers
1300 Clay Street
Oakland, California 94612

Gee Heckscher
Architectural Resources Group
1301 53rd St
Port Townsend, Washington 98368

Judith Mitrani-Reiser
Johns Hopkins University
Dept. of Civil Engineering
3400 N. Charles St., Latrobe 109
Baltimore, Maryland 21218

Peter Morris
Davis Langdon
1331 Garden Highway, Suite 310
Sacramento, California 95833

Farzad Naeim
John A. Martin and Associates, Inc.
950 S. Grand Ave., 4th Floor
Los Angeles, California 90015

Keith Porter
University of Colorado
Dept. of Civil, Environmental, and Architectural Engineering
Engineering Center Office Tower 428
1111 Engineering Drive
Boulder, Colorado 80309

Hope Seligson
MMI Engineering
2100 Main Street, Suite 150
Huntington Beach, California 92648

Risk Management Products Consultants

Travis Chrupalo
2 Lanai Court
Chico, California 95973

D. Jared DeBock
University of Colorado
939 Cedwick Drive
Lafayette, Colorado 80026

Armen Der Kiureghian
ADK & Associates
1974 18th Avenue
San Francisco, California 94116

Scott Hagie
John A. Martin & Associates, Inc.
950 South Grand Avenue
Los Angeles, California 90015

Curt B. Haselton
California State University, Chico
Dept. of Civil Engineering
209F Langdon Hall
Chico, California 95929

Russell Larsen
Magnusson Klemencic Associates
1301 Fifth Avenue, Suite 3200
Seattle, Washington 98101

Juan Murcia-Delso
University of California, San Diego
Dept. of Structural Engineering
409 University Center
9500 Gilman Drive – MC0085
La Jolla, California 92093

P. Benson Shing
University of California, San Diego
Dept. of Structural Engineering
409 University Center
9500 Gilman Drive – MC0085
La Jolla, California 92093

Scott Shell
Esherick Homsey Dodge & Davis Architects
500 Treat Avenue, Suite 201
San Francisco, California 94110

Farzin Zareian
University of California, Irvine
Dept. of Civil and Environmental Engineering
Irvine, California 92697

Structural Performance Products Team

Andrew S. Whittaker (Team Leader)
University at Buffalo
Dept. of Civil Engineering
230 Ketter Hall
Buffalo, New York 14260

Laura Lowes
University of Washington
Dept. of Civil and Environmental Engineering
Box 352700
Seattle, Washington 98195

Gregory Deierlein
Stanford University
Dept. of Civil & Environmental Engineering
240 Terman Engineering Center
Stanford, California 94305

Nicolas Luco
U. S. Geological Survey
Box 25046 – DFC – MS 966
Denver, Colorado 80225

John D. Hooper
Magnusson Klemencic Associates
1301 Fifth Avenue, Suite 3200
Seattle, Washington 98101

Andrew T. Merovich
A. T. Merovich & Associates, Inc.
1950 Addison Street, Suite 205
Berkeley, California 94704

Yin-Nan Huang
127 Paramount Pkwy
Buffalo, New York 14223

Structural Performance Products Consultants

Jack Baker
Stanford University
Dept. of Civil & Environmental Engineering
240 Terman Engineering Center
Stanford, California 94305

J. Daniel Dolan
Washington State University
Dept. of Civil and Environmental Engineering
405 Spokane Street, Sloan 101
P.O. Box 642910
Pullman, Washington 99164

Dhiman Basu
University at Buffalo
Dept. of Civil Engineering
230 Ketter Hall
Buffalo, New York 14260

Charles Ekiert
12 Hillcrest Drive
Hamlin, New York 14464

Andre Filiatrault
Multidisciplinary Center for Earthquake
Engineering Research, University at Buffalo
105 Red Jacket Quadrangle
Buffalo, New York 14261

Aysegul Gogus
University of California, Los Angeles
Dept. of Civil Engineering
Los Angeles, California 90095

Kerem Gulec
University at Buffalo
Dept. of Civil Engineering
Buffalo, New York 14260

Dawn Lehman
University of Washington
Dept. of Civil and Environmental Engineering
214B More Hall
Seattle, Washington 98195

Jingjuan Li
4747 30th Avenue NE B118
Seattle, Washington 98105

Eric Lumpkin
6353 NE Radford Drive, Apt. #3917
Seattle, Washington 98115

Juan Murcia-Delso
University of California, San Diego
Dept. of Structural Engineering
409 University Center
9500 Gilman Drive – MC0085
La Jolla, California 92093

Hussein Okail
University of California, San Diego
Dept. of Structural Engineering
409 University Center
9500 Gilman Drive – MC0085
La Jolla, California 92093

Charles Roeder
University of Washington
Dept. of Civil and Environmental Engineering
233B More Hall
Seattle, Washington 98195

P. Benson Shing
University of California, San Diego
Dept. of Structural Engineering
409 University Center
9500 Gilman Drive – MC0085
La Jolla, California 92093

Christopher Smith
Stanford University
Dept. of Civil Engineering
MC:4020, Building 540
Stanford, California 94305

Victor Victorsson
1742 Sand Hill Road, Apt. 308
Palo Alto, California 94304

John Wallace
University of California, Los Angeles
Dept. of Civil Engineering
5731 Boelter Hall
Los Angeles, California 90095

Nonstructural Performance Products Team

Robert E. Bachman (Team Leader)
RE Bachman Consulting
25152 La Estrada Drive
Laguna Niguel, California 92677

Philip J. Caldwell
Schneider Electric
7 Sleepy Hollow Lane
Six Mile, South Carolina 29682

Andre Filiatrault
Multidisciplinary Center for Earthquake
Engineering Research, University at Buffalo
105 Red Jacket Quadrangle
Buffalo, New York 14261

Robert P. Kennedy
RPK Structural Mechanics Consulting, Inc.
28625 Mountain Meadow Road
Escondido, California 92026

Helmut Krawinkler (deceased)
Stanford University
Dept. of Civil & Environmental Engineering
240 Terman Engineering Center
Stanford, California 94305

Manos Maragakis
University of Nevada, Reno
Dept. of Civil Engineering
Mail Stop 258
Reno, Nevada 89557

Eduardo Miranda
Stanford University
Dept. of Civil & Environmental Engineering
Terman Room 293
Stanford, California 94305

Gilberto Mosqueda
University at Buffalo
Dept. of Civil, Structural, and Environmental Engineering
Buffalo, New York 14260

Keith Porter
University of Colorado
Dept. of Civil, Environmental, and Architectural Engineering
Engineering Center Office Tower 428
1111 Engineering Drive
Boulder, Colorado 80309

Nonstructural Performance Products Consultants

Richard Behr
Pennsylvania State University
Dept. of Architectural Engineering
104 Engineering Unit A
University Park, Pennsylvania 16802

John Eidinger
G&E Engineering Systems
PO Box 3592
Olympic Valley, California 96146

Gregory S. Hardy
Simpson Gumpertz & Heger
4000 MacArthur Blvd. Suite 710
Newport Beach, California 92660

Christopher Higgins
Oregon State University
220 Owen Hall
Corvallis, Oregon 97333

Gayle S. Johnson
Halcrow
500 12th Street, Suite 310
Oakland, California 94607

Paul Kremer
430 Canterbury Drive
State College, Pennsylvania 16802

David L. McCormick
Simpson Gumpertz & Heger
The Landmark @ One Market, Suite 600
San Francisco, California 94105

Ali M. Memari
Pennsylvania State University
104 Engineering Unit A
University Park, Pennsylvania 16802

William O'Brien
The Pointe
501 Vairo Boulevard
State College, Pennsylvania 16803

John Osteraas
Exponent
149 Commonwealth Drive
Menlo Park, California 94025

Xin Xu
7 Xibei Xincun, Room 403
Wuxi, Jiangsu 214062, P.R.China

Fragility Review Panel

Bruce R. Ellingwood
School of Civil and Environmental Engineering
Georgia Institute of Technology
790 Atlantic Drive
Atlanta, Georgia 30332

Stephen Mahin
University of California
Dept. of Civil Engineering
777 Davis Hall, MC 1710
Berkeley, California 94720

Robert P. Kennedy
RPK Structural Mechanics Consulting, Inc.
28625 Mountain Meadow Road
Escondido, California 92026

Validation/Verification Team

Charles Scawthorn (Chair)
C. Scawthorn & Associates
744 Creston Road
Berkeley, California 94708

David Bonneville
Degenkolb Engineers
235 Montgomery Street, Suite 500
San Francisco, California 94104

Jack Baker
Stanford University
Dept. of Civil & Environmental Engineering
240 Terman Engineering Center
Stanford, California 94305

Hope Seligson
MMI Engineering
2100 Main Street, Suite 150
Huntington Beach, California 92648

Special Reviewers

Thalia Anagnos
San Jose State University
General Engineering Office 169
San Jose, California 95192

Fouad M. Bendimerad
125B 24th Avenue
San Mateo, California 94403